The Development of Candidate Therapeutics for Transmissible Spongiform Encephalopathies

By

Katarzyna Zolnierczyk

Thesis submitted to the University of Nottingham

for the Degree of

Doctor of Philosophy

February 2021

School of Veterinary Medicine and Science

Sutton Bonington Campus

Loughborough

Leicestershire

LE12 5RD

Author's declaration

I declare that, except where reference is made to the contribution of others, that this thesis is the product of my own work and has not been submitted for any other degree at the University of Nottingham or any other institution.

Signature 

Katarzyna Joanna Zolnierczyk

Abstract

Previous studies have shown that addition of recombinant prion into a cell free prion replication assay – PMCA inhibits the formation of PrP^{Sc}. Previously naturally existing versions of ovine prion protein were tested: rARQ, rARR and rVRQ within this assay. Of these, rVRQ was the most potent inhibitor of amplification of different scrapie isolates (IC50 value 120 nM) and bovine BSE (IC50 – 171 nM). The main aim of this study was to produce additional molecular clones for expression of recombinant ovine prion protein where codon 136 had been mutated to code for different amino acids. These rPrPs were tested in dose response experiments in order to investigate whether the change at 136 position in ovine PrP could impact on the ability to inhibit or stop the prion protein misfolding compared to previously tested rVRQ. In order to produce rPrP mutants at codon 136, site-directed mutagenesis was used. All rPrPs were purified by metal affinity chromatography taking advantage of the metal binding properties of PrP molecule. All mutated rPrPs were added to protein misfolding cyclic amplification (PMCA) at different concentration and compared to rVRQ. After amplification, samples were digested with Proteinase K (100 µg/ml) and quantified on immunoblots. The best inhibitors were tested with different ovine scrapie (ARQ/VRQ, VRQ/VRQ, AHQ/VRQ), bovine BSE and ovine BSE isolates (ARQ/ARQ). The results showed that three of the recombinant prion proteins: rRRQ, rKRQ and rPRQ (with arginine, lysine and proline at 136 position, respectively) were found to inhibit the PrP^{Sc} misfolding significantly better than naturally occurred rVRQ.

The structure of rPrP variants and amino acid substitution at 136 position were analysed and different length peptides containing the valine, arginine, lysine and proline at 136 position were designed. None of these peptides analysed in PMCA gave similar levels of inhibition to the equivalent full length recombinant prion protein response. Moreover, structural analysis showed that introduction of longer amino acids at position 136 did not alter the whole scaffold of prion protein. In addition, the longer side chains for $arginine_{136}$ and $lysine_{136}$ or pyrrolidine loop in proline could result in more interatomic bonding in comparison to $valine_{136}$ and therefore could act to stabilize the whole PrP molecule. Furthermore, the presence of the longer side chains of $arginine_{136}$ and $lysine_{136}$ would not predict further structure changes because of the 'structural' pocket present on the opposite site of position 136 in ovine PrP.

The Rov9 cell line could be persistently infected with processed (heated and sonicated) scrapie brain homogenate SSBP1 (VRQ/VRQ) and SSBP1 derived, NaPTA precipitated PrP^{Sc}. In both cases, PrP^{res} was detected in cell lysates from induced with 1 µg/ml doxycycline and when 500 µg of total protein was digested with 20 µg/ml of PK followed by PrP^{res} concentration by centrifugation. The best inhibitory rPrPs were used in experiments to prevent the infection with SSBP1 isolate or reduce the PrP^{res} in

persistently infected Rov9 cells. As a result, addition of 250 nM of rRRQ, rKRQ and rPRQ prevented the infection of Rov9 cells at culture passage 1. The rPrP variants showed more promising results than natural rVRQ. In contrast, no significant reduction of PrP^{res} was observed when persistently infected Rov9 cells were treated with 250 nM of either variants or natural rPrPs for 4 days.

Overall, this work demonstrated a novel therapeutic approach for prion diseases using recombinant prion proteins. The recombinant protein treatment was effective not only in scrapie model but also among other TSEs and therefore these rPrPs or analogous strategy could be applied as potential human TSE therapeutic.

Acknowledgments

A dream does not become reality through magic; it takes sweat, determination and hard work.

Colin Powell

Firstly, I would like to offer my special thanks to my supervisors Professor Kevin Gough (School of Veterinary Medicine and Science) and Dr Ben Maddison (RSK-ADAS) for their patience, continuous support, motivating and pushing me towards research goals. Without them, this work would not be possible.

I would also like to thank members of RSK-ADAS group; Claire Baker for her ongoing mental and technical support and encouragement, Keith Bishop for his outstanding jokes, Dr Jon Owen and Dr Helen Rees for always being there for me. I must also thank my friend and lab partner Juan Fernandez Bonfante for sharing the knowledge, experience and fun with me during the route through PhD.

I would like to thank all the group members and friends from Vet School: Maria Tsoumpeli, Anitha Varghese, Morena Santi, Kieran Pitchers, Dr Alison Grey, Britany Clarke, Dr Robert Workman and many others who helped me throughout my time in the laboratory and office. Your encouragement and kindness helped me a lot through these hard-working years.

I am also very grateful to Professor David Gartner (UoN, Vet School) and Dr Ingrid Dreveny (UoN, CBS) for their help at various stages of my PhD.

My gratitude and wishes extends to my loving family: Sebastian, my mum and dad, my best brother and others for understanding, support, uplifting throughout the PhD journey and most of all for keeping me sane.

And the last but not least thanks go to you – the Reader – for your time and patience. Hope you will find this work interesting.

Contents

List of figures

List of tables

Abbreviations

°C	Degrees Celsius
α-syn	α-synuclein
2YT	2 x yeast tryptone media
2YT-AG	2 x yeast tryptone media with ampicillin and glucose
2YT-AI	2 x yeast tryptone media with ampicillin and IPTG
3-D	Three-dimensional
A	Alanine
Å	Ångstroms
aa	Amino acid
AD	Alzheimer's Disease
ALS	Amyotrophic lateral sclerosis
ANOVA	Analysis of variance
APHA	Animal and Plant Health Agency
APP	Amyloid precursor protein
Aβ	Amyloid β
BASE	Bovine amyloidotic spongiform encephalopathy
BSA	Bovine serum albumin
BSE	Bovine Spongiform Encephalopathy
C	Cysteine
C-BSE	Classical Bovine Spongiform Encephalopathy
CD	Circular dichroism
CDI	Conformation-dependent immunoassay
CGN	Cerebellar granule neurons
CNS	Central nervous system
CR	Congo Red

CSA	Conformational stability assay
CSF	Cerebrospinal fluid
Cu	Copper
CWD	Chronic wasting disease
D	Aspartic acid
D-PBS	Dulbecco Phosphate Buffered Saline, sterile PBS for cell culture
DC	Dendritic cells
DLB	Dementia with Lewy bodies
DMSO	Dimethylsulfoxide
DNA	Deoxyribonucleic acid
dNTPs	Deoxynucleotides
dox	Doxycycline
dpi	Days post infection
E	Glutamic acid
EC50	Half maximal effective concentration
EDTA	Ethylene diamine tetra-acetic acid
EEG	Electroencephalogram
EMEM	Eagle's Minimum Essential Medium
ENS	Enteric nervous system
EU	European Union
EV	Extracellular vesicles
F	Phenylalanine
Fabs	Recombinant antibodies fragments
FBS	Fetal Bovine Serum
fCJD	Familial Creutzfeldt-Jakob disease
FDC	Follicular dendritic cells
Fe(III)-TMPyP	Fe(III)-meso-tetra(N-methyl-4-pyridyl)porphine

FFI	Fatal Familial Insomnia
FI	Fatal Insomnia
FPLC	Fast liquid protein chromatography
FTIR	Fourier-transform infrared
g	Gram
G	Glycine
GALT	Gut-associated lymphoid tissue
Gdn-HCl	Guanidinium hydrochloride
GPI	Glycosylphosphatidylinositol
GSS	Gerstmann-Sträussler-Scheinker syndrome
GST	Glutathione S-transferase
H	Histidine
h	Hour
hGH	Human Growth hormone
HRP	Horseradish peroxidase
I	Isoleucine
IMAC	Immobilised metal affinity chromatography
i.p.	Intraperitoneal
IAPP	Islet amyloid polypeptide
IC50	The concentration of an inhibitor where the response is reduced by half
iCJD	Iatrogenic Creutzfeld-Jakob Disease
IHC	Immunohistochemistry
iPSC	Induced pluripotent stem cells
IPTG	Isopropyl β-D-1-thiogalactopyranoside
K	Lysine
kb	Kilobase pair
kDa	Kilo Dalton

kT/e	Electrostatic potential unit in PyMOL
L	Leucine
LB	Lewy Bodies
LDS	Lithium dodecyl sulphate
LRS	Lymphoreticular system
M	Methionine or Molar
MAP	Microtubule-associated proteins
MDBK	Madin-Darby Bovine Kindey
MeOH	Methanol
mg	Milligrams
ml	Millilitre
mM	Millimolar
mRNA	Messenger ribonucleic acid
MV	Microvesicles
MWCO	Molecular weight cut off
N	Asparagine
NaPTA	Sodium phosphotungistic acid
NFT	Neurofibrillary tangles
ng	Nanogram
nm	Nanometre
NMR	Nuclear magnetic resonance
NSP	National Scrapie Plan
OD	Optical density
OR	Octapeptide repeat
ORF	Open reading frame
P	Proline
PBS	Phosphate Buffered Saline

PBST	Phospate Buffered Salinie with Tween20
PCR	Polymerase chain reaction
PD	Parkinson's Disease
pdb	Protein Data Bank
Pen/Strep/Glu	Penicillin, Streptomycin, Glutamine
PIRIBS	parallel in-register intermolecular β-sheet
PK	Proteinase K
PMCA	Protein Misfolding Cyclic Amplification
PMDs	Protein Misfolding Diseases
PPS	Pentosane polysulphate
PRNP	Human prion protein gene
Prnp	Animal prion protein gene
PrP	Prion protein
PrP27-30	Protease-resistant core of PrP^{Sc}
PrP^{C}	Cellular prion protein
PrP^{res}	PK resistant form of prion protein
PrP^{Sc}	Disease associated prion protein
PVDF	Polyvinylidene difluoride
Q	Glutamine
R	Arginine
RAMALT	Recto-anal mucosa-associated lymphoid tissue
rhamPrP	Recombinant hamster prion protein
RNA	Ribonucleic acid
rPrP	Recombinant prion protein
RT-QuIC	Real time quaking induced conversion
S	Serine
sCJD	Sporadic Creutzfeldt-Jakob Disease

SDS	Sodium dodecyl sulphate
SDS-PAGE	Sodium dodecyl sulphate-polyacrylamide gel electrophoresis
SiO_2	Silicon dioxide
SMA	Powdered milk
SNCA	α-synuclein gene
SOD	Superoxide dismutase
sPMCA	Serial protein misfolding cyclic amplification
T	Threonine
TBS	Tris buffered saline
TBST	Tris buffered saline with 0.05 % tween 20
ThT	Thioflavin T
TNTs	Tunnelling nanotubes
TSE	Transmissible Spongiform Encephalopathy
µg	Microgram
µl	Microliter
µM	Micromolar
V	Valine or Voltage
v/v	Volume per volume
vCJD	New variant Creutzfeldt Jakob Disease
VPSPr	Variable Protease-Sensitive Prionopathy
W	Tryptophan or Watts
w/v	Weight per volume
x g	Gravitational force
Y	Tyrosine

Chapter 1: Introduction

1.1 Transmissible Spongiform Encephalopathies

Transmissible spongiform encephalopathies (TSEs, also known as prion diseases) are a group of progressive, fatal neurodegenerative disorders with no treatment or cure. Among this group are both human and animal diseases. These disorders are characterised by spongiform changes within the neural tissue resulting in neuronal loss and this occurs without an inflammatory reaction. Furthermore, the incubation period is typically very long (Prusiner, 1998; Belay, 1999). The main pathological event that is thought to occur in these diseases is the conversion of a benign cellular protein (cellular prion protein, PrP^{C}) into a unique conformation called PrP^{Sc}. This misfolded protein then accumulates in neuronal tissue, a process accompanied by neurodegeneration.

1.1.1 Human Prion Diseases

Human prion diseases can be inherited (familial), transmitted (acquired via medical procedures (iatrogenic)) or meat consumption) and sporadic. Inherited forms of human TSEs include familial Creutzfeldt Jakob Disease (fCJD), FFI (fatal familial insomnia) and GSS (Gerstmann-Sträussler-Scheinker syndrome) (Belay, 1999; Chesebro, 2003). Inherited human prion diseases are mostly associated with point mutations within the prion protein gene (*PRNP*) or changes in the number of octapeptide-repeats within the protein sequence (Belay, 1999). In FFI, for example, a mutation at codon 178 in the *PRNP* gene results in substitution of aspartic acid (D) to asparagine (N). This event is the main trigger for the disease development and no exposure to the TSE agent is needed for the progression of inherited TSE forms (Forloni *et al.*, 2013). Additionally, two different mechanisms were proposed for sporadic TSE occurrence in humans (sCJD and sporadic FI (fatal insomnia)) (Puoti *et al.*, 2012). The first suggests that there is a sporadic, somatic mutation, which causes PrP^{Sc} formation and aggregation, while the second mechanism describes spontaneous formation of PrP^{Sc} in neural tissues (Belay, 1999; Colby and Prusiner, 2011). Furthermore, there is no clear evidence that exposure to the TSE agent might trigger the sporadic TSE development in patients (Chesebro, 2003). On the other hand, transmitted prion diseases have been described as a direct result of prion disease agent exposure. For example, iatrogenic CJD (iCJD) developed in patients treated with prion contaminated growth hormone or gonadotropins and after brain tissue implants from TSE infected patients. Furthermore, PrP^{Sc} was also transferred into healthy patients during the use of contaminated electroencephalogram (EEG) electrodes or neurosurgical instruments (Will, 2003).

A distinct TSE in humans is kuru, an acquired disease described in the Papua New Guinea Fore people, spread through the ritualistic ingestion of TSE infected brain tissue of dead tribe members (Belay, 1999). vCJD was similarly acquired through the oral route as a result of BSE transmission to human via BSE contaminated meat (Will *et al.*, 1996; Chesebro, 2003). In comparison to sporadic CJD, vCJD is characterised by early disease symptoms and other distinct neuropathological changes within the brain tissue (Chesebro, 2003).

Also, an atypical human prion disease – Variable Protease-Sensitive Prionopathy (VPSPr) – has been described. VPSPr exhibits distinct features from other human prion diseases. In these cases, the PrP from patients has distinct biochemical characteristics to previously analysed human TSEs, for example it is unusually sensitive to proteases. Furthermore, the clinical disease progression is relatively slow and brain tissues show different PrP immunostaining patterns in comparison to other human TSEs (Gambetti *et al.*, 2008; Zou *et al.*, 2010, 2013).

1.1.2 Animal prion diseases

Animal TSEs include a range of diseases affecting food related animal species. These include scrapie in sheep and goats, BSE (bovine spongiform encephalopathy) in cattle and CWD (chronic wasting disease) in deer.

Scrapie was the first described prion protein disease, although the scrapie agent was unknown at the time (Stockman, 1913). Susceptibility and resistance to scrapie in sheep seems to depend mainly on the polymorphisms at positions 136, 154 and 171 within the PrP protein sequence (Belt *et al.*, 1995; Goldmann, 2008). Furthermore, a different type of sheep scrapie, now described as atypical or Nor98, was identified in Norway in 2003 (Benestad *et al.*, 2003). In comparison to classical scrapie, atypical scrapie was described in animals with ARR (alanine$_{136}$, arginine$_{154}$, arginine$_{171}$) genotype which is highly resistant to classical scrapie but also in ARQ (alanine$_{136}$, arginine$_{154}$, glutamine$_{171}$) and AHQ (alanine$_{136}$, histidine$_{154}$, glutamine$_{171}$) animals (Benestad *et al.*, 2003; Moum *et al.*, 2005; Arsac *et al.*, 2007; Luhken *et al.*, 2007). In addition, polymorphisms at positions 141 (change from leucine (L) to phenylalanine (F)) were found in atypical scrapie cases that may influence susceptibility (Moum *et al.*, 2005; Luhken *et al.*, 2007). Furthermore, phenylalanine at 141 position was usually found associated with ARQ polymorphisms in sheep ($A_{136}F_{141}R_{154}Q_{171}$) (Luhken *et al.*, 2007; Andréoletti *et al.*, 2011; Silva *et al.*, 2018). The main difference between these two forms of scrapie is that classical scrapie can spread through the lymphatic system as well as the central nervous system (CNS) and peripheral nervous system, while PrP^{Sc} deposits in atypical scrapie affected sheep were limited to brain (Benestad *et al.*, 2003; Buschmann *et al.*, 2004; Nentwig *et al.*, 2007; Vascellari *et al.*, 2007; Vidal *et al.*, 2008; Maddison, Baker, *et al.*, 2010; Andréoletti *et al.*, 2011). Different patterns of spongiform changes in the brain were noted for atypical scrapie compared to classical scrapie, suggesting that PrP^{Sc} deposits are distributed in a different way (Benestad *et al.*, 2003). In addition, atypical scrapie was described as a spontaneous disease affecting older animals rather than an infectious disease, with probable influence from genetic or environmental factors (Benestad *et al.*, 2008; Fediaevsky *et al.*, 2009). The PrP^{Sc} of these two diseases also differs biochemically, after Proteinase K (PK) treatment, western blot analysis of atypical scrapie cases displays distinct PrP^{Sc} band patterns to classical scrapie. First of all, these two forms of scrapie differ in a number of bands on western blot with classical scrapie having 3 bands and Nor98 having up to 5 bands. Secondly, the di-glycosylated band

shows higher molecular weight for atypical scrapie than classical, giving bands at around 31 kDa and 27-28 kDa, respectively. Moreover, a fast migrating band was detected for atypical scrapie at around 11-12 kDa or 7-8 kDa, whereas for classical scrapie display the smallest band is at around 19 kDa (Arsac *et al.*, 2007; Benestad *et al.*, 2008).

BSE is a prion protein disease in cattle. It was firstly described in the United Kingdom in 1986 (Wells *et al.*, 1987). BSE is a unique prion disease that can cross the species barrier and appear in unrelated species via natural infections. Because of this feature, it was linked to human vCJD and BSE-like tissue changes in greater kudu and goats (Will *et al.*, 1996; Cunningham *et al.*, 2004; Spiropoulos *et al.*, 2011). In addition, it has been reported, that BSE also had some atypical forms called L- (also known as bovine amyloidotic spongiform encephalopathy – BASE) and H-BSE. One of the differences between classical BSE (C-BSE) and the atypical forms is the migration profile of the PK-resistant PrP^{Sc} bands shown on western blots. In all forms of BSE, three bands are present on blots but in H-type, the PK resistant core migrates higher than C-BSE and in L-BSE this migrates lower (Biacabe *et al.*, 2007; Jacobs *et al.*, 2007). Furthermore, C-type BSE seems to be more resistant to PK digestion than the atypical forms of BSE (Jacobs *et al.*, 2007). After tissue staining, the pattern of L-BSE amyloid plaques was different than in classical BSE, whereas for H-type there were no differences that allow to differentiate from C-BSE types based on PrP^{Sc} deposits in brain (Casalone *et al.*, 2004; Sisó *et al.*, 2007). Moreover, atypical BSE forms were described as sporadic affecting older animals compared to infectious C-BSE (Biacabe *et al.*, 2004).CWD (chronic wasting disease) is a prion disease found in the *Cervidae* family, including elk, deer, reindeer and moose. It was reported in both free-ranging and captive animals, with transmission routes being investigated. Within the CWD cases, abnormal prion protein was detected in tonsil lymph nodes, follicular dendritic cells and also in gut associated lymphoid tissues (Sigurdson *et al.*, 1999; Miller *et al.*, 2004). Some reports indicate that the CWD occurrence might be associated with some polymorphisms within the *Prnp* gene, however the correlation between polymorphism and disease susceptibility or resistance is not as strong as in scrapie cases (Johnson *et al.*, 2003; Robinson *et al.*, 2012; Hoover *et al.*, 2017).All animal prion diseases are a major concern for food security because these TSEs affect food chain species and the transmission routes still remain unclear. Furthermore, there is a possibility that they might be transferred to humans, as BSE causing vCJD has shown. Therefore, surveillance programs and regulations were established to monitor animal TSE cases and try and reduce their incidence in food producing animals.

1.1.3 Prion diseases occurrence

In the UK, the most common animal prion diseases have been scrapie in sheep and BSE in cattle. The first scrapie case was described in 1853 in the UK, and since then many scrapie cases have been reported both in the UK and around the world (Stockman, 1913). In the UK in recent times, scrapie was an endemic disease in sheep and goats. In order to help with the reduction of scrapie prevalence in the UK, in 2001 the National Scrapie Plan (NSP) was introduced **(Table 1.1.1)**. The program consisted of identifying sheep as being in 1 of 5 genotype groups based on susceptibility to classical scrapie, where group 5 is the highest scrapie susceptibility and group 1 is the lowest risk for scrapie development (Goldmann, 2008). The NSP aimed to breed sheep in the UK to increase the levels of genetic resistance of the UK flock to scrapie. This breeding programme along with increased surveillance and culling of diseased animals resulted in the incidence of classical scrapie disease being 0 cases in 2018 (Animal and Plant Health Agency, 2019b). BSE was recognised in 1986 in UK cattle and became established as an epidemic (Belay, 1999). Nearly 180,000 cases of BSE were confirmed in the UK with the peak of the epidemic in early 1990s (Animal and Plant Health Agency, 2019a). Moreover, the first reported case of BSE outside the UK was in 1989 in Ireland and then more BSE cases were described in Europe and North America. Since then, the number of classical BSE cases has decreased due to effective control measures and in 2017 for the first time since the BSE outbreak, no cases of classical BSE were reported (World Organisation for Animal Health, 2019). Although the disease source might be eliminated (thought to be BSE contaminated meat and bone meal feed), it is possible that infectious prions could be present in the environment and act as a reservoir of infectivity.

Chronic wasting disease (CWD) was first reported in captive deer in the USA State of Colorado in late 1960s. Subsequently, cases in wild deer were confirmed (Williams and Young, 1980). Since then, the disease has spread in free-ranging cervids and is established in 24 US states or Canadian provinces (*Centers for Disease Control and Prevention*, 2019). Furthermore, CWD was also reported in South Korea after a CWD infected elk was imported from Canada (Sohn *et al.*, 2002). In addition, the first European case was reported in March 2016 in Norway. From that time, Norway has detected 23 cases of CWD (data until September 2019). The first reported case of CWD in the European Union (EU) was in Finland (March 2018) and since then, new cases were also reported in Sweden (Koutsoumanis *et al.*, 2019). So far, there are no cases of CWD reported in the UK and the risk of importing infectivity is estimated to be very low (Gale and Roberts, 2018).

In humans, the most common form of human prion disease is sporadic sCJD with the number of sCJD cases increasing in the UK from 48 in 2000 to 135 cases in 2018. Worldwide, sCJD occurred at 2.06 cases per million in 2018. Also, iatrogenic and genetic CJD cases are being reported at lower levels (NCJDRSU, 2019). Moreover, it is now

established that BSE transmission to humans via consumption of meat contaminated with infectious prions has affected 178 people in the UK with the last reported case of new variant CJD (vCJD) in 2016 (NCJDRSU, 2019).

Table 1.1.1 Ovine genotypes occurring in sheep in the UK and their degree of resistance/susceptibility to scrapie according to the National Scrapie Plan. Adapted from (DEFRA, 2001).

Genotype	Resistance/susceptibility to the disease	Suitability for breeding
ARR/ARR	Resistant to scrapie	Yes
ARR/AHQ ARR/ARH ARR/ARQ	Resistant to scrapie	Yes, but with caution
AHQ/AHQ AHQ/ARH AHQ/ARQ ARH/ARH ARH/ARQ ARQ/ARQ	Little resistance to scrapie	Yes, but with caution
ARR/VRQ	Susceptible to scrapie	No
AHQ/VRQ ARH/VRQ ARQ/VRQ VRQ/VRQ	Highly susceptible to scrapie	No

1.1.4 TSE transmission

TSE transmission is a considerable concern after the interspecies transmission of BSE to humans and other animal species via presence of cattle BSE in meat/feed. Despite this, there is no evidence of other TSEs transmissibility to distinct, non-related species outside of a laboratory setting. However, the possible routes of infectious prion secretion and excretion, environmental storage, and animal uptake are being investigated **(Table 1.1.2)**.

Infectious prions are released from the body of sick or dead animals via many routes (Gough, Baker, *et al.*, 2015). For both classical scrapie and CWD, TSE agent is shed from nasal and oral secretion, in urine, faeces, milk, blood, antler velvet and skin. In addition, possible transmission of infectivity through placenta from infected mothers to offspring (*in utero* transmission) was described for both scrapie and CWD (Race, Jenny and Sutton, 1998; Tuo *et al.*, 2001, 2002; Andréoletti *et al.*, 2002; Miller and Williams, 2003; Nalls *et al.*, 2013). Infectivity could also derive from decomposed or buried carcasses of infected animals for many years after death (Brown and Gajdusek, 1991).

Table 1.1.2. Evidence of possible transmission routes for prion diseases.

Disease	Excretion/secretion or transmission route	Reference
Animal TSEs		
Classical scrapie	Saliva	(Maddison, Rees, *et al.*, 2010; Gough *et al.*, 2012)
	Milk	(Maddison, Whitelam and Gough, 2007; Konold *et al.*, 2008; Maddison *et al.*, 2009)
	Skin	(Thomzig *et al.*, 2007)
	Placenta	(Race, Jenny and Sutton, 1998; Tuo *et al.*, 2001, 2002; Andréoletti *et al.*, 2002)
	Urine	(Murayama *et al.*, 2007)
C-BSE	Contaminated meat and tissues (and to different species)	(Will *et al.*, 1996; Bruce *et al.*, 1997; Bons *et al.*, 1999; Cunningham *et al.*, 2004; Jeffrey, González, *et al.*, 2006; Jeffrey, Martin, *et al.*, 2006)
CWD	Saliva	(Sigurdson *et al.*, 1999; Mathiason *et al.*, 2006; Haley *et al.*, 2009; Denkers, Telling and Hoover, 2011; Henderson *et al.*, 2013)
	Nasal/aerosol	(Denkers *et al.*, 2013)
	Semen	(Kramm *et al.*, 2019)
	Urine	(Haley *et al.*, 2009)
	Faeces	(Cheng *et al.*, 2016)
	Antler velvet/skin	(Angers *et al.*, 2009)
	Blood	(Mathiason *et al.*, 2006)
	Placenta	(Miller and Williams, 2003)
Human TSEs		
vCJD	Blood	(Llewelyn *et al.*, 2004)
iCJD	Neurological medical equipment (*eg.* EEG equipment)	(Bernoulli, Siegfried and Baumgartner, 1977; Will and Matthews, 1982; Will, 2003)
	Contaminated growth hormone (hGH)	(Centers for Disease Contol, 1985; Gibbs *et al.*, 1985; Koch *et al.*, 1985)
	Dura mater grafts	(Thadani *et al.*, 1988; Will, 2003)

Once released to the environment, prions can bind to soil minerals, remain infectious and act as a disease reservoir (Johnson *et al.*, 2006; Genovesi *et al.*, 2007; Maddison *et al.*, 2015). In the environment, TSE infectivity can survive for several years. Studies showed that CWD derived PrP^{Sc} was found on the surfaces 2 years after CWD affected

animals were present, and scrapie infectivity was detected on a farm even after a 16 year period (Williams, 2005; Georgsson, Sigurdarson and Brown, 2006). In this period of time, susceptible animals can come into contact with prions on fomites or soil particles containing the PrP^{Sc} could be taken up by an animal. It has also been suggested that plants could bind and retain the PrP^{Sc} from soil via roots, leading to transport of the TSE agents to leaves and stems creating another source of infectivity (Pritzkow *et al.*, 2015). Moreover, research conducted by Maddison *et al*., showed the presence of PrP^{Sc} on metal, concrete, wood and plastic fomites on a farm, indicating environmental reservoirs of prion (Maddison, Baker, *et al.*, 2010). Another study conducted by Konold *et al.*, demonstrated that scrapie could indeed be transmitted via these fomites when susceptible sheep were exposed to them (Konold *et al.*, 2015). A further study investigated the possibility of prion transmission after binding to fomites (wood, rock, cement, aluminium, glass, stainless steel or polypropylene). Not only were prions able to bind to these surfaces but the PrP^{Sc} could seed *in vitro* amplification assays and was infectious in hamster bioassays. Furthermore, the same study found that, animals could take up the environmental prions by direct exposure such as by licking or sniffing. Also, direct transfer of the prions to the bedding site also resulted in infection of the animals, although this transmission method gave the lowest attack rate (Pritzkow *et al.*, 2018). Further studies have also shown that scrapie prions can be spread via dust on an 'infected farm'. It was also shown that PrP^{Sc} were detected on the surfaces that were not in any direct contact with sick animals, Indeed, scrapie PrP^{Sc} was found in the dust samples collected at 30 m distance from farm buildings (Gough, Baker, *et al.*, 2015).

In order to investigate the risk of prion transfer from interred tissues of dead animals, mouse passaged BSE was experimentally buried for a 5 year period and area surrounding soils and rainwater samples that has passed through the site were collected and analysed. It appeared that the BSE infectivity survived at very high titres in the brain tissue for the study duration. Additionally, only limited migration of prion through the soil was observed. However, some prion was seen in rainwater that had passed through the burial site. This research showed the importance of having contained burial sites for any prion infected animals and in particular for those affected with BSE (Somerville *et al.*, 2019).

1.2 Cellular prion protein

The normal prion protein, also known as cellular prion protein PrP^{C}, is a membrane attached glycoprotein encoded by a host *Prnp* gene. In humans *PRNP* gene is localised on the short arm of chromosome 20 and is built from 2 exons, with the entire open reading frame (ORF) for prion protein localised within the second exon (Prusiner, 2004; Mead, 2006). PrP^{C} has several distinct domains and also undergoes post translational modification **(Figure 1.2.1)**. Briefly, PrP^{C} is translated from the mRNA in the endoplasmic reticulum and after the polypeptide chain is created, the N-terminal signal peptide and GPI-anchor signals are cleaved (Hope *et al.*, 1986). The

glycosylphosphatidylinositol (GPI) anchor is added to serine (S) at position 231 and then the protein is carried through the Golgi apparatus, where the N-glycan chains are added to some of the asparagine residues at positions 181 and 197. The N-terminal domain of PrP^C is built from a nonapeptide (PQGGGGWGQ) followed by nine octapeptide repeats (OR) with 4-6 copper ion binding sites (Acevedo-Morantes and Wille, 2014). On the C-terminal, cysteines (C) at positions 179 and 214 are connected with a disulphide bond. The processed and glycosylated PrP^C is transported to the cell surface and attached to lipid rafts in the cell membrane through the GPI anchor (Maiti and Surewicz, 2001; Mead, 2006; Acevedo-Morantes and Wille, 2014). Mammalian PrP protein sequences are homologous in more than 90 % of residues and only differ in, for example, N-glycosylation or disulphide bond sites (Groschup, Harmeyer and Pfaff, 1997).

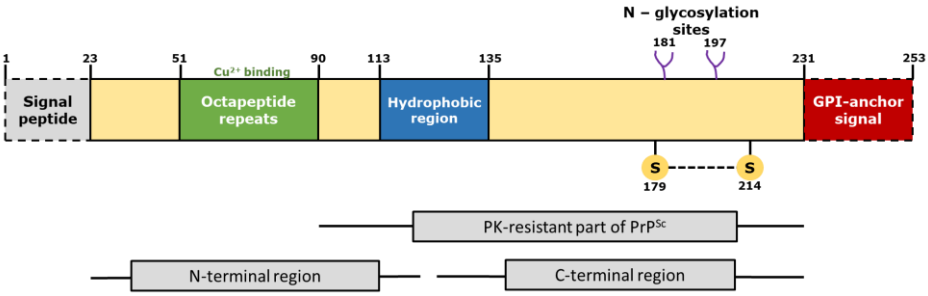

Figure 1.2.1. Human PrP^C structure. After translation, human PrP consists of 253 amino acids and its N-terminus contains: a signal peptide (1-22), octapeptide repeats with Cu^{2+} binding sites (51-90), a hydrophobic region (113-135), and on the C-terminus: a disulphide bond between cysteines at positions 179 and 214, two N-glycosylation sites on asparagine at 181 and 197 residues and a GPI-anchor signal peptide. GPI – glycosylphosphatidylinositol, PK – proteinase K. Adapted from (Acevedo-Morantes and Wille, 2014), modified.

On the other hand, the sheep *Prnp* gene is localised on chromosome 13 and in comparison to the human gene, ovine *Prnp* contains 3 exons and 2 introns. The whole ORF is contained within the longest, 3rd exon. Furthermore, the ovine prion protein is longer than human PrP and contains 254 amino acids and bovine PrP^C contains 264 amino acids (Yoshimoto *et al.*, 1992; Goldmann, 2008). The main difference between the PrP sequences between species is usually the presence of different numbers of octapeptide repeats in the protein sequence (Yoshimoto *et al.*, 1992; Schläpfer *et al.*, 1999).

Many attempts have been made to obtain complete three-dimensional (3-D) structure of PrP^C, however the most accurate structural information comes from nuclear magnetic resonance (NMR) studies of recombinant prion protein **(Figure 1.2.2)**. So far, NMR data has been obtained for the globular, C-terminal structure of recombinant mouse,

hamster, sheep, human and bovine PrP (Donne *et al.*, 1997; Riek *et al.*, 1997; Zahn *et al.*, 2000; Lopez Garcia *et al.*, 2002; Haire *et al.*, 2004). In general, within the globular domain (C-terminus) of the prion protein three α-helices and an anti-parallel β-sheet is present. Furthermore, the disulphide bridge connects helices 2 and 3 (Riesner, 2003). The N-terminus of PrP is more flexible than the globular C-terminus and as mentioned before, its main feature is an OR region with copper ion binding sites and a hydrophobic region (Zahn *et al.*, 2000; Riesner, 2003). Overall, the benign cellular prion protein structure contains more α-helices than β-sheets and because the PrP sequence is highly conserved between mammalian species, the 3-D structure between species is very similar (Zahn *et al.*, 2000).

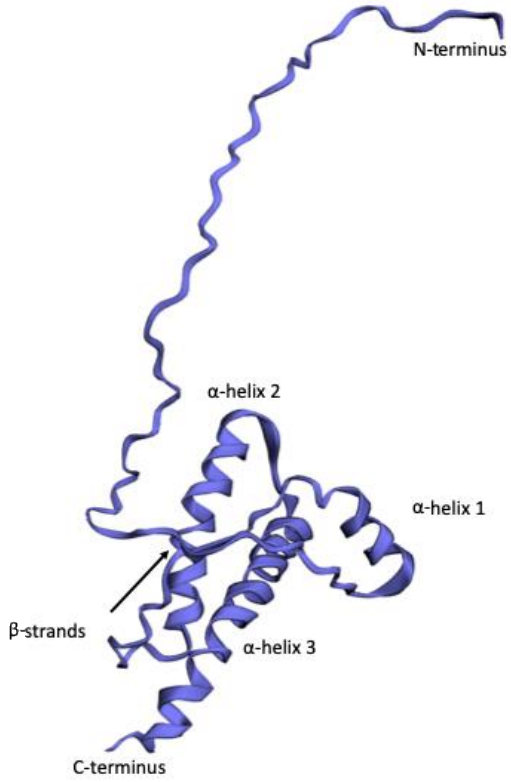

Figure 1.2.2. Ovine PrP^C structure. Protein N-terminus is flexible, whereas the C-terminus is highly structured and contains three α-helices and an anti-parallel β-sheet. The figure was generated using Phyre2 and EzMol1.3 software.

Cellular prion protein is attached through the GPI anchor to lipid rafts on the cell membrane. Research using antibodies against different parts of the prion protein (C-, N-terminus and central protein regions) has also localised the PrP^C to different cellular structures within murine cells: *e.g.* on the Golgi complex, endoplasmic reticulum, and on the plasma membrane (Naslavsky *et al.*, 1997; Mironov *et al.*, 2003). Moreover, PrP^C was also found in the cell nuclei and mitochondria (Gu *et al.*, 2003; Hachiya *et al.*, 2005; Morel *et al.*, 2008; Sorice *et al.*, 2012). In addition, for some brain regions like hippocampus, thalamus and neocortex, cellular prion protein was also observed in the

neuron's cytoplasm. Despite the fact that PrP^C is synthesised at relatively high levels in neurons in the CNS compared to other tissues and cell types, the amount of mRNA differs between brain regions from relatively high levels in hippocampus or neocortex to very low levels in internal regions of the cerebellum. The same amounts of PrP^C were found in the pre- and postsynaptic membranes. Apart from brain tissue and CNS, relatively high expression levels of PrP^C were also found in heart and lungs, while lower levels were found in spleen or intestinal epithelial cells, keratinocytes and brain endothelial cells (Manson *et al.*, 1992; Morel *et al.*, 2004, 2008; Viegas *et al.*, 2006; Wulf, Senatore and Aguzzi, 2017).

The biological function of the normal prion protein is still being investigated and several possible roles have been suggested. Its presence in pre- and postsynaptic membranes might be correlated to synaptic ion channels and receptor control. Moreover, some studies indicate that PrP^C probably participates in neurobiological processes like memory and sleep regulations, while other authors describe a possible role for PrP in murine embryo development (Manson *et al.*, 1992; Mironov *et al.*, 2003; Wulf, Senatore and Aguzzi, 2017). Furthermore, a role for prion protein in apoptosis was described and different sources indicate that PrP might act as either a protector or an apoptosis stimulator and the function is determined by PrP^C intra- or extracellular localization (Sorice *et al.*, 2012). Alternatively, the presence of PrP^C in the nucleus of actively dividing cells suggests that it might take part in cell division (Morel *et al.*, 2008). Furthermore, GPI-anchored PrP^C might contribute in cell–cell and cell–extracellular matrix adhesion and even mediate some signals between these structures For example for intestine endothelium enterocytes, where PrP^C was found to interact with adhesion proteins *e.g.* β- or γ-catenin (Morel *et al.*, 2004; Besnier *et al.*, 2015). As mentioned previously, the PrP sequence contains copper binding sites, therefore a role in copper binding and metabolism is also possible. Moreover, copper binding with the cellular prion protein might activate some protein shape changes from α-helices to β-sheets, therefore it is possible that copper binding promotes PrP^{Sc} formation or even starts the pathogenic process (Stöckel *et al.*, 1998).

1.3 Disease associated prion protein

The first scrapie cases in England were dated back to 1853. From that time, many different attempts to characterise the 'scrapie agent' were performed (Stockman, 1913). Until Prusiner's seminal publication in 1982, scrapie and other neurodegenerative diseases were thought to be caused by a 'slow virus' (Hadlow, 1959; Hadlow *et al.*, 1980). The term 'prion' was introduced by Prusiner for small 'proteinaceous infectious particles'. This 'particle' was described as UV radiation, ionisation resistant and stable in high temperatures (Prusiner, 1982). Moreover, the prion protein coding mRNAs were analysed and compared between healthy and diseased brains. Oesch and co-workers reported that both forms of prion protein – healthy and misfolded – are encoded by the same gene and its expression is at the same level between healthy and diseased brain

tissues. They suggested that during post translational modifications PrP might be converted into two different forms. However, Taraboulos *et al*., published that one of the post translational alterations – N-glycosylation – had no impact on resistant prion protein levels (Oesch *et al.*, 1985; Taraboulos *et al.*, 1990). Since this time, many attempts have been performed and a range of methods used to describe the prion agent. Research showed that the PrP^{C} and disease associated prion protein, PrP^{Sc}, have the same amino acid sequence but they differ in their secondary and tertiary structure and also in biochemical properties with the major structural difference between them being the content of α-helixes and β-sheets. The amount of α-helix content changes from 40 % in PrP^{C} to 30 % in PrP^{Sc}, while nearly undetectable amounts of β-sheets in PrP^{C} increase to 45 % in PrP^{Sc}. This structural conversion is the major factor involved in prion disease associated tissue neurodegeneration (Pan *et al.*, 1993). Furthermore, in comparison to cellular prion protein, PrP^{Sc} has a protease resistant core and is insoluble in detergents (Taraboulos *et al.*, 1990; Pan *et al.*, 1993). Proteinase K digestion only partially digests PrP^{Sc} (around 80 amino acids are truncated from both N- and C-termini) leaving the protease resistant core, also called as PrP27-30, while under the same conditions, cellular prion protein is completely digested (Oesch *et al.*, 1985). In addition, the truncated PrP^{Sc} is still infectious (Wille *et al.*, 2002). When PK digested samples are analysed on a western blot, a characteristic three band pattern is shown, with bands derived from the 3 possible glycosylation states of PrP protein: un-glycosylated, mono-glycosylated and di-glycosylated (Hunter, 2003). Furthermore, the size and relative abundance of each band differs between prion diseases and this feature is one of the distinguishing methods for prion disease strains (Jacobs *et al.*, 2011). Structurally modified PrP^{Sc} is prone to aggregate within the tissue creating amyloid fibrils and these aggregates of misfolded PrP^{Sc} in the brain tissue are characteristic for prion diseases (Taraboulos *et al.*, 1990).

1.3.1 PrP^{Sc} dissemination within the body

The understanding of the mechanisms involved in PrP^{Sc} infection of various cells and tissues is extremely important in order to understand TSE pathogenesis (Brown, 1997). The most common way of prion infection in natural infections is via the oral route, however other routes cannot be excluded. But whether and how the disease will develop depends on many different factors including host PrP genotype, TSE strain and genotype, and the dose of TSE agent (Beekes and McBride, 2000; Van Keulen, Vromans and Van Zijderveld, 2002). For infectious prion spread within tissues, expression of cellular prion protein on the cell membrane is necessary (Brandner *et al.*, 1996; Caughey *et al.*, 2009). After prions are delivered orally, they travel to the intestine and cross the intestinal epithelium. Many different intestine epithelium cells have been implicated in prion transport and mechanisms have been proposed. The first hypothesis describes PrP^{Sc} entering the intestine epithelium due to the β-sheet rich structure, while other theory shows that the epithelial cells such as M cells or dendritic cells capture

infected prions from the intestine lumen (Cobb and Surewicz, 2009; Natale *et al.*, 2011). Next, the PrP^{Sc} is transported along the epithelium, where it is phagocytosed by either macrophages or dendritic cells and transported to gut-associated lymphoid tissue (GALT). Here, transported cells are in contact with follicular dendritic cells (FDC) on the Peyer's patches. FDCs express high levels of cellular prion protein and their main role is to catch and present antigen on their surfaces. Therefore, these cells can trap and keep infectious prions on their cell membranes and are replication sites for prions in lymphoreticular system (LRS) tissues (McCulloch *et al.*, 2011; Bradford, Crocker and Mabbott, 2014). The PrP^{Sc} then starts to accumulate and amplify within the GALT (Beekes and McBride, 2000; Cobb and Surewicz, 2009). Studies using transmissible mink encephalopathy showed that PrP^{Sc} may be accumulated in the spleen, however other research with mouse adapted scrapie (263K strain) demonstrated that accumulation of prions in spleen was not an absolute requirement (Hadlow, Race and Kennedy, 1987; Race, Oldstone and Chesebro, 2000). The dissemination routes and involvement of particular LRS tissues is likely to be dependent of host *Prnp* genotype, the strain of invading prion and the entry route to a body **(Figure 1.3.1)**. Prion strains that are more neuroinvasive could propagate more efficiently in lymphoid tissues and intensify neuroinvasion. Furthermore, the spreading process could depend on the size of prion aggregates, with smaller aggregates able to penetrate the peripheral nerves more easily than large amyloid deposits. In addition, stability of the specific strain aggregates may also play a role – instable strains will generate high doses of small infectious prion particles. These small fragments facilitate effective spreading of infectivity within peripheral nerves. As a result, higher strain stability can cause longer disease incubation times (Bett *et al.*, 2012). These multiple factors explain why there are many differences in finding PrP^{Sc} deposits in different tissues at different disease stages between cases. In sheep scrapie, the LRS involvement depends on *Prnp* genotype. Langeveld *et. al.,* reported that VRQ (both homo and heterozygote) animals showed PrP^{Sc} positive deposits in LRS much earlier than in the brain tissue. The only exception from this are sheep with genotype VRQ/ARR, which usually show no LRS involvement but with some exceptions (Ersdal *et al.*, 2003; Langeveld *et al.*, 2006). In addition, no deposits in LRS were reported for either atypical scrapie or CH1641 strains (Benestad *et al.*, 2003; Jeffrey, González, *et al.*, 2006). It is considered that after accumulation in the GALT, PrP^{Sc} starts neuroinvasion, spreading firstly to the enteric nervous system (ENS) and next to the CNS (Natale *et al.*, 2011). It was described that PrP^{Sc} moves to neurons associated with GALT or epithelial cells through direct contact via axons or dendrites (Natale *et al.*, 2011). This transport might be possible *e.g.* due to significantly reduced or even absent myelin layer on nerves (Kimberlin, Hall and Walker, 1983). In addition to that, FDC have also been found close to sympathetic nerve fibres, suggesting that this could also be a route into the peripheral nervous system (PNS) (Glatzel and Aguzzi, 2000; Davies *et al.*, 2006). The involvement of the sympathetic nervous system was described *e.g.* in vCJD patients (Haïk *et al.*, 2003).

Once in the PNS, PrP^{Sc} could travel using either axonal or non-axonal transport or even using the Schwann cells (Glatzel and Aguzzi, 2000; Glatzel *et al.*, 2001). A 'domino mechanism' has been described, in which transported PrP^{Sc} entering a neuronal tissue acts as a template for the PrP^{C} expressed in that tissue, which then misfolds (Race, Oldstone and Chesebro, 2000; Glatzel *et al.*, 2001; Natale *et al.*, 2011). Moreover, the PrP^{Sc} could be transferred between nerves and into the CNS by retrograde transport (Bartz, Kincaid and Bessen, 2002). The analysis and understanding of PrP^{Sc} spread within the body may help to develop new therapeutic approaches and targets (Bradford, Crocker and Mabbott, 2014).

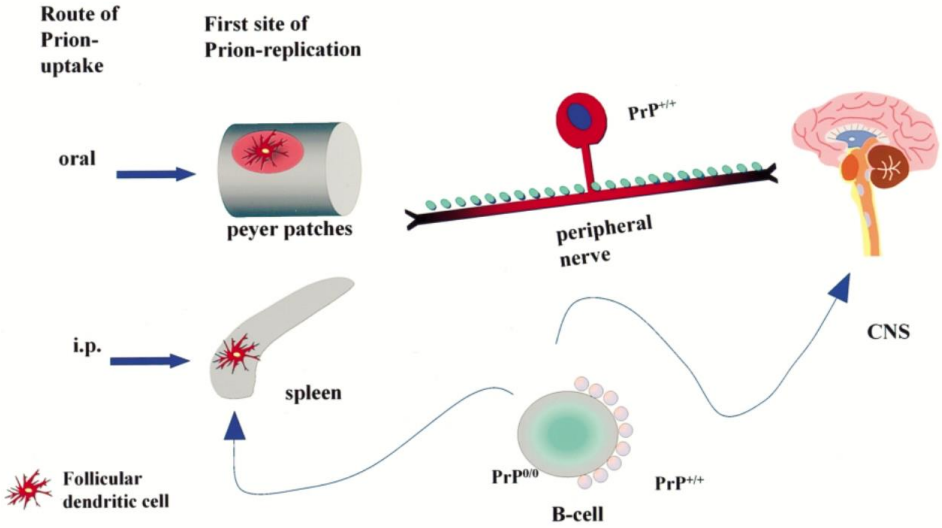

Figure 1.3.1. The PrP^{Sc} neuroinvasion route depends on the administration route. After oral administration, PrP^{Sc} is more likely to propagate within GALT, from where it spreads to the peripheral nervous system through peripheral nerves. Next, it enters the CNS. After intraperitoneal injection, B-cells were described to play a crucial part in the spread into the spleen and CNS. i.p. – intraperitoneal, CNS – central nervous system. Adapted from (Glatzel and Aguzzi, 2000) (licence nr 5064751273253).

1.3.2 Prion protein propagation

Analysis of the formation and structure of β-sheet rich prion protein aggregates is a challenge. As mentioned, the PrP^{Sc} aggregates are insoluble in detergents, heterogenic and the protein structure is fibrillar. Therefore methods based on NMR or X-ray crystallography were unsuccessful (Spagnolli *et al.*, 2019). However, methods like FTIR (Fourier-transform infrared) spectroscopy and CD (circular dichroism), showed that PrP^{Sc} is characterised by high beta sheet content but details of the fibril formation process were still unknown (Requena and Wille, 2014). One of the crucial methods for visualising PrP^{Sc} is electron microscopy with some structure modelling (Requena and Wille, 2014). Using both, cryo-electron microscopy and structural analysis, a 4-rung β-solenoid model was described with two types of parallel β-helical folds the right- and left-handed β-helices (Wille *et al.*, 2002; Govaerts *et al.*, 2004; Vázquez-Fernández *et al.*, 2016). Left-handed β-helices **(Figure 1.3.2, A)** are formed by triangular rungs with usually 18 residues per rung and each triangle made of six residues. Then, parallel rungs can trimerize **(Figure 1.3.2, B and C)** where the three monomers assemble together at the β-sheet level. Moreover, the α-helices and glycans attached to the PrP structure are located outside the main fibril core. In comparison to left-handed β-helices, right-handed β-helices are described as larger in diameter and much less regular. In addition to that, each rung in right-handed β-helices could be formed from 22 to 25 residues (Govaerts *et al.*, 2004). In both kinds of β-helices, when the whole rung is formed, the most lower or upper parts can act as a 'sticky surface' and template for the unfolded prion proteins **(Figure 1.3.3)** (Wille and Requena, 2018). Furthermore, the differences in amino acid compositions on the rungs can cause many variations in the whole fibril structure, that could be the source of different prion strains (Wille and Requena, 2018). In addition, a different model of PrP^{Sc} structure – PIRIBS (parallel in-register intermolecular β-sheet) was also described, however this model is not entirely consistent with structural analysis data (Wickner *et al.*, 2018; Baskakov *et al.*, 2019). These proposed mechanisms of prions conversion are crucial for any structural therapeutic approaches that targets the misfolding process and PrP^{Sc} accumulation in the nervous tissue (Spagnolli *et al.*, 2019).

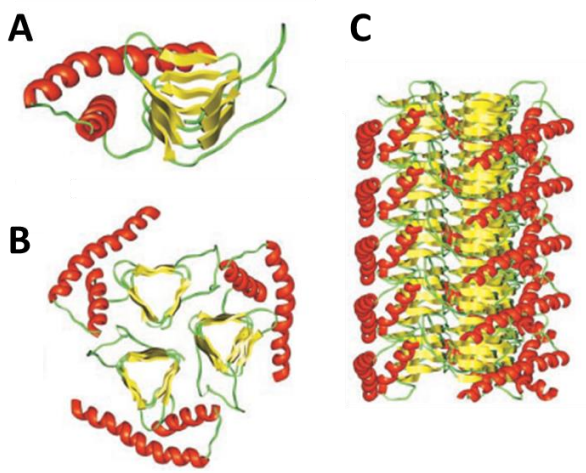

Figure 1.3.2. Modelling of the 87-174 residues of PrP27-30. **A** – monomeric model of PrP27-30. **B** – Trimeric model of PrP27-30 monomers with α-helices located outside the main structure. **C** – PrP27-30 fibre model. Adapted from (Govaerts *et al.*, 2004) (Copyright (2004) National Academy of Sciences, U.S.A.).

Whether the PrP^{C} conversion occurs on the cell membrane or during protein transport is still poorly understood, however, a two-step seeded polymerization mechanism was described for PrP^{C} conversion. In the first part, PrP^{Sc} aggregates – 'seeds' - bind PrP^{C} and in the second step, PrP^{C} undergoes structural changes and is converted into PrP^{Sc}. In the 4-rung β-solenoid model, structure extension is provided by the lowermost or/and the uppermost rungs. These can act as a template for the unstructured or structured PrP^{C}. Arriving cellular PrP^{C} would interact with β-solenoid structure, create or change its conformation and self-template into a β-sheet rich molecule **(Figure 1.3.3)** (Wille and Requena, 2018). The PrP^{Sc} aggregates and fibrils then accumulate within the cell or extracellularly, usually within the CNS or lymphoid tissue (Moore, Taubner and Priola, 2009).

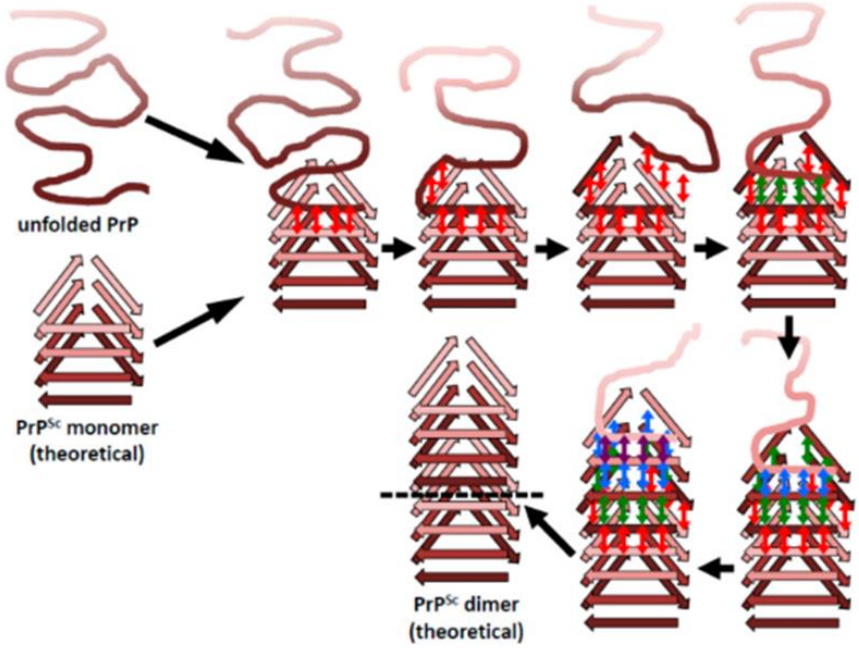

Figure 1.3.3. Schematic PrP^{Sc} fibril extension with the approaching unfolded PrP^{C}. This model shows only the uppermost rung extension, whereas additional extension from the lowermost rung has been proposed. The incoming unstructured PrP^{C} molecule links to the β-solenoid structure and mimics the β-sheet rich configuration. Adapted from (Wille and Requena, 2018) (licence under the CC by 3.0).

1.4 Mutations and polymorphisms within the *Prnp* gene

Various mutations within the human prion protein gene can cause inherited prion diseases such as GSS, FFI and fCJD. Mutations within the *PRNP* gene usually include point mutations, where a single nucleotide is substituted and results in an amino acid change within the protein sequence. Other types of mutation found in the *PRNP* gene are insertion or deletion mutations usually within the OR region. In FFI, a mutation causing the change from aspartic acid (D) into asparagine (N) at position 178 in human PrP is thought to determine the disease (Medori *et al.*, 1992; Medori and Tritschler, 1993). Also, other missense mutations are associated with GSS. These include substitutions at different positions alongside the protein chain as well as insertion of the larger octapeptide fragments into the peptide chain (Hsiao *et al.*, 1989, 1992; Kitamoto, Lizuka and Tateishi, 1993; Laplanche *et al.*, 1999). Similarly, fCJD was correlated with single amino acid changes in the protein sequence and addition of octapeptide repeats (Goldfarb *et al.*, 1991; Kitamoto, Lizuka and Tateishi, 1993; Peoc'h *et al.*, 2000). In addition, polymorphisms were described within the prion protein amino acids sequence. These changes, in comparison to genetic mutations, are sequence variations that are common in the population. As a result, polymorphisms in both human and animal PrP do not lead to the prion diseases directly, however they may determine the possibility of developing a prion disease as they can determine susceptibility to the acquired

disease (Belt *et al.*, 1995; Acevedo-Morantes and Wille, 2014). The most common polymorphism in the human gene is an amino acid change at codon 129. Here, the methionine (M) is substituted with valine (V) (Mead, 2006). Both, V/V and M/M homozygotes are over-represented in sporadic and iatrogenic CJD, whereas the M/V patients are described to have a level of resistance for these diseases. In variant CJD most cases were represented by 129 M/M with only one case reported recently being M/V (Mastrianni, 2010; Brown *et al.*, 2012; Acevedo-Morantes and Wille, 2014; Mok *et al.*, 2017). In contrast, polymorphism at position 219, where glutamate (E) is substituted with lysine (K), correlates with a resistant genotype for sporadic CJD (Acevedo-Morantes and Wille, 2014). Heterozygotes E/K were found to be underrepresented in sporadic CJD cases (Shibuya *et al.*, 1998). In addition, both E/K and K/K patients could have an increased susceptibility to vCJD (Kobayashi *et al.*, 2015).

Similar to in humans, polymorphisms in animal *Prnp* genes can influence susceptibility to acquired prion diseases. A well-studied example is sheep where distinct *Prnp* genes have an impact on scrapie. These variations include a codon change at positions 136 (alanine in valine), 154 (arginine in histidine) and 171 (glutamine in arginine/histidine), abbreviated as ARQ, ARR, ARH, VRQ *etc*. (Belt *et al.*, 1995; Goldmann, 2008). ARR genotypes are associated with the highest disease resistance, whereas the VRQ genotype is correlated with disease susceptibility (Goldmann *et al.*, 1994). These amino acid substitutions are the most commonly found, however other rare mutations at these positions have been reported *e.g.* T (threonine) instead of A/V at position 136, leucine (L) at position 154 and lysine (K) at position 171 (Billinis *et al.*, 2004; Goldmann, 2008). However, these amino acid changes were not correlated to increased or decreased disease susceptibility (Billinis *et al.*, 2004). Polymorphisms in goat PrP in relation to classical scrapie have also been described. In contrast to sheep PrP, the goat prion protein sequence is not polymorphic at 136 position, but the presence of histidine (H) at position 154 was described to have an impact on atypical scrapie development (Benestad *et al.*, 2008; Mead, Lloyd and Collinge, 2019). Furthermore, the most studied polymorphisms in caprine PrP include changes at 222 position (Q/K) and N to S or D at 146 position. These changes are correlated to scrapie resistance in European populations of goats (Acutis *et al.*, 2006; Goldmann *et al.*, 2011; Papasavva-Stylianou *et al.*, 2011). In addition, a change at position 32 that translates into a stop codon has been described as natural in Norwegian Dairy Goats. This results in the presence of animals naturally lacking PrP (Benestad *et al.*, 2012). In compare to ovine and caprine, the bovine prion protein sequence displays less alterations, with the most common change being alterations within the octapeptide repeats number (Goldmann, 2008). Moreover, a deletion or an insertion of a 12 or 23 base pair sequence in the *Prnp* gene promoter was recognised and corelated to susceptibility to BSE (Sander *et al.*, 2004). Lastly, PrP polymorphisms that have an impact on CWD development were described. In elk, a change at position 132, where methionine is replaced with leucine was reported. This position corresponds to human 129 codon and research showed that

homozygotes M/M at 132 codon correlates with susceptibility to CWD in both farmed and wild Rocky Mountain elk and wapiti (O'Rourke *et al.*, 1999; Perucchini *et al.*, 2008). Moreover, three other polymorphic positions (95, 96 and 116) were described in white-tailed deer, where histidine, serine and glycine, respectively, were in the minority for CWD cases (Mead, Lloyd and Collinge, 2019).

1.4.1 Prion strain concept

Many different factors can lead to phenotypic variation between different prion diseases such as scrapie, BSE, CJD and also between distinct prion isolates within some of these diseases. Two possible mechanisms were described for the generation of 'new' prion strain that differs from the original PrP^{Sc} **(Figure 1.4.1)**. Firstly, the cloud hypothesis reports that the single prion strain consists of multiple PrP^{Sc} conformers. Only a subgroup of these PrP^{Sc} conformers would develop within the new host and environment, therefore creating a new prion strain. Secondly, the deformed template theory hypothesised that none of the present conformers could adapt in the new environment leading to production of novel PrP^{Sc} derived from the original strain that would fit to the new host (Makarava and Baskakov, 2013). These two hypotheses are not exclusive, and both could participate in the emerge of new prion strains. Moreover, these explain the difference in prion diseases phenotypes. When these become stable over multiple transmissions within the same host they are known as prion strains (Collinge *et al.*, 2007; Makarava and Baskakov, 2013). Moreover, these variations are being considered as biochemical changes and are not caused by genetic background (Murdoch and Murdoch, 2015). To analyse different variants, prion diseases were usually transmitted to rodent models. After the first transmission, incubation periods were usually long, however after subsequent passages within the same species and the same genetic background, some phenotypic changes, incubation times and other disease features stabilised (Gough, Rees, *et al.*, 2015). So far, the best described rodent model for prion strain typing is mice. However, there are some drawbacks to this approach. These include the facts that many animals are required, the disease incubation periods are long and it is very difficult to determine the infection efficiency (Thackray *et al.*, 2008). Furthermore, there are cases of both classical (*e.g.* ARQ/ARQ and ARQ/VRQ genotypes) and atypical scrapie, that cannot be transferred into specific mouse lines (Bruce *et al.*, 2002; Thackray, Hopkins, *et al.*, 2012). Recently, a bank vole model was described for TSE bioassays. In comparison to the mouse models, bank voles show susceptibility to all tested scrapie isolates, sporadic and familial CJD, BSE and CWD (Cartoni *et al.*, 2005; Nonno *et al.*, 2006; Agrimi *et al.*, 2008; Di Bari *et al.*, 2008, 2013; Watts *et al.*, 2014). They also display much shorter incubation times, therefore bank voles are thought to be the most universal prion acceptor (Watts *et al.*, 2014). The only TSE that shows lower transmission levels in bank voles is Variable Protease-Sensitive Prionopathy (Nonno *et al.*, 2019). Overall, prion strain typing bioassays in mammalian species require time, ethical consideration and are very costly. Therefore,

other methods or hosts need to be developed in order to reduce the use of animals, time of experiments and financial requirement. Recent studies showed that *Drosophila melanogaster* – fruit fly – can be used in a prion bioassay. The fruit fly was engineered to express ovine PrP and after oral exposure showed phenotypic changes characteristic for prion diseases like reduction of locomotion. One of the major features of this model is that fruit fly species multiply very quickly and the organism's genetics is well known (Thackray, Muhammad, *et al.*, 2012). However, all models based on non-mammalian species need to be considered carefully as whist they can demonstrate PrP pathology and could be used for transmission studies, the use of rodent models still allows more complex analysis and disease type differentiation (Younan *et al.*, 2018). In addition, recent studies showed that *Drosophila* flies have been engineered to express rodent PrP with human FFI or fCJD mutations and this approach allowed comparison of the mutations' effects on the flies. These tools could be potentially used to discover new prion diagnostic markers or therapeutics (Thackray *et al.*, 2017).

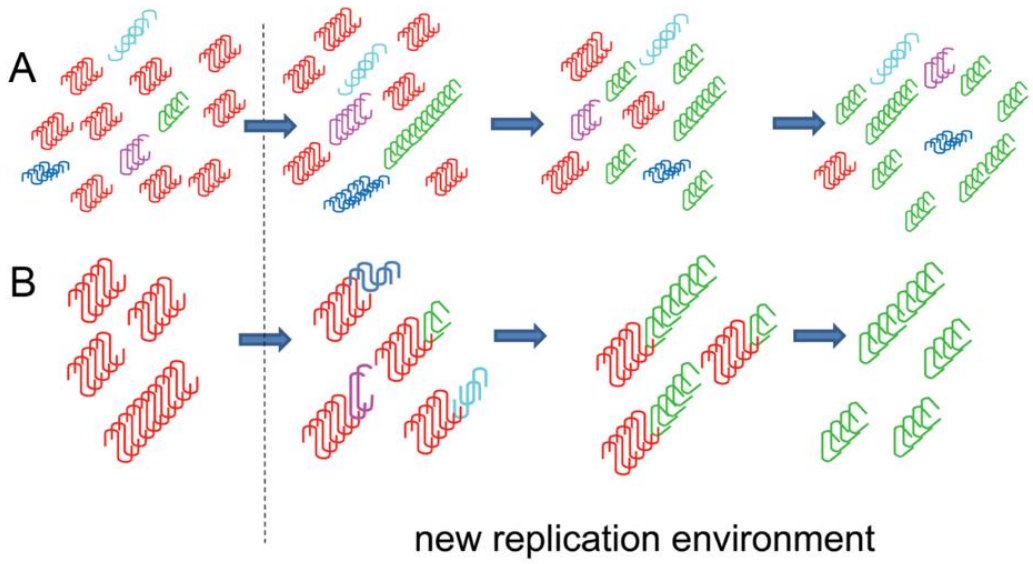

Figure 1.4.1. The cloud and deformed templating hypotheses. **A** – The cloud hypothesis the demonstrates that the single prion strain consists of multiple PrP^{Sc} conformers (shown in different colours). Only a subgroup of these PrP^{Sc} conformers would develop within the new host and environment. **B** – the deformed template theory presents that none of the PrP^{Sc} conformers adapt in the new host environment leading to production of novel PrP^{Sc} derived from the original isolate. Adapted from (Makarava and Baskakov, 2013) (licence under the CC by 3.0).

Other than animal bioassays, biochemical prion strain typing assays have been developed. Biochemical analysis uses the PK cleavage and glycosylation patterns of PrP^{Sc} on western blotting (Cobb and Surewicz, 2009). The glycosylation patterns are compared between different TSE isolates using an antibody that binds to the protease-

resistant core region of PrP. An example is the differentiation of scrapie and BSE in sheep. In addition, the molecular weight of the lower, un-glycosylated band in scrapie is higher than that for BSE and can be used in diagnosis. Also, the highest, di-glycosylated band, is more abundant in BSE than in scrapie (Hill *et al.*, 1998; Stack, Chaplin and Clark, 2002; Thuring *et al.*, 2004; Jacobs *et al.*, 2011). In another example, the atypical forms of scrapie show 4 bands on the western blotting and these bands have lower molecular weights when compared to classical scrapie cases (Arsac *et al.*, 2007). Moreover, thermolysin (a thermostable protease) has also been applied in biochemical strain typing methods as an alternative to PK. The digestion pattern for this protease also allowed the differentiation of scrapie and BSE. In addition, the analysis was not affected by scrapie type or host genotype (Owen *et al.*, 2007). Further tests involve the use of PK digestion followed by prion protein core antibody detection alongside monoclonal P4 antibody detection. The latter binds to an epitope situated near the N-terminus of PrP that is partially or completely lost following digestions of BSE PrP^{Sc} with PK, but is retained in scrapie PrP^{Sc}. From western blotting analysis, the core antibody:P4 western blot signal ratios were lower for BSE compared to classical scrapie cases (Stack, Chaplin and Clark, 2002; Jeffrey, González, *et al.*, 2006). It has been noted that some scrapie cases were hard to differentiate using the methods mentioned above. One of the most difficult isolates to differentiate from BSE was an experimental scrapie isolate maintained in sheep – CH1641 (Foster and Dickinson, 1988). Recently, a method that uses serial *in vitro* prion replication (a method called protein misfolding cyclic amplification, PMCA) allowed the differentiation of ovine BSE from CH1641. After 5 days of *in vitro* amplification with alternating PrP^{C} substrates AHQ/AHQ and VRQ/VRQ, only BSE PrP^{Sc} was amplified and not CH1641 or any of the atypical or classical scrapie isolates tested. The main feature of this method is that it substitutes the use of animal model in the assay and allows to differentiate between two very closely related prion strains (Taema *et al.*, 2012). Additionally, alternative to PMCA method – real time quaking induced conversion (RT-QuIC) – was described for prion propagation and was also used in prion strain typing experiments for human and animal TSEs (Orrú, Groveman, *et al.*, 2015; Masujin *et al.*, 2016; Levavasseur *et al.*, 2017).

Alternative methods for identifying prion strains within ruminants use immunohistochemical (IHC) examination of tissues. 'PrP^{Sc} profiling' is a method that uses antibodies against specific PrP domains to determine intra- and extra-cellular locations of PrP^{Sc} within a brain tissue (González, Martin and Jeffrey, 2003; González *et al.*, 2005). Moreover, 'PrP^{Sc} epitope mapping' applies antibodies to define specific epitopes across the PrP^{Sc} length within the brain and LRS cells and in extracellular matrix (Jeffrey, González, *et al.*, 2006). The use of antibodies in PrP^{Sc} profiling and epitope mapping was used to determine different morphological types of PrP^{Sc}, association with cells type and levels of PrP^{Sc} accumulation within multiple neuroanatomical sites. Based on these features both methods helped with distinguishing between scrapie and BSE cases (Jeffrey *et al.*, 2001; Jeffrey, Martin, *et al.*, 2006).

Methods based on prion stability analysis have also been proposed. These involve conformational stability assays (CSA) and conformation-dependent immunoassay (CDI). The main feature of these methods is to monitor changes in protease resistance (CSA) or epitope accessibility during a process that incrementally denatured PrP^{Sc} (CDI) (Safar *et al.*, 1998; Peretz, 2001).

The presence of many different prion strains has been determined by distinct disease phenotypes within the same host species. However, the variations seen were explained as being due to different conformations of PrP^{Sc} aggregates rather than the presence of other factors that might determine the prion strain features (Cobb and Surewicz, 2009). Therefore, the findings regarding the differences between prion isolates still fully supports the prion-only hypothesis developed by Prusiner (Prusiner, 1998).

1.5 Methods used in TSE research for prion protein amplification

1.5.1 Protein misfolding cyclic amplification

Protein misfolding cyclic amplification (PMCA) is a technique which facilitates the conversion of cellular PrP^{C} into the protease resistant PrP^{Sc} *in vitro*. PMCA was developed by Saborio *et al.* (Saborio, Permanne and Soto, 2001). In this method, the PrP^{Sc} acts as a template for the cellular prion protein, and the conversion is fully dependent on the presence of the misfolded PrP^{Sc}. This *in vitro* protein replication method is thought to simulate the exact process of PrP^{Sc} formation found *in vivo* and can faithfully replicate prion infectivity. The reaction consists of two steps: incubation, which allows the formation of protein aggregates, and sonication, which break down the aggregates into oligomers. Every created oligomer can then act as a template for further seeding of aggregation **(Figure 1.5.1)**. Moreover, the properties of newly synthesised PrP^{Sc} through PMCA are the same as for the PrP^{Sc} found in TSE affected brains – they are proteinase K resistant, insoluble in detergents and infectious in rodent bioassays (Saborio, Permanne and Soto, 2001; Shikiya and Bartz, 2011). PMCA is a very useful tool in prion disease research and there are now many examples that it can be used for prion protein detection in brain tissue, secreta or excreta *e.g.* urine, blood, faeces, milk or saliva, elk antler velvet or deer semen and reproductive system tissues (Castilla *et al.*, 2005; Maddison, Whitelam and Gough, 2007; Murayama *et al.*, 2007; Angers *et al.*, 2009; Krüger *et al.*, 2009; Maddison *et al.*, 2009; Gough and Maddison, 2010; Maddison, Baker, *et al.*, 2010; Kramm *et al.*, 2019). Moreover, the PMCA method was also been used for the detection of a wide range of animal and human prion types including vCJD, FFI, scrapie, CWD and classical and H-type BSE from brain homogenates and other tissues (Saá, Castilla and Soto, 2006; Maddison, Whitelam and Gough, 2007; Gough, Bishop and Maddison, 2014; Redaelli *et al.*, 2017; Barria *et al.*, 2018; Kramm *et al.*, 2019). In addition, PMCA was also used to differentiate between experimental BSE and the BSE like scrapie isolate CH1641 – an isolate that shares BSE-like biochemical properties but is not transmissible to mice (Jeffrey, González, *et al.*, 2006;

Taema *et al.*, 2012). However, despite many attempts there are no evidence that sCJD could be amplified and detected using PMCA (Giaccone and Moda, 2020).

PMCA was developed for the misfolding of prion protein but it has also been used for α-synuclein (α-syn) or tau fibril formation. Production of α-syn fibrils is a slow and variable process but applying the PMCA method increased the speed of this process. Moreover, the generated α-synuclein aggregates had the same biophysical and biochemical features as α-synuclein fibrils produced *in vivo* (Herva *et al.*, 2014; Jung *et al.*, 2017). Also, PMCA can be used to convert the monomeric tau into long filaments of protein aggregates (Meyer *et al.*, 2014).

1.5.2 Real time quaking induced conversion

RT-QuIC is a variant of the PMCA technique, where instead of a sonication step, intensive shaking is used, and a Thioflavin T (ThT) fluorescence assay monitors in real time amyloid formation, as opposed to western blot analysis of protease-resistant protein **(Figure 1.5.1)**. Shaking breaks down the formed PrP aggregates into multiple reactive seeds (Kang *et al.*, 2017). RT-QuIC was firstly used by Atarashi and co-workers who found this method to be easier and faster to perform than standard PMCA (Atarashi, Sano, *et al.*, 2011). They used recombinant PrP (rPrP) as a substrate for resistant prion protein formation when seeded with hamster cerebrospinal fluid (CSF) derived prions (Atarashi *et al.*, 2008). Later, human peripheral tissues and sheep CFS were used as seed. QUIC allowed the correct differentiation between healthy and disease samples (Orrú *et al.*, 2009). Next, RT-QuIC has been used to detect prion protein in sCJD cases. Atarashi *et al.* detected the PrP^{Sc} in 14 out of 16 (87.5 %) CJD cases, while none of the negative samples showed elevations in ThT fluorescence (Atarashi, Satoh, *et al.*, 2011). Based on these results, two international and independent trials of PrP^{Sc} detection from CJD cases using patients CFS were run and all laboratories correctly identified all positive cases (McGuire *et al.*, 2016). Moreover, obtaining some biopsy materials from patients is a complicated and invasive process. Therefore, research into finding less invasive procedure of collecting tissues was investigated. For example, Orru and co-workers tested whether RT-QuIC could be used to determine sCJD prion protein presence in the olfactory epithelium. Testing materials were obtained from patients by a nasal brushing procedure and RT-QuIC analysis was found to be sensitive and accurate for PrP^{Sc} detection (Orrú *et al.*, 2014). Furthermore, other human prion diseases like familial CJD, GSS, and FFI were detected through RT-QuIC with high sensitivity (Sano *et al.*, 2013). In addition, this method has also been applied for the recognition of animal prion diseases. Orru *et al*. used cattle brain homogenates from classical (C-BSE) and atypical forms of BSE. They detected and even distinguished between different types of BSE using RT-QuIC (Orrú, Favole, *et al.*, 2015). Moreover, the use of RT-QuIC in deer infected with CWD has been described and the technique allowed the detection of prion even before clinical signs appeared (Hoover *et al.*, 2017). There is also evidence of positive disease recognition from samples collected ante-mortem and post-mortem from

deer and elks. These include analysis of faeces, saliva, recto-anal mucosa-associated lymphoid tissue (RAMALT), nasal brush samples, urine, CSF and lymph nodes (Haley *et al.*, 2013, 2014, 2016; Henderson *et al.*, 2013; John, Schätzl and Gilch, 2013; Cheng *et al.*, 2016).

Even though the RT-QuIC method was first described for prion diseases, a similar assay was developed for α-synuclein detection in CSF for other protein misfolding diseases like dementia with Lewy bodies (DLB) and Parkinson's Disease (PD) (Fairfoul *et al.*, 2016; Sano *et al.*, 2017).

All described cases of using RT-QuIC show high specificity and sensitivity for both animal and human protein misfolding disease. Its further development has the potential to deliver a powerful, *ante-mortem* diagnostic tool and can also help with disease surveillance. However, RT-QuIC products have not been shown to be infectious in an animals *in vivo* assays so the method may have less applications for screening for therapeutics or in understanding prion infectivity (Groveman *et al.*, 2017; Haley and Richt, 2017).

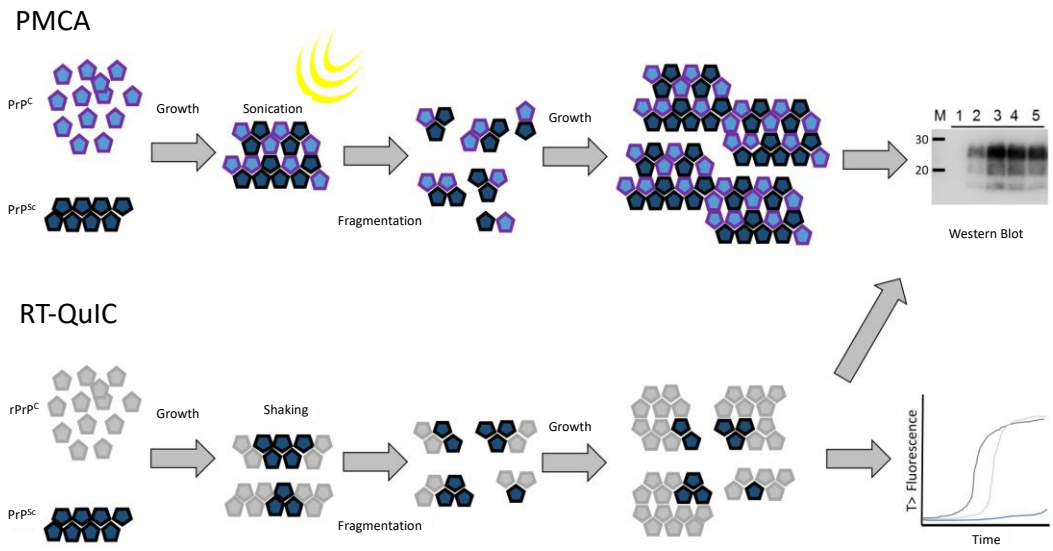

Figure 1.5.1. Comparison between PMCA and RT-QuIC. PMCA (top) involves incubation and sonication cycles. In this method, PrP^{Sc} interacts with PrP^{C} and converts it into PrP^{Sc} aggregates. Sonication breaks the aggregates into smaller oligomers, which then act as seeding nuclei over the next incubation step. RT-QuIC (bottom) is analogous to PMCA but it uses shaking instead of sonication to break the PrP^{Sc} aggregates. While PMCA formed PrP^{Sc} aggregates are protease resistant and usually detected by western blotting, QUIC formed amyloid fibrils are detected in real time by ThT binding and fluorescence. Adapted from (Gough, Rees, *et al.*, 2015) (licence under the CC by 4.0).

1.6 Cell culture models for prion diseases

Prion disease bioassays in rodents are an extremely useful tool to determine the prion strain type, infectivity rates and titres, although they are slow and require the use of many animals (Neale *et al.*, 2010). Therefore, research into TSE infection permissive cells lines have been extensively investigated. The use of cell models increases the speed of infection and disease incubation. Moreover, PrP^{Sc} infected cell lines help to investigate the cell-cell spreading mechanisms of PrP^{Sc}, prion protein metabolism and also to characterize prion strains (Harris, 1999; Solassol, Crozet and Lehmann, 2003). Furthermore, cell culture methods also allow the analysis of PrP^{C} and PrP^{Sc} levels and infection rates. In addition, cell culture models can also be used for faster therapeutic compound screening or finding possible infection markers with the highest physiological and diagnostic gain (Solassol, Crozet and Lehmann, 2003). Moreover, it was investigated whether, strain characteristics change with cell model multiplications. Analysis using different murine strains and several cell lines, as well as RK13 cells with murine, ovine and vole derived strains showed that clinical signs, incubation rates and brain vacuolation patterns remain unchanged with cell multiplication (Birkett *et al.*, 2001; Arjona *et al.*, 2004; Arima *et al.*, 2005; Courageot *et al.*, 2008). Furthermore, cell lysates were shown to be infectious to transgenic mice bioassays (Vorberg *et al.*, 2004). Whilst a single cell line is able to propagate more than one strain (Vilette, 2008) a limitation of the reported models is that not all prions strains/isolates can infect the cell lines (van der Merwe *et al.*, 2015).

1.6.1 Cell models for animal prion diseases

The first successful attempt to infect the mouse neural cell line – SMB – was carried out in 1970. The cells were inoculated with mouse adapted scrapie Chandler strain (Clarke and Haig, 1970). Later, infection of mouse neuroblastoma cells – N2a - with scrapie was described and N2a cells remain one of the most intensively studied and used models for prion infections (Race, Fadness and Chesebro, 1987; Vilette *et al.*, 2001). Since then, both neural and non-neural cell lines have been found to be susceptible to prions and to be able to maintain prion infection **(Table 1.6.1)** (Solassol, Crozet and Lehmann, 2003). Moreover, it was also found that mouse prions could be successfully transmitted into cells from different species. For example, in 1984 the rat cell line PC12 was infected with mouse adapted scrapie prion strain 139A (Rubenstein, Carp and Callahan, 1984). In addition, rodent adapted prion isolates were found to propagate in mouse fibroblast cell line NIH/3T3 and gave high levels of PrP^{Sc} post infection and after multiple passages. Moreover, cerebellar granule neurons (CGN) isolated from transgenic mice expressing ovine, hamster or murine PrP were found to be susceptible and propagate sheep, hamster and murine TSE isolates, respectively (Cronier *et al.*, 2007). In addition, the rabbit epithelial cell line RK13 cells were engineered to express different species PrP^{C} in a doxycycline induced manner (Vilette *et al.*, 2001; Courageot *et al.*, 2008). When mouse or bank vole PrP^{C} was expressed in these cells, the cell cultures were permissive

to different prion isolates including mouse adapted scrapie and vole adapted ovine BSE (Courageot *et al.*, 2008).

Vilette *et al.*, presented transgenic RK13 cells as an infection model with sheep scrapie, not previously adapted to rodents (Vilette *et al.*, 2001). The RK13 cell line variant Rov9 was engineered with doxycycline regulated expression system for ovine PrP (VRQ type) (Vilette *et al.*, 2001). Later, it was found that Rov9 cells are also permissive and maintain the infection of other natural scrapie isolates (Neale *et al.*, 2010). Moreover, a Schwann cell like line – MovS – was isolated from transgenic mice expressing ovine VRQ (Archer *et al.*, 2004). This cell line was found to be permissive to many natural scrapie isolates and in addition, infected MovS cells propagated infectivity as measured by mouse bioassays (Archer *et al.*, 2004; Neale *et al.*, 2010).

In addition to natural and rodent adapted scrapie isolates, other TSEs have been propagated in cell cultures. Tark *et al.*, exposed the MDBK (Madin-Darby Bovine Kindey) cells to natural BSE brain homogenate. MDBK cells were engineered to overexpress bovine PrP^C using the lentivirus expression system and these cells maintained the BSE infection (Tark *et al.*, 2015). After transmission to mice, BSE infected cells showed similar brain lesion profiles to that observed in cattle C-BSE however they differed slightly in their biochemical features (Suh *et al.*, 2017). Moreover, a brain derived MDB (mule deer brain) cell line has been successfully infected with CWD. Microsomes from CWD infected brain homogenates were shown to infect cells and the infection rates were stable over passages (Raymond *et al.*, 2006). In addition, differentiated neurosphere cultures derived from mouse brain cells expressing the elk PrP^C were successfully infected with non-adapted CWD (Iwamaru *et al.*, 2017). In addition, new approach of engineering murine cells to express bank vole PrP^C was proposed to increase their susceptibility to prion infection (Walia *et al.*, 2019). As mentioned before, bank vole PrP was found to be the most susceptible to conversion within the range of tested species, therefore this model may help to establish and analyse other prion strains' infections in cell cultures (Watts *et al.*, 2014; Walia *et al.*, 2019). In addition, 33 different cell lines were challenged with different natural and experimental scrapie and BSE isolates. These cells lines were chosen from a eukaryotic species bank of Veterinary Medicine cell lines (Collection of Cell Lines in Veterinary Medicine – CCLV). The final 33 cell lines derived from different age and tissues of cattle, sheep, goat, mink, cat, wild and domestic pig, deer, human, hamster, rabbit and mouse. Among them, the bovine derived MDBK-PES cell line was infected with natural scrapie but not BSE. In addition, this study provided the first evidence showing infection and propagation of ARQ/ARQ natural scrapie in cell culture models, as previously VRQ homozygotes or ARR/VRQ isolates were shown to be infectious (Oelschlegel *et al.*, 2015).

Table 1.6.1. Neural and non-neural cell lines susceptible to prion infection. Adapted from (Grassmann *et al.*, 2013; van der Merwe *et al.*, 2015), modified.

Cell line	Cell line origin	Species	Infecting Prion Strain		References
			Human	Animal	
Neural					
SMB	Mesodermal cells	Mouse	-	Mo-Scrapie (Chandler, 22F, 79A)	(Clarke and Haig, 1970; Birkett *et al.*, 2001; Kanu *et al.*, 2002)
N2a	Neuroblastoma cells	Mouse	-	Mo-Scrapie (RML, 22L, Chandler, 139A)	(Taraboulos *et al.*, 1990; Nishida *et al.*, 2000; Alais *et al.*, 2008; Abdulrahman *et al.*, 2017; Thapa *et al.*, 2018; Bourkas *et al.*, 2019)
GT1	Hypothalamic cells	Mouse	mo-CJD mo-GSS, kuru	Mo-Scrapie (RML, Chandler, 139A, 22L)	(Schatzl *et al.*, 1997; Nishida *et al.*, 2000; Arjona *et al.*, 2004; Arima *et al.*, 2005; Miyazawa, Emmerling and Manuelidis, 2011)
SN56	Cholinergic septal neuronal cells	Mouse	-	Mo-Scrapie (Chandler)	(Baron *et al.*, 2006)
PC12	Pheochromocytoma cells	Rat	-	Mo-Scrapie (139A)	(Rubenstein, Carp and Callahan, 1984; Rubenstein *et al.*, 1991)
Mov-S	Neuroglia cells	Mouse	-	Ov-Scrapie (PG127, field isolates)	(Archer *et al.*, 2004; Neale *et al.*, 2010)
MDB	Brain cells	Deer	-	CWD	(Raymond *et al.*, 2006)
SH-SY5Y	Neuroblastoma cells	Human	sCJD brain	-	(Ladogana *et al.*, 1995)
CAD5	Neuronal tumor cells	Mouse	-	CWD, Mo-scrapie (22L, RML, 79A, Me7) Mo-BSE (301C)	(Mahal *et al.*, 2007; Abdulrahman *et al.*, 2017; Bourkas *et al.*, 2019; Walia *et al.*, 2019)
MSC 80	Schwann cells	Mouse	-	Mo-Scrapie (Chandler)	(Follet *et al.*, 2002)
NSC	CNS stem cells	Mouse	-	Mo-Scrapie (22L)	(Milhavet *et al.*, 2006)
iPSC	Induced pluripotent stem cells derived astrocytes	Human	sCJD and	-	(Krejciova *et al.*, 2017;

			vCJD brains		Groveman *et al.*, 2019)
CGN	Cerebellar granule neurons	Mouse	sCJD, iCJD, vCJD	Mo-scrapie (139A, 22L, ME7), Ha-scrapie (Sc237, 139H), Ov-scrapie (127S)	(Cronier *et al.*, 2007; Hannaoui *et al.*, 2014)
Non-neural					
RK13 (expressing mouse, ovine (Rov9), bank vole, elk (RKE) PrP^C)	Kidney epithelial cells	Rabbit	Mo-GSS, Mo-sCJD	Mo-Scrapie (Chandler, 22L, ME7), Ov-scrapie (field isolates), CWD	(Vilette *et al.*, 2001; Vella *et al.*, 2007; Courageot *et al.*, 2008; Lawson *et al.*, 2008; Bian *et al.*, 2010; Neale *et al.*, 2010)
NIH/3T3	Fibroblasts	Mouse	-	Mo-Scrapie (22L)	(Vorberg *et al.*, 2004)
L929	Fibroblasts	Mouse	-	Mo-Scrapie (22L, RML, ME7)	(Vorberg *et al.*, 2004; Mahal *et al.*, 2007; Grassmann *et al.*, 2013)
C2C12	Myoblasts	Mouse	-	Mo-Scrapie (RML, 22L, ME7)	(Herbst *et al.*, 2013)
MEF	Embryonic fibroblasts	Mouse	-	CWD, Mo-scrapie (22L)	(Abdulrahman *et al.*, 2017; Walia *et al.*, 2019)
MSC-L	Mesenchymal stromal cells	Mouse	Mo-vCJD, Mo-GSS	-	(Cervenakova *et al.*, 2011)
MDBK (MDBK-PES)	Kidney cells	Bovine	-	Scrapie, BSE	(Oelschlegel *et al.*, 2015; Tark *et al.*, 2015)
SP-SC	Spleen stromal cells	Mouse	Mo-vCJD Mo-GSS	-	(Akimov *et al.*, 2008)

Mo – mouse passaged
Ha – hamster passaged
Ov – ovine isolates

As well as their value in diagnostics, the use of cell culture models could help with the characterisation and understanding of the involvement of different nervous system cell types in prion propagation. Primary cell cultures may also allow the study of cell degeneration mechanisms after exposure to infectious prions. Cronier and co-workers analysed neurons and astrocytes after inoculation with scrapie. It was found that both cell types take part in PrP^{Sc} propagation and could be the primary replication site for prion proteins (Cronier, Laude and Peyrin, 2004).

1.6.2 Cell models for human prion diseases

The use of cell lines to model prion diseases has been established for a range of animal TSE isolates. Furthermore, some early reports demonstrated that sporadic CJD can infect human derived cell lines – neuroblastoma SH-SY5Y (Ladogana *et al.*, 1995). However, the use of this human cell line was never reported again for human TSE cell infection assays (Groveman *et al.*, 2019). Another human model susceptible for infection with sCJD brain was described more than 20 years later. In this study, the use of induced pluripotent stem cells (iPSC) was reported. The iPSC were differentiated into astrocytes and were able to replicate three different sCJD isolates (Krejciova *et al.*, 2017). Moreover, human iPSC can organise into structures called cerebral organoids and therefore can be used as a brain tissue model (Lancaster and Knoblich, 2014; Groveman *et al.*, 2019). These larger structures were also tested for permissiveness to sCJD prions and were found to be susceptible. This novel model gave new perspectives on prion disease modelling and might increase the understanding of PrP^{Sc} pathogenesis in brain tissue (Groveman *et al.*, 2019).

Furthermore, a RK13 cell variant expressing human PrP was described, however this attempt failed to propagate human PrP^{Sc} (Lawson *et al.*, 2008). In contrast, RK 13 cells expressing mouse PrP^{C} were found to propagate mouse passaged human GSS isolate – Fukuoka 1 (Courageot *et al.*, 2008). In addition, murine GT hypothalamic cells were found to be susceptible for infection with CJD. For these assays, 'slow' (SU) and 'fast' (FU) virulent Asian CJD isolates were used. Infections with both strains showed the presence of PrP^{Sc} after mutiple passages (Arjona *et al.*, 2004; Manuelidis *et al.*, 2007). Apart from sCJD isolates, a murine GT hypothalamic cell line has been shown to propagate vCJD and kuru PrP^{Sc} (Miyazawa, Emmerling and Manuelidis, 2011). Moreover, murine spleen-derived stromal cells were susceptible to 'fast' virulent strain of sCJD as well as a vCJD isolate (Akimov *et al.*, 2008).

Some primary cell cultures infected with human PrP^{Sc} have also been established. Cronier and co-workers demonstrated the use of a transgenic mouse model expressing human PrP^{C} as a source for primary neuronal cell line CGN (cerebellar granule neurons). The CGN cells were exposed to murine adapted CJD isolates and were found to be permissive (Cronier *et al.*, 2007). Later, the primary CGN cells were also found to be susceptible to brain homogenates of various human sCJD, vCJD and iCJD isolates (Hannaoui *et al.*, 2014).

1.6.3 PrP^{Sc} spread between cells in cell culture

Despite the availability of many different cell types that are permissive to prion infection, the cellular PrP^{Sc} transmission routes between cells are still being investigated (Mattei *et al.*, 2009). Firstly, research showed that PrP^{C} can be transferred between different cell lines *in vitro*. This used M17 cell line (human neuroblastoma) expressing the PrP^{C} and IA cells (human erythroleukemia) that lack PrP^{C}, grown in co-cultures. The study

also demonstrated that direct cell-to-cell contact was necessary for successful PrP^{C} uptake (Liu *et al.*, 2002). It was next established that as well as cellular prion protein being transferred between cells *in vitro,* PrP^{Sc} was also transferred. Prion infected cells were described that released the PrP^{Sc} and triggered the conversion of PrP^{C} into PrP^{Sc}. There are several described routes for the spreading of infectious prions between cells **(Figure 1.6.1)**, however the conversion of PrP^{C} into PrP^{Sc} seems to occur at the cell membrane level (Aguzzi and Lakkaraju, 2016; Vilette *et al.*, 2018). Cell-to-cell transmission may involve the use of membrane-bound extracellular vesicles (EV) like microvesicles or exosomes packed with PrP^{Sc}, tunnelling nanotubes (TNTs) and direct cell-to-cell contact (Aguzzi and Lakkaraju, 2016). Firstly, the role of exosomes, cytoplasmic organelles has been described. In general, exosomes are created within the cell in order to remove non-functional proteins from cells or mediate some cell functions (Vella *et al.*, 2008). Fevrier and co-workers analysed the scrapie prion infected Rov and Mov cells and found that infectious prions were present in culture media. Ultracentrifugation fractions were analysed and showed that PrP^{Sc} was linked with exosomes and this was confirmed by electron microscopy analysis. In addition, PrP^{Sc} contained within exosomes retained its infectivity in mouse bioassay (Fevrier *et al.*, 2004). Later, a range of cells types, RK13 expressing mouse PrP, GT1 hypothalamic cells, neuroblastoma N2a cells, dendritic cells and lymphocytes, were infected with different scrapie isolates and the secretion of PrP^{Sc} from cells was associated with exosomes (Vella *et al.*, 2007; Alais *et al.*, 2008; Castro-Seoane *et al.*, 2012; Coleman *et al.*, 2012). The involvement of microvesicles (MV) in intracellular prion transport has also been described. MVs are usually smaller than exosomes and are membrane-bounded structures displaying some adhesion molecules on their surfaces. Usually secreted by blood cells, platelets or endothelial cells, MVs were found to be carriers for PrP^{Sc} (Mattei *et al.*, 2009). After release of either exosomes or MVs into the extracellular matrix, the structures would form direct contact with other cells, fuse and insert the PrP^{Sc} into the cell (Caughey *et al.*, 2009; Guo and Lee, 2014).

Another possible route for transmission of PrP^{Sc} between cells are tunnelling nanotubes. These tubular structures are made from microtubules and F-actin (Ahmed and Xiang, 2011). Moreover, TNTs are formed *de novo* in order to provide a transfer route between cells (Rustom *et al.*, 2004). TNTs are packed with cytoskeletal and motor proteins and can transport cell organelles, membrane vesicles and also nucleic acids, calcium cations, proteins and even pathogens (Gerdes and Carvalho, 2008; Sisakhtnezhad and Khosravi, 2015). Research using the fluorescent labelling of PrP^{C} and live cell imaging showed that tunnelling nanotubes transport cellular prion protein between murine neuron like cells (CAD cells) *in vitro*. Furthermore, TNTs could mediate the transfer of fluorescently labelled infectious prion between dendritic cells (DC) and neurons. TNTs were formed after overnight incubation and PrP^{Sc} was transported between DC and CAD cells *in vitro* (Gousset *et al.*, 2009). Moreover, a possible TNT mediated transfer for prion proteins

was also described between astrocyte–astrocyte, and astrocyte–neuron pathways (Victoria *et al.*, 2016).

The third mechanism for PrP^{Sc} transport is through direct cell-to-cell contact. Kanu and co-workers used SMB cells infected with mouse adapted scrapie and showed that propagation of infectious prions is possible through direct cell-cell contact. Furthermore, no membrane associated PrP^{Sc} were found in cell culture media indicating that EVs were not mediating transfer of prions (Kanu *et al.*, 2002). In addition, prions added directly to cell media could enter cells by direct cell membrane penetration or endocytosis (Guo and Lee, 2014).

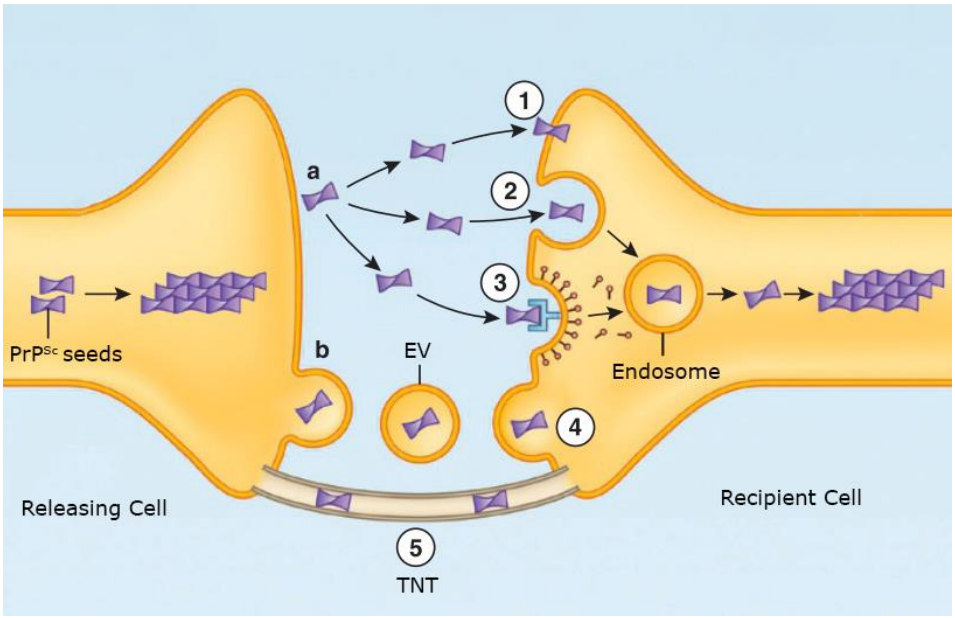

Figure 1.6.1. Possible transmission routes of PrP^{Sc} between cells. a – uptake of media floating PrP^{Sc} monomers through (1) direct penetration of recipient cell membrane, (2) endocytosis or (3) receptor-mediated endocytosis. b – PrP^{Sc} seeds that are released within extracellular vesicles (EV) integrate with recipient cell membrane (4). PrP^{Sc} seeds transport between cells might also take place via cytoskeletal structures - tunnelling nanotubes (TNTs) (5). Adapted from (Guo and Lee, 2014), modified.

The existence of different PrP^{Sc} transmission routes between cells in distinct cell culture models could lead to the conclusion that different prion strains and isolates could influence the route of transmission (Paquet, Langevin, *et al.*, 2007; Arellano-Anaya *et al.*, 2015). Furthermore, all of the mentioned *in vitro* analyses are difficult to examine in *in vivo* situations. However, *in vivo* research has showed that EVs could be isolated from many types of animal body fluids including CFS, urine, saliva, milk or even blood and plasma (Vilette *et al.*, 2018). In addition, some EV derived from plasma, urine or CFS were found to be PrP^{C} positive indicating that this might also be the way of spreading infectious PrP^{Sc} (Robertson *et al.*, 2006; Vella *et al.*, 2008; Gough and Maddison, 2010; Conde-Vancells and Falcon-Perez, 2012). On the other hand, detection

of TNTs *in vivo* is a very challenging process. There are no TNT specific markers and visualisation methods in solid tissues face some technical difficulties and do not provide sensitive and robust data. In addition, conditions required to detect PrP^{Sc} in these tissues are very specific and together with difficulties connected with TNT detection make it impossible for visualisation of PrP^{Sc} in TNTs *in vivo* (Vilette *et al.*, 2018).

1.7 Prion diseases as an example of protein misfolding diseases

The aggregation of misfolded proteins leading to a serious disease is not an exclusive hallmark for prion diseases. It affects a larger range of proteins and these disorders are grouped as protein misfolding diseases (PMDs). PMDs are caused by a change in a protein's conformation into β-sheet rich organised structures and this change in protein structure appears to be the only disease trigger. Most PMDs appear sporadically and have no genetic background however some could be inherited (Moreno-Gonzalez and Soto, 2011). Misfolded protein aggregates are observed in more than 20 human PMDs **(Table 1.7.1)**, including Alzheimer's disease (AD), Parkinson's Disease (PD), Huntington Disease, type II diabetes and amyotrophic lateral sclerosis (ALS) (Moreno-Gonzalez and Soto, 2011).

Table 1.7.1. Examples of human PMDs.

Disease	Protein involved	Misfolded protein location	Occurrence
TSE (prion diseases)	Prion protein	Extracellular	Sporadic, inherited, infectious
Parkinson's disease	α-synuclein	Cytoplasmic	Sporadic, inherited
Alzheimer's disease	Aβ, tau	Extracellular	Sporadic, inherited
Huntington's Disease	Huntingtin	Nuclear	Inherited
Diabetes type 2	Islet amyloid polypeptide (IAPP)	Extracellular	Sporadic
Amyotrophic lateral sclerosis (ALS)	Superoxide dismutase (SOD)	Cytoplasmic	Sporadic, inherited

1.7.1 Alzheimer's disease

Alzheimer's disease (AD) is known from its first case in 1906 in Germany and is one of the most common protein misfolding disorders. AD affects mainly people over 65 years old, however familial AD form also occurs in younger patients. In general, the disease is characterised by changes in behaviour and personality and progressive memory loss (Liu *et al.*, 2019). AD symptoms are caused by intracellular aggregates of misfolded proteins tau and amyloid β (Aβ). These two proteins create so-called neurofibrillary tangles and neurotic plaques in the brain tissue, respectively. Amyloid β is a 4 kDa protein, that is created by the proteolysis from glycosylated transmembrane amyloid precursor protein (APP), that is synthesised in neurons (Glenner and Wong, 1984; Weidemann *et al.*, 1989; Wirak *et al.*, 1991; Lee *et al.*, 2008). There is evidence indicating that it plays a role in cell growth and viability, may be a receptor for a glycoprotein F-spondin and participate in neuronal repair and development (Ho and Sudhof, 2004; O'Brien and Wong, 2011). Moreover, Aβ plays a role in synaptic release regulation (Abramov *et al.*, 2009). The majority of APP peptides that are produced are Aβ(1-40) and Aβ(1-42). It has been suggested that the misfolded Aβ(1-42) is mostly found to be correlated with disease (Jarret, Berger and Lansbury, 1993; Bayer *et al.*, 1999).

Tau protein aggregates create neurofibrillary tangles (NFT). In healthy tissue, tau proteins are microtubule-associated proteins (MAP) that bind and stabilise cell or organelle movement. They are also involved in cell shape maintenance (Weingarten *et al.*, 1975). Moreover, tau proteins undergo some posttranslational modifications with phosphorylation being the most important one. It has been suggested that the role of tau proteins in the tissue depends on the phosphorylation state (Buée *et al.*, 2000). Tau protein has been detected in many different tissues such as rat heart, kidneys, skeletal muscles, lungs and liver, but mainly in neurons axons (Lee, Goedert and Trojanowski, 2001; Gu, Oyama and Ihara, 2002). In AD, tau is hyperphosphorylated and not able to form microtubules within neurons. Instead, it aggregates in insoluble inclusions, the NFTs. As a result, the presence of NFT becomes toxic to cells as the intracellular transport is disrupted (Ballatore, Lee and Trojanowski, 2007), leading to changes in cytoskeleton structure and function (Roy *et al.*, 2005). Overall, the presence of NFT in the brain tissue is one of the main hallmarks of AD (Grundke-iqbals *et al.*, 1986; Kondo *et al.*, 1988).

1.7.2 Parkinson's disease

Parkinson's disease (PD) is a neurodegenerative disease characterised by the presence of Lewy Bodies (LB) and nerve cell loss. LB appears intracellularly, mainly in the cytoplasm of neurons within different brain regions with its highest abundance in substantia nigra and hypothalamus (Forno, 1995; Soto, 2003). The main component of LBs are misfolded α-syn aggregate filaments about 5-10 nm long. In general, α-syn is 140 amino acids long (Spillantini *et al.*, 1997, 1998) and encoded by the *SNCA* gene

located on the chromosome 4. It is expressed to the highest levels in brain tissue but is also found in lungs, placenta and kidneys (Ueda *et al.*, 1993). The function of α-syn is not fully known, however it may be involved in synaptic protein release (Narayanan and Scarlata, 2001). Moreover, α-syn contains some fatty-acid binding regions, therefore it might also have a role in fatty acid metabolism (Sharon *et al.*, 2001).

1.8 Misfolded protein cross-seeding

Every protein misfolding disease is characterised by the presence of protein aggregates specific to the illness and these aggregates can exhibit similar features like β-sheet rich structure, morphology and tissue staining pattern. Moreover, it is possible they might also recruit other proteins and create cross-seeded protein aggregates (Morales, Moreno-Gonzalez and Soto, 2013). The recruitment of protein to misfold is called 'homologous seeding' when engaging the same protein, or 'heterologous seeding', also known as 'cross-seeding' when different proteins are involved. The seeding process is based on the nucleation hypothesis, which consists of two steps, lag and elongation phases (Kocisko *et al.*, 1994; Soto, Estrada and Castilla, 2006). During the lag process, a nuclei is formed from misfolded protein oligomers. This phase is relatively slow and its main determinant is the formation speed of a nucleus of thermodynamically stable β-sheet rich conformer (Morales, Green and Soto, 2009). *In vivo*, this process can be spontaneous, determined by some genetic mutations or acquired. Following the nuclei formation, the elongation step is rapid. The seeds bind to cellular protein and compel it to change conformation. Furthermore, the lag phase could be accelerated by addition of already formed nuclei of different kinds of seeds (Soto, 2001). Such seeding provides an explanation for vCJD that appears in younger patients (Collinge *et al.*, 1996; Morales, Moreno-Gonzalez and Soto, 2013). Moreover, *in vitro* results also demonstrate that the production of misfolded protein during PMCA is accelerated by addition of misfolded protein seeds (Katorcha *et al.*, 2017).

In addition, many scientific sources described the co-occurrence of different pathologic misfolded proteins in human brain tissue and from *in vivo* and *in vitro* studies. These include Aβ occurring with α-syn for both AD and PD (Paik *et al.*, 1998; Masliah *et al.*, 2001; Mandal *et al.*, 2006; Tsigelny *et al.*, 2008), Aβ with prion protein for AD (Morales *et al.*, 2010), tau protein with α-synuclein for AD and PD (Arima *et al.*, 1999; Giasson *et al.*, 2003; Ishizawa *et al.*, 2003; Muntané *et al.*, 2008; Waxman and Giasson, 2011) and α-synuclein with prion protein for TSEs (Haïk *et al.*, 2002; Adjou *et al.*, 2007; Vital *et al.*, 2007, 2009; Mougenot *et al.*, 2011; Masliah *et al.*, 2012; Katorcha *et al.*, 2017). The co-occurrence of different protein aggregates within the same PMD is a quite common occurrence. An interesting hypothesis described by Katorcha and co-workers suggests that the determining factor for protein cross-seeding other protein aggregates might be the similarity in protein folding pattern rather than amino acids sequences or seed homology with the 'substrate' protein (Katorcha *et al.*, 2017). The impact of cross-

seeding events needs to be better understood in order to deliver improved diagnostic and therapeutic approaches for PMDs (Morales, Green and Soto, 2009).

1.9 Therapeutics for prion diseases

Prion diseases are fatal and characterised by a very prolonged asymptomatic incubation period. There is no treatment or cure for disease development. When developing therapeutic to TSE diseases, many factors must be considered *e.g.* availably of the therapeutic to cross the blood-brain barrier, and that the treatment cannot be toxic for the patient (Forloni *et al.*, 2013). To date, many therapeutic approaches have been tested *in vitro* and *in vivo*, targeting the cellular PrP, misfolded PrP^{Sc} or even the whole process of PrP^{C} misfolding **(Figure 1.9.1)** (Trevitt and Collinge, 2006). Therapeutics, which target PrP^{C} involve mostly switching off the *Prnp* gene by classical gene knockout or RNA interference (Trevitt and Collinge, 2006; White and Mallucci, 2009). Furthermore, a range of drugs were screened and analysed in terms of decreasing or even stopping PrP^{Sc} formation, examples include amphotericin B, antimalarial drugs: quinacrine and mefloquine, congo red (CR), pentosane polysulphate (PPS), heparin, antibodies, peptides and recombinant proteins (Chabry, Caughey and Chesebro, 1998; Kocisko *et al.*, 2003; Bertsch *et al.*, 2005; Forloni *et al.*, 2013; Yuan *et al.*, 2013). Most of these agents successfully inhibited PrP^{Sc} formation in cell-free system or mouse neuroblastoma cells, however *in vivo* the majority did not delay the disease onset or the drug appeared to be toxic for the organism. Both quinacrine and mefloquine were able to cross the blood-brain barrier but lacked activity to block PrP^{Sc} formation in *in vivo* models (Kocisko *et al.*, 2003; Kocisko and Caughey, 2006a; Rochet, 2007). Moreover, quinacrine has been tested in hospital trials on patients. One of the clinical trials was started in the UK and included familial, iatrogenic, sporadic and variant CJD patients. This study was called PRION-1 and showed that the drug did not affect the progression of prion diseases and CJD patients mortality rates did not change in comparison to untreated patients (Collinge *et al.*, 2009). In addition, another quinacrine clinical study was performed in the US between 2005 and 2009. Repeatedly, there was no significant difference in survival time of sCJD in compare to placebo controls (Geschwind *et al.*, 2013). Another drug that has been tested on prion disease patients was PPS. In the UK, this drug was delivered to 5 vCJD patients intraventricularly. The majority of them showed longer survival, however post mortem research showed no differences in pathological changes in the brain tissue (Newman *et al.*, 2014). A similar study was performed in Japan with iCJD, fCJD and sCJD patients. However in this case, there were no differences in the patients survival times, suggesting that the response to this drug was disease or patient specific (Tsuboi, Doh-Ura and Yamada, 2009; Teruya and Doh-Ura, 2017). Doxycycline was also tested in clinical trials. In Italy and in France, patients with sCJD and fCJD were treated orally but the therapy showed no differences in disease progression or patient survival between placebo and doxycycline treated patients (Haïk *et al.*, 2014). In addition to that, another preventive study with patients

affected with FFI was started in Italy, in which FFI patients will be exposed for doxycycline treatment for 10 years. To date, no results from this trial have been published (Forloni *et al.*, 2015).

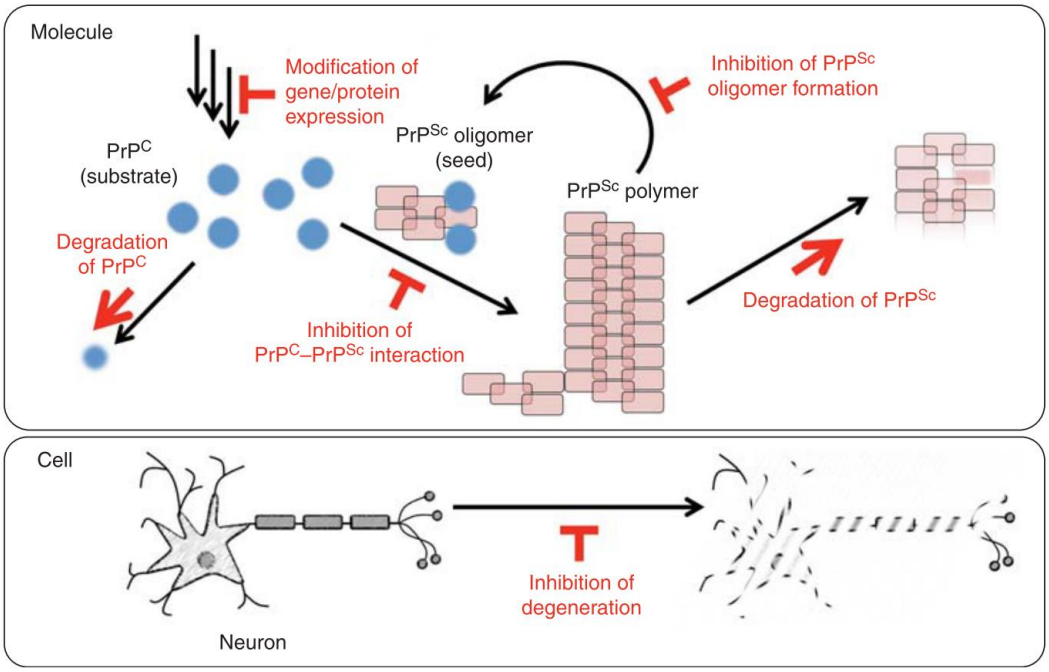

Figure 1.9.1. Possible targets for prion disease treatments. These targets include modification of the *Prnp* gene or PrP^{C} expression level. Therapies might be also directed towards degradation of cellular PrP, or limitation of the interaction between PrP^{C} and PrP^{Sc}. In addition, degradation of PrP^{Sc} and inhibition of PrP^{Sc} derived oligomer formation were also proposed as therapeutic targets. Furthermore, on the cell level, therapeutics could inhibit neuronal degeneration. Adapted from (Teruya and Doh-Ura, 2017) (Copyright to Cold Spring Harbour Laboratory Press).

Testing the therapeutic potential of polyclonal and monoclonal antibodies that bind to PrP^{C} or PrP^{Sc} have been reported, and antibodies can have an inhibiting effect on PrP^{Sc} formation in cell cultures and in the spleen in an *in vivo* model (White *et al.*, 2003; Trevitt and Collinge, 2006). A monoclonal antibody 6H4 was investigated in N2a cell culture inhibition. 6H4 binds to mouse PrP residues 144-152 corresponding to helix 1 in the PrP structure. When added to N2a cell infected with scrapie, the monoclonal antibody cured the scrapie infected cells. In addition to that, 6H4 molecule added to the cell culture media was also found to prevent the scrapie infection in these cells (Enari, Flechsig and Weissmann, 2001). Generated in transgenic mice lacking the PrP^{C}, antibodies were raised against two human PrP^{Sc} isoforms: α and β. When these were applied to Rov9 cells infected with scrapie, both kinds of antibody blocked accumulation of misfolded PrP^{Sc} (Beringue *et al.*, 2003, 2004). Furthermore, another study involved screening 145 different monoclonal antibodies in order to determine its effect on PrP^{Sc} formation in two cell culture models: Rov9 and N2a. Amongst them, two antibodies,

Sha31 and BAR236 that binds the central and C-terminal region, respectively, were shown to have the highest inhibition response. They produced IC50 value of 0.6 nM for N2a cells in the initial screening (Féraudet *et al.*, 2005). In addition, monoclonal antibodies ICSM18 and ICSM35 were also assessed in mice that were infected peripherally with scrapie agent. These antibodies recognise region 146-159 and 91-110, respectively (Beringue *et al.*, 2003; White *et al.*, 2003). Results showed that levels of PrP^{Sc} in spleen were significantly reduced and survival time was increased for animals treated peripherally with antibodies (White *et al.*, 2003). In addition to that, Peretz *et al.,* investigated recombinant antibodies fragments (Fabs) for their ability to inhibit prion protein propagation in mouse ScN2a cells. They tested a range of concentrations and found out that the D18 antibody was the most effective and significantly reduced the level of PrP^{Sc} in cells (Peretz *et al.*, 2001). Because the Fab bound to the 132-156 region in mouse PrP^{C} is was suggested that it blocks or changes the site of interaction with PrP^{Sc} (Williamson *et al.*, 1998; Peretz *et al.*, 2001). In contrast, Fabs that were binding to the C-terminal of N-terminal of PrP were found to have no inhibitory effect (Peretz *et al.*, 2001). Furthermore, polyclonal antibodies were also used in a ScN2a cell model and demonstrated inhibition of *de novo* PrP^{Sc} accumulation (Gilch *et al.*, 2003). All of these examples highlight the potential for antibodies to be used for prion diseases therapies, however, their use is still limited (White *et al.*, 2003). Only recently, an ICSM18 derivative human antibody – PRN100 - was given to small number of patients with different staged of sCJD in clinical trials in the UK. Thus, the outcomes are still not presented (White *et al.*, 2003; Dyer, 2018; Aguzzi and Frontzek, 2020).

Heterologous or homologous recombinant prion protein can also inhibit TSE disease progression *in vitro* and *in vivo*. Priola and co-workers showed that expression from a non-homologous *Prnp* gene, which differed from host *Prnp*, was able to interfere with misfolded prion protein aggregation and could prevent its accumulation (Priola *et al.*, 1994). Moreover, Skinner *et al.*, conducted *in vivo* research, where mice were inoculated with a scrapie strain and two doses of recombinant hamster PrP (rhamPrP). The rhamPrP proteins was administered intracerebrally at the inoculation time and orally on the following day (Skinner *et al.*, 2015). At the end of the study, 50 % of animals treated with the high dose of rhamPrP were free of any scrapie signs at the time of death, however animals developed some characteristic TSE-related brain tissue changes. Furthermore, addition of recombinant PrP was also reported to inhibit ovine and bovine PrP^{Sc} amplification *in vitro* (Workman, Maddison and Gough, 2017). Further *in vitro* research showed that homologous recombinant prion protein was reported to act as an inhibitor and was more effective than introduced heterologous rPrPs (Yuan *et al.*, 2013). Studies to date indicate that the addition of any recombinant PrP might significantly delay the PrP^{Sc} accumulation, however the mechanism is still unclear. Yuan and colleagues reported that inhibition of PrP^{C} misfolding involves both the N- and C-terminal regions of PrP, suggesting that PrP^{Sc} binding sites are contributed to by sites across the whole PrP molecule. In addition, recombinant PrP proteins bind to misfolded PrP^{Sc} and

therefore might block the possible sites for cellular PrP to interact (Yuan *et al.*, 2013). However, synthetic peptides made from only the central part of hamster PrP were tested for inhibition of *in vitro* amplification and could successfully inhibited PrP^{C} conversion. This data indicated that the PrP protein central region might be the most important domain in its interaction within PrP^{Sc} in the misfolding process (Chabry, Caughey and Chesebro, 1998).

1.10 Study aims

The central hypothesis to this study was that mutated recombinant PrP could be a potent inhibitor of PrP^{Sc} formation.

This hypothesis was tested through the following aims:

Verification of rVRQ as an inhibitor for scrapie prion misfolding

It was demonstrated previously that addition of recombinant prion protein into PMCA inhibit the infectious prion protein amplification (Yuan *et al.*, 2013). Later, Workman investigated hamster recombinant PrP, rARQ, rVRQ and rARR. Of these natural variants and a heterologous rPrP, rVRQ was found to inhibit the scrapie amplification most efficiently (Workman, 2017). As a starting point to the present study, the aim was to reproduce and confirm the rVRQ inhibition pattern with representative scrapie isolate ARQ/VRQ PG1361/05. The rVRQ was tested at different concentrations and then IC50 values was calculated and compared to previously obtained results.

Preparation and screening of ovine rPrP mutants as inhibitors of PrP^{Sc} formation

Previous data showed that polymorphisms at position 136 of ovine scrapie has a considerable influence not only of the susceptibility to natural scrapie but also on the efficacy of rPrP inhibition of PrP^{Sc} formation. In order to investigate whether other point mutations at 136 position will increase or decrease the inhibition level of scrapie isolate, all possible amino acid changes at this position were made using site directed mutagenesis. Once mutations were confirmed, all rPrP proteins were expressed in *E. coli* and purified. All variants were compared to rVRQ to identify improvements in inhibition efficacy. More potent inhibitors were characterised in terms of IC50 values.

Investigation of rPrP mutants with different prion disease isolates

The best rPrP inhibitors of scrapie ARQ/VRQ PG1361/05 were then analysed with other scrapie isolates, as well as bovine and ovine BSE. First of all, optimal PMCA and serial PMCA conditions were determined for the amplification of these disease isolates. Once determined, the previously tested rPrP were added into PMCA rounds at specific concentrations and final rounds of amplifications were analysed and inhibitor efficacies determined.

Investigation of peptides from rPrP mutants as inhibitors of PrP^{Sc} amplification and structural analysis of rPrP proteins

Previously, the potential use of synthetic peptides instead of recombinant proteins in prion disease inhibition was demonstrated (Chabry, Caughey and Chesebro, 1998; Yuan *et al.*, 2013). This current study aimed to design and produce various ovine PrP derived peptides of different lengths, each containing the 136 position. These were screened for inhibition properties and compared to equivalent rPrP inhibition. Additionally, to

investigate how a single amino acid change at position 136 in ovine PrP influenced changes in a 3-D structure of the whole protein, the structures of rPrPs were analysed *in silico* and compared.

Application of rPrP inhibition of prion formation to a cell cultures model of scrapie infection

It has been shown that TSE permissible cells lines have had a huge potential in understanding mechanisms of disease development, prion protein conversion and assessing therapeutics (Vilette *et al.*, 2018). In this project, the aim was to infect Rov9 cells expressing ovine PrP (genotype VRQ) with ovine scrapie isolates/strains. After the establishment of infection, the efficacy of rPrPs to inhibit scrapie development in cells were assessed.

Chapter 2: Materials and Methods

2.1 Brain tissue samples details

Both healthy and TSE positive brain tissue samples were obtained from the Animal and Plant Health Agency (APHA) or the Roslin Institute (University of Edinburgh). All sample details are shown in **Table 2.1.1**.

Table 2.1.1. Details of healthy and TSE positive samples.

Isolate number	Description	Host	Genotype	TSE status
PG0648/09	Brain 16	Ovine	VRQ/VRQ	Healthy
PG0146/12	Brain 42	Ovine	VRQ/VRQ	Healthy
PG0211/12	Brain 51	Ovine	AHQ/AHQ	Healthy
PG0209/12	Brain 49	Ovine	AHQ/AHQ	Healthy
Bovine	Bovine	Bovine	Bovine	Healthy
PG1361/05	Scrapie	Ovine	ARQ/VRQ	TSE
PG1207/03	Scrapie	Ovine	VRQ/VRQ	TSE
PG1499/02	Scrapie	Ovine	AHQ/VRQ	TSE
J3011	CH1641 scrapie	Ovine	AHQ/AHQ	TSE
J2935	CH1641 scrapie	Ovine	ARQ/AHQ	TSE
SE1945/0035	BSE	Bovine	Bovine	TSE
PG1693/03	BSE	Ovine	ARQ/ARQ	TSE
SSBP1	Scrapie	Ovine	VRQ/VRQ	TSE
PG1212/03	Scrapie	Ovine	VRQ/VRQ	TSE
PG1517/01	Scrapie	Ovine	VRQ/VRQ	TSE

2.2 Production of non-available clones of rPrP mutants

2.2.1 Plasmid preparations

In order to produce recombinant prion proteins with specific mutations at position 136, site directed mutagenesis was performed. The plasmid pet22b(+) containing the rVRQ (valine$_{136}$, arginine$_{154}$ and glutamine$_{171}$) sequence was purified from *E. coli* (NovaBlue, isolate BL21 (DE3), Novagen). Briefly, DE3 were grown in 5 ml of 2 x Yeast Tryptone (2YT) media containing 100 µg/ml of ampicillin and 3 % (w/v) glucose (2YT-AG) from glycerol stock overnight at 37 °C with shaking. Then, bacteria were harvested by centrifugation at 17000 x g for 3 minutes. For plasmid preparation, a Qiagen Kit (QIAprep Spin Mini Prep Kit) was used according to the protocol. Briefly, after centrifugation, supernatant was removed and bacteria were re-suspended in 250 µl of buffer P1 and next, 250 µl of P2 buffer was added and samples were mixed. 350 µl of buffer N3 was added, samples were centrifuged for 10 minutes at 17000 x g. Then, 800 µl of supernatant were added in the kit provided column and centrifuged for 1 minute at 17000 x g. The flowthrough was discarded and the column was washed with 700 µl

of buffer PB. Samples were centrifuged as described before and once the flowthrough was removed, columns were centrifuged for an additional minute. Next, columns were moved to a new tube, 30-50 µl of EB buffer was added and incubated for 2 minutes at room temperature. Samples were then pulsed at 17000 x g and columns were discarded. The DNA concentration was estimated by Nanodrop (Thermo Scientific). This DNA was then used as a template in the inverse PCR.

2.2.2 Inverse PCR primer design

Non-overlapping primers were designed, so that the forward primer starts at the mutation site, and the reverse primer is complimentary to the sequence before the mutation position **(Figure 2.2.1)**.

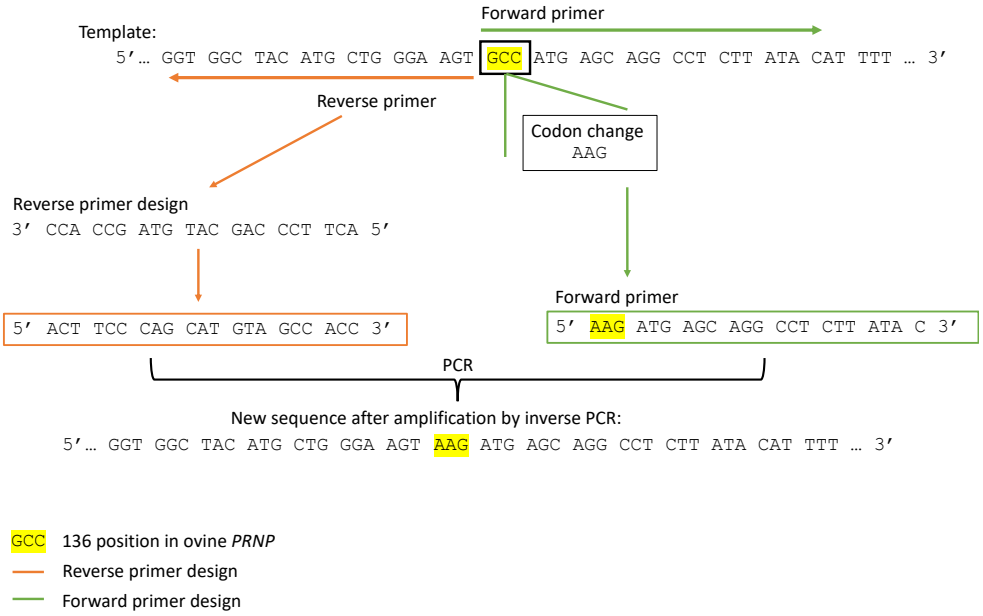

Figure 2.2.1. Representative scheme for inverse PCR primer design for 136 position mutation in ovine PrP. Forward primer starts at the mutation site and first codon was mutated in order to obtain proper mutation at 136 mutation. The reverse primer is complimentary to the sequence before the mutation position. Reverse primer is universal for each rPrP.

All the primers were phosphorylated at the 5' end. Primer sequences with their melting temperatures are showed in **Table 2.2.1**. Each primer was resuspended in ultrapure water to a final concentration of 100 µM. Primers were stored at -20 °C until further use.

Table 2.2.1. Inverse PCR primers.

Primer name[1]	Sequence 5′ → 3′[2]	Melting temperature [°C]
rPrP-Rev	acttcccagcatgtagccacc	61.8
rPrP-For-K	aagatgagcaggcctcttatac	58.4
rPrP-For-G	ggcatgagcaggcctcttatac	62.1
rPrP-For-W	tggatgagcaggcctcttatac	60.3
rPrP-For-Q-(1)	cagatgagcaggcctcttatac	60.3
rPrP-For-Q-(2)	caaatgagcaggcctcttatac	58.4
rPrP-For-P	cccatgagcaggcctcttatac	62.1
rPrP-For-T	accatgagcaggcctcttatac	60.3
rPrP-For-D	gacatgagcaggcctcttatac	60.3
rPrP-For-E	gagatgagcaggcctcttatac	60.3
rPrP-For-M	atgatgagcaggcctcttatac	58.4

[1]Rev – reverse, For – forward, the amino acid change is indicated in the primer name: V – valine, K – lysine, G – glycine, W – tryptophan, Q – glutamine, P – proline, T – threonine, D – aspartic acid, E – glutamic acid, M – methionine.
[2]aag – amino acid codon change

2.2.3 Inverse PCR

Inverse PCR was performed as described in **Table 2.2.2**. Q5 Reaction Buffer (cat. no. B9027S), dNTPs (cat. no. N0447S), Q5 High GC Enhancer (cat. no. B9028A) and Q5 High Fidelity DNA Polymerase (cat. no. M0491L) were purchased from New England BioLabs. PCR primers were obtained from Eurofins. All PCR reactions were carried on in PCR machine LifeECO, BioER.

PCR reactions were performed with initial denaturation at 95 °C for 5 minutes. Next, 30 cycles of denaturation at 95 °C for 30 seconds, annealing at 61 °C for 30 seconds and elongation at 72 °C for 5 minutes were completed. For some cases, gradient inverse PCR was performed with annealing temperatures ranging from 50 to 63 °C. Lastly, the final extension was performed for 10 minutes at 72 °C. When necessary, PCR products were stored at either 4 °C or -20 °C.

Table 2.2.2. Reagents concentration and volumes used in inverse PCR.

Reagent	Reaction concentration	Volume [µl]
Q5 Reaction Buffer	1x	10
dNTPs	0.4 µM	2
DNA template	0.2 ng/µl	1
Forward primer	0.3 µM	1.5
Reverse primer	0.3 µM	1.5
Q5 High GC Enhancer	1x	10
Q5 Polymerase	20 U/ml	0.5
H_2O	Up to 50 µl	23.5

2.2.4 Agarose Gel Electrophoresis

PCR products were analysed on a 1 % (w/v) agarose gel. Briefly, 1 g of agarose was re-suspended in 1 x TAE buffer (40 mM Tris, 20 mM acetic acid, 1 mM EDTA) and Nancy-520 (Sigma-Aldrich) was added to a final concentration of 1 mM. All samples were mixed with Gel Loading Dye (cat. no. B70256, New England BioLabs) and 60 µl of each sample were loaded on the gel. As a DNA size reference, 1 kb DNA Ladder was used (cat. no. N3232S, New England BioLabs). The agarose gel was run for 45 minutes at 100 V. Gels were visualised using a BioRad Imager.

2.2.5 Gel Extraction

PCR products of the expected size were extracted from the gel using the Nucleospin Gel and PCR clean up kit following the manufacturer's instructions (Macherey-Nagel). Briefly, PCR products were cut from the gels and placed in tubes. Then, tubes were weighed and NTI buffer was added to the sample. Next, samples were incubated for 10 minutes at 50 °C with vortexing every 2 minutes. Fully dissolved gel products were loaded on the columns and centrifuged at 11000 x g for 30 seconds. Flow through was discarded and columns were washed twice with 700 µl of NT3 buffer and centrifuged again. Afterwards, columns were centrifuged for 3 minutes at 11000 x g in order to dry the silica. PCR products were eluted using 20 µl of buffer NE. DNA concentrations were estimated using NanoDrop (Thermo Scientific).

2.2.6 Digestion with DpnI

In order to remove the DNA template from the mixture, 20 µl of eluted DNA was mixed with 2 µl of CutSmart Buffer (cat. no. B7204S, New England BioLabs) and 1 µl of DpnI

enzyme (cat. no. R0176S, New England BioLabs). Samples were incubated for 2 h at 37 °C. Next, enzyme was heat inactivated at 80 °C for 20 minutes.

2.2.7 PCR clean up

Samples were purified using the same kit as for the gel extraction (Macherey-Nagel) with some modifications. Briefly, 70 µl of DEPC water and 140 µl of NTI buffer were added and the samples and incubated for 10 minutes at 50 °C. Then, samples were added to the columns and centrifuged at 11000 x g for 30 seconds. Flow through was discarded. Next, 700 µl of NT3 buffer were added to the columns and centrifuged at 11000 x g for 30 seconds. This step was repeated once. Columns were centrifuged for another 3 minutes in order to dry the silica and then placed in a clean tube, 20 µl of NE buffer were added and samples were incubated for 2 minutes at room temperature. Samples were then centrifuged at 11000 x g for 1 minute and DNA concentration was measured by NanoDrop.

2.2.8 Ligation

4 µl of Ligase Buffer (cat. no. B020S, New England BioLabs), 0.4 µl of T4 DNA Ligase (cat. no. M0202S, New England BioLabs) and 150 ng of DNA were mixed together and up to 40 µl of DEPC water was added to each reaction. Then, samples were incubated at 16 °C overnight and enzyme heat inactivated for 10 minutes at 65 °C.

2.2.9 Transformation

Competent DE3 *E. coli* NovaBlue cells (Novagen) were thawed on ice and 4 µl (150 ng) of DNA was added to the cells (20 µl of cells per transformation). Samples were incubated on ice for 5 minutes and quickly transferred at 42 °C for 30 seconds. Next, samples were incubated on ice for 2 minutes. Then, 80 µl of pre-warmed SOC media was added to the cells, mixed and 50 µl of cells were plated on the 2YT-AG (yeast tryptone with 100 µg/ml ampicillin and 3 % (w/v) glucose) plates. Bacteria were grown overnight at 37 °C.

2.2.10 Bacteria cultures

Single colonies from agar plates were selected and grown in 5 ml of 2YT-AG media overnight at 37 °C. Plasmid preparation was performed as previously described **(2.2.1)**. Glycerol stocks were prepared in 50 % of glycerol and stored at -80 °C for further use.

2.2.11 Sequencing

10 µl of 100 ng/µl of DNA were sent for Sanger sequencing (Source BioScience). All samples were sequenced using T7 Forward primer derived from the company stock. Sequencing results were analysed using SnapGene Viewer software (GSL Biotech LLC).

2.3 Expression and purification of recombinant prion proteins

2.3.1 Recombinant prion protein expression

Bacterial glycerol stocks were grown at 37 °C overnight in 10 ml of 2YT-AG media. Cultures were then diluted 1/100 and transferred into 250 ml of 2YT-AG media and grown at 37 °C with 180 rpm shaking until OD_{600} reached 0.4. Afterwards, bacteria were centrifuged at 1500 x g at 4 °C and resuspended in 250 ml of 2YT media with 100 µg/ml of ampicillin and 1 mM IPTG (isopropyl β-D-1-thiogalactopyranoside) (2YT-AI) followed by overnight growth at 37 °C with shaking. Bacteria were centrifuged at 1500 x g at 4 °C for 30 minutes, supernatant was removed and pellets were stored at -20 °C until required. Bacteria pellets were then re-suspended in 10 ml of lysis buffer (50 mM NaH_2PO_4, 300 mM NaCl, pH 8.0, 0.1 % (v/v) NP-40, 10 mg/ml lysozyme, 1 tablet of Protease and Phosphatase Inhibitor (Thermo Scientific)) and incubated at 37 °C for 1 h. Then, 240 µl of 1 mg/ml DNase (cat. no. DN25, Sigma) and 120 µl of 1 M $MgCl_2$ were added and incubated at room temperature for 15 minutes. The lysate was then centrifuged at 9600 x g for 20 minutes and supernatant was removed. Bacterial pellets were washed three times using 10 mM Tris, pH 8.0, 0.1 % (v/v) NP-40. After the first wash, 20 minutes incubation on ice was performed. Every wash was followed by centrifugation at 9600 x g for 20 minutes. Afterwards, supernatant was removed and bacterial pellet re-suspended in 20 ml of solubilisation buffer (8 M Urea, 50 mM NaH_2PO_4, 300 mM NaCl, pH 7.5). Pellet solubilisation was performed overnight at room temperature and then samples were centrifuged at 9600 x g for 1 h. Supernatant was collected and stored at 4 °C until required.

2.3.2 Protein purification

Recombinant proteins were purified using the Fast Protein Liquid Chromatography (FPLC) on an AKTA prime FPLC machine (GE Healthcare). Briefly, the column (cat no. 71-7005-00 AZ, HiTrap™ Chelating High Performance Column) was charged with 50 mM $CuSO_4$, washed and supernatant containing the protein of interest was passed through the column. Recombinant prion proteins were eluted using imidazole gradient (0 – 0.5 M) in elution buffer (50 mM NaH_2PO_4, 300 mM NaCl, pH 7.5). Afterwards, the protein purity was analysed on the polyacrylamide gel stained with Instant Blue (Expedeon) and fractions with rPrPs were pooled together. Protein concentration was estimated using Bradford assay **(2.3.3)** and then protein was frozen at –80 °C in the elution buffer with 20 % (w/v) sucrose until required.

2.3.3 Bradford Assay

Bovine Serum Albumin (BSA) standard curve (1.4 mg/ml – 0.25 mg/ml) was prepared by diluting the BSA stock solution (2 mg/ml) in sample buffer. Briefly, 1.4, 1.0, 0.5 and 0.25 mg/ml standards were made in tubes and 5 µl of each standard and samples were put in duplicates on the Nunc-Immuno Maxisorp ELISA 96 well plate (Thermo Scientific)

and 250 µl of Bradford Reagent (cat. no. B6916, Sigma) were added into wells. Plates were incubated for up to 15 minutes and the absorbance at 595 nm was measured in the Tecan plate reader (Tecan GENios). Blank absorbance values (sample buffer only) were subtracted from each measurement and an average value was calculated. Average value was plotted against concentration and the amount of protein in samples was read from the curve.

2.3.4 Protein concentration and dialysis

Before every experiment with the recombinant prion protein, rPrPs were thawed and the protein concentration was estimated with Bradford Reagent (see chapter **2.3.3**). Protein batches were then concentrated using the Pierce Protein Concentrators with a molecular weight cut off (MWCO) of 10K (cat. no. 88516, Thermo Scientific) and a 2-step dialysis was performed on ice using the 0.5 ml G2 dialysis cassettes with the same MWCO – 10K (cat. no. 88250, Thermo Scientific). Briefly, 400 µl of protein concentrate was loaded into a previously hydrated cassette and the protein was dialysed in buffer 1 (PBS with 10 % (w/v) sucrose) for 1 h on ice and then dialysed for 1 hour in buffer 2 (PBS only). Sample was then recovered from the cassette and a Bradford assay was performed in order to estimate the protein concentration. Dialysed recombinant prion proteins were stored at 4 °C until further use.

2.4 Recombinant PrP mutants and PrP peptides analysis

2.4.1 Protein Misfolding Cyclic Amplification with scrapie isolate PG1361/05

Protein misfolding cyclic amplification (PMCA) was used to amplify prion and assess any inhibitory properties of the recombinant PrP or peptides of PrP. Each reaction was performed in clear 0.2 ml tubes (Sarstedt). Routinely, scrapie strain PG1361/05 (genotype ARQ/VRQ) was the source of the PrP^{Sc} seed, while the 10 % healthy brain 16 (genotype VRQ/VRQ) was the source of PrP^{C} substrate. A range of concentrations of rVRQ (0.25 nM – 1200 nM) and rVRQ mutants were added to samples before the amplification started. As seed, 5 µl of 1 % scrapie PG1361/05 brain homogenate was added into every reaction to a final reaction volume 100 µl. PMCA was performed for 24 h with repeat cycles of 40 seconds of sonication and 29 min 20 seconds incubation at 37 °C (48 cycles in total). Power was set to 180 – 200 W (S-4000 Misonix, Ultrasonic Liquid Processors). Amplification products were stored at -20 °C.

2.4.2 Serial Protein Misfolding Cyclic Amplification

In serial Protein Misfolding Cyclic Amplification (sPMCA) multiple rounds of sonication and incubation at 37 °C were used. Again, this method was used to assess the inhibitory ability of rPrP. After round 1 (24 h), PMCA reaction products were diluted 1/3 into fresh PrP^{C} substrate (negative brain homogenate) and amplified for another 24 h (up to 5 PMCA rounds were performed). Amplification conditions were as detailed in **2.4.1**. In inhibition sPMCA, different TSE isolates were tested with 50 nM of rRRQ, rKRQ and rPRQ

added into every PMCA round. For round 1 of serial PMCA, seeds of PrP^{Sc} were added as follows: 0.5 µl of 10 % brain homogenate for PG1361/05 (ARQ/VRQ), PG1207/03 (VRQ/VRQ), and 5 µl of 10 % brain homogenate for ovine scrapie PG1499/02 (AHQ/VRQ), bovine BSE (SE1945/0035), ovine BSE (PG1693/03, ARQ/ARQ) and CH1641 like scrapie isolates – J3011 (AHQ/AHQ) and J2935 (ARQ/AHQ). Round 1 PMCA products were diluted 3/7 into fresh PrP^{C} substrate. All mentioned scrapie isolates were amplified in VRQ/VRQ (brain 16) substrate, whereas the bovine BSE was amplified in bovine substrate. Ovine BSE PG1693/03 amplification was tested in VRQ/VRQ (brain 16) substrate in all rounds of amplification and also in AHQ/AHQ (brain 51 – for rounds 1, 3 and 5) and VRQ/VRQ (brain 42 – for rounds 2 and 4) substrates. On the other hand, CH1641 like scrapie isolates: J3011 and J2935 were amplified in AHQ/AHQ negative brain homogenate (brain 49).

2.4.3 Peptides design and inhibition

In order to identify whether fragments of recombinant prion proteins that include the 136 position are still able to inhibit the misfolding process, non-overlapping peptides derived from ovine prion protein were designed and ordered **(Figure 2.4.1)** (Biomatik, GeneCust). Two different peptide sizes were designed for rVRQ, rRRQ, rKRQ and rPRQ, 33 amino acids (aa) and 18 aa long. In addition, a 43 aa long peptide, residues OvR130-173, was designed for rRRQ, containing position 136, 154 and 171. Furthermore, sequence for the fragment OvV112-144 was randomised and used as a control. All peptides were acetylated on the N-terminus and amidated on the C-terminus. Peptides information including names, mutations, sequences and molecular weights are described in **Table 2.4.1**.

Table 2.4.1. Ovine peptides.

Name[1]	Mutation at 136 position	Sequence[2]	Length[3]	MW[4] [g/M]
ovRND	-	GMGVGGKMRAARAPVHYLIAGAALMVGGLSH FS	33 aa	3325.24
OvV122-139	V	GAVVGGLGGYMLGSVMSR	18 aa	1751.84
OvR122-139	R	GAVVGGLGGYMLGSRMSR	18 aa	1809.66
OvK122-139	K	GAVVGGLGGYMLGSKMSR	18 aa	1780.74
OvP122-139	P	GAVVGGLGGYMLGSPMSR	18 aa	1749.96
OvV112-144	V	MKHVAGAAAAGAVVGGLGGYMLGSVMSRPLI HF	33 aa	3267.54
OvR112-144	R	MKHVAGAAAAGAVVGGLGGYMLGSRMSRPLI HF	33 aa	3325.32
OvK112-144	K	MKHVAGAAAAGAVVGGLGGYMLGSKMSRPLI HF	33 aa	3297.6
OvP112-144	P	MKHVAGAAAAGAVVGGLGGYMLGSPMSRPLI HF	33 aa	3266.37
OvR130-173	R	GYMLGSRMSRPLIHFGNDYEDRYYRENMYRY PNQVYYRPVDQYS	43 aa	5606.16

[1]RND – randomised, V – valine, R- arginine, K – lysine, P – proline;
[2]The amino acid change has been underlined in peptide sequence;
[3]aa – amino acid;
[4]MW – molecular weight;

Peptides were resuspended in the buffers recommended by the company. Therefore, peptides ovRND, OvV112-144, OvR112-144, OvK112-144 and OvP112-144 were resuspended in 80 % (v/v) acetonitrile. Peptide OvV122-139 was resuspended in 2 % (v/v) HCOOH, 18 % (v/v) acetonitrile. Peptides OvR122-139, OvK122-139, OvP122-139 were resuspended in ultrapure water. For peptide OvR130-173, the supplier did not provide the recommended buffer, therefore peptide net charge was calculated using an on-line calculator pepcalc and peptide was resuspended in water (Lear and Cobb, 2016). Resuspended peptides were aliquoted and stored at -20 °C.

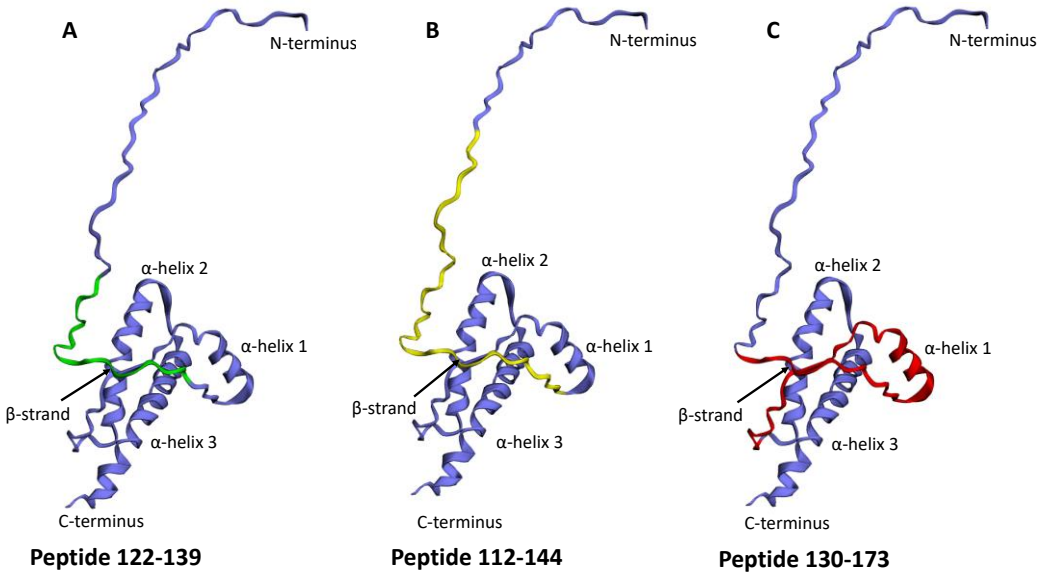

Figure 2.4.1. Peptide alignment on ovine PrP^C structure. **A** – 18 amino acids long peptide showed in green on the PrP^C structure. **B** – 33 amino acid long peptide showed in yellow on the PrP^C structure. **C** – 43 amino acids long peptide showed in red on the PrP^C structure. All peptides contain the 136 position. Peptide 130-173 (43 amino acids shown in red in **C**) contains position 136, 154 and 171 in ovine PrP protein. The figure was generated using Phyre2 and EzMol1.3 software.

2.4.4 Testing peptides and solvent inhibition of PMCA

It was investigated if different concentrations of acetonitrile and acetonitrile with formic acid could interfere with misfolded prion protein amplification. Different concentration of acetonitrile (from 2.7 to 0.005 % (v/v)) and the mixture of formic acid with acetonitrile (from 0.04 % (v/v) HCOOH, 0.3 % (v/v) acetonitrile to 0.00007 % (v/v) HCOOH, 0.0006 % (v/v) acetonitrile) were added to PMCA reactions. It was then tested whether the designed peptides can inhibit the amplification of prion protein better in comparison to the recombinant proteins rVRQ, rRRQ, rKRQ and rPRQ. The PMCA reactions were performed as previously described **(2.4.1)**.

2.4.5 Proteinase K digestion of PMCA products

PK stock solution was prepared at 0.2 mg/ml with 0.045 % (w/v) SDS. Amplified samples were mixed 50:50 by volume with PK stock solution, giving a final PK concentration of 100 µg/ml. Then samples were incubated at 37 °C for 1 h in a water bath. PK digestion was stopped by freezing the samples at -80 °C for 5 minutes.

2.4.6 Sodium dodecyl sulphate-polyacrylamide gel electrophoresis (SDS-PAGE) and western blotting

NuPAGE™ 12 % Bis-Tris gels (cat. no. NP0342, Invitrogen) were placed in the XCell SureLock™ Mini (Invitrogen) and the 1 x MOPS buffer (cat. no. NP0001, Invitrogen) was added. 15 µl of each sample was mixed with 5 µl of 4 x LDS Sample Buffer (cat. no. NP0008, Invitrogen) with 5 % (v/v) β-mercaptoethanol and boiled at 100 °C for 10 minutes. 10 µl of SeeBlue™ Plus2 Pre-Stained Protein Standard (cat. no. LC5925, Invitrogen) and 20 µl of each sample were loaded into gels and electrophoresis performed for 1 h at 200 W. Proteins were then stained with InstantBlue (Expedeon) and destained with ultrapure water. Gel images were captured using the ChemiDoc™ Imaging System (BioRad). Alternatively, gels were used for western blotting, in which proteins were transferred onto polyvinylidene difluoride (PVDF) membrane. The wet transfer was performed for 75 minutes at 30 V in NuPAGE 1 x Transfer Buffer (cat. no. NP00061, Invitrogen). Then, membranes were blocked overnight in 5 % (w/v) milk powder (SMA) in 1 x TBST at 4 °C.

2.4.7 Dot blot and PrP^{Sc} detection

PK digested samples were mixed with 4 x LDS Sample Buffer (cat. no. NP0008, Invitrogen) with 5 % (v/v) β-mercaptoethanol, boiled at 100 °C for 10 minutes and 2.5 µl of each were spotted onto nitrocellulose membrane (cat. no. 10600002, Amersham Protran) in duplicates. Membranes were then left to dry for 5 minutes and blocked overnight in 5 % (w/v) SMA in TBS with 0.05 % (v/v) Tween 20 (TBST) at 4 °C. Blocked overnight dot blots were incubated with SHA31 monoclonal antibody 1:40000 in 0.5 % (w/v) SMA in TBST for 1.5 h. SHA31 antibody binds to the epitope YEDRYYRE, which in ovine prion protein is equivalent to positions 145-152 (Féraudet *et al.*, 2005). Then, blots were washed 3 x 10 minutes with 0.5 % (w/v) SMA in TBST and incubated for 1 hour with a 1:2000 dilution of secondary antibody (cat. no. P0447, polyclonal goat anti-mouse HRP, Dako) in 0.5 % (w/v) SMA in TBST. Afterwards, blots were washed 4 x 10 minutes in 0.5 % (w/v) SMA in TBST and once in ultrapure water. Then, membranes were incubated with HRP substrate EZ-ECL (Biological Industries), sealed in clear plastic and visualised using the ChemiDocTM Imaging System (BioRad).

2.4.8 rVRQ mutants screening for inhibition of PMCA

All rPrP mutants details are provided in **Table 2.4.2**. These 136 position rVRQ mutants were screened at 100 nM and compared to rVRQ at 1200 (100% inhibition control) and 100 nM (direct comparison control). Inhibitors that appeared to have higher inhibition than the rVRQ were chosen for further analysis and the estimation of the IC50 value. To do this, a range of mutant concentrations were added to amplification reaction and then the samples underwent PMCA as previously described. PK digestion was performed and 2.5 µl of each sample was added on dot blots in duplicates and incubated with

primary and secondary antibodies, as described previously. Membranes were visualised using ChemiDoc Imaging System (BioRad).

Table 2.4.2. rPrPs mutants at 136 position details.

Mutation[1]	Mutant name	MW[2] [Da]
V	rVRQ	22782.19
V → I	rIRQ	22796.22
V → F	rFRQ	22830.24
V → N	rNRQ	22797.16
V → S	rSRQ	22770.14
V → R	rRRQ	22839.25
V → C	rCRQ	22786.22
V → L	rLRQ	22796.22
V → Y	rYRQ	22846.23
V → H	rHRQ	22820.2
V → K	rKRQ	22811.2
V → G	rGRQ	22740.1
V → W	rWRQ	22869.3
V → Q	rQRQ	22811.2
V → P	rPRQ	22780.2
V → T	rTRQ	22784.2
V → D	rDRQ	22798.2
V → E	rERQ	22812.2
V → M	rMRQ	22814.3

[1]V – valine, I – isoleucine, F – phenylalanine, N – asparagine, S – serine, R – arginine, C – cysteine, L – leucine, Y – tyrosine, H – histidine, K – lysine, G – glycine, W – tryptophan, Q – glutamine, P – proline, T – threonine, D – aspartic acid, E – glutamic acid, M – methionine;
[2]Molecular weight (MW) was calculated from its protein sequence using the ExPASy calculator, Da – daltons

2.4.9 Analysis

The dotblot images were analysed using the ImageJ software **(Figure 2.4.2)** (Schneider, Rasband and Eliceiri, 2012). First of all, average light density for a defined spot area was measured for 100 % inhibition control. Then, this value was subtracted from the average light density for all spots measured on that same blot. Percentage of inhibition was calculated and compared to either uninhibited or 100 nM rVRQ control. Values were plotted in GraphPad Prism. For all data distribution was established using normality tests. Then, equivalent parametric or non-parametric statistical test was used. In order to calculate the half maximal inhibitory concentration (IC50 values), non-linear regression analysis with log inhibitor versus response (normalised slope) model was used.

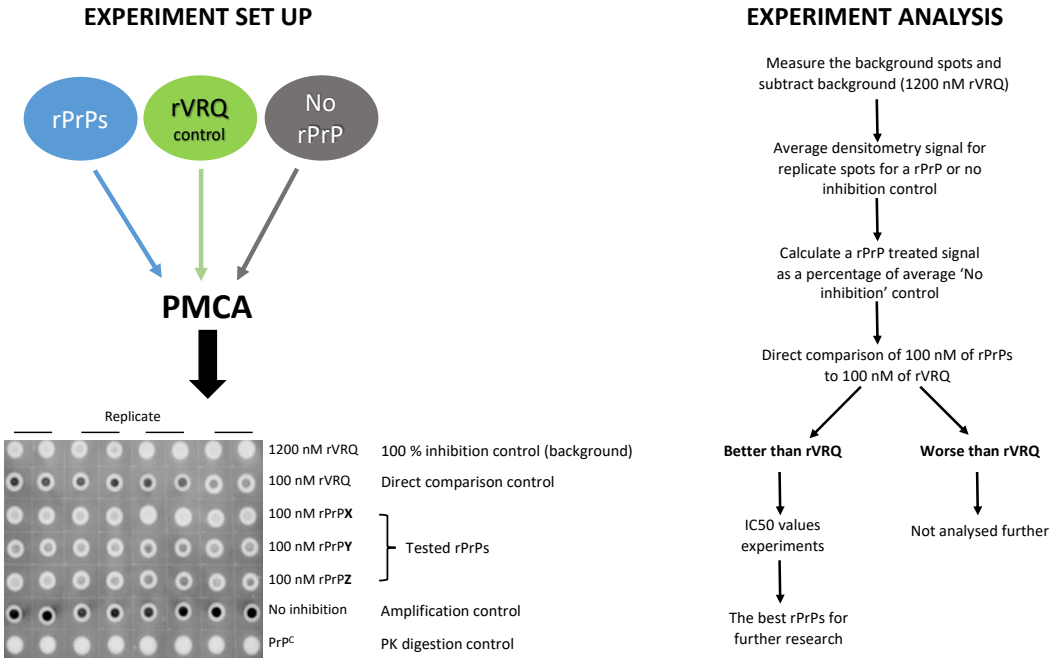

Figure 2.4.2 Flowchart of experiment set up and analysis for testing the rPrPs in PMCA. PrP^{Sc} was amplified in the absence or presence of rVRQ or different rPrPs. 1200 nM of rVRQ was treated as a background control, whereas 100 nM rVRQ was a direct comparison control. In first experiments rPrPs were added at 100 nM into the PMCA. PrP^{C} control was also included on the blot and acted as a background/PK digestion control. When dotblots were analysed, firstly the background spots for 1200 nM rVRQ were measured and subtracted from blot. Then, average densitometry signal for rPrPs and no inhibition control spots were measured. For each rPrP (including 100 nM rVRQ) percentage of no inhibition control average was calculated. The values were next compared to rVRQ at 100 nM. rPrPs that were better than rVRQ were further analysed in IC50 values experiments, whereas rPrPs worse than rVRQ were not analysed further.

2.5 Structural analysis of rPrP mutants at 136 position

In order to assess and predict the impact of specific mutation at 136 position in ovine PrP, structures of recombinant prion proteins were analysed. As an example of PDB data entry, we used previously deposited file 2N53. This entry showed the solution structure of ovine PrP with valine at 136 position (Munoz-Montesino *et al.*, 2016). We used this file to extract the NMR analysis in PYMOL by using the PYMOL commend '`show all_states`' (Schrodinger, 2010). The ClustalW on-line tool was used for sequences alignment (Higgins, Thompson and Gibson, 1996). Then, rPrP structures pdb files were created using the online tool DynaMut with the mutation effect prediction resource (Rodrigues, Pires and Ascher, 2018). Pdb files were downloaded and data were analysed using PyMOL software (Schrodinger, 2010).

2.6 Inhibition of α-synuclein misfolding with rRRQ

Recombinant α-syn was a gift from a research group member Juan Fernandez Bonfante. Methodology for α-syn fibrils formation was optimised and described by Juan Bonfante Fernandez (personal communication). Briefly, 20 μM of monomeric α–synuclein was spiked with misfolded α–synuclein from PD patients brains or healthy control brains. Recombinant prion protein with R at 136 position (rRRQ) at concentrations 1, 50 or 100 nM was added into the reactions. In addition, also rKRQ and PRQ were added at 50 nM. Then, samples were amplified with 40 seconds of sonication and 29 minutes 20 seconds of incubation at 37 °C with power was set to 100 – 120 W (S-4000 Misonix, Ultrasonic Liquid Processors). Amplification was performed for 72 h. Next, samples were digested with PK at 17 μg/ml and products were analysed on the NuPAGE™ 4-12 % Bis-Tris gels (cat. no. NP0322, Invitrogen) in 1 x MES buffer (cat. no. NP0002, Invitrogen). Gels were run for 30 minutes at 200 V and stained with Instant Blue **(2.4.6)**.

2.7 Rov9 cell culture

Rov9 are a cell line created from rabbit kidney epithelial cells - RK13. These cells were transfected with pTRE plasmid containing ovine PrP sequence (VRQ variant). In addition, the level of ovine PrP is controlled by the presence of doxycycline (Vilette *et al.*, 2001). Rov9 cells were a gift from Hubert Laude (Virologie et Immunologie Moléculaires, Jouy-En-Josas, France). Cells were visualised using the inverted biological microscope (Ceti). All cells images were taken with Panasonic DMC-FS7 camera and cropped in GIMP (version 2.10.14). Moreover, Rov9 cells persistently infected with SSBP1 were a gift from Dr Fiona Houston (Roslin Institute). These cells were used as a comparison to our infected cells.

2.7.1 Rov9 cells maintenance

The main stock of Rov9 cells was maintained in Eagle's Minimum Essential Medium (EMEM, cat. no. M2279, Sigma) at 37 °C, 5 % CO_2 in a humidified incubator. To generate this, the liquid nitrogen stored cell stock was thawed and immediately re-suspended in EMEM with 5 % (v/v) Fetal Bovine Serum (FBS, Fisher Scientific) and 1 % (v/v) of total pre-mixed solution of Penicillin, Streptomycin and Glutamine (Pen/Strep/Glu, cat. no. G1146, Sigma). Media with addition of FBS and Pen/Strep/Glu is referred to as media complete. Next, cells were centrifuged at 300 x g for 5 minutes and supernatant was discarded. Then, Rov9 cells were re-suspended in 5 ml of EMEM complete and grown in a 25 cm^2 tissue culture flask (Greiner Bio-One) at 37 °C, 5 % CO_2.

After Rov9 cells reached around 70-80 % confluence, sub passage of cells was performed. Briefly, flasks with Rov9 cells were washed with Dulbecco Phosphate Buffered Saline (D-PBS) with $MgCl_2$ and $CaCl_2$ (cat. no. D8662, Sigma). Then, cells were detached from the tissue culture flasks using 0.25 % (w/v) trypsin – EDTA (cat. no. T4049, Sigma). Cells were collected in complete media to neutralise the trypsin-EDTA

solution and centrifuged for 5 minutes at 300 x g. Supernatant was discarded, Rov9 cells were washed in D-PBS and centrifuged again. The wash step was repeated twice. Afterwards, cell pellets were re-suspended in EMEM complete. Part of the cells was mixed with 0.4 % trypan blue solution (cat. no. 15250-061, Gibco) in order to assess cell viability. Cell count and viability was analysed using the Neubauer Haemocytometer counting chamber and Ceti Inverted Microscope. Then, Rov9 cells were seeded at 1/5 or 1/8 ratio in EMEM complete. One T75 cm^2 flask (Greiner Bio-One) with Rov9 cells in EMEM complete was maintained for the whole experiment.

Cell culture experiments were interrupted by a sudden University laboratory closure due to the Covid-19 pandemic. Therefore, samples were collected and frozen with addition of freezing mix (80% (v/v) FBS and 20 (v/v) % of dimethylsulfoxide (DMSO)) at -80 °C.

2.7.2 Rov9 cells storage

For longer storage cells were frozen and stored at either -80 °C or in liquid nitrogen. For both storage strategies, cells were prepared as follows. When Rov9 cells reached about 80 % confluence, they were washed 1 x with D-PBS, trypsinised and counted as described in chapter **2.7.1**. Next, freezing mix and media complete were mixed together in 1:1 ratio and slowly added on the cells. The cell density was 1 x 10^6 cells/ml. For longer term storage, cells were moved to a container with isopropanol and placed at -80 °C for 3 days. After this period, cells were moved to liquid nitrogen and stored until required. For short term storage, cells were immediately placed on ice and then at -80 °C until required.

2.7.3 Induction of PrP expression in Rov9 cells

Rov9 cells were seeded on T75 cm^2 flask at a density 0.7 x 10^6 cells or 12 well plate (ThermoFisher Scientific) at 0.1 x 10^6 cells per well. Seeded cells were grown for 48 h or until they reached 90 % confluence in EMEM complete. Then, in order to express the ovine PrP^C in Rov9 cell membranes, cells were stimulated with 1 µg/ml of doxycycline (cat. no. D9891, Sigma) and incubated for 48 h in OPTI MEM complete (5 % FBS, 1 % Pen/Strep/Glu, cat. no. 11524456, Gibco) for 48 h. Next, cells were washed with D-PBS and lysed in lysis buffer (50 mM Tris, 0.5 % (v/v) Triton X-100, 0.5 % (w/v) sodium deoxycholate, pH 7.4) for 10 minutes on ice. Then, cell lysates were centrifuged for 2 minutes at 400 x g. Finally, supernatants were collected and stored at -20 °C for further analysis.

2.7.4 Investigation of PrP^{Sc} amplification in sPMCA from scrapie isolates used as inocula in cell culture

sPMCA with multiple rounds of sonication and incubation at 37 °C was used for amplification of scrapie isolates used in cell culture to assess their amplification in VRQ/VRQ substrate. For that purpose, 10 µl of each 10 % SSBP1, PG1207/03, PG1212/03 and PG1517/01 (all VRQ/VRQ) were mixed with 90 µl of negative brain

homogenates (B16) and amplified for round 1 (24 h). After round 1, PMCA reaction products were diluted 1/3 into fresh PrP^C substrate (negative brain homogenate) and amplified for another 24 h (up to 5 PMCA rounds were performed). In addition, serial PMCA for PG1361/01 was also performed and 0.5 µl of 10 % scrapie PG1361/05 brain homogenate was added into every reaction to a final reaction volume 100 µl. Amplification conditions were as detailed in chapter **2.4.1**.

2.7.5 Infection of Rov9 cells with scrapie

Rov9 cells were seeded on 12 well plates at 0.1 x 10^6 cells per well and grown at 37 °C in EMEM complete for 48 h. Then, media was discarded and cells were washed 1 x with D-PBS. OPTI MEM complete with or without 1 µg/ml of doxycycline was added and cells were incubated for 48 h. Next, infectious inoculas were prepared (as specified for each method below) and 1 ml of media with or without PrP^{Sc} was added onto the cells and incubated for 3 days at 37 °C, 5 % CO_2 in a humidified incubator. After this time (72 h post infection), media was discarded and fresh OPTI MEM media complete with or without 1 µg/ml of doxycycline was added on the cells and incubated for 48 h. After that time (120 h post infection), media was discarded and cells were washed with 1 x D-PBS. Next, D-PBS was discarded and cells were passaged. Briefly, 500 µl of 1 x Trypsin/EDTA was added and cells were incubated for 5 minutes at 37 °C, 5 % CO_2. Cells were then collected into sterile 1.5 ml tube and 500 µl of media complete was added. Cells were washed 2 x with sterile PBS and then seeded further on two wells on 12-well plates in OPTI MEM complete with or without 1 µg/ml of doxycycline. This was the passage 1 of cells infected with scrapie. Then, cells were grown for 7 days. Afterwards, cells from 1 well were collected using 1 x Trypsin/EDTA and these cells were seeded further, whereas the cells from second well was washed 2 x with PBS and lysed with 500 µl of lysis buffer. These steps were repeated for every infection condition from passage 2 onwards.

2.7.5.1 Rov9 cells infection with brain homogenates

Healthy and scrapie brain homogenates were used for Rov9 cells infection. Briefly, 10 % negative brain homogenate – B16 (VRQ/VRQ) and 10 % scrapie positive brain homogenates SSBP1 (VRQ/VRQ), PG1207/03 (VRQ/VRQ), PG1212/03 (VRQ/VRQ), PG1517/01 (VRQ/VRQ) or PG1361/05 (ARQ/VRQ) were added on non-induced or induced for 48 h with 1 µg/ml doxycycline Rov9 cells at ratios 1/500, 1/80 and 1/40 (2 µl, 12.5 µl or 25 µl of 10 % brain per 1 ml of media, respectively). In addition, brain homogenates buffer controls were added on the cells at the same ratios as scrapie brain homogenates. These included conversion buffer (0.5 % (w/v) sodium deoxycholate, 0.5 % (v/v) NP-40 in PBS) control and brain homogenate buffer (0.15 M NaCl, 1 % (v/v) Triton X-100, 4 mM EDTA, Protease Inhibitor Cocktail) control. Next, cells were incubated with inoculas in OPTI MEM complete with or without 1 µg/ml doxycycline for 72 h and then media was replaced with OPTI MEM complete with or without 1 µg/ml

doxycycline. Culture was maintained for another 48 h, after which 1 passage was performed.

In other alternative experiments, scrapie brain homogenates SSBP1 (VRQ/VRQ), PG1207/03 (VRQ/VRQ), PG1212/03 (VRQ/VRQ) or PG1517/01 (VRQ/VRQ) aliquots were heated at 80 °C for 20 minutes sonicated for 2 minutes (180-200 W) (4000 Misonix, Ultrasonic Liquid Processors) at 37 °C. Treated brain homogenates were mixed with OPTI MEM media with or without 1 µg/ml doxycycline and added on the induced Rov9 cells in 1/40 (25 µl of 10 % brain for PG1207/03, PG1212/03, PG1517/01) or 1/80 (12.5 µl of 10 % brain homogenate for SSBP1) ratio. Then, cells were incubated for 72 h at 37 °C, 5 % CO_2 and infectious inocula were replaced with OPTI MEM complete with or without 1 µg/ml doxycycline. Samples were incubated for further 48 h, after which cells were passaged. After splitting, cells were further maintained for 7 days before passaging further.

2.7.5.2 Inoculation of Rov9 cells with PrP^{Sc} precipitated from brain homogenates using silicon dioxide

Silicon dioxide (SiO_2) has been reported to bind and precipitate resistant prion protein (Rees *et al.*, 2009). Therefore, it was used here to concentrate PrP^{Sc} from brain homogenates. Brain homogenates (10 or 20 % (w/v)) were prepared by mixing 50:50 with D-PBS. Then, 50 µl of each diluted brain homogenate was mixed with 25 µl of 20 % (w/v) SiO_2 slurry in PBS (cat. no. 637238, Sigma). Samples were sealed and incubated with rotation for 3 h at room temperature. Then, samples were centrifuged for 10 minutes at 400 x g. Supernatants were collected for further analysis, whereas precipitates were re-suspended and washed with in 0.1 % (w/v) SDS. Then, samples were centrifuged again at 400 x g for 3 minutes. Supernatants were collected for further analysis. Each pellet was then re-suspended in 1 % (w/v) SDS and vortexed for 2 minutes. Next, samples were centrifuged at 400 x g for 2 minutes and supernatants containing PrP^{Sc} were collected.

In order to exchange the buffer from 1 % (w/v) SDS to D-PBS that is suitable for cell culture, samples were precipitated using absolute methanol (MeOH). Briefly, the PrP^{Sc} solution was mixed with ice-cold MeOH in 5:1 ratio and incubated for 1.5 h at -20 °C. Then, samples were centrifuged at 21 000 x g for 30 minutes at RT. Supernatants were discarded and protein pellets were re-suspended in D-PBS. For short term storage, samples were kept at 4 °C, whereas for long term storage, samples were kept at -20 °C. 10 or 20 µl of these SiO_2 extracted products were added per 1 ml of OPTI MEM complete with 1 µg/ml doxycycline on cells and incubated for 72 h at 37 °C, 5 % CO_2. After 72 h, media was discarded and fresh OPTI MEM complete with 1 µg/ml doxycycline was added on cells and incubated in the same conditions for further 48 h. Cells were then passaged and incubated for another 5 days in OPTI MEM complete with 1 µg/ml doxycycline. After

5 days, half of the cells were lysed, PK digested and analysed on western blotting, whereas the other half was seeded on a cell culture dish and grown further.

2.7.5.3 Inoculation of Rov9 cells with PrP^{Sc} precipitated from brain homogenates using NaPTA

Sodium phosphotungistic acid (NaPTA) has been reported to bind misfolded PrP^{Sc} and allows the purification and concentration PrP^{Sc} from brain homogenates (Safar *et al.*, 1998). In order to precipitate PrP^{Sc} from 10 % brain homogenates SSBP1, PG1207/03 (VRQ/VRQ genotypes), PG1361/05 (ARQ/VRQ) were digested with PK at 50 µg/ml for 1 h at 37 °C. Digestion was stopped by freezing the samples at -80 °C for 5 minutes. Then, samples were warmed to RT. 4 % (w/v) NaPTA solution (cat. no. P6395, Sigma) was prepared, pre-warmed at 37 °C and added to PK digested samples to a final NaPTA concentration 0.3 % (v/v). Samples were incubated for 30 minutes at 37 °C and then centrifuged for 30 minutes at 20 000 x g. Supernatants were removed and pellets were re-suspended in D-PBS. For short term storage, samples were kept at 4 °C, whereas for longer storage samples were kept at -20 °C.

30 µl of NaPTA precipitated PrP^{Sc} were added per 1 ml of OPTI MEM complete with 1 µg/ml doxycycline and incubated for 72 h at 37 °C, 5 % CO_2. Then, scrapie inoculas were discarded and fresh OPTI MEM complete with 1 µg/ml doxycycline was added on the cells and incubation at 37 °C, 5 % CO_2 was performed for another 48 h. After that time (120 h post infection, 5 dpi) cells were collected, frozen and stored until further notice at -80 °C. This experiment was interrupted by sudden facility closure due to Covid-19 pandemic. When possible, cells were retrieved from -80 °C storage and analysed further.

2.7.6 BCA assay

For protein content estimation in cell lysates, Pierce™ BCA Protein Assay Kit was performed as described in company protocols for a microplate procedure (ThermoFisher Scientific). Briefly, BSA standards at concentrations 2000 – 0 µg/ml were prepared in lysis buffer. Each standard and sample in duplicate (25 µl) were added into wells (Nunc-Immuno Maxisorp ELISA 96 well plate; ThermoFisher Scientific). Next, 200 µl of BCA Working Reagent was added per well and plates were incubated for 30 minutes at 37 °C. After the incubation plates were read at 595 nm (FLUOstar, BMG Labtech). Blank absorbance values (lysis buffer only) were subtracted from each measurement and average values were calculated for each sample and standard. Then, values were plotted against concentration and the amount of protein in samples was read from the curve.

2.7.7 PrP^{res} concentration from cell lysates

500 µg of protein from each protein lysate was digested with 20 µg/ml of PK for 1 h at 37 °C. The digestion was stopped by freezing at -80 °C for 5 minutes. After thawing, samples were centrifuged for 1 h at 20 000 x g. Supernatant was removed and PrP^{res}

pellets were re-suspended in 15 µl of PBS. 5 µl of 4 x LDS Sample Buffer (cat. no. NP0008, Invitrogen) with 5 % (v/v) β-mercaptoethanol was added and samples were boiled for 10 minutes at 100 °C. Then, SDS-PAGE, western blotting and immunodetection with SHA31 antibodies were performed as described previously **(2.4.6, 2.4.7)**.

2.7.8 The detection of PrP^{res} in cell lysates using serial PMCA

For the first round of PMCA, 10 µl of each cell lysate were mixed with 90 µl of TSE negative brain homogenate B16 (VRQ/VRQ). For negative control, 10 µl of lysis buffer instead of cell lysate were mixed with 90 µl of B16. For a positive control, scrapie PG1361/05 (ARQ/VRQ) diluted 1/10 diluted in lysis buffer was used. Each condition was run in triplicates. Samples were amplified for 24 h with 40 seconds of sonication and 29 minutes 20 seconds incubation at 37 °C cycles with power set to 180 – 200 W (S-4000 Misonix, Ultrasonic Liquid Processors). Then, samples were diluted 1/3 into fresh B16 and amplified for another 24 h. Five rounds of PMCA were performed. All amplification products were stored at -20 °C for further analysis. The dotblot and western blot analysis was performed as previously described.

2.7.9 Preventing infections of Rov9 cells with recombinant PrPs

rVRQ, rRRQ, rKRQ, rPRQ and rARR were concentrated and dialysed prior to each experiment as described in chapter **2.3.4**. In addition, Bradford assay was performed to estimate the protein content before every protein use **(2.3.3)**. 50 or 250 nM of each recombinant protein was mixed with heated and sonicated 10 % SSBP1 brain homogenate (VRQ/VRQ) in OPTI MEM media with or without 1 µg/ml doxycycline. Brain/media/rPrP mixture was incubated for 1 h at 37 °C and added on the cells on the infection day. rPrP was kept on the cells after each cells subculture.

2.7.10 Curing Rov9 PrP^{res} infections with recombinant PrPs

Persistently infected with SSBP1 (VRQ/VRQ) cells were seeded on the 12 well plate with density 0.1 x 10^6 cells per well with or without 250 nM of each rPrPs. Cell were incubated in OPTI MEM complete with 1 µg/ml doxycycline for 4 days at 37 °C, 5 % CO_2 humidified incubator. After 4 days, cells were washed 2 x with PBS and 500 µl of lysis buffer was added. Cells were lysed on the plate for 10 minutes, lysates were collected and centrifuged for 5 minutes at 400 x g. Supernatants were collected and stored at -20 °C for further analysis.

2.7.11 Data analysis

The densitometry for all western blots was measured in ImageJ using the gel analysis tool (Schneider, Rasband and Eliceiri, 2012). Where possible data distribution was established using normality tests. According to the values distribution, equivalent statistical tests were used in order to analyse the data.

Chapter 3: The production of rPrP mutants at position 136

3.1 Introduction

TSE diseases have been recognised since the first description of scrapie in 1853 but, they still lack any successful therapeutic (Stockman, 1913; Forloni *et al.*, 2013). Many agents have been tested in both *in vitro* and *in vivo* with few then being assessed in clinical trials. Amongst them are drugs, antibodies, peptides but also recombinant prion proteins. All of these target cellular PrP, PrP^{Sc} or the protein misfolding process (Trevitt and Collinge, 2006).

In ovine PrP three common polymorphisms at 136, 154 and 171 positions have been recognised as having serious impact on scrapie development. The paradigm is that VRQ are the most susceptible to classical scrapie and ARR the most resistant (DEFRA, 2001). This research will focus on using recombinant ovine PrP with variations at position 136 as a therapeutic agent for prion disease. Previous research demonstrated that recombinant ovine PrP with valine (VRQ) acted as a better inhibitor *in vitro* for various prion diseases isolates than PrP with alanine (ARQ) at 136 position (Workman, Maddison and Gough, 2017). Moreover, it was also tested whether ARR also inhibit the *in vitro* amplification of isolates. The research showed that the rARR was the least potent inhibitor with the highest IC50 value compared to VRQ, ARQ and hamster recombinant PrPs (Workman, Maddison and Gough, 2017). The first aim of this research was to obtain recombinant ovine PrPs with different mutations at 136 position.

3.2 Results

3.2.1 Availability of rPrP mutants

Within the study, valine at position 136 in rVRQ was mutated into the other 18 amino acids. Clones of nine rVRQ mutants within the expression vector pET22b(+) were available at the outset of the study: IRQ, FRQ, NRQ, SRQ, RRQ, CRQ, LRQ, YRQ and HRQ. For these clones, the presence of the specific mutation was confirmed by Sanger Sequencing. The other 9 recombinant prion protein clones (KRQ, GRQ, WRQ, QRQ, PRQ, TRQ, DRQ, ERQ and MRQ) were produced by site directed mutagenesis during this study.

3.2.2 Inverse PCR for making recombinant prion proteins

Firstly, inverse PCR was carried out with positive samples (with the DNA of interest) and compared to negative samples (no template). DNA for 8 samples was confirmed as positive on the agarose gel (producing a band of ~6 kb), while there was no PCR product for one sample, rQRQ **(Figure 3.2.1)**. Furthermore, the forward primer for QRQ (1) with mutation codon CAG did not work in different amplification temperatures in the inverse PCR **(Figure 3.2.2**, **A),** therefore a new forward primer for rQRQ with a CAA codon to mutate position 136 to glutamine (rPrP-For-Q(2)) was designed. Inverse PCR was performed with the rPrP-For-Q(2) primer and annealing temperatures in the range 58 – 60 °C were tested. In all mentioned temperatures, PCR product was positive **(Figure 3.2.2**, **B**). All clone variants were produced and Sanger sequenced to confirm the presence of the correct mutations.

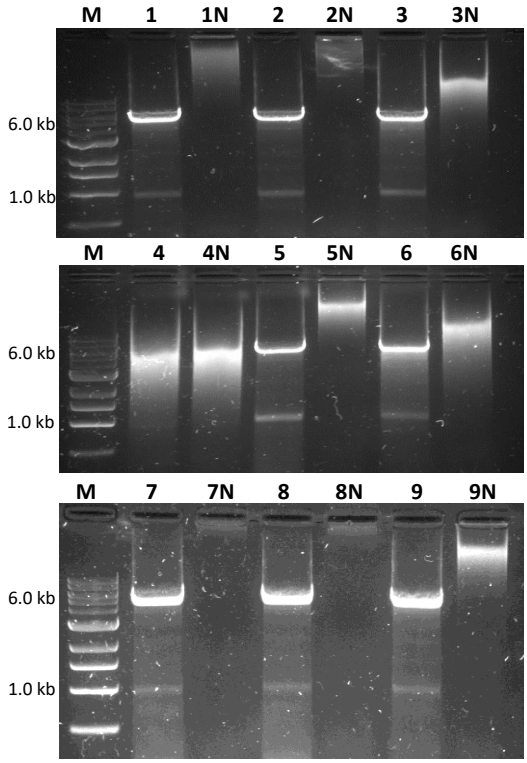

Figure 3.2.1. Inverse PCR amplification of site directed PrP mutants. Template vector (pet22b(+)) containing the *Prnp* gene for rVRQ was amplified by inverse PCR (annealing temperature 61 °C) using primers to mutate the equivalent codon at position 136 in ovine PrP. DNA products were assessed for a band at 6.2 kb on 1 % agarose gel. For some negative samples, bands were visible on the gel and could suggest primers dimerization or samples contaminants. M – DNA marker, 1 – KRQ, 2 – GRQ, 3 – WRQ, 4 – QRQ, 5 – PRQ, 6 – TRQ, 7 – DRQ, 8 – ERQ, 9 – MRQ, N – the equivalent negative samples.

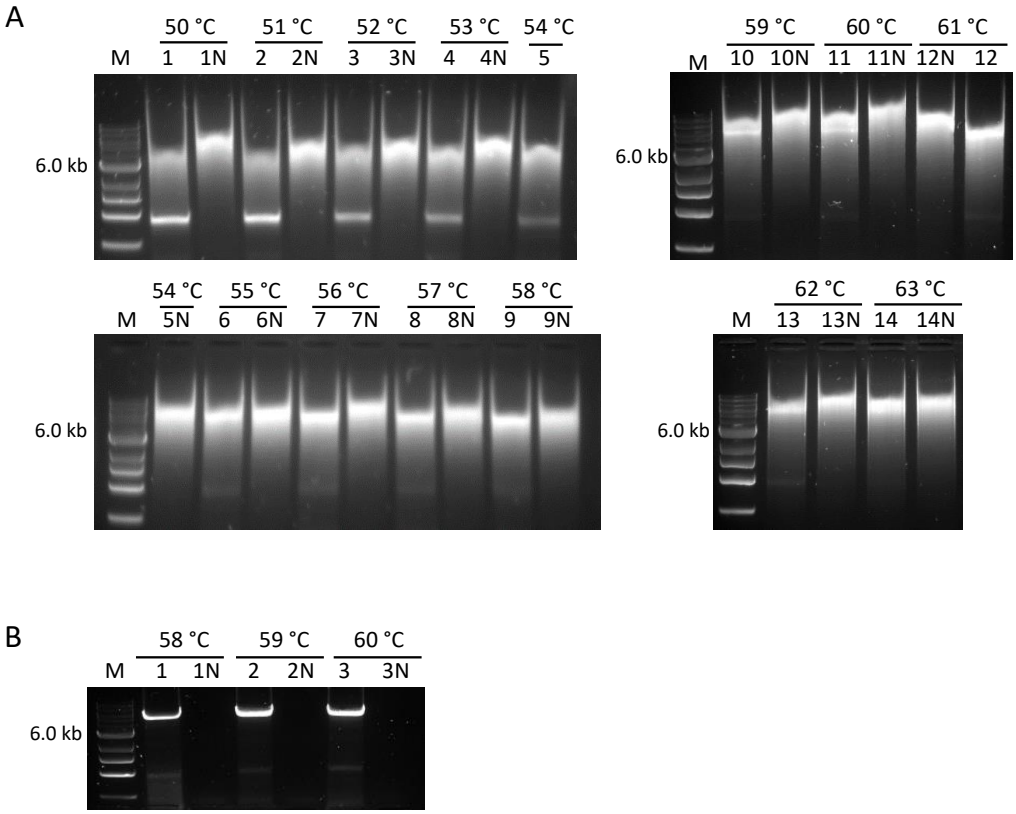

Figure 3.2.2. Gradient inverse PCR amplification of rQRQ with rPrP-For-Q(1) primer **(A)** and rPrP-For-Q(2) primer **(B)**. Template vector (pet22b(+)) containing the *Prnp* gene for rVRQ was amplified by gradient inverse PCR to mutate the codon at position 136 in ovine PrP. The annealing temperatures **A** – 50-63 °C using primer rPrP-For-Q(1) and **B** – 58-60 °C using the primer rPrP-For-Q(2) were tested. DNA products were assessed for a band at 6.2 kb on 1 % agarose gel. M – DNA marker, 1 – 14 – different annealing temperatures, N – equivalent negative control (no DNA template).

3.2.3 Purification of recombinant prion proteins

Recombinant prion proteins were expressed and purified. Bacteria were grown and purified using FPLC using purified by immobilised metal affinity chromatography (IMAC) taking advantage of the metal binding properties of the PrP octapeptide repeat region. Eluted FPLC fractions were analysed by SDS-PAGE and gels stained with Instant Blue **(Figure 3.2.3)**.

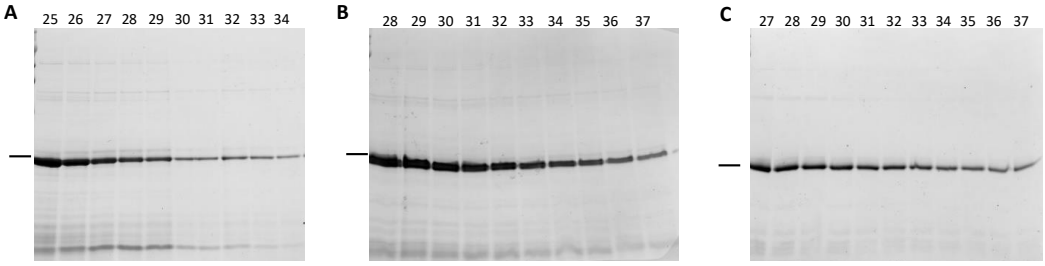

Figure 3.2.3. Representative SDS-PAGE gel analysis of rVRQ, rRRQ and rERQ (~23 kDa) purification fractions. 15 µl of each fraction were analysed on the gel stained with Instant Blue. **A** – rVRQ, **B** – rRRQ, **C** – rERQ, 25 – 37 eluted fractions. A 24 kDa marker is indicated on the left side of each gel.

For eluate fractions containing purified rPrP were pooled and stored at -80 ˚C with addition of 20 % sucrose. Overall, from 1 L of bacterial culture, from 10 – 15 ml of pure rPrP were collected with concentration range being from 0.3 to 0.5 mg/ml.

3.2.4 Dialysis of recombinant prion proteins

Before use, the concentrations of thawed rPrP stocks were analysed by Bradford Assay to re-estimate protein content. When concentrations were below 0.5 mg/ml, rPrPs were concentrated using Pierce™ Protein Concentrator PES with 10 kDa molecular weight cut off. All rPrPs were then dialysed and protein bands were analysed on SDS-PAGE gels. For rIRQ, rFRQ, rNRQ, rSRQ, rRRQ, rCRQ, rLRQ, rYRQ and rHRQ only dialysed fractions were analysed on the gel **(Figure 3.2.4, A)**, whereas for rVRQ, rKRQ, rGRQ, rWRQ, rQRQ, rPRQ, rTRQ, rDRQ, rERQ, rMRQ purified non-dialysed and dialysed proteins were analysed **(Figure 3.2.4, B)**. Purity of dialysed PrPs was estimated by densitometry analysis using ImageJ.

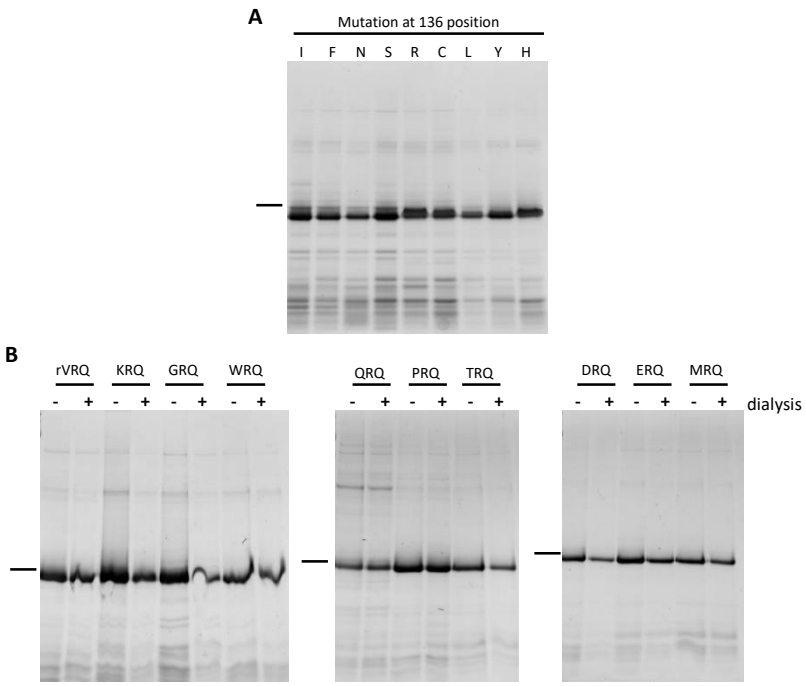

Figure 3.2.4. Examples of purity analysis and the effects of dialysis on recombinant rPrPs. **A** – dialysed rIRQ, rFRQ, rNRQ, rSRQ, rRRQ, rCRQ, rLRQ, rYRQ and rHRQ. **B** – non-dialysed (-) and dialysed (+) rVRQ, rKRQ, rGRQ, rWRQ, rQRQ, rPRQ, rTRQ, rDRQ, rERQ and rMRQ. Each rPrP was purified, fractions were pooled together, concentrated, where necessary, and dialysed for 1 h with PBS with 10 % sucrose, 0.25 M imidazole and then 1 h with PBS only. 15 µl of each fraction were analysed on the gel stained with Instant Blue. A 25 kDa marker is indicated on the left side of each gel. The purity of each rPrP was calculated using the ImageJ densitometry tool: the density of entire gel lane for each rPrP was measured and compared to the main band density. The percentage of protein purity was calculated from obtained in the software values.

The representative purity for dialysed rPrPs calculated according to the SDS-PAGE gels analysis **(Figure 3.2.4)** is as follows rIRQ: 38 %, rFRQ: 48 %, rNRQ: 59 %, rSRQ: 36 %, rRRQ: 38 %, rCRQ: 46 %, rLRQ: 64 %, rYRQ: 43 %, rHRQ: 43 %, rVRQ: 60 %, rKRQ: 56 %, rGRQ: 76 %, rWRQ: 72 %, rQRQ: 66 %, rPRQ: 50 %, rTRQ: 78 %, rDRQ: 77 %, rERQ: 62 % and rMRQ: 69 %. In addition, dialysis caused the reduction of protein concentration by around 30-40 %. Moreover, different batches of recombinant proteins needed to be made and the process was consistent. This included re-purification and/or re-dialysis. All dialysed rPrPs were stored at 4 °C until use.

3.3 Discussion

The change from alanine to valine at 136 position seems to have significant impact on the inhibition of misfolding process for prion diseases isolates (Workman, 2017; Workman, Maddison and Gough, 2017). To investigate whether other amino acid substitutions at this position in the prion protein will possess greater inhibitor properties to rVRQ, the codon for valine at 136 was mutated into other amino acids. While some of the recombinant proteins were previously made within the research group (IRQ, FRQ, NRQ, SRQ, RRQ, CRQ, LRQ, YRQ and HRQ), the others were produced during this study using site directed mutagenesis. This method allowed the successful mutation and production of the other recombinant prion proteins (KRQ, GRQ, WRQ, QRQ, PRQ, TRQ, DRQ, ERQ, MRQ). To my knowledge and to date, mutation of 136 position of ovine PrP into other amino acids was performed for the first time. rARQ ($alanine_{136}$) was not produced and analysed in this study as it was previously determined as less potent than rVRQ inhibitor (Workman, 2017; Workman, Maddison and Gough, 2017). In contrast, rVRQ which was also analysed previously, was used as a control in this study.

The purification of cellular PrP from brain (Turk *et al.*, 1988; Pan, Stahl and Prusiner, 1992; Pergami, Jaffe and Safar, 1996) usually resulted in low protein recovery: up to 20 % of total PrP^C from brains and low yield (Pan, Stahl and Prusiner, 1992; Pergami, Jaffe and Safar, 1996). Therefore, PrP brain isolation protocols were replaced with recombinant protein production systems. In this research, we used the NovaBlue DE3 *E. coli* organism to produce recombinant ovine PrP. This protein expression system is highly accessible and produces a relatively high quantity of bacteria expressing recombinant protein in a short period of time (Rosano and Ceccarelli, 2014).

In this research, recombinant ovine PrP was purified exploiting the ability of the octapeptide repeats within the prion protein sequence to bind metals. This allowed the purification of the prion protein that does not include any additional affinity tags in a one-step purification (Rezaei *et al.*, 2000; Yin, Zheng and Tien, 2003). Purification of recombinant prion protein based on metal affinity of octapeptide repeats was firstly described by Razaei's group and produced stable and monomeric PrP (Rezaei *et al.*, 2000). Here, we used Sepharose columns charged with copper ions that display the strongest affinity to PrP compared to nickel, cobalt or zinc (Pan, Stahl and Prusiner, 1992). Recovery of the recombinant prion protein was maximised by the use of urea to solubilise inclusion bodies. In addition, the FPLC was also carried out under denaturing conditions. Previously, in order to obtain recombinant PrP, different tags were added to the protein sequence. First of all, production of hamster or human prion protein with glutathione S-transferase (GST) tag was described (Weiss *et al.*, 1995; Völkel, Blankenfeldt and Schomburg, 1998; Corsaro *et al.*, 2002). The addition of GST tag increased the solubility and stability of rPrP. Moreover, purification of human PrP fragment (90-231) was possible in native conditions. In this case, PrP did not accumulate within inclusion bodies but was expressed in the cytosolic fractions of

bacterial cells, therefore was accessible with native purification conditions (Corsaro *et al.*, 2002). However, addition of the GST tag caused problems with isolation of the PrP or the obtained product was unstable (Weiss *et al.*, 1995). Addition of GST tag added extra steps to the procedure with one being addition of detergents like Triton X-100 to increase the protein-tag complex solubility (Bell *et al.*, 2013). Moreover, a 26 kDa GST tag has a propensity to dimerize, that could affect the properties of PrP (Kimple, Brill and Pasker, 2013). Alternatively, a poly-histidine tag has been attached to either C- or N-terminus of bovine or human PrP. The PrP was then purified using denaturing conditions on purification columns charged with Ni^{2+} ions (Negro *et al.*, 1997; Jackson *et al.*, 1999; Shin *et al.*, 2008). Again, addition of the poly-histidine tag can alter the properties of the rPrP.

After the purification, only the purest PrP fractions were pooled together and kept for further analysis. The method used here is consistent with the previous research, where recombinant ovine VRQ, ARQ, ARR and hamster PrP were purified (Workman, 2017). Additionally, all recombinant proteins in this research were produced using the same methodology. After purification, dialysis was performed to remove the imidazoles and sucrose from the final PrP pool. It was previously found that the presence of imidazoles has interfered with the *in vitro* amplification of bovine and ovine BSE but not with classical scrapie (Workman, 2017). In this research, each rPrP was dialysed in order to remove the co-eluted proteins and imidazoles from the buffer so that the rPrP produced in this research were consistent with previous analysis of rPrP inhibition during PMCA (Workman, 2017). Analysis of the purity of the recombinant proteins demonstrated that it was contaminated with relatively low amounts of smaller PrP fragments or co-eluting bacterial proteins (Mehlhorn *et al.*, 1996). However, the rVRQ produced in this research had the same degree of inhibition as the one reported by Workman *et al.* (Workman, Maddison and Gough, 2017). This suggest that the presence of minor co-eluted protein did not affect the PrP inhibition properties.

Chapter 4: Quantification of the ability of rPrP mutants at position 136 to inhibit prion replication

4.1 Introduction

The importance of successful development of therapeutic agents for prion diseases increased after the BSE outbreak in the UK that resulted in a new prion disease – vCJD (Will *et al.*, 1996). The pace of prion research accelerated after the development of PMCA, a method that allows in effective *in vitro* replication of prions, assisting in the development of diagnostics and also providing a model to screen for potential therapeutics (Saborio, Permanne and Soto, 2001). It has been described that the *in vitro* produced disease associated PrP displayed similar characteristics to that isolated from diseased brains, like protease resistance, detergent resistance and infectivity (Saborio, Permanne and Soto, 2001; Shikiya and Bartz, 2011). PMCA allows to study of inhibition mechanisms for prion conversion in more detail and can be used in preliminary screening of inhibitory mechanisms of PrP^{res} formation. However, this method could not completely replace the cell culture models that are slower but an excellent, valuable and viable tool for screening prion diseases therapeutic compounds in the cellular context (Skinner *et al.*, 2015; Moda, Bolognesi and Legname, 2019). The limitations of cell culture are the limited number of natural prion isolated that can be used to infect cells and in contrast, PMCA has been shown to amplify most prion isolates (Moda, Bolognesi and Legname, 2019). In therapeutic agents screening, PMCA has been used in a few cases. Barret *et al.,* studied the effect of quinacrine and tetracycline on 263K scrapie hamster brain homogenate amplification in healthy hamster brain homogenate using PMCA. In this work, both molecules reduced the formation of PrP^{res} in the *in vitro* amplification (Barret *et al.*, 2003). Furthermore, another research used PMCA as a tool for investigating the inhibition of CWD with quinacrine (Bian, Kang and Telling, 2014). PMCA was also used for inhibition effect study of an iron tetrapyrrole – Fe(III)-TMPyP (Fe(III)-meso-tetra(N-methyl-4-pyridyl)porphine). This potential therapeutic reagent was found to inhibit the cell-free amplification of mouse 22L and Dawson isolate scrapie strain (Massignan *et al.*, 2016).

Since the interaction between PrP^{C} and PrP^{Sc} is a crucial part for creating disease associated prion aggregates, it has been investigated what the impact is of any interruptions of this process (Seelig, Goodman and Skinner, 2016). The use of recombinant prion proteins in inhibition research is not a new concept. Moreover, both, heterologous and homologous PrPs were used in various studies. It was firstly determined in scrapie infected MNB cells (mouse neuroblastoma) that the expression of heterologous (hamster) PrP interfered with production and aggregation of PrP^{res} (Priola *et al.*, 1994). Later on, Horiuchi and co-workers using a different approach, cell free conversion assay, and demonstrated that hamster prion protein could interfere with mice PrP^{Sc} formation (Horiuchi *et al.*, 2000). Furthermore, expression of rabbit PrP was shown to stop the conversion to PrP^{res} in scrapie infected MNB cells (Vorberg *et al.*, 2003). In the research of Yuan and co-workers, heterologous (mouse, bank vole and bovine) and homologous PrP were screened for their inhibitory capabilities of iCJD amplification during PMCA. They found out that the heterologous PrPs inhibition was

much less efficient than homologous (Yuan *et al.*, 2013). The use of homologous PrP in inhibitory PMCA also was presented by Workman. He has investigated how addition of different variants of recombinant ovine PrP slowed down the PMCA process of different scrapie isolates. The results showed that the inhibition efficacy changed with the genotype of rPrP used (Workman, 2017; Workman, Maddison and Gough, 2017).

There has also been successful *in vivo* research in using recombinant hamster PrP in a scrapie mouse model. Animals were inoculated with RML-Chandler scrapie isolate and additionally rhamPrP was also administered into animals. The result of this study showed that the rhamPrP treatment not only delayed the onset of disease symptoms like loss of motor function but also increased the animal survival time (Skinner *et al.*, 2015). In addition, another study confirmed the previous research that mice infected with RML-Chandler strain and treated with high doses (0.7 mg/ml) of rhamPrP significantly increased the animal survival and delayed the symptoms onset. In addition, animals that were treated with high dose of heterologous recombinant PrP showed less PrP^{res} deposits in the brain in comparison to animals treated with low dose (0.35 mg/ml) or without rhamPrP (Seelig, Goodman and Skinner, 2016).

A proposed inhibition mechanisms suggests that homologous PrP binding to the resistant PrP^{Sc} blocks the possible structural binding sites for PrP^{C} (Yuan *et al.*, 2013). Furthermore, heterologous rPrP inhibition showed that recombinant PrP binding destabilises aggregates and no seed for further amplification were produced (Jarrett and Lansburry, 1993). An additional *in vivo* mechanism suggests that the presence of heterologous prion protein stimulated an immune response and this event resulted in a decrease of PrP^{Sc} production (Skinner *et al.*, 2015).

In this study, we investigated how the change of a single amino acid at position 136 in ovine PrP affected its ability to inhibit prion replication. Previously, it was determined that amongst rhamPrP, rARQ, rVRQ and rARR, rVRQ showed the highest inhibition (Workman, 2017). Here, rVRQ and 18 rPrPs with mutations at position 136 were tested for their ability to inhibit the replication of scrapie isolate PG1361/05 (ARQ/VRQ). It was demonstrated before that this particular classical scrapie isolate was easily amplified within one PMCA round (24 h), therefore it is an effective model for screening rPrP inhibition (Workman, 2017). Each rPrP was first tested at 100 nM, which is around the previously reported IC50 value for rVRQ. Then, rPrPs with more effective inhibition properties than rVRQ were characterised by calculating IC50 values. This value is an indicator of inhibitory efficacy and reports the concentration of rPrP at which the amplification of PrP^{res} was reduced by half (Georgakis *et al.*, 2020).

4.2 Results

4.2.1 rVRQ as a PrP^{Sc} replication inhibitor

rVRQ (recombinant prion protein valine$_{136}$) was tested in PMCA as a scrapie PG1361/05 ARQ/VRQ inhibitor. A range of rVRQ concentrations (1200 – 50 nM) were added into PMCA. Firstly, PK digested 1200 rVRQ inhibition and no inhibition products were analysed on western blot in order to see the characteristic for the scrapie triple band pattern **(Figure 4.2.1**, **B)**. In addition, also an amplified and PK digested TSE negative sample was analysed by western blot and no signal was produced. Next, inhibition samples and control samples were analysed on dotblots **(Figure 4.2.1, A)**. For reference, additional no inhibition and designated 100 % inhibition (1200 nM rVRQ, the low signals were likely to be from the PrP^{Sc} seeded into the PMCA reaction) controls were included in each experiment. In addition, to assess the PK digestion efficacy, PrP^{C} controls were displayed on each dotblot. All dotblots images were analysed using the ImageJ software. First of all, the average background value was calculated from density measures of all 1200 nM rVRQ repeats. Then, the average background value was subtracted from all other values. For each experiment, IC50 value was calculated according to signal intensities for each inhibitory sample to no inhibition samples **(Figure 4.2.2)**. The calculated IC50 values for three repeat experiments were 115 nM, 89 nM and 139 nM. The average IC50 value for rVRQ calculated from three independent experiments was 114 nM.

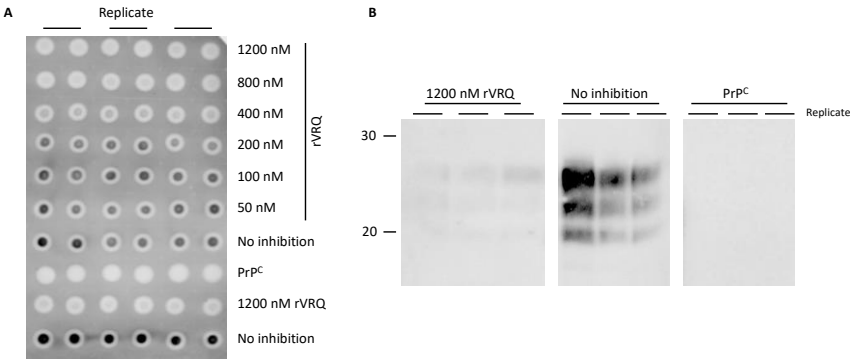

Figure 4.2.1. Representative analysis of rVRQ inhibition of ovine scrapie ARQ/VRQ PG1361/05. **A** – representative dotblot analysis. 2.5 µl of each sample was loaded on the nitrocellulose membrane in duplicate. Experiment was performed three times, each including triplicates analysis as shown here. Additional of 1200 nM rVRQ and 'no inhibition' controls were included. **B** – representative western blot showing almost complete inhibition of scrapie ARQ/VRQ amplification with 1200 nM rVRQ in comparison to 'no inhibition' samples. Western blots show the characteristic triple band pattern for scrapie. PrP^C – TSE negative brain substrate only control. Molecular weight is indicated on the left side on the blot (kDa). 20 µl of PK digested amplified products were analysed per reaction.

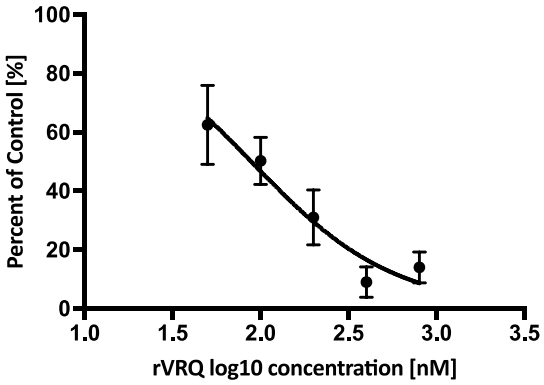

Figure 4.2.2. Representative data for rVRQ inhibition. Graph displays the percent of control versus logarithmic concentration of rVRQ for classical scrapie strain ARQ/VRQ (PG1361/05). Range of rVRQ concentrations (1200 – 50 nM) were tested. 1200 nM rVRQ was treated as a blot background control, therefore was not displayed on the graph. The IC50 value calculated from this data was 89 nM. The mean IC50 value calculated for rVRQ from three independent experiments was 114 nM.

4.2.2 Screening of rVRQ mutants for prion replication inhibition properties

In order to investigate whether the 136 position mutants inhibit the scrapie ARQ/VRQ (PG1361/05) amplification more or less than rVRQ, rPrPs were tested at 100 nM and compared to rVRQ at 100 nM. In addition, 1200 nM rVRQ was included in each experiment as a 100 % inhibition control. Therefore, the density values for 1200 nM rVRQ were subtracted from each blot. Also, PrP^{C} controls (no PrP^{Sc} seed added to the PMCA) were displayed on each dotblot as a PK digestion controls. Each sample was performed in quadruplicate **(Figure 4.2.3, A)**. The density of each sample was measured using ImageJ software. Then, the percent of no inhibition control was calculated for samples. Next, the average signal as a percent of the uninhibited sample for each rPrP type from each experiment was calculated. And these values were calculated in at least two independent experiments. For rIRQ, rFRQ and rNRQ one batch of protein was tested in two independent experiments. In this case, the result showed that 100 nM of rIRQ, rFRQ and rNRQ inhibits the amplification of scrapie ARQ/VRQ (PG1361/05) less effectively or at the same level as rVRQ **(Figure 4.2.3**, **B)**. Statistical analysis using one-way non-parametric ANOVA – Kruskal-Wallis test (H=48.28, $p<0.05$) followed by Dunn's multiple comparisons test showed no significant differences between these groups (IRQ p value>0.9999, FRQ p value>0.9999, NRQ p value=0.4882). Therefore, these rPrPs were not analysed further.

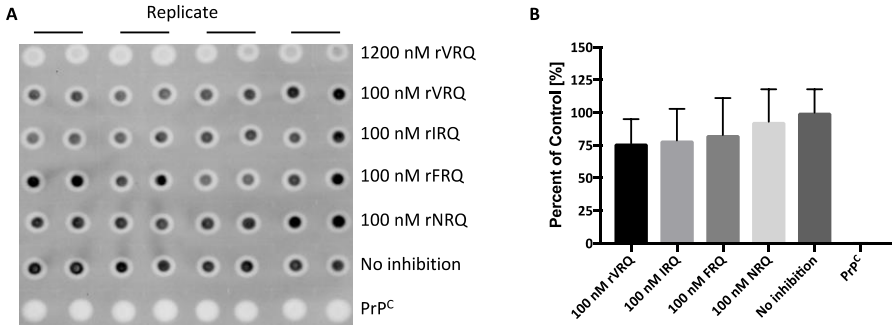

Figure 4.2.3. Effect of 100 nM rVRQ, rIRQ, rFRQ and rNRQ on scrapie ARQ/VRQ PG1361/05 amplification. **A** – representative dotblot comparing 100 nM rIRQ, rFRQ and rNRQ to 100 nM rVRQ. 2.5 µl of each sample were added on the dotblot in duplicate. Each control was run in quadruplicates. PrP^{C} was included on the dotblot as a PK digestion control. 1200 nM rVRQ was included as a 100 % inhibition control. **B** – plot displays the mean percent of the signal compared to the no inhibition control values for 100 nM inhibition using rIRQ, rFRQ and rNRQ within two experiments in comparison to rVRQ at the same concentration. The data for 100 nM of rPrP was compared to 100 nM rVRQ and statistical Kruskal-Wallis test followed by Dunn's multiple comparison test were performed in GraphPad Prism 8. There were no significant statistic differences (H=48.28, p value>0.05) reported between 100 nM rVRQ and 100 nM IRQ ($p>0.9999$), FRQ ($p>0.9999$) and NRQ ($p=0.4882$). 1200 nM rVRQ was treated as a background

control for each experiment and is not displayed on the graph. PrP^C – TSE negative brain substrate only was used in PMCA.

For rSRQ, rRRQ, rCRQ, rLRQ, rYRQ and rHRQ, four independent experiments were performed and two batches of rPrPs were used. The analysis **(Figure 4.2.4)** showed that 100 nM rSRQ and rHRQ did not inhibited the scrapie PrP^{Sc} amplification better that 100 nM rVRQ. On the other hand, 100 nM of rRRQ ($p<0.0001$), rCRQ ($p=0.0012$), rLRQ ($p<0.0001$) and rYRQ ($p=0.0039$) displayed higher inhibition than 100 nM rVRQ. These differences were reported as statistically different using the Kruskal-Wallis followed by Dunn's multiple comparison test. Kruskal-Wallis statistic was calculated separately for rSRQ, rRRQ, rCRQ ($H=135.4$, $p<0.05$) and rLRQ, rYRQ, rHRQ ($H=134.1$, $p<0.05$). Therefore, these recombinant proteins were analysed further. rHRQ was not reported as significantly different but as the trend suggested it may display more effective inhibition, it was included in further analysis.

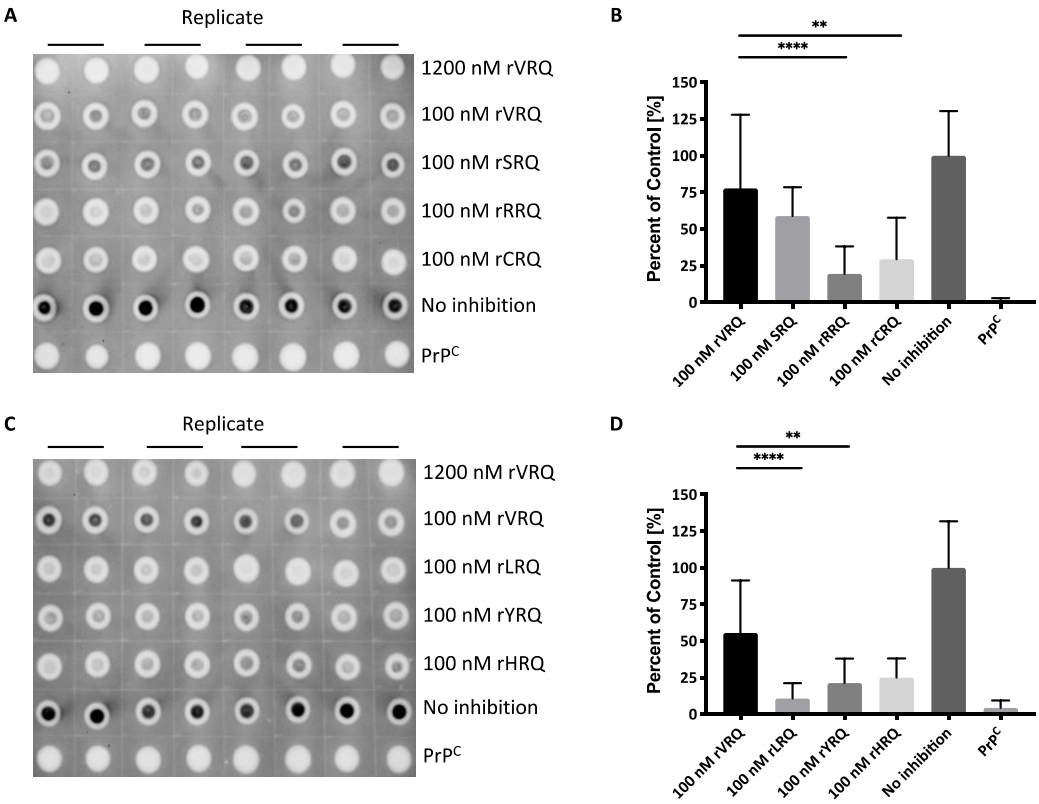

Figure 4.2.4. Effect on 100 nM rVRQ, rSRQ, rRRQ, rCRQ, rLRQ, rYRQ, rHRQ on ARQ/VRQ scrapie PG1361/05 amplification. **A, C** – representative dotblots comparing 100 nM of rPrPs to 100 nM rVRQ. 2.5 µl of each sample were added on the dotblot in duplicate. Each control was run in quadruplicates. PrP^C was included on the dotblot as a PK digestion control. 1200 nM rVRQ was included as a 100 % inhibition control. **B, D** – plots display the mean percent of signal compared to the no inhibition control values for 100 nM inhibition of rPrPs for four experiments in comparison to rVRQ at the same concentration. 1200 nM rVRQ was treated as a background control for each experiment and is not displayed on the graph. The data for 100 nM of rPrP was compared to 100 nM rVRQ and statistical Kruskal-Wallis test followed by Dunn's multiple comparison test were performed in GraphPad Prism 8. Kruskal-Wallis statistics were calculated separately for experiments rSRQ, rRRQ, rCRQ ($H=135.4$, $p<0.05$) and rLRQ, rYRQ, rHRQ ($H=134.1$, $p<0.05$). Significant differences (p value<0.05) are reported between 100 nM rVRQ and 100 nM RRQ (****, p value<0.0001), CRQ (**, p value=0.0012), LRQ (****, p value<0.0001) and YRQ (**, p value=0.0039). 1200 nM rVRQ was treated as a background control for each experiment and is not displayed on the graph. * - $p\geq0.05$; ** - $p\geq0.01$; *** - $p\geq0.001$; **** - $p\geq0.0001$. PrP^C – TSE negative brain substrate.

Recombinant proteins with K, G, W, Q, P, T, D, E, M at 136 position, one batch of each protein were similarly tested in two independent experiments. Kruskal-Wallis statistics were calculated separately for rKRQ, rGRQ, rWRQ ($H=63.29$, $p<0.05$), rQRQ, rPRQ,

rWRQ (H=49.88, p<0.05) and rDRQ, rERQ, rMRQ (H=64.58, p<0.05). Analysis showed **(Figure 4.2.5)** that rGRQ, rWRQ, rQRQ, rTRQ, rDRQ and rMRQ displayed similar or lower inhibition at 100 nM when compared to 100 nM rVRQ. In addition, the variations between rPrPs replicates were very high. For these reasons, recombinant prion proteins with glycine (G), tryptophan (W), glutamine (Q), threonine (T), aspartic acid (D) and methionine (M) were not analysed further. rKRQ, rPRQ and rERQ showed higher inhibition when compared to rVRQ and the statistical Kruskall-Wallis test followed by Dunn's multiple comparison test showed statistically significant differences between these groups (rKRQ *p* value=0.0399, rPRQ *p* value=0.0059 and rERQ *p* value=0.0428). Consequently, rKRQ, rPRQ and rERQ were analysed further.

To conclude, all the produced rPrPs were tested at 100 nM level and compared to 100 nM rVRQ. Amongst them, rPrPs having arginine, cysteine, leucine, tyrosine, histidine, lysine, proline and glutamic acid displayed enhanced inhibition compared to valine and were chosen for further analysis.

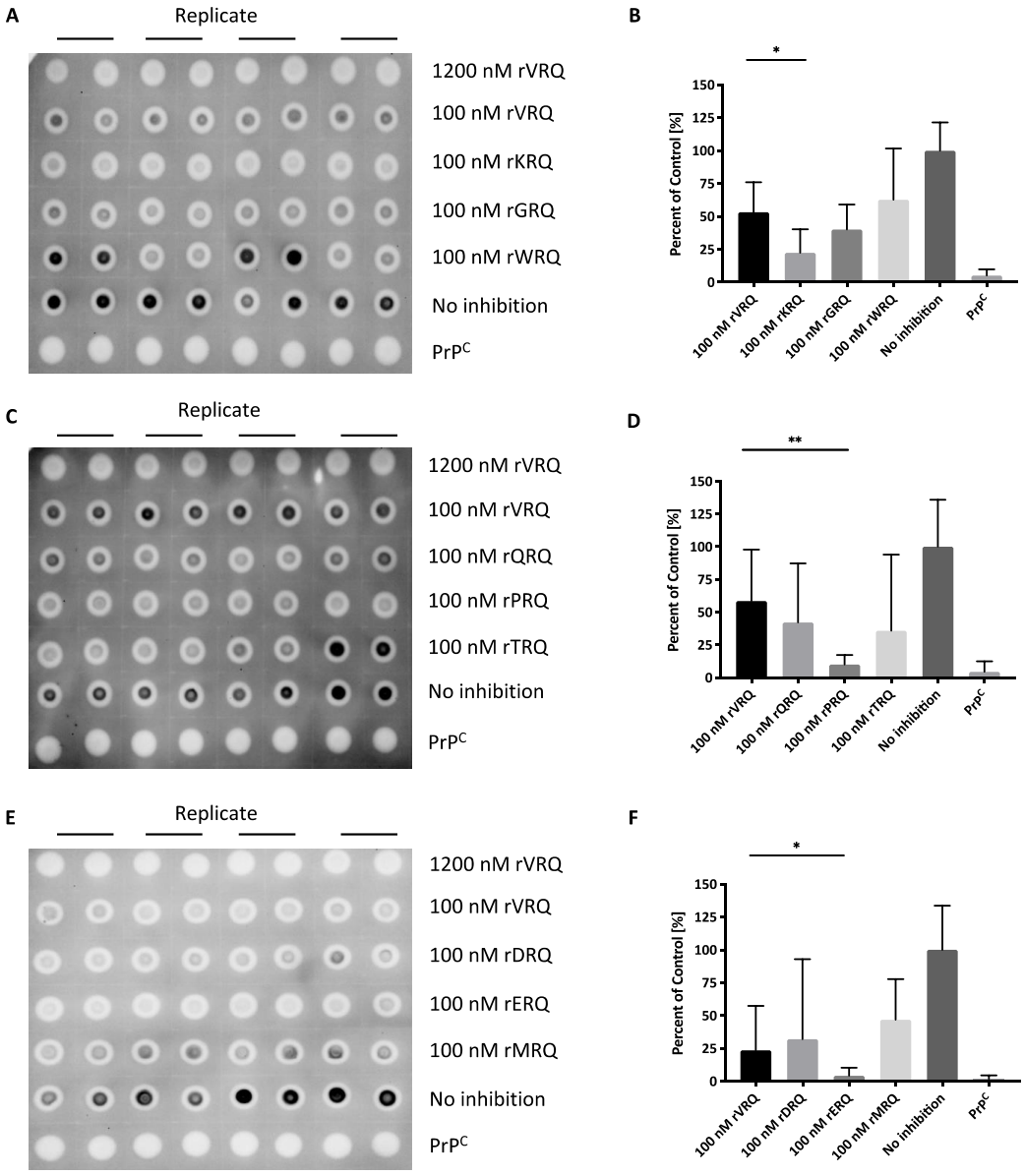

Figure 4.2.5. Effect of 100 nM rVRQ and 100 nM of mutants produced by site directed mutagenesis on ARQ/VRQ scrapie PG1361/05 amplification. **A, C, E** – representative dotblots comparing 100 nM of each rPrP to 100 nM rVRQ. 2.5 µl of each sample were added on the dotblot in duplicate. Each control was run in quadruplicates. PrP^C was included on the dotblot as a PK digestion control. 1200 nM rVRQ was included as a 100 % inhibition control. **B, D, E** – plots display the mean signal as a percentage of the no inhibition control values for 100 nM inhibition of rPrPs for two experiments in comparison to rVRQ at the same concentration. The data for 100 nM of rPrP was compared to 100 nM rVRQ using statistical Kruskal-Wallis test followed by Dunn's multiple comparison test in GraphPad Prism 8. Kruskal-Wallis statistics were calculated seperetely for rKRQ, rGRQ, rWRQ ($H=63.29$, $p<0.05$), rQRQ, rPRQ, rWRQ ($H=49.88$, $p<0.05$) and rDRQ, rERQ, rMRQ ($H=64.58$, $p<0.05$). Significant differences ($p>0.05$) are reported between 100 nM rVRQ and 100 nM KRQ (*, $p=0.0399$), rPRQ (**,

p=0.0059), rERQ (*, p=0.0428). 1200 nM rVRQ was treated as a background control for each experiment and is not displayed on the graphs. * - $p \geq 0.05$; ** - $p \geq 0.01$; *** - $p \geq 0.001$; **** - $p \geq 0.0001$; PrP^C – TSE negative brain substrate.

4.2.3 IC50 value determination for rPrPs with potentially enhanced inhibition properties compared to rVRQ

Eight rPrPs were chosen for dose response experiments. A range of rPrPs concentrations were added into PMCA reactions, where scrapie ARQ/VRQ PG1361/05 isolate was amplified. For rRRQ, rCRQ, rLRQ, rYRQ and rHRQ, 1200 – 12.5 nM of each rPrP were added, whereas for rKRQ, rPRQ and rERQ 100 – 0.25 nM were added into PMCA. Each experiment consisted of 4 replicates. PK digested PMCA products were analysed on dotblot as previously described. 1200 nM of rVRQ was included in each experiment as a 100 % inhibition control. In addition, PrP^C control was included in order to assess the PK digestion efficiency. Addition of 1200 and 800 nM of each rPrP, inhibited the amplification to 100 % (data not shown) therefore, further repeats consisted only of values 400 – 12.5 nM **(Figure 4.2.6)** or 100 – 0.25 nM **(Figure 4.2.8)** of each rPrP. For each experiment, IC50 value was calculated according to signal intensities for each inhibitory sample to no inhibition samples **(Figure 4.2.7)**. The IC50 values calculated for rRRQ were 16 and 1 nM. The data reproducibility for rCRQ, rLRQ, rYRQ, rHRQ was poor. For example, rCRQ seemed to inhibit the scrapie *in vitro* amplification in 100 % at concentrations 400 nM but from this point variations between replicates were high as were the differences between experiments, IC50 vales calculated from two independent experiments were 112 nM and 11 nM. rLRQ was found to stop the scrapie isolate amplification at 400 nM but further inhibitor dilutions resulted in lack of reproducibility between experiments, the calculated IC50 values were 17 nM and 1 nM. For rYRQ and rHRQ, densitometry analysis over two independent experiments revealed IC50 values were 45 nM and 78 nM for rYRQ and 90 nM and 69 nM for rHRQ.

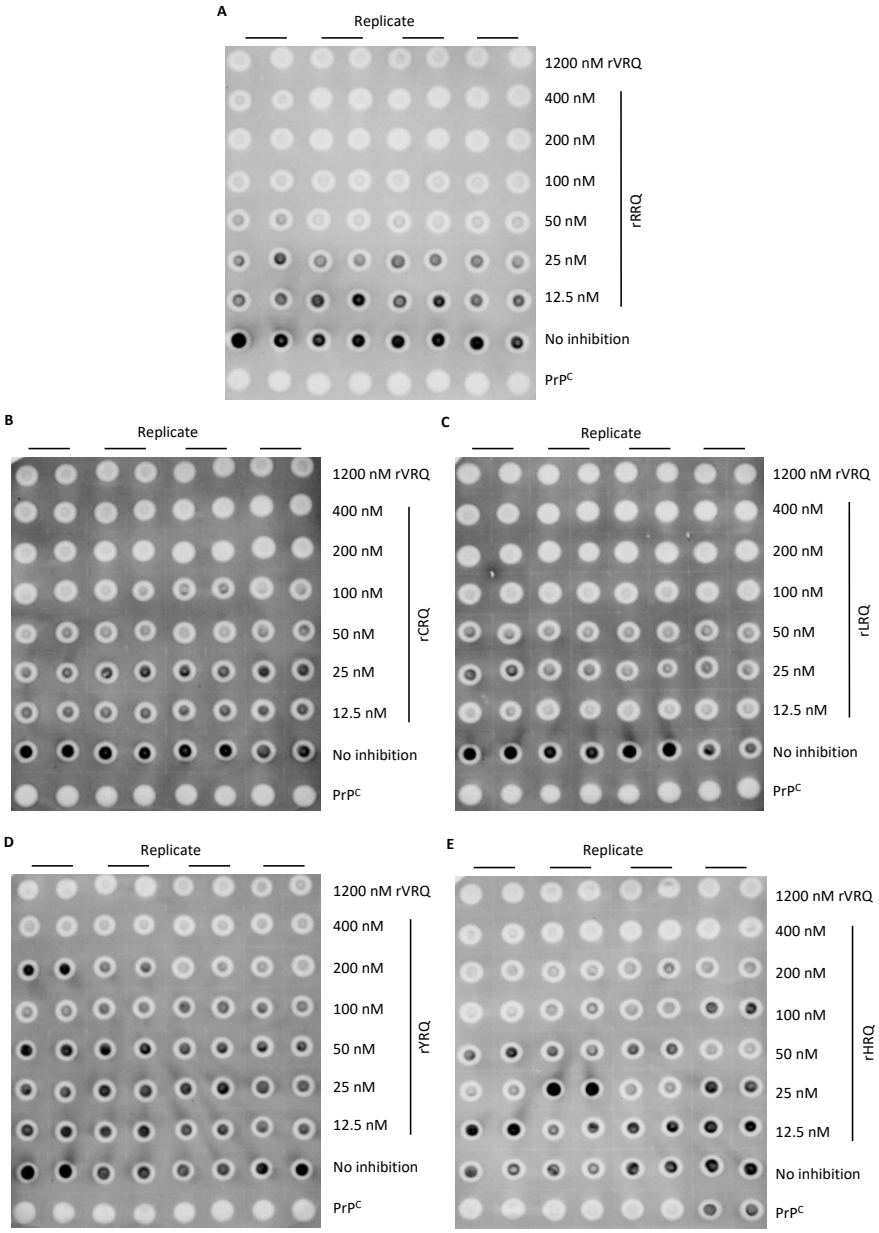

Figure 4.2.6. Representative dotblots showing the dose response inhibition of ARQ/VRQ scrapie PG1361/05 with rRRQ **(A)**, CRQ **(B)**, rLRQ **(C)**, rYRQ **(D)**, rHRQ **(E)**. 2.5 µl of each sample was added on the dotblot in duplicate. Each control was run in quadruplicates. 1200 nM rVRQ was used as a 100 % inhibition control. PrP^C – TSE negative brain homogenate.

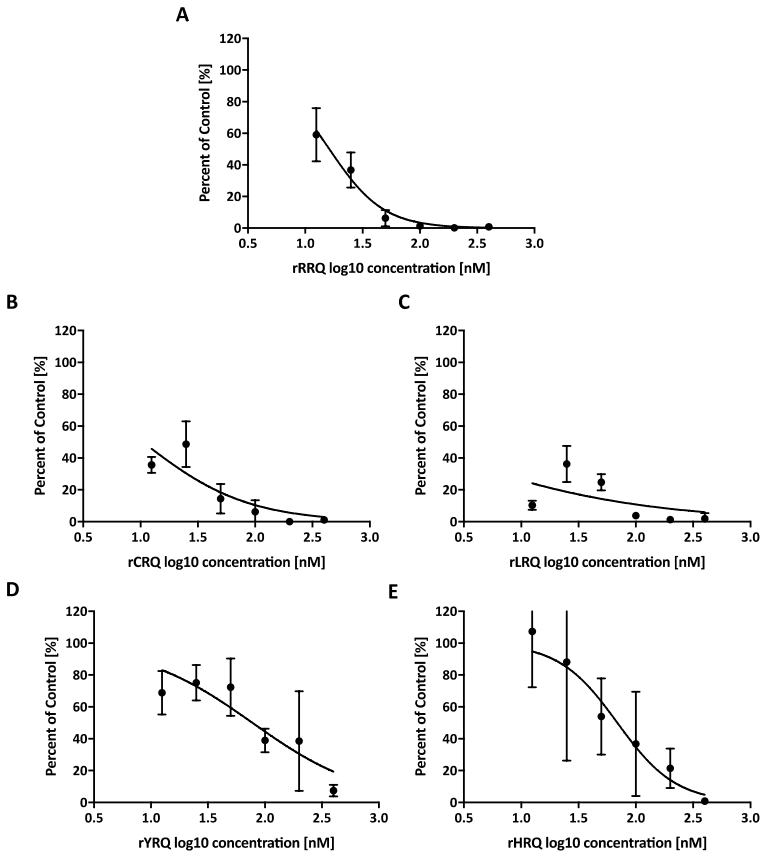

Figure 4.2.7. Representative plots displaying percent of uninhibited versus logarithmic concentration for rRRQ **(A)**, rCRQ **(B)**, rLRQ **(C)**, rYRQ **(D)**, rHRQ **(E)** inhibition of scrapie ARQ/VRQ PG1361/05. From these graphs IC50 values were calculated for each rPrPs as 16 nM for rRRQ, 11 nM for CRQ, 1 nM for LRQ, 78 nM for YRQ and 69 nM for HRQ. These rPrPs were tested in 400 – 12.5 nM concentration range. 1200 nM rVRQ was used as a blots background control and it was not displayed on the graphs.

For rKRQ, rPRQ and rERQ over the range of concentrations from 100 to 0.25 nM **(Figure 4.2.8)** IC50 values were calculated as follows rKRQ – 2 nM, rPRQ – 2 nM and rERQ – 95 nM in the first experiment **(Figure 4.2.9)**. In addition, for rKRQ second calculated IC50 value was 1 nM, what together with the first experiment gave average IC50 value 2 nM for rKRQ. For rPRQ second experiment, we could not calculate the IC50 values, however based on dotblot and graphs analysis the IC50 value was below 20 nM. In addition, only one experiment for rERQ inhibition was performed and due to its hight IC50 value this rPrP was not variations between replicated was not analysed further.

Additionally, inhibition of rRRQ was also tested in the range 100 to 0.001 nM with ARQ/VRQ scrapie isolate (data not shown). However, 100 nM of rRRQ still showed the 100 % inhibition of scrapie amplification, the lowest inhibitor concentrations showed no inhibition that could be related to the difficulty of accurately measure this amount of protein. On the other hand, IC50 was calculated from the experiment and was 15 nM.

This, together with two other IC50 values that were calculated for rRRQ (16 nM, 1 nM, 15 nM) gave an average IC50 value for rRRQ – 11 nM.

To conclude, from eight rPrPs where IC50 values were calculated, all displayed values lower than rVRQ as predicted from the initial screens using 100 nM rPrP. Three proteins, rRRQ, rKRQ and rPRQ, were chosen for further analysis as they displayed the lowest IC50 values **(Table 4.2.1)**.

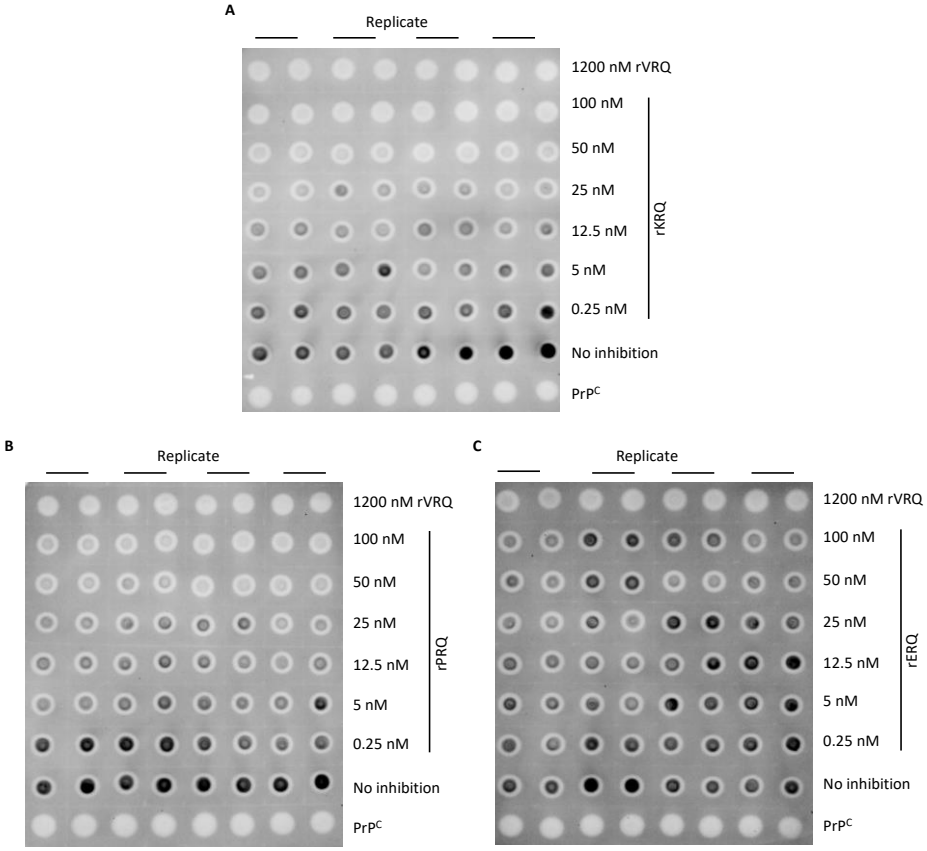

Figure 4.2.8. Inhibition of scrapie ARQ/VRQ PG1361/05 with 100 – 0.25 nM of rKRQ **(A)**, rPRQ **(B)** and rERQ **(C)**. 2.5 µl of each sample were added on the dotblot in duplicate. Each control was run in quadruplicates. 1200 nM rVRQ was used as a 100 % inhibition control. PrP^C – TSE negative brain homogenate.

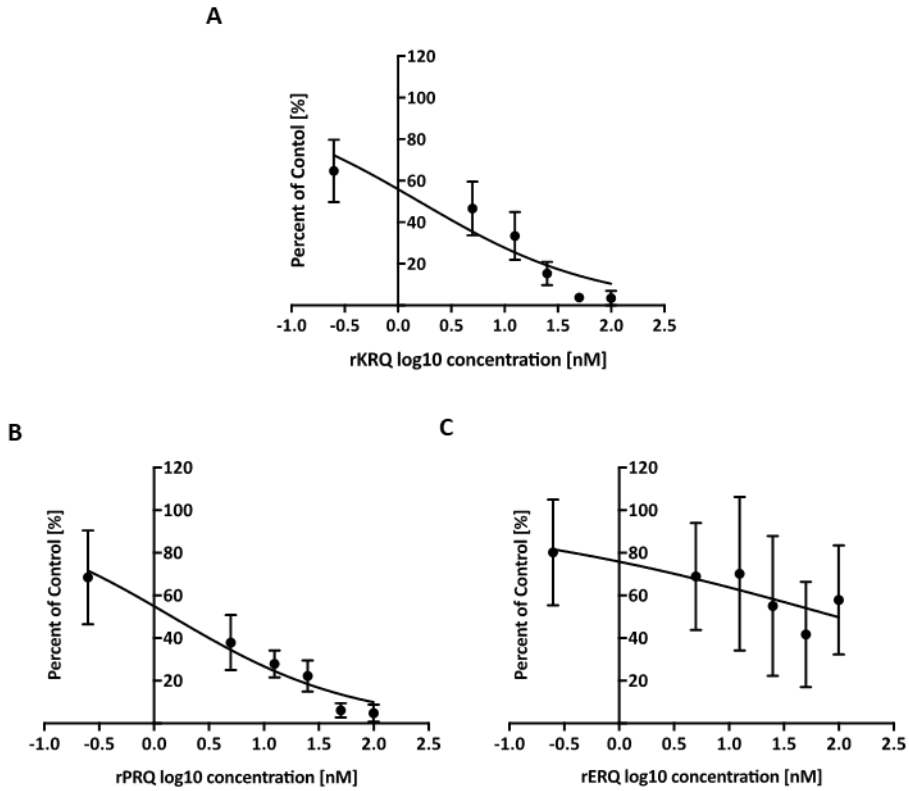

Figure 4.2.9. Representative plots displaying percent of uninhibited versus logarithmic concentration for rKRQ **(A)**, rPRQ **(B)** and rERQ **(C)** inhibition of scrapie ARQ/VRQ PG1361/05. IC50 value was calculated for each rPrPs as 2 nM for rKRQ, 2 nM for PRQ and 95 nM for ERQ. These rPrPs were tested in 100 – 0.25 nM concentration range. 1200 nM rVRQ was used as a blots background control and it was not displayed on the graphs.

Table 4.2.1. IC50 values comparison for rVRQ mutants.

rPrP mutant	IC50 (1)	IC50 (2)
rVRQ	Average: 114 nM[1]	
rRRQ[2]	16 nM	1 nM
rCRQ	112 nM	11 nM
rLRQ	17 nM	1 nM
rYRQ	45 nM	78 nM
rHRQ	90 nM	69 nM
rKRQ	2 nM	1 nM
rPRQ	2 nM	<20 nM[3]
rERQ	95 nM	NA[4]

[1]Average IC50 value for rVRQ was calculated from three independent experiments

[2]Also, third experiment was performed, where IC50 = 15 nM (100 – 0.001 nM)

[3]For experiment where we could not calculate the IC50 values, an estimated value was reported based on dotblots and graphs

[4]IC50 value estimation experiment was not performed

4.2.4 rRRQ, rKRQ and rPRQ analysis at lower concentrations

In order to assess whether the rKRQ and rPRQ are inhibiting the scrapie ARQ/VRQ amplification more efficiently than rRRQ, the inhibitors were compared at 10, 5 and 1 nM **(Figure 4.2.10, A, C)**. When analysing these data, in order to pass the normality tests, one value for 10 nM rRRQ had to be excluded from data (second replicate, second repeat). The experiment showed that when looking at 10 nM and 5 nM inhibition, rRRQ was more efficient than rKRQ. The differences at these concentrations were analysed using the statistical mixed-effects model (two-way ANOVA with missing values) followed by Sidak's multiple comparisons test ($F=29.28$, $p<0.05$). The results showed that rRRQ inhibited amplification of PG1361/05 scrapie ARQ/VRQ significantly better than rKRQ at 10 nM and 5 nM (p values < 0.0001). In contrast, there was no statistically significant difference when comparing these two proteins at 1 nM level **(Figure 4.2.10, B)**. Furthermore, rPRQ was compared to rRRQ **(Figure 4.2.10, D).** Data from this experiment passed the normality tests, therefore the statistical analysis using two-way ANOVA with Sidak's multiple comparison was performed ($F=2.053$, $p<0.05$). The test showed that rRRQ and rPRQ were not statistically different between at 10 and 5 nM ($p>0.05$). In contrast, rRRQ appeared to have a higher inhibition level at 1 nM than rPRQ (p value $=0.0170$). In addition, rPRQ results were very variable at this concentration, so that it was hard to fully predict the inhibition efficacy at 1 nM. Moreover, the statistical differences could be also explained by rRRQ variability between experiments.

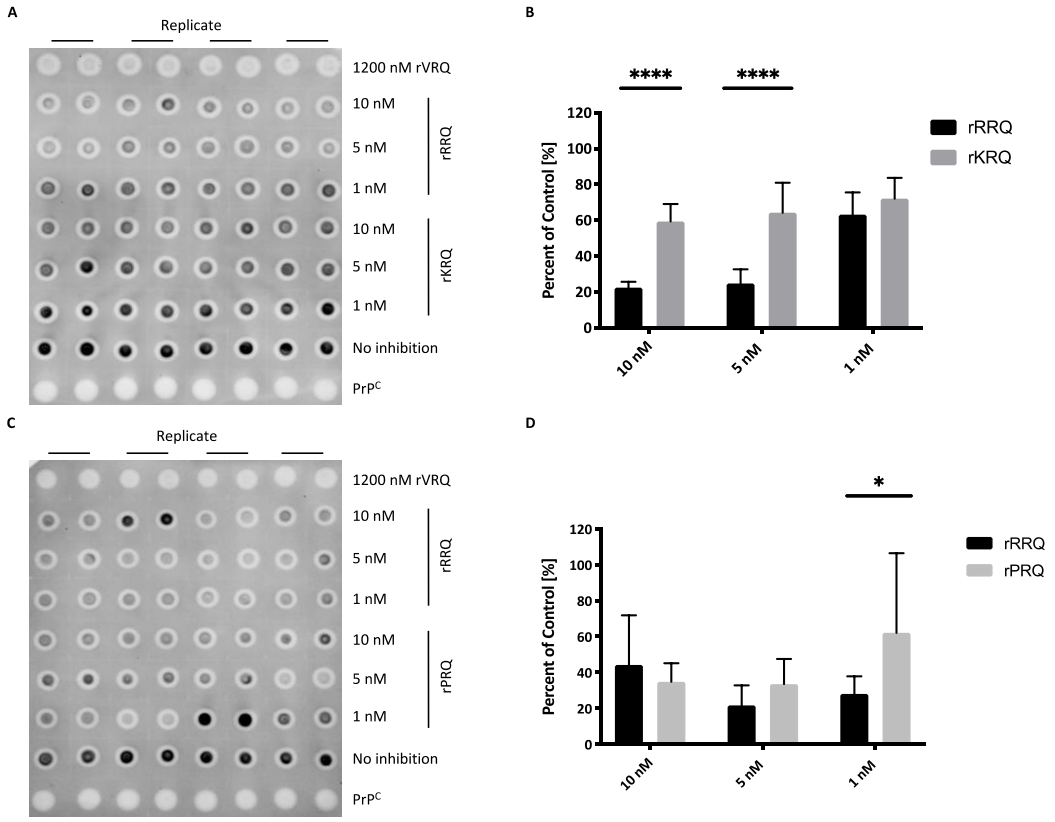

Figure 4.2.10. Inhibition of rRRQ in compare to rKRQ (A, B) and rPRQ (C, D) at 10, 5 and 1 nM of scrapie ARQ/VRQ PG1361/05. **A, C** – representative dotblots showing the direct comparison of rRRQ and rKRQ **(A)** and rRRQ and rPRQ **(C)** at 10, 5 and 1 nM. 2.5 µl of each sample were added on the dotblot in duplicate. Each control was run in quadruplicates. 1200 nM rVRQ was used as a 100 % inhibition control. PrP^C – TSE negative brain homogenate. **B, C** – graphs display comparison of rRRQ to rKRQ and rRRQ to rPRQ at 10, 5 and 1 nM concentration. The data for rKRQ and rRRQ were analysed using mixed-effects model (two-way ANOVA for missing values) and Sidak's multiple comparisons test ($F=29.28$, $p<0.05$). The test showed that rRRQ at 10 nM and 5 nM inhibit amplification of scrapie significantly better that rKRQ at the same concentrations ('****' - *p* values <0.0001). For 1 nM comparison there was no significant statistical difference between rRRQ and rKRQ (*p* value = 0.2954). For rRRQ and rPRQ comparison, two-way ANOVA with Sidak's multiple comparisons test were used ($F=2.053$, $p<0.05$) and the significant difference was only at 1 nM level ('*', *p* value =0.0170). Both, 10 and 5 nM of rPRQ and rRRQ has similar impact on scrapie PG1361/05 inhibition (*p* value =0.07677 (10 nM) and *p* value =0.6253 (5 nM)).

4.3 Discussion

Protein misfolding cyclic amplification provides a tool for investigating the misfolding process of prion protein (Saborio, Permanne and Soto, 2001). In this research, PMCA was modified and in addition to template (PrP^{Sc}) and substrate (PrP^{C}), homologous, full length, ovine recombinant PrP was added. The difference between recombinant PrP produced in bacteria (*E. coli*) and brain derived PrP^{C} is that the recombinant PrP does not undergo any posttranslational modifications, therefore, it lacks the N-glycans and GPI anchor (Kim *et al.*, 2009; Yuan *et al.*, 2013). Previously, Workman and colleagues tested recombinant ovine prion proteins: rVRQ, rARQ ($alanine_{136}$, $arginine_{154}$, $glutamine_{171}$) and rARR ($alanine_{136}$, $arginine_{154}$, $glutamine_{171}$). They have calculated the IC50 for these recombinant proteins inhibiting the scrapie ARQ/VRQ isolate PG1361/05 and calculated average IC50 values 122 nM for rVRQ, 228 nM for rARQ and 505 nM for rARR when analysing the products on dotblot. In addition, the same samples were analysed on western blots and showed the IC50 values 85 nM for rVRQ, 200 nM for rARQ and 515 nM for rARR (Workman, 2017; Workman, Maddison and Gough, 2017). In both methods, the result showed that rVRQ was the most potent inhibitor. As the dotblot is a higher throughput assay we therefore decided to conduct only dotblots for the inhibition analysis in the current study. In addition, Workman *et al.* also tested heterologous PrP (rhamPrP) in this scrapie inhibition model. This version of rPrP had IC50 value of 181 nM (dot blot analysis), which showed that this rPrP also acted as an inhibitor of scrapie ARQ/VRQ amplification *in vitro*. Moreover, reported IC50 value for rhamPrP was lower than for tested rARQ or rARR in the same research (Workman, 2017). The data produced in the current study confirmed that recombinant ovine rVRQ can inhibit scrapie ARQ/VRQ isolate PG1361/05 prion protein amplification *in vitro*. The average calculated IC50 value for rVRQ was 114 nM, correlating with the 122 nM value previously obtained for the same PG1361/05 (ARQ/VRQ) scrapie isolate (Workman, 2017).

All eighteen rPrPs were first compared at 100 nM to 100 nM rVRQ (all variants excluding ARQ), which is around its IC50 value. At this stage, it was found that rRRQ, rCRQ, rLRQ, rYRQ, rHRQ, rKRQ, rPRQ and rERQ inhibited the amplification of scrapie isolate (PG1361/05, ARQ/VRQ) better than rVRQ. In order to analyse them further, PMCA including a range of rPrP concentrations was performed. At this point, IC50 values for rCRQ (122 and 11 nM) varied between the repeats, whereas IC50 calculated for rYRQ (45 and 78 nM), rHRQ (90 and 69 nM) and ERQ (95 nM) were high in compare to other tested rPrPs. For these reasons, rCRQ, rYRQ, rHRQ and ERQ were not analysed further in the current study. Additionally, for some rPrP it was challenging to accurately estimate IC50 values. The tested concentrations did not allow to produce full sigmoidal curve and usually the curves did not reach the top plataur. Therefore, IC50 values were calculated beyond the range of tested concentration. At this stage, four of the tested recombinants showed significantly higher inhibition in *in vitro* amplification of ovine scrapie PG1361/05 than rVRQ and the data was reproducible between experiments. These were rRRQ, rLRQ,

rKRQ and rPRQ, with arginine, leucine, lysine and proline at 136 position, respectively. Additionally, third experiment for IC50 values calculations was performed for rRRQ and involved range of concentrations from 100 nM to 0.001 nM. The calculated IC50 was 15 nM and confirmed that rRRQ was one of the strongest inhibitor for PG1361/05 amplification. The average IC50 value calculated from three independent experiments for rRRQ was 11 nM. In addition, two IC50 values for rKRQ were calculated and gave an average value 2 nM (1 nM and 2 nM). The rRRQ, rKRQ and rPRQ were then directly compared in the same experiments at lower concentrations (10, 5 and 1 nM) and it was found that the differences between them in inhibition of scrapie ARQ/VRQ PG1361/05 amplification were very similar. This could suggest that rRRQ and rKRQ gave similar levels of inhibition in PMCA, whereas rPRQ inhibiton degree. It has to be taken into account that the statistical differences between rPRQ and rRRQ at 1 nM could also be explained by rRRQ variability between experiments. At this point, rLRQ was not analysed in direct comparison at lower concentrations and it was decided to proceed and analyse rRRQ, rKRQ and rPRQ further.

Inhibition of PK resistant prion formation using both homologous and heterologous prion protein has been reported previously. Yuan and co-workers compared homologous (human PrP) and heterologous (mouse, bank vole and bovine) recombinant prion protein inhibition in human prion protein amplification during PMCA. They found that the addition of homologous human rPrP was more effective than the heterologous (Yuan *et al.*, 2013). Moreover, *in vitro* research by Priola and colleagues used the model of scrapie infected mouse neuroblastoma – MNB – cell line. They showed that the addition of heterologous prion protein inhibits resistant PrP formation and accumulation (Priola *et al.*, 1994). In addition, Skinner *et al*., used an *in vivo* model, where scrapie infected mice were treated with two different levels (high and low dose) of recombinant hamster PrP. The heterologous protein was injected (for high dose 31.5 µg, 15.75 µg for low dose) together with the scrapie dose intracerebrally and also orally on the following day (70 µg for high dose, 35 µg for low dose). After 108 days post infection, brain and spleen tissue staining showed that all animals were infected with scrapie and addition of heterologous recombinant PrP did not prevent the disease progression, although addition of high dose treatment reduced the amount of PrP^{Sc} accumulation in analysed tissues. Furthermore, when the experiment was finished (452 days post infection), 50 % of animals with high dose treatment still not developed any clinical symptoms in compare to low dose treatment and mock infected animals (Skinner *et al.*, 2015). Overall, the current research and described examples showed that usage of rPrPs could inhibit the prion replication *in vitro* and *in vivo*.

Within the literature, multiple mutations and polymorphisms have been recognised in the *Prnp* gene. In the ovine PrP, codons 136, 154 and 171 play very important roles in disease development and as mentioned before, some of the genotypes are scrapie susceptible (like VRQ) or resistant (like ARR) (Goldmann, 2008). From the range of rPrP

variants at codon 136 tested in the current study, rRRQ, rKRQ and rPRQ were the most effective inhibitors of *in vitro* scrapie replication and all were more effective than natural variants. Whilst none of the most effective variants have been reported in the nature, tyrosine at position 136 was found in both scrapie affected and healthy sheep populations in Greece, Iran, Turkey and China at low frequencies (Billinis *et al.*, 2004; Alvarez *et al.*, 2011; Guan *et al.*, 2011; Frootan *et al.*, 2012; Meydan *et al.*, 2012). First reports about presence of T at 136 position came from Greece, where 216 sheep from different country regions and flocks were screened for PrP genotypes. It was described that the possibility of scrapie development in sheep with genotype ARQ/TRQ was at the same level as for animals with ARQ/ARQ. Moreover, ARQ/TRQ heterozygotes showed lower risk of scrapie than animals with VRQ/VRQ (Billinis *et al.*, 2004). So far, it is the only published research that describe the presence of T_{136} in scrapie affected animals. Furthermore, in Chinese healthy Hu sheep from two country regions T was also found at 136 position. The researchers screened 180 animals in which the highest frequency allele was A_{136}, whereas T_{136} had the lowest frequency in this group. In addition, new low frequency genotypes were reported: ARQ/TRK, ARQ/TRR and TRR/TRQ (Guan *et al.*, 2011). Additionally, ARQ/TRQ, TRQ/TRQ, TRQ/ARR and TRQ/VRQ genotypes were reported at low frequencies across different breeds in both Turkey and Iran (Alvarez *et al.*, 2011; Frootan *et al.*, 2012). Because of its rare presence, association of mentioned genotypes with scrapie is hard to determine (Goldmann *et al.*, 2005). Amongst the published data, only Billinis *et al.* reported T_{136} in scrapie affected sheep, therefore any conclusions regarding its impact on disease resistance/susceptibility cannot be predicted (Billinis *et al.*, 2004). Moreover, any outcomes need to be treated with caution and more genotypes distribution screening in sheep populations needs to be analysed (Billinis *et al.*, 2004; Goldmann *et al.*, 2005; Meydan *et al.*, 2012). This is important in planning new breeding strategies that help to eliminate genotypes prone to scrapie in sheep (Goldmann *et al.*, 2005). In addition, in the majority of these sheep populations ARQ was the most frequent allele and in some breeds and VRQ (the most scrapie susceptible genotype) was not found (Billinis *et al.*, 2004; Goldmann, 2008; Alvarez *et al.*, 2011; Guan *et al.*, 2011; Frootan *et al.*, 2012; Meydan *et al.*, 2012). In the current research, it was investigated how the substitution from V to T changed the inhibition of scrapie in *in vitro* amplification. We found that the rTRQ was a less effective inhibitor than rVRQ. Apart from commonly and less known polymorphisms described at 136 position, also 137 and 138 positions display amino acid changes (Goldmann *et al.*, 2005). These substitutions include changes from M to T and S to R, respectively. Similarly, it is hard to determine the impact of these changes on disease appearance because of their low frequency in sheep populations (Goldmann *et al.*, 2005; Saunders *et al.*, 2006). However, one study showed that the presence of tyrosine at 137 position together with the ARQ/ARQ and ARQ/AHQ genotypes had a protective effect when sheep were challenged experimentally with scrapie or BSE (Vaccari *et al.*, 2007).

Chapter 5: Assessment of rPrP 136 codon mutants as inhibitors of replication of distinct prion strains and other misfolding proteins

5.1 Introduction

Protein misfolding diseases are characterised by the presence of disease specific protein aggregates. These proteins differs in secondary and tertiary structure without any changes within the protein sequences (Soto, 2001). One of the most important features of misfolded proteins aggregates is that they consist of β-sheets rich structures (Moore, Taubner and Priola, 2009). Based on that, a potential molecule could bind to these elements and reduce the further processes of fibrils formation. This would potentially decrease or even stop the disease development pace. To date, no successful therapeutic agents targeting either specific protein aggregates or any amyloid compounds present in brain tissue have progressed to the clinic. Furthermore, any therapeutic approaches towards prions diseases could be further tested for the application to other protein misfolding (Panegyres and Armari, 2013; Thompson *et al.*, 2013). Several studies have described PMDs as diseases with co-occurrence of different misfolded proteins within the tissue of the same patient (Katorcha *et al.*, 2017). For example, α-synuclein deposits were detected in sCJD, fCJD and iCJD patients and scrapie (Haïk *et al.*, 2000, 2002; Vital *et al.*, 2009; Kovacs *et al.*, 2011). Therefore, potential successful therapeutics could not only slow down the misfolding process of each protein, they could inhibit and reverse the misfolding and aggregation processes for multiple proteins and also prevent any cross seeding of misfolding proteins (Soto and Estrada, 2005).

The interactions of PrP and other proteins that misfold could play an important role in the pathogenesis of PMDs (Han *et al.*, 2006). It has been described that the cell membrane localised PrP^C interacted with β-sheet rich conformers like Aβ, yeast produced PrP or β-peptides. Furthermore, these interactions were inhibited by the use of PrP and Aβ oligomer specific antibody (A11) (Kayed *et al.*, 2003; Resenberger *et al.*, 2011). These findings showed that PrP^C could potentially interact with β-sheet rich structures within misfolded proteins like Aβ, α-syn or tau (Resenberger *et al.*, 2011). In addition to that, studies showed that PrP^C exhibited high affinity for binding synthetic amyloid β (1-42) oligomers and low affinity for binding the Aβ monomers (Laurén *et al.*, 2009; Bove-Fenderson *et al.*, 2017). Moreover, PrP^C regions responsible for PrP – Aβ interactions have been mapped. Chen *et al*., found that the deletion of PrP^C N-terminal region (either residues 23-90 or 92-110) resulted in total loss of human PrP and human Aβ binding (Chen, Yadav and Surewicz, 2010). The later research confirmed the importance of N-terminal part of PrP in Aβ oligomers binding (Nieznanski *et al.*, 2014). In contrast, the highly structured C-terminus of cellular prion protein was not reported to be involved in any interactions of PrP and Aβ oligomer, however research performed by Bove-Fenderson and co-workers indicated the involvement of both C- and N-terminus of PrP as necessary (Chen, Yadav and Surewicz, 2010; Bove-Fenderson *et al.*, 2017). Since there is evidence indicating that PrP can interact with misfolded Aβ, research into the development of therapeutic towards their dependency were carried out. It was shown that full length human PrP (PrP23-231) and a C-terminus truncated version

inhibited the fibrillization of amyloid β, when investigated by ThT fluorescence. In contrast, N-terminally truncated PrP had no inhibition effect on amyloid β oligomerisation (Nieznanski *et al.*, 2012).

Multiple studies showed that the amyloid β aggregates could bind to PrP^C resulting in decreased levels of amyloid oligomerisation, however not much is known about the relation of α-syn and tau with prion protein and some research showed conflicted outcomes (Corbett *et al.*, 2020). Ferreira and co-workers communicated that α-syn could interact with PrP^C. They reported PrP as an important linker between α-synuclein oligomers and their synaptic toxicity. Moreover, it was found that PrP/α-synuclein interaction is regulated by a member (Fyn kinase) of Src tyrosine kinase family (SFK) that are commonly found within neurons (Um and Strittmatter, 2013; Ferreira *et al.*, 2017). Additionally, the same Fyn kinase was associated with PrP^C mediated Aβ toxicity (Um *et al.*, 2012; Um and Strittmatter, 2013). The toxic effects of α-synuclein oligomers in synaptic structures were inhibited by inactivation by a PrP^C specific antibody targeting the 93-109 region of PrP^C (Ferreira *et al.*, 2017). Also, recently published work showed α-synuclein soluble aggregates bind to PrP but the affinity of that process depended on an aggregation form. Furthermore, the binding affinity for α-synuclein soluble aggregates was similar to Aβ soluble aggregates. On the other hand, work from La Vitola and colleagues revealed neither binding nor any interactions between the PrP^C and α-synuclein oligomers (La Vitola *et al.*, 2019).

The third most common protein found in protein misfolding diseases is tau. It was found that recombinant full length tau protein is capable of forming tau-PrP complexes in *in vitro* research. Moreover, the binding affinity was dependent on the number of octapeptide repeats within the recombinant prion protein (Wang *et al.*, 2008). These findings suggested that PrP could moderate some of the tau aggregates damaging effects on synaptic functions (Hu *et al.*, 2018; Ondrejcak *et al.*, 2018). These outcomes were supported by the most recent work by Corbett, where soluble tau aggregates were bound to PrP, however with less affinity than the soluble aggregates of Aβ or α-synuclein (Corbett *et al.*, 2020). In addition, co-immunoprecipitation studies revealed that recombinant tau protein could not only interact with native PrP^C but also PrP^{Sc} derived from 263K scrapie strain (Han *et al.*, 2006).

PrP as a protein might exhibit disaggregating properties (Nieznanski *et al.*, 2014). On this basis along with the reported interaction of PrP^C with other misfolded proteins, it could be hypothesised that PrP could provide a potential therapeutic of not only TSE but also other protein misfolding diseases (Nieznanska *et al.*, 2018). As stated, it has been shown that PrP inhibits the Aβ oligomers formation. However, no studies investigating its possible inhibitions of formation α-synuclein or tau oligomers have been reported. In the current study, our main focus was on testing recombinant prion proteins (rRRQ, rKRQ and rPRQ) in a spectrum of ruminant TSEs. This involved classical ovine scrapie,

bovine BSE and ovine BSE isolates. In addition, the rPrPs were also used to investigate possible inhibitions mechanisms of α-synuclein fibril formation during PMCA.

5.2 Results

5.2.1 Optimisation of scrapie, bovine and ovine BSE isolate amplification

In order to analyse whether the rPrP mutants can act as an inhibitor for other prion disease isolates, amplification conditions for each isolate were tested and optimised. Isolates of ovine scrapie PG1207/03 (VRQ/VRQ) and PG1499/02 (AHQ/VRQ) were found to amplify over 4 rounds in VRQ/VRQ, whereas bovine BSE (SE1945/0035) amplified in bovine brain substrate over 5 rounds **(Figure 5.2.1, B)**. In addition, PG1361/05 (ARQ/VRQ) was found to amplify consistently over 4 rounds in VRQ/VRQ substrate, and round 5 reactions were used as a control that should be inhibited by the rPrPs **(Figure 5.2.1, A)**.

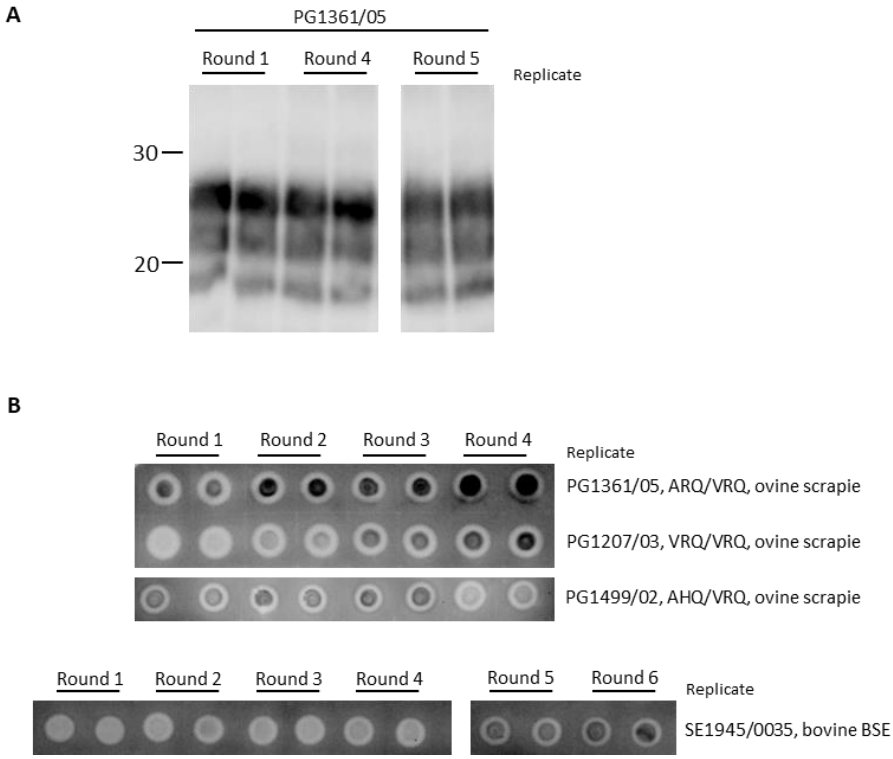

Figure 5.2.1. Representative western blots and dotblots of ovine scrapie and bovine BSE isolate amplification in serial PMCA. **A** – amplification of scrapie PG1361/05 (ARQ/VRQ) isolate over PMCA rounds 1, 4 and 5. This ovine isolate was amplified in VRQ/VRQ brain substrate. Samples show characteristic triple band pattern for scrapie. Molecular weight markers (kDa) are indicated on the left side on the blot. 20 µl of amplified, PK digested products were analysed per lane. Duplicates PMCA reactions were analysed on western blot. **B** – amplification of ovine scrapie isolates PG1361/05 (ARQ/VRQ), PG1207/03 (VRQ/VRQ), PG1499/02 (AHQ/VRQ) isolates and bovine BSE (SE1945/0035) over PMCA rounds. Ovine scrapie isolates were amplified in VRQ/VRQ substrate, whereas the bovine BSE was amplified in bovine brain. 0.5 µl of 10 % brain homogenate of PG1361/05 and PG1207/03 was added into round 1. For scrapie

PG1499/02 and bovine BSE (SE1945/035), 5 µl of 10 % brain homogenates were added into round 1 of PMCA. After each round, PMCA products were PK digested and 2.5 µl of each sample in duplicate were added on the dotblot.

Moreover, ovine BSE – PG1693 (ARQ/ARQ) isolate – was amplified using VRQ/VRQ substrate only and also the method described previously where two different substrates are being used: for rounds 1, 3 and 5, AHQ/AHQ substrate, and for rounds 2 and 4, VRQ/VRQ (Taema *et al.*, 2012). The ovine BSE amplified better using the latter procedure **(Figure 5.2.2)**, therefore this method was applied for inhibitor testing. Furthermore, also BSE-like scrapie, CH1641 isolates J3011 (AHQ/AHQ) and J2935 (ARQ/AHQ) were amplified in AHQ/AHQ substrate but over 5 rounds of PMCA but there was no amplification product (data not shown). Therefore, these isolates were not analysed further.

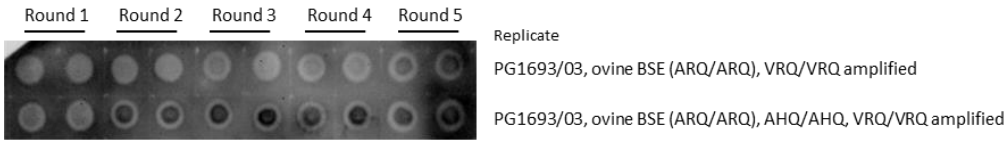

Figure 5.2.2. Amplification of ovine BSE – PG1693/03 (ARQ/ARQ) over 5 PMCA rounds. Top row shows amplification of ovine BSE in VRQ/VRQ substrate only. Bottom row shows amplification of ovine BSE in two different substrates: AHQ/AHQ for rounds 1, 3, 5 and VRQ/VRQ for rounds 2 and 5. For each PMCA, 5 µl of 10 % ovine BSE brain homogenate was added into round 1 of PMCA. After each round, PMCA products were PK digested and 2.5 µl of each sample was added on the dotblot in duplicate.

5.2.2 Optimisation of round 5 ovine scrapie PG1361/05 inhibition with rRRQ

In order to analyse the inhibition of round 5 of serial PMCA amplifications, the control ovine scrapie isolate PG1361/05 (ARQ/VRQ) was inhibited with rRRQ. Different amounts of scrapie spike from round 4 of PMCA were added into round 5 and amplified as described before. The amounts were 30, 15, 7.5 and 3.75 µl of round 4 product into 70, 85, 92.5 and 96.25 µl of TSE negative VRQ/VRQ brain, respectively. In addition, 100 nM of rRRQ was added into each reaction and products were PK digested. The higher concentration of rRRQ (9 x greater than reported average IC50 value) was chosen because it was hypothetisezed that higher inhibitor concentrations could act as stronger inhibitors of different prion strains and prion diseases amplification. This idea was also based on and supported by previous research where higher than IC50 concentrations of rVRQ was used to inhibit across prion disease isolates in 100 % (Workman, Maddison and Gough, 2017). The experiment was performed in triplicates **(Figure 5.2.3, A)**. The dotblot analysis showed that addition of 30 µl of round 4 scrapie spike was the most efficient method, in which both the amplification and inhibition of round 5 with 100 nM rRRQ was clearly visible. Moreover, addition of 30 µl of round 4 allowed to compare all isolates regardless the variability of amplification efficiency for different disease isolates. Therefore, a dilution of 3:7 of round 4 spike into round 5 was used in further experiments.

A second optimisation step involved adding 30 µl of round 4 PrP^{Sc} (PG1361/05, ARQ/VRQ scrapie) but with a range of rRRQ concentrations (100, 200 and 400 nM) **(Figure 5.2.3, B)**. These samples were compared to uninhibited control. The experiment was performed in triplicate. The densitometry analysis showed that all used rRRQ concentrations inhibited the round 5 amplification of ovine scrapie ARQ/VRQ PG1361/05 by around 70 % when compared to non-inhibited. Moreover, there were no inhibition differences in PrP^{Sc} signal between 100, 200 and 400 nM of rRRQ. This result suggested that 100 nM of rRRQ might have inhibited round 5 amplification of control scrapie isolate by 100 % and the sample signal on the dotblot came from the amount of PrP^{Sc} spike added into round 5. Therefore, it was established what negative control should be used for these experiments. Samples in which 30 µl of round 4 scrapie PG1361/05 was mixed with 70 µl of negative brain homogenate (VRQ/VRQ, brain 16) was kept at -20 °C for the period of amplification (24 h). These samples were compared to amplified controls and then all samples were PK digested and analysed on the dotblot **(Figure 5.2.3, C)**. The result showed that samples with no amplification gave high PrP^{Sc} positive signal on the dotblot indicating that the amount of amplified PrP^{Sc} after 4 rounds of PMCA for ovine scrapie (PG1361/05) could be detected. It was decided to use the non-inhibited and non-amplified samples as a background control for inhibition with rPrPs of serial PMCA experiments. When this was applied, both dotblots with either different amounts of round 4 spike going to round 5 or different amounts of rRRQ going into round 5, rRRQ inhibited the round 4 to round 5 amplification of ovine ARQ/VRQ PG1361/05 scrapie in 100 % when analysed in additional experiments on the same blots (data not shown).

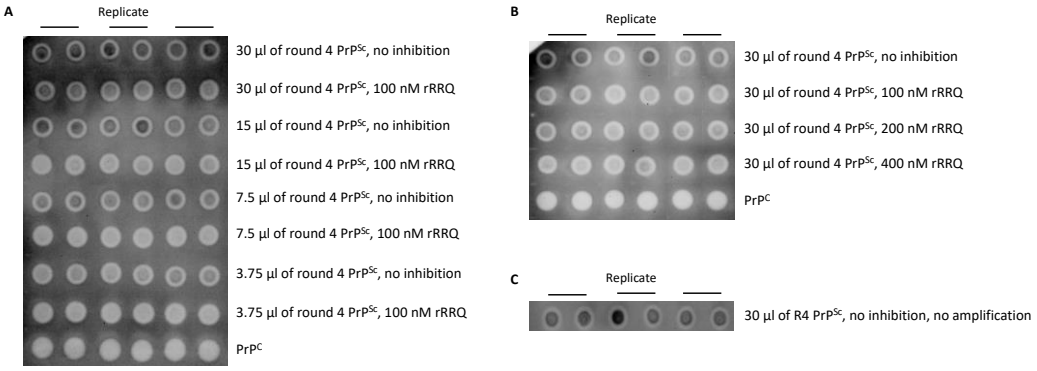

Figure 5.2.3. Dotblots showing the amplification and inhibition result of different amount of round 4 PrP^{Sc} of ovine scrapie PG1361/05 (ARQ/VRQ) and different concentrations of rRRQ added in round 5 of PMCA. **A** – 30, 15, 7.5 and 3.75 µl of round 4 PrP^{Sc} was added into 70, 85, 92.5 and 96.25 µl of negative brain homogenate (VRQ/VRQ, brain 16), respectively. The samples were amplified with or without addition of 100 nM rRRQ for 24 h. **B** – dotblot shows amplification of round 4 scrapie PG1361/05 (ARQ/VRQ) PrP^{Sc}, where 30 µl of round 4 spike was mixed with 70 µl of negative brain (VRQ/VRQ, brain 16). Amplification was performed with and without 100, 200 and 400 nM of rRRQ. **C** – representative dotblot shows the signal level for non-inhibited and non-amplified samples with 30 µl of R4 ARQ/VRQ scrapie PrP^{Sc} going into 70 µl of negative brain homogenate (VRQ/VRQ, brain 16). During the amplification time, non-amplified samples were stored at -20 °C. 2.5 µl of PK digested products were analysed on dotblot. Experiment was performed in triplicate. PrP^{C} – negative brain homogenate, R4 – round 4;

5.2.3 Optimization of the amount of rPrP inhibiting the round 5 of ovine scrapie ARQ/VRQ PG1361/05 amplification

It was previously established that 400 nM of rVRQ added into serial PMCA inhibited the classical ovine scrapie, bovine and ovine BSE isolates to 100 % (Workman, Maddison and Gough, 2017). Therefore, we applied the same approach for screening other recombinant prion proteins with the classical ovine scrapie isolate PG1361/05 (ARQ/VRQ). Accordingly, 400 nM of rVRQ or 100 nM of rRRQ, rKRQ and rPRQ were added into round 5 of PMCA and seed from round 4 PrP^{Sc} was added into VRQ/VRQ negative brain homogenate at ratio 3:7 and amplified. Furthermore, no amplification/no inhibition samples were included in the analysis and its average signal was used as a dotblot background control **(Figure 5.2.4, A)**. The data from the dotblot were analysed in two different ways. Firstly, each rPrP was compared to no inhibition samples. Secondly, the potential differences between rPRQ and other rPrP levels of inhibiton at 100 nM were compared. The result showed that on average 400 nM rVRQ inhibited the round 5 scrapie amplification by 96 %, 100 nM of rRRQ by 100 %, 100 nM rKRQ by 88 % and 100 nM of rPRQ by 55 % **(Figure 5.2.4, B)**. These data were then statistically analysed using the Tukey's multiple comparisons test ($F=27.47$, $p<0.05$). The analysis showed that the differences between 400 nM rVRQ and No inhibition ($p<0.0001$), 100 nM rRRQ and No inhibition ($p<0.0001$), 100 nM KRQ and No inhibition ($p<0.0001$) and rPRQ and No inhibition ($p=0.0004$) were statistically significant. In addition, some significant differences between rPrPs efficacy were also present. 400 nM rVRQ ($p=0.0103$), 100 nM rRRQ ($p=0.0047$) and 100 nM rKRQ ($p=0.0491$) inhibited amplification of ovine scrapie significantly better than 100 nM rPRQ **(Figure 5.2.4, C)**. Moreover, there were no statistically significant differences between level of inhibition of the scrapie isolate between 400 nM rVRQ and 100 nM rRRQ ($p=0.9974$) or 100 nM rKRQ ($p=0.9591$). These results suggest that addition of 100 rRRQ and rKRQ inhibited the amplification of scrapie isolate PG1361/05 (ARQ/VRQ) at a similar to 400 nM rVRQ.

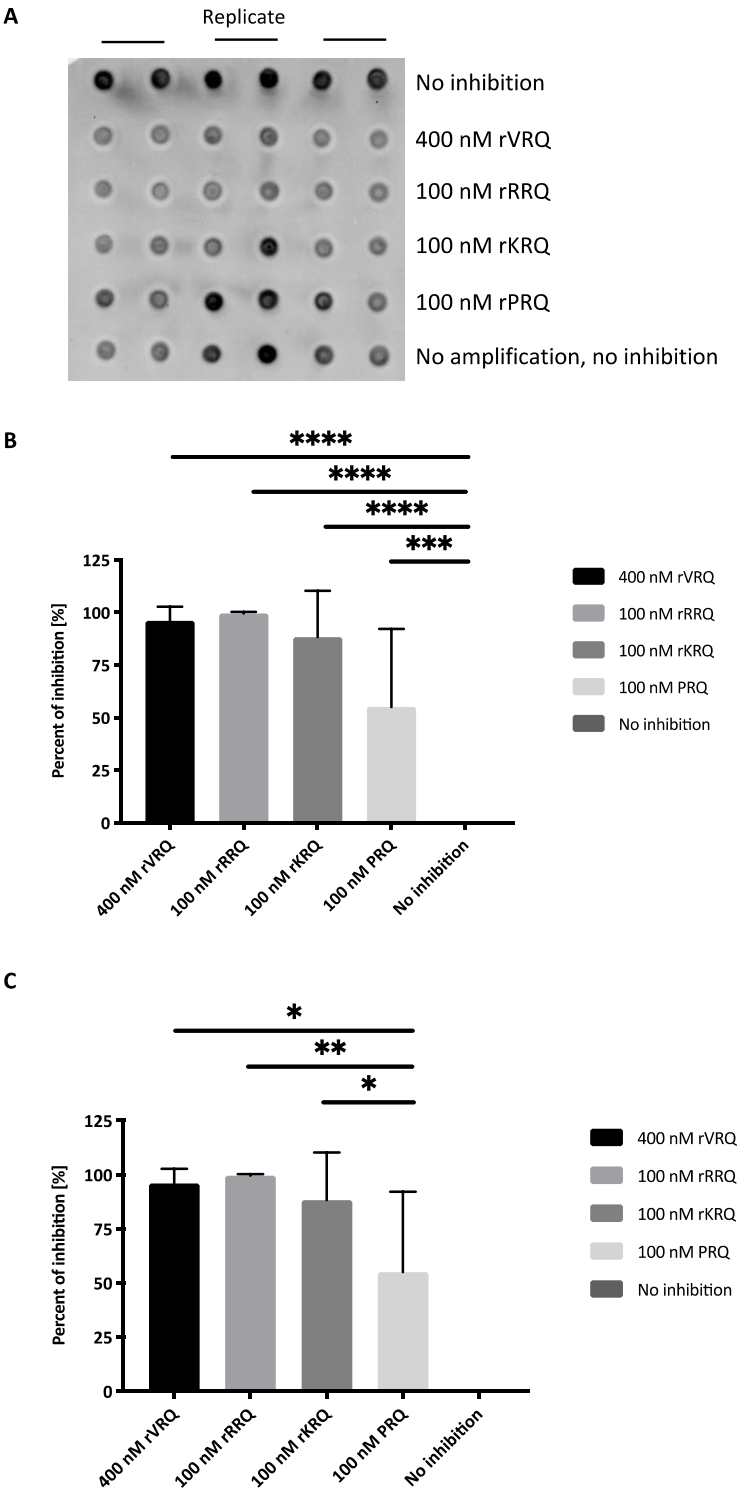

Figure 5.2.4. Inhibition of round 5 of serial PMCA ovine scrapie ARQ/VRQ PG1361/05 with 400 nM rVRQ, 100 nM rRRQ, rKRQ and rPRQ. **A** – representative dotblot shows inhibition pattern for 400 nM rVRQ, 100 nM rRRQ, rKRQ and rPRQ in comparison to no inhibition samples. Round 5 amplification samples signals subtracted with no inhibition and no amplification samples. 2.5 µl of PK digested products were analysed on the dotblot. **B** – graph shows the percent inhibition for 400 nM rVRQ, 100 nM rRRQ, rKRQ,

rPRQ in round 5 of PMCA for ovine scrapie ARQ/VRQ PG1361/05 compared to no inhibitor being present. The percent of inhibition was displayed on the graphs as it showed the power of each tested rPrP in compare to controls in a better way. According to one-way ANOVA followed by Tukey's multiple comparisons test ($F=27.47$, $p<0.05$), significant statistical differences ($p<0.0001$) were reported on the graphs between each rPrP and No inhibition sample: 400 nM rVRQ ('****', $p<0.0001$), 100 nM rRRQ ('****', $p<0.0001$), 100 nM rKRQ ('****', $p<0.0001$) and rPRQ ('***', $p=0.0004$). **C** – graph shows the percent inhibition for 400 nM rVRQ, 100 nM rRRQ, rKRQ, rPRQ in round 5 of PMCA for ovine scrapie ARQ/VRQ PG1361/05 compared to no inhibitor being present. Here, statistical differences in the inhibition response levels between rPrP are indicated. Based on Tukey's multiple comparisons test ($p<0.0001$), statistical differences are reported between 400 nM rVRQ and rPRQ ('*', $p=0.0103$), 100 nM rRRQ and rPRQ ('**', $p=0.0047$) and 100 nM KRQ and rPRQ ('*', $p=0.0491$). * - $p\geq0.05$; ** - $p\geq0.01$; *** - $p\geq0.001$; **** - $p\geq0.0001$;

5.2.4 Ovine scrapie, bovine BSE and ovine BSE isolate inhibition

The addition of 100 nM of rRRQ into round 5 PMCA inhibited the scrapie amplification in 100 %. Because of the fact that the recorded IC50 values for tested rPrPs were lower than 50 nM and for some lower than 20 nM, it was decided to change the concentration of rPrPs in PMCA to 50 nM and investigate its effect. Moreover, other tested rPrPs presented less efficacy when only round 5 was inhibited, therefore we tested whether addition of 50 nM of rPrPs into every PMCA round could improve their performance. Furthermore, it was investigated if rRRQ, rKRQ and rPRQ also inhibit other prion isolates, when 50 nM of each rPrP were added to every PMCA round. All prion isolates were amplified for up to round 5 and the rounds with the most consistent amplification for no inhibition samples were analysed. Inhibited with recombinant PrP samples were compared to non-inhibited but amplified samples. Non-amplified samples were prepared at the same time as other samples but stored at -20 °C for the PMCA running time. Round 5 was chosen for analysis of classical ovine scrapie isolates and a bovine BSE isolate and round 4 was analysed for ovine BSE **(Figure 5.2.5)**. These rounds showed the most consistent amplification of no inhibition samples, therefore could be analysed for inhibition responses.

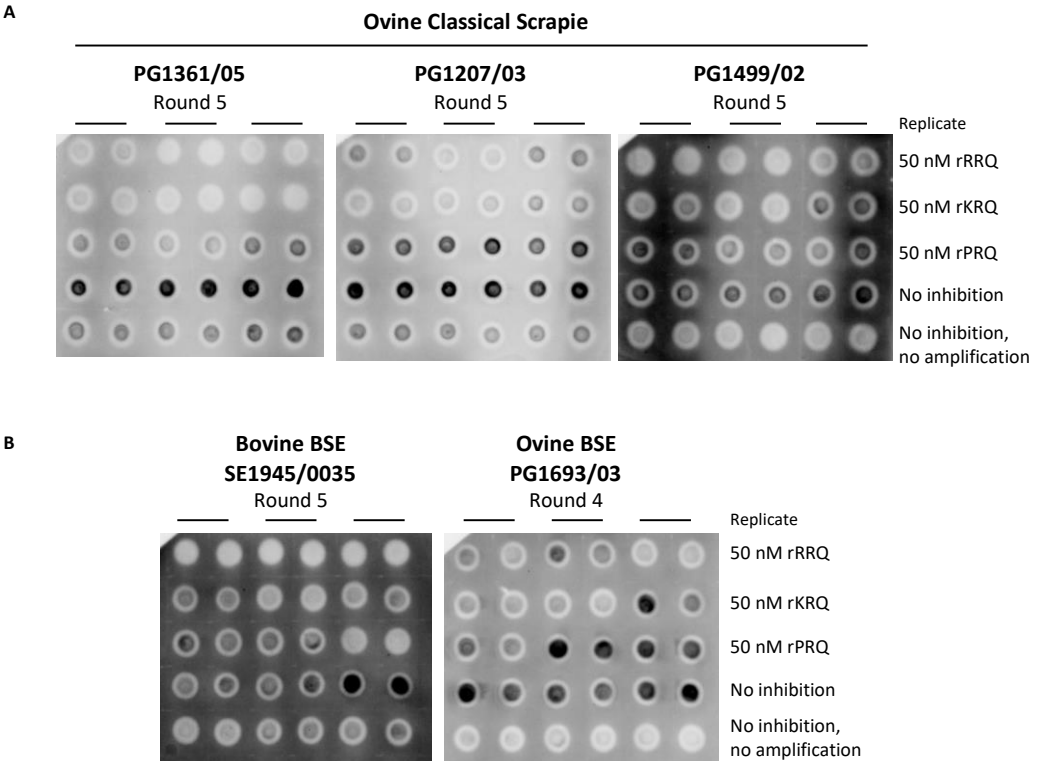

Figure 5.2.5. Representative dotblots for serial PMCA round 5 (classical scrapie and bovine BSE isolates) and round 4 (ovine BSE) shows inhibition with 50 nM of each rRRQ, rKRQ and rPRQ. **A** – inhibition of round 5 of PMCA with 50 nM rRRQ, rKRQ and rPRQ for classical scrapie isolates PG1361/05 (ARQ/VRQ), PG1207/03 (VRQ/VRQ) and PG1499/02 (AHQ/VRQ). 50 nM of rRRQ, rKRQ and rPRQ was added into every PMCA round. **B** – inhibition of PMCA round 5 of bovine BSE (SE1945/0035) and round 4 of ovine BSE (PG1693/03). 50 nM of rRRQ, rKRQ and rPRQ was added into every PMCA round. PMCA products were PK digested and 2.5 µl was analysed on the dotblot in duplicates.

During densitometry analysis, the average signal for no inhibition/no amplification samples was subtracted from the densitometry signals for other samples in ImageJ. Analysis **(Figure 5.2.6)** of round 5 of scrapie isolates showed that on average rRRQ inhibited the scrapie isolates PG1361/05 (ARQ/VRQ), PG1207/03 (VRQ/VRQ) and PG1499/02 (AHQ/VRQ) by 99 %, 90 % and 82 %, respectively. Furthermore, rRRQ also showed high inhibition for both bovine (SE1945/0035) and ovine BSE (PG1693/03, ARQ/ARQ) with average inhibition of 98 % and 64 %, respectively. rKRQ inhibited scrapie isolates PG1361/05, PG1207/03 and PG1499/02 in 100 %, 97 % and 57 %, respectively, and round 5 of bovine BSE was inhibited by 81 % and ovine BSE by 60 %. rPRQ inhibition has been found to be at levels 84 %, 40 % and 46 % for round 5 of scrapie isolates PG1361/05, PG1207/03 and PG1499/02, respectively, and for round 5 of bovine BSE by 68 % and round 4 of ovine BSE by only 18 %. From these results, recombinant ovine rRRQ with arginine at position 136 was found to be the most potent

inhibitor across different prion diseases isolates with a mean of 87 %. This was followed by rKRQ (79 %) and rPRQ (52 %). Additionally, two-way ANOVA (F=2.44, p<0.05) with Dunnett's multiple comparison test was performed on this data in order to compare differences between for each rPrP within isolates. The statistically significant differences were reported for rRRQ between control scrapie PG1361/05 and ovine BSE isolate (PG1693/03) (p=0.0253) and for rPRQ between scrapie PG1361/05 and scrapie PG1207/03 (p=0.0036) and ovine BSE PG1693/03 (p=0.001). When rKRQ was analysed, no statistically significant differences in inhibition were found between scrapie PG1361/05 and other tested isolates (p>0.05). This outcome suggested that from the pool of tested rPrPs, rKRQ was the best inhibitor among all tested isolates derived from different TSEs and its response didn't differ significantly between isolates. However, high standard deviations for rPrP could suggest that both rRRQ and rKRQ showed similar inhibtion rates among tested prion diseases isolates.

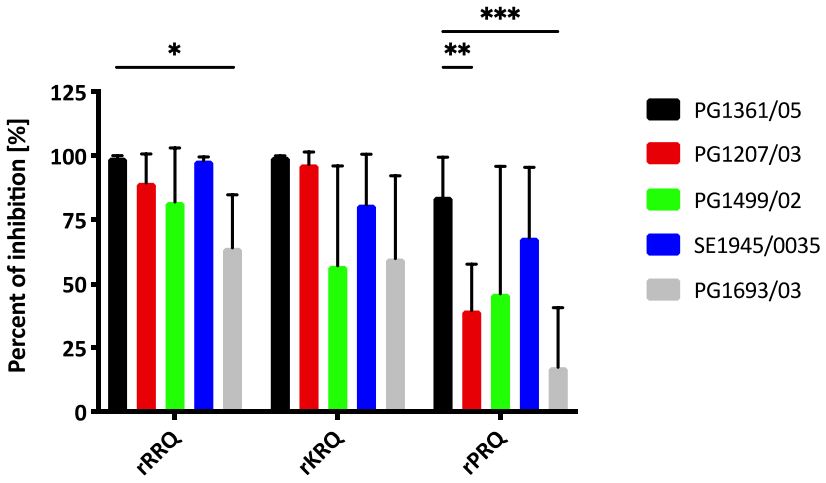

Figure 5.2.6. Percent of inhibition for rRRQ, rKRQ and rPRQ in round 5 of PMCA for ovine scrapie isolates PG1361/05 (ARQ/VRQ), PG1207/03 (VRQ/VRQ), PG1499/02 (AHQ/VRQ), bovine BSE (SE1945/0035) and round 4 of ovine BSE (PG1693/03). The background signals of non-amplified, non-inhibited samples were subtracted from blots. The densitometry values for other samples were obtained from dotblots and the percent of inhibition was calculated using the non-inhibited control. Graph shows the data from three replicates per rPrP. Two-way ANOVA (F=2.44, p<0.05) with Dunnett's multiple comparison test was performed. Statistical differences were found for rRRQ between scrapie PG1361/05 and ovine BSE PG1693/03 ('*', p=0.0253) and rPRQ between control scrapie PG1361/05 and scrapie PG1207/03 ('**', p=0.0036) and ovine BSE PG1693/03 ('***', p=0.001). * - p≥0.05; ** - p≥0.01; *** - p≥0.001; **** - p≥0.0001;

5.2.5 Inhibition of α-synuclein fibrils formation

In order to investigate, whether rRRQ, rKRQ or rPRQ could act as an inhibitor for α-synuclein fibril formation during PMCA, recombinant prion proteins were added at 50 nM concentration prior to PMCA. Recombinant α-syn was seeded with healthy control (HC) and Parkinson's Disease patients (PD) samples and compared to samples treated with rPrPs. Samples were amplified with 40 seconds of sonication followed by 29 minutes 20 seconds of incubation at 37 °C (144 cycles). Products were digested with PK (17 μg/ml) and analysed on the SDS-PAGE. Signal values were measured in ImageJ and the percent of control was calculated. The control for α-synuclein + PD with rPrP was α-synuclein + PD only, whereas for α-synuclein + HC with rPrP was compared to α-synuclein + HC. Moreover, all samples were amplified in 1 x PBST, therefore rPrP in PBST controls were also included in the experiment as further controls. Results showed spontaneous fibrillization of recombinant α-syn and recombinant α-syn with healthy control. Moreover, misfolding of α-syn seeded with Parkinson's Disease samples showed similar to HC seed product. Furthermore, the addition of 50 nM of rRRQ **(Figure 5.2.7)** did not inhibit the α-synuclein fibril formation in all tested cases (recombinant α-syn on its own, seeded with HC and PD samples). The data were compared using statistical one-way ANOVA ($F=0.1969$, $p<0.05$) with Tukey's multiple comparisons test, which showed that there were no statistically significant differences between any tested groups. In addition, also other concentrations – 1 nM and 100 nM of rRRQ – were tested in this experiment but showed results similar to 50 nM rRRQ (data not shown). Moreover, rKRQ and rPRQ were also tested at 50 nM and displayed no inhibition of α-synuclein fibrils formation (data not shown).

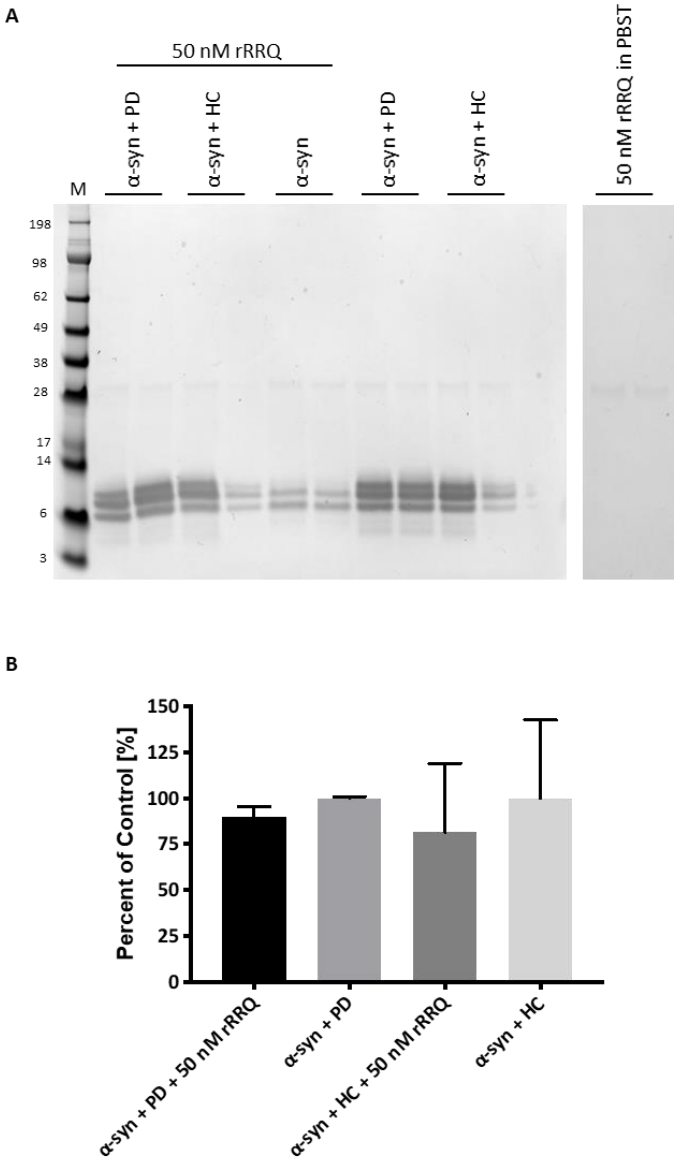

Figure 5.2.7. Representative SDS-PAGE gel image and graph analysis for 50 nM rRRQ inhibition of α-synuclein fibrils formation. **A** – representative SDS-PAGE gel image showing lack of inhibition of α-synuclein fibrils with 50 nM rRRQ. Protein marker was indicated on the left site of the gel (kDa). Each sample was digested with PK at 17 µg/ml and 15 µl of the product was analysed on the SDS-PAGE. Gel was stained with Instant Blue. **B** - graph shows the percent signal with rRRQ compared to the relevant control (shown as 100% signal). The control for α-synuclein with PD and with rRRQ was α-synuclein with PD only, whereas α-synuclein with HC and rRRQ were compared to α-synuclein with HC only. Data were analysed using one-way ANOVA ($F=0.1969$, $p<0.05$) followed by Tukey's multiple comparisons test and showed no statistical differences between groups. α-syn - α-synuclein (no seeding representing *de novo* formation of fibrils); PD – Parkinson's Disease sample seed; HC – healthy control sample seed; M – marker, PBST – phosphate buffer with 0.05 % Tween 20.

5.3 Discussion

This study focused on attempts to inhibit a range of TSE isolates in ruminants and also a completely unrelated protein misfolding disease with mutant rPrPs. In the previous chapter, it has been shown that amongst all produced recombinant prion proteins, three – rRRQ, rKRQ and rPRQ – were identified as demonstrating the greatest potential to decrease the *in vitro* amplification of an ARQ/VRQ classical scrapie isolate. Here, we investigated the inhibition impact of these recombinant PrPs on the replication of other prion isolates. Besides ovine classical scrapie isolate - PG1361/05 (ARQ/VRQ) – two further classical scrapie isolates were used. These were PG1207/03 (VRQ/VRQ) and PG1499/02 (AHQ/VRQ). In addition, bovine BSE (SE1945/0035) and ovine BSE (PG1693/03, ARQ/ARQ) were tested. First of all, the amplification efficiency of these isolates was analysed in various negative brain homogenates. Classical scrapie isolates were found to successfully amplify in VRQ/VRQ substrate over 4 rounds of PMCA. Moreover, bovine BSE was amplified in bovine substrate, and ovine BSE isolate was amplified using a previously established method, where two substrates (AHQ/AHQ and VRQ/VRQ) are alternated (Taema *et al.*, 2012). In addition, distinctive experimental scrapie isolate samples CH1641 (isolates J3011 and J2935) were amplified over four rounds of PMCA but no PrP^{Sc} was detected. Therefore, in this research isolate CH1641 was not analysed further. In comparison to this, Workman *et al*., found that CH1641 isolate J2935 amplified over 5 rounds in AHQ/AHQ substrate (Workman, Maddison and Gough, 2017). In contrast, CH1641 like scrapie isolates was reported not to amplify over 5 or 10 rounds in neither VRQ/VRQ nor AHQ/AHQ substrate (Taema *et al.*, 2012). Discrepancies between the studies may be due to differences in amplification condition used such as the amplitude or could be due to the subtle effects of using distinct sonication machines/horns.

For PG1361/05, 0.5 µl of PrP^{Sc} going into round 1 showed high levels of PrP^{Sc} amplification. On this basis we hypothesized that the amount of PrP^{Sc} going into round 5 would be high and detectable on dotblot without round 5 amplification. To test that, we firstly added various amounts of PG1361/05 round 4 product into round 5 of PMCA and performed the amplification. The result showed that the highest PrP^{Sc} signal was when 3/7 of round 4 was added into round 5. Furthermore, PrP^{Sc} amplified even when adding only 3.75 µl of round 4 spike. This amount of PrP^{Sc} spike resulted in no background signals, therefore, would have been ideal for screening inhibitors. But other isolates did not amplify as efficiently as this scrapie isolate therefore higher seeding volume (3/7) was used. Secondly, different rRRQ concentration were tested with 3/7 ratio of round 4 into round 5 of PMCA for control classical scrapie PG1361/05. It was noticed that there were no differences between used rRRQ concentration. Additionally, to test the exact signal of round 4 amplified PrP^{Sc} going into round 5 (3/7 ratio), we prepared the sample as for non-inhibition control but 24 h amplification was replaced by sample storage. The experiments showed that the round 4 PrP^{Sc} spike was detectable on dotblots and could act as a negative (background) control for dotblots. Furthermore,

for some cases, the signal for no amplification, no inhibition controls was higher than inhibited samples. This suggested that the amplification was inhbited in 100 % but and the signal came from the previous round seed.

Workman and colleagues established that addition of 400 nM rVRQ inhibited the serial amplification of PG1361/05 by 100 %. Primary tests with control isolate PG1361/05 involved screening 400 nM of rVRQ and compared it to 100 nM rRRQ, rKRQ and rPRQ (as they had lower IC50 values than rVRQ). At this point, results showed that there were no significant differences in inhibition of ARQ/VRQ scrapie isolate between 400 nM rVRQ and 100 rRRQ or rKRQ. Moreover, inhibition with 100 nM rPRQ had lower efficiency and larger variability than for the other rPrPs. At this point, the 400 nM rVRQ and 100 nM rRRQ and rKRQ inhibited the round 5 amplification at the same level showing that rRRQ and rKRQ are potentially more efficient inhibitors than rVRQ, as also indicated by the relative IC50 values.

After the optimisation of the serial PMCA conditions for the amplification of each TSE isolate, rounds with the most consistent amplification across the experimental repeats were chosen for densitometry analysis. Round 5 for every classical scrapie isolate (PG1361/05, PG1207/03 and PG1499/02) and bovine BSE (SE1945/0035) were analysed, whereas for ovine BSE (PG1693/03) round 4 of PMCA was analysed. As a background control, either round 5 or round 4 were prepared the same way as the no inhibition control, however, no amplification was carried out and samples were frozen for the PMCA duration time. This control showed the exact amount of PrP^{Sc} spike going into the final round of PMCA and provided the background signal in the blots. Additionally, after discussions and consideration it was decided to lower the amount of rPrP used in PMCA from 100 nM to 50 nM. The reported IC50 values for rPrPs were lower than 20 nM. Basing on the molecular weight and obtained concentration for each rPrP, it was possible to include as accurately as possible 50 nM of each PrP. Moreover, for some isolates round 5 amplification products had already large amounts of PrP^{Sc} what could have an impact on the rPrP performance. Therefore, for testing other isolates, rPrPs at 50 nM were added into every PMCA round.

Workman *et al*., showed that rVRQ acted as a strong inhibitor for various TSE isolates. Classical scrapie isolates (PG1361/05 (ARQ/VRQ) and PG1563/02 (VRQ/VRQ)), mouse passaged classical scrapie (two G338 scrapie and two Apl338 scrapie isolates, all VRQ/VRQ), ovine BSE isolates (PG0392/04 and PG1693/04, both ARQ/ARQ) and bovine BSE isolates (SE1929/0729 and SE1945/0035) were tested. In every case, rVRQ at 400 nM inhibited the prion protein amplification with a mean inhibition of 84 % (Workman, 2017; Workman, Maddison and Gough, 2017). In the current study, our final tests involved using rPrP at 50 nM in every PMCA round. This amount of recombinant protein inhibited round 1 of classical scrapie isolate (PG1361/05, ARQ/VRQ) by 100 %. In this assay, the mean percent of inhibition for rRRQ (at 100 nM) across all tested TSE isolates was 87 % which was marginally higher than previously reported value for rVRQ at 400

nM – 84 % (Workman, 2017; Workman, Maddison and Gough, 2017). Furthermore, rRRQ inhibited classical scrapie isolates as well as bovine BSE and ovine BSE. rKRQ also displayed high mean inhibition value for all tested isolates – 79 %. rKRQ showed similar inhibition efficiency for classical ovine scrapie isolates – PG1361/05 and PG1207/03 and bovine BSE in comparison to rRRQ. While testing the third recombinant prion protein rPRQ, it was found that the variations between replicates and experiments were high and the protein had a lower mean percent of inhibition (52 %). In addition, statistical analysis for rPrPs for control classical scrapie isolate (PG1361/05) and different TSE isolates revealed that rKRQ was the best inhibitor among all tested isolates. It's percent of inhibition did not differ significantly between the control isolate and other TSE isolates. This was followed by rRRQ which only displayed the difference between PG1361/05 and ovine BSE. In contrast, rRRQ had the highest mean inhibition for all isolates from all tested rPrP. On the other hand, rPRQ showed differences in inhibition between PG1361/05 and another classical scrapie PG1207/03 and ovine BSE. Interestingly, for any of the tested rPrPs no significant differences were reported between ovine classical scrapie PG1361/05 and other species TSE – bovine BSE. This result confirm the data obtained for rVRQ, which had the same inhibition level for ovine scrapie and bovine BSE (Workman, 2017). These data confirm the hypothesis that recombinant prion protein could act as an inhibitor for a wide spectrum of animal TSE isolates independently from the genotype differences between the recombinant PrP^{C} and the seeding PrP^{Sc}, and the prion strain being amplified (Workman, 2017).

It was also investigated whether rPrP could act as inhibitor for an unrelated protein misfolding processes. Here, α-syn aggregates were produced according to a PMCA method developed by research group member Juan Fernandez Bonfante (personal communication). The method can amplify synthetic α -synuclein monomers into fibrils either without seed (*de novo* formation) or after seeding with either PD or healthy brain samples. It has been shown that the seeded samples contain distinct fibril conformers compared to *de novo* fibrils (Juan Bonfante, personal communication). An analogous method has also been reported and the α-synuclein aggregates shown to display similar biochemical and biophysical characteristic as *in vivo* α-synuclein aggregates (Herva *et al.*, 2014). Moreover, commonly known anti-amyloid compounds like CR or curcumin have been tested by this method. The PMCA products showed significant decrease in ThT positive structures after Congo Red or curcumin treatment. Also, SDS-PAGE results were consistent with these findings and less PK-resistant α-synuclein was produced in the presence of the inhibitors (Herva *et al.*, 2014). Here, it was tested whether the recombinant ovine prion proteins could inhibit the *in vitro* formation of α-synuclein aggregates. Based on the finding by Nieznanski, in which prion protein was described as having disaggregating properties, we tested if it inhibits α-synuclein aggregates production (Nieznanski *et al.*, 2014). This preliminary outcome showed that in the PMCA system, rPrPs did not prevent or decrease the extent of fibril formation. Previously, research produced conflicting outcomes regarding the PrP – α-synuclein interactions

(Ferreira *et al.*, 2017; La Vitola *et al.*, 2019; Corbett *et al.*, 2020). Furthermore, the method of α-synuclein oligomers production was different in each case and none of these previous studies involved fibril production by PMCA. One study used 300 seconds of shaking every 10 minutes before the ThT fluoresce reading (Corbett *et al.*, 2020). Other two studies used either shaking for 6 days at 37 °C or incubation of α-synuclein at 37 °C for 48 h without shaking (Ferreira *et al.*, 2017; La Vitola *et al.*, 2019). In addition to the different methodologies for fibril production, all three studies produced *de novo* α-synuclein aggregates and reactions were not seeded with Parkinson's Disease samples. Therefore, it is possible that fibrils produced in our research (and between studies), could exhibit different features and misfolding pattern for samples seeded with HC or PD samples.

To conclude, three recombinant prion protein produced in this research – rRRQ, rKRQ and rPRQ – were found to inhibit various TSE isolates but not the formation of misfolded α-synuclein during PMCA.

Chapter 6: PrP derived peptides as inhibitors of prion replication

6.1 Introduction

The use of peptides derived from recombinant proteins shows an opportunity to design new therapeutics that mimics natural processes (Lau and Dunn, 2018). In addition, peptides could be engineered to have higher biological activity, membrane penetration and be less toxic than the full-length proteins. Furthermore, peptide production has lower cost (Baig *et al.*, 2018). Peptide inhibitors have been used in a range of neurodegenerative diseases. For Aβ, β-sheet breakers were described. These compounds specifically recognise and bind amyloid β fragments and prevent the oligomer and/or fibril formation (Funke and Willbold, 2012). In the Aβ aggregation studies, sequence KLVFFA (Aβ residues 16-21) and its modifications were used (Soto *et al.*, 1996; Tjernberg *et al.*, 1996; Funke and Willbold, 2012). This peptide is derived from the hydrophobic, fibrillogenic fragment of the Aβ N-terminus (Barrow *et al.*, 1992). The peptide not only bound to the monomeric full-length protein but also prevented its polymerization into fibrils by blocking the formation of β-sheet rich structures (Soto *et al.*, 1996; Tjernberg *et al.*, 1996; Nieznanska *et al.*, 2018). Additionally, other research investigated how the substitution of any amino acid in the HHQKLVFFAEDVG (Aβ residues 13-25) sequence changes the impact on Aβ aggregation. For that purpose, overlapping peptides were designed. As a result, the replacement of any amino acid in the sequence equivalent to Aβ residues 13-25 with proline resulted not only in better peptide solubility but most importantly in significant reduction of fibrils formation (Wood *et al.*, 1995). Moreover, a similar approach was used for the inhibition of tau fibrils formation. Pir and colleagues used a recombinant tau fragment (residues 258-360) with inserted prolines. The tau fibrils formation was investigated in multiple experiments involving Thioflavin S fluorescence, atomic force microscopy and N2a cell culture. The outcome showed that the modified tau fragment affected the aggregation process in a dose-dependent manner (Pir *et al.*, 2019).

PrP^{sen} to PrP^{res} conversion and PrP^{res} accumulation has been inhibited using prion protein derived peptides in cell free conversion assays and MNB scrapie infected cells (Chabry, Caughey and Chesebro, 1998; Chabry *et al.*, 1999). Among many overlapping hamster and mouse amino acid sequences tested, peptides homologous to the central parts of PrP were the most successful and showed the potential for this approach for further usage among other prion diseases (Chabry *et al.*, 1999). Moreover, N-terminus PrP derived peptides were also found to inhibit the Aβ fibrils formation and their neurotoxic effects on cells (Nieznanski *et al.*, 2012; Fluharty *et al.*, 2013; Nieznanska *et al.*, 2018). It was presented that two binding sites (residues 23-31 and 95-105) on the PrP^{C} could interact with the Aβ (Chen, Yadav and Surewicz, 2010). Based on that, the PrP fragment containing the PrP^{C} residues 23-111 (N1 peptide) was designed and tested. It was found that N1 inhibited the oligomers fibrils formation in polymerization assays (Fluharty *et al.*, 2013). In addition, further research presented that full length PrP was found to have similar effectiveness as the N1 peptide, whereas the C-terminal fragment had no

inhibitory activity on Aβ fibril formation (Nieznanski *et al.*, 2012). Moreover, the shortest possible molecule with the ability to inhibit amyloid β misfolding was investigated using the ThT fluorescence assays and transmission electron microscopy analysis. The two N1 derived peptides (PrP23-50 and PrP90-112) interfered with amyloid formation, however, the process was less effective than for the N1 peptide (Nieznanska *et al.*, 2018).

In the previous research, synthetic hamster peptides were shown to interact with PrP^{sen} and demonstrated inhibitory effect in cell free scrapie conversion assays (Chabry, Caughey and Chesebro, 1998). The most successful peptides were highly homologous in other species PrP sequences (Chabry *et al.*, 1999). In this research, we propose similar mechanisms for ovine prion protein conversion during PMCA and that fragments or peptides from ovine PrP can inhibit prion formation. In this chapter, we focused on designing and producing ovine PrP derived peptides in order to investigate which part of the structure and/or sequence might have an impact on the inhibition of *in vitro* prion protein misfolding. We analysed rVRQ, rRRQ, rKRQ and rPRQ derived peptides of different lengths. The sequences of these peptides were carefully designed to include the known polymorphisms at positions 136, 154 and 171 in ovine PrP. Peptide design included predicted structural analysis in order to select the residues in the protein sequence that could be important for β-sheet formation and molecule stabilization. Furthermore, the predicted protein structure was used as a tool for predicting the various amino acids substitutions on protein structure, function and bindings (Teng *et al.*, 2010). Here, models were created for rARQ, rRRQ, rKRQ and rPRQ with focus on the amino acid substitutions at position 136 in those recombinant proteins. These four recombinant proteins were compared to those previously deposited in Protein Data Bank VRQ model (pdb entry 2N53) that showed less efficient inhibition than rRRQ, rKRQ and rPRQ in *in vitro* misfolding (Workman, Maddison and Gough, 2017).

6.2 Results

6.2.1 Optimisation of peptides' solvent concentration in PMCA

Acetonitrile was used as solvent for all peptide Ov112-144 fragments, as specified by the manufacturer. In order to assess any peptide solvents inhibitory effects in PMCA, a range of concentrations of acetonitrile was added to PMCA and samples were amplified as previously described **(Figure 6.2.1)**. The solvent concentrations required to be added in the PMCA reactions were calculated from peptides concentrations. Results were compared to samples amplified in PBS. Densitometry analysis showed that 2.7 % of acetonitrile, that is an equivalent amount of solvent in 50 µM of peptide, had a significant inhibition effect on amplifications of PG1361/05 scrapie (ARQ/VRQ). On average, it inhibited the scrapie amplification by 64 %. Furthermore, the 0.05 % and 0.005 % of acetonitrile that would correspond to 1 µM and 100 nM peptide concertation, respectively, slowed down the prion protein misfolding by 30 %. This result shows that there is acetonitrile related inhibition of misfolding of prion protein.

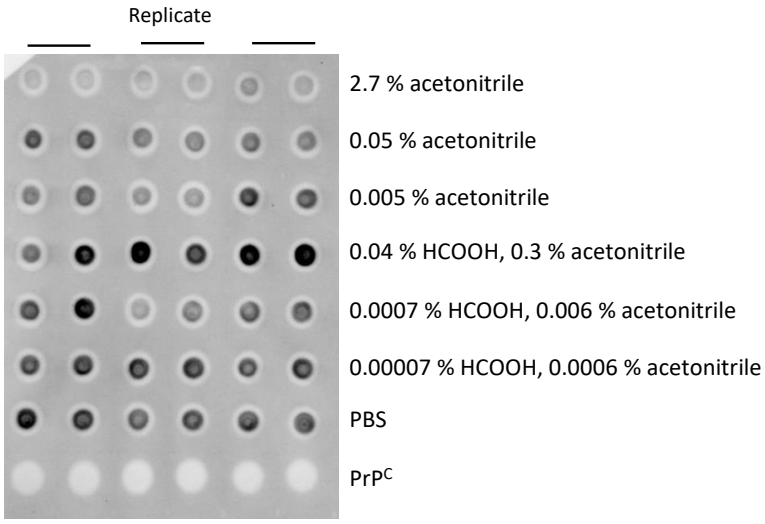

Figure 6.2.1. Solvent impact on scrapie ARQ/VRQ PG1361/05 *in vitro* amplification. Different amounts of acetonitrile and formic acid (HCOOH) were added into PMCA and amplified for 24 h. 2.5 µl of PK digested products were analysed on dotblot in duplicate. Samples contain specific solvent were compared to samples amplified in PBS. PrP^C – negative brain homogenate.

Furthermore, for peptide OvV122-139, manufacturer solubility tests showed that this peptide is resuspended in acetonitrile and formic acid (HCOOH). Therefore, different concentrations according to peptide concentrations were tested with the highest being 0.04 % HCOOH, 0.3 % acetonitrile for 50 µM peptide and the lowest - 0.00007 % HCOOH, 0.0006 % acetonitrile for 100 nM of peptide OvV122-139. The dotblot analysis showed that the mixture of formic acid and acetonitrile had no impact on the ovine

scrapie prion protein misfolding during the PMCA. Additionally, OvR, OvK and OvP122-139 were resuspended in water and their solvent impact on PMCA was not assessed.

6.2.2 Peptides inhibition of ovine scrapie PG1361/05 amplification

rRRQ derived peptides (OvR112-144 and OvR122-139) were screened at concentrations of 50 µM, 1 µM and 100 nM and compared to 50 nM rRRQ and no inhibition controls **(Figure 6.2.2)**. 50 µM of peptide was equivalent to 2.7 % of acetonitrile in the PMCA reaction, therefore PrP^{C} in 2.7 % of acetonitrile was also analysed. For each peptide concentration, non-inhibited control with equivalent solvent concentration was studied. So that, 50 nM rRRQ, 50 µM, 1 µM and 100 nM of OvR122-139 were compared to PG1361/05 amplification in PBS. Then, 50 µM of OvR112-144 was compared to PG1361/05 amplification with 2.7 % acetonitrile, 1 µM of OvR112-144 was compared to PG1361/05 amplification with 0.05 % acetonitrile and 100 nM of OvR112-144 to PG1361/05 amplification in 0.005 % acetonitrile. Data shows that the addition of 2.7 % acetonitrile already inhibited the amplification of PG1361/05, therefore it is difficult to investigate the inhibition of 50 µM of OvR112-144 peptide, which contain 2.7 % acetonitrile. In such case, any PrP^{Sc} signal decrease came from solvent rather than peptide derived inhibition. PMCA samples containing 1 µM and 100 nM of this peptide did not inhibit amplification. On the other hand, 50 µM of OvR122-139 inhibited the misfolding on average by 30 %, whereas 1 µM and 100 nM had no inhibitory effect.

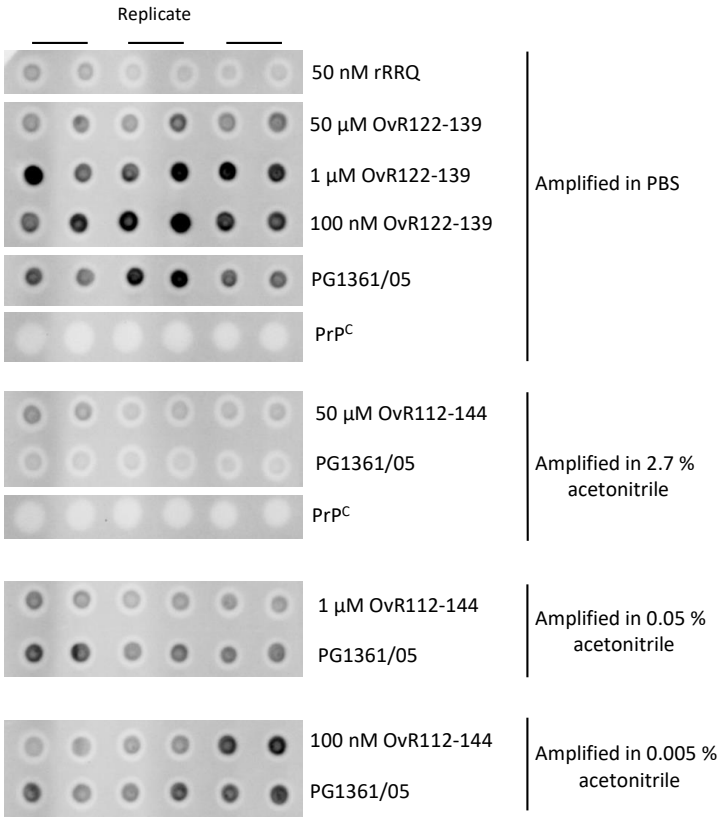

Figure 6.2.2. Representative dotblot shows inhibition of ovine scrapie PG1361/05 (ARQ/VRQ) with rRRQ and OvR peptides. 50 nM rRRQ, 50 µM, 1 µM and 100 nM of OvR122-139 were compared to PG1361/05 amplified in PBS. PrP^C amplified in PBS was included as a PK digestion control. 50 µM OvR112-144 was compared to PG1361/05 amplified in the presence of 2.7 % acetonitrile and PrP^C in 2.7 % acetonitrile was included as a digestion control. 1 µM of OvR112-144 was compared to PG1361/05 amplified with addition of 0.05 % acetonitrile. 100 nM of OvR112-144 was compared to PG1361/05 amplified in 0.005 % of acetonitrile. Amplification products were PK digested and 2.5 µl of each sample were added on the dotblot in duplicate. PrP^C – negative brain homogenate.

Possible inhibition of OvR122-139, PMCA with higher concentrations of this peptide (50 – 150 µM) was investigated **(Figure 6.2.3)**. The results showed again that there was around 30-40 % of signal decrease for 50 µM of that peptide in compare to non-inhibition samples, however higher concentrations showed no inhibition. Based on this, we concluded that there is no significant OvR122-139 inhibition of ovine scrapie PG1361/05. The 30-40 % signal decrease for 50 µM peptide on the dotblot could be PMCA variation rather than peptide derived inhibtion.

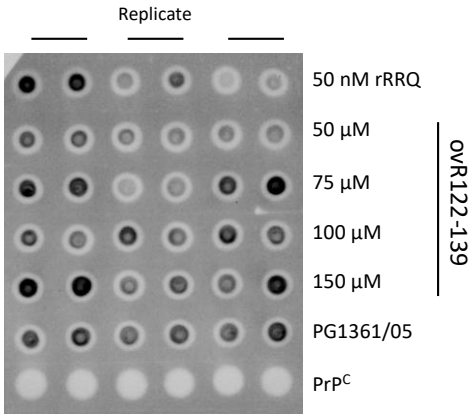

Figure 6.2.3. Representative dotblot showing the inhibition of ovine scrapie PG1361/05 (ARQ/VRQ) with 50 nM rRRQ and 50 – 150 µM of OvR122-139 peptide. This peptide was re-suspended in water and further dilutions were made in PBS. All inhibition samples were compared to no inhibition control – PG1361/05 that was also diluted in PBS. PrP^C (negative brain homogenate) was included as a background control and to assess PK digestion efficacy. All samples were PK digested and 2.5 µl of each sample was added on dotblot in duplicate.

Further peptides were also tested for rVRQ, rKRQ and rPRQ. The longer peptide for each mutation (OvV112-144, OvK112-144, OvP112-144) and a randomised peptide (OvRND) were tested at 1 µM and 100 nM. 50 µM was not assessed further as this resulted in an acetonitrile concentration of 2.7 % that interfered with PMCA. In addition, the shorter peptides OvK122-139 and OvP122-139 were analysed at 50 µM, 1 µM and 100 nM as they were resuspended in water and then diluted in PBS. In addition, OvV122-139 was resuspended in formic acid and acetonitrile, and these concentrations of solvents were not affecting misfolding *in vitro*. In all cases, there was no peptide inhibition of scrapie ARQ/VRQ PG1361/05 **(Appendix)**.

The peptide that consists of three ovine polymorphic positions 136, 154 and 171 was designed with R at 136 position (OvR130-173) was also produced. There was no suggested solvent from the manufacturer, therefore the overall peptide net charge was calculated using the online calculator pepcalc to be 1.1 at pH 7 (Lear and Cobb, 2016). The value suggested good water solubility, therefore the peptide was resuspended in ultrapure water and further dilutions were performed in PBS. The range of peptide concentrations (50 µM – 1 nM) were added into PMCA reactions **(Figure 6.2.4)**. The dotblot analysis showed that OvR130-173 had no inhibitory effect on amplification of ovine scrapie PG1361/05 ARQ/VRQ isolate.

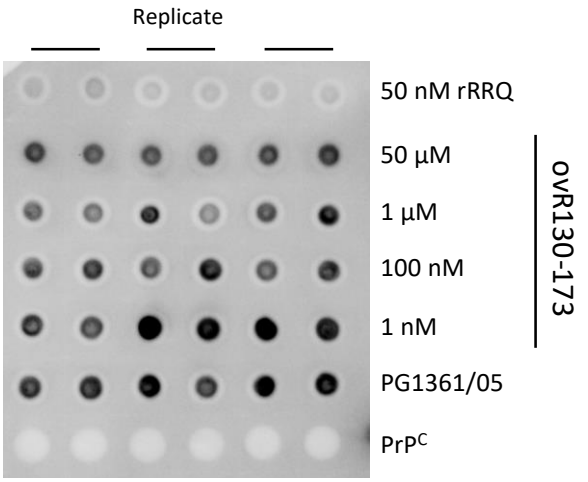

Figure 6.2.4. Representative dotblot determining the inhibition of ovine scrapie ARQ/VRQ (PG1361/05) with 50 nM rRRQ and range of concentrations (50 µM – 1 nM) OvR130-173). The peptide included all three polymorphic positions in ovine PrP and included arginine at 136 and 154 position and glutamine at 171 position (RRQ). Peptide was re-suspended in water and further dilutions were made in PBS. All inhibition samples were compared to no inhibition control – PG1361/05 that was also diluted in PBS. PrP^C (native brain homogenate) was included as a background control and to test PK digestion efficacy. All samples were PK digested and 2.5 µl of each sample was added on dotblot in duplicate.

In summary, the various peptides derived from rVRQ, rRRQ, rKRQ and rPRQ and containing the residue at 136 showed no inhibitory effect on the PrP^{Sc} formation *in vitro*.

6.2.3 Structural overview of the rPrP mutants

6.2.3.1 Structure of ovine PrP with valine at 136 position

As a model the wild-type ovine PrP (accession code: 2N53) with valine$_{136}$, arginine$_{154}$ and glutamine$_{171}$ was taken from the Protein Data Bank (PDB), entry 2N53 **(Figure 6.2.5, B)** (Munoz-Montesino *et al.*, 2016). The structure analysis in PyMOL showed 3 α-helices within the core PrP structure **(Figure 6.2.5, A)**. During the PyMOL analysis of the 2N53 entry those helices were reported at positions: α-helix 1: 146-156, α-helix 2: 174-194 and α-helix 3: 202-232. In addition, there is one anti-parallel β-sheet present in the structure (131-134 and 162-165), however it was not shown in the images generated by the pdb files downloaded from the website.

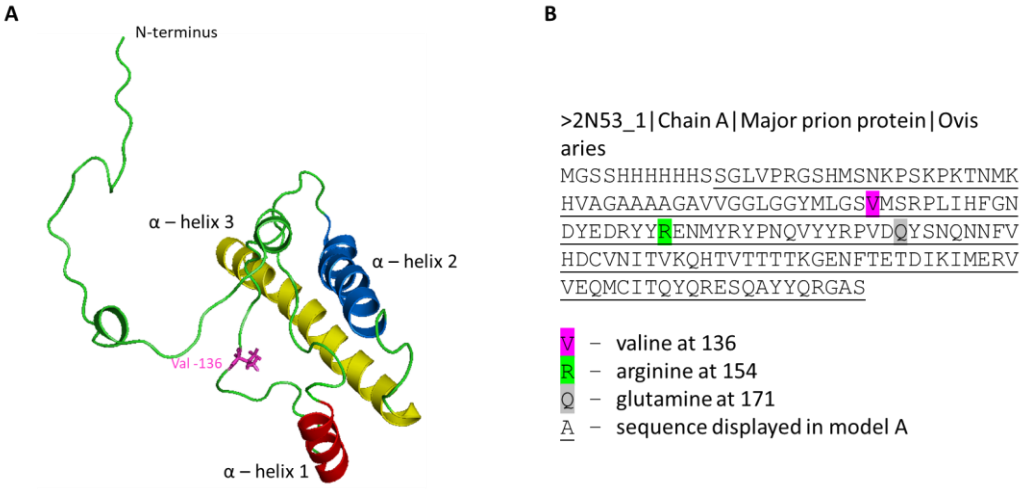

Figure 6.2.5. The most-representative model of the PrP structure (**A**) and sequence (**B**) of the 2N53 protein bank database entry. **A** – structure of ovine prion protein with valine at 136 position (pink) was generated using 2N53 .pdb file and PyMOL (version 0.99). The model contains residues 92 (S) – 234 (S) of ovine prion protein and does not contain the poly-his tag. 1st α-helix is indicated in red, 2nd α-helix – blue, 3rd α-helix – yellow. **B** – ovine prion protein amino acid sequence. Valine (pink), arginine (green) and glutamine (grey) are marked as known polymorphic positions 136, 154 and 171, respectively. Also, the displayed on **A** sequence was underlined.

Moreover, it was also investigated how the valine position at 136 varies between different NMR model ensembles. From different models' alignment **(Figure 6.2.6, A)** it was noticed that the N-terminus of the ovine PrP was highly flexible and presented large variations between NMR coordinates. Moreover, these variations between models existed until residue 131 (tyrosine), at which the models started to create a more organised amino acid chain with similar coordinates for each NMR entry. After a closer look at the 136 position region **(Figure 6.2.6, B)**, it was observed that the positions

around 136 valine might have different NMR coordinates in different NMR models suggesting flexibility.

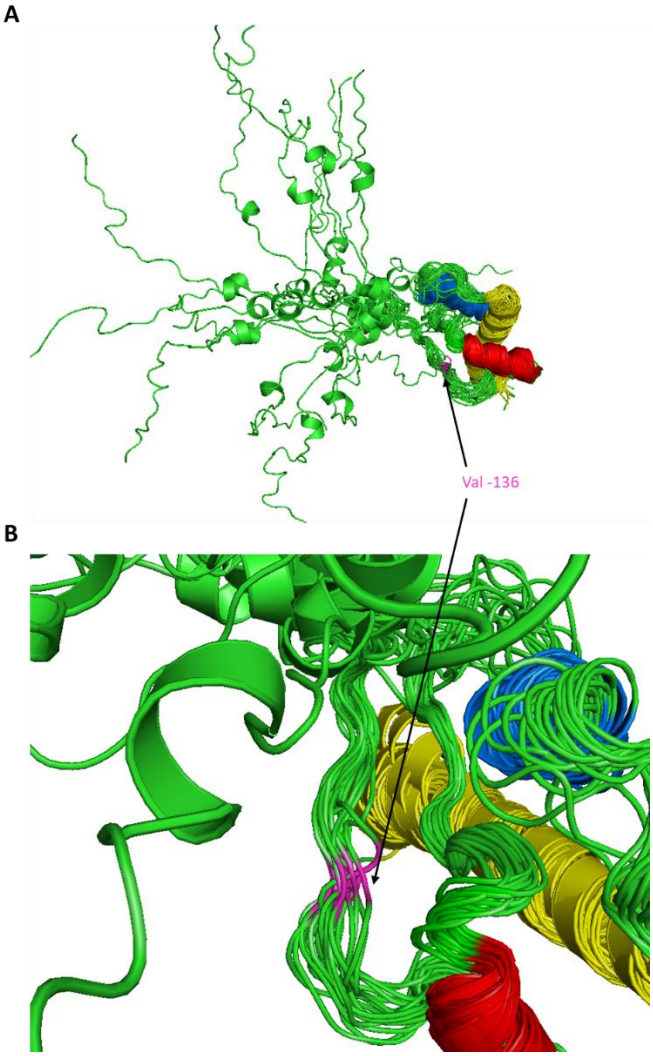

Figure 6.2.6. NMR ensembles of solution models of ovine prion protein with valine at 136 position (2N53 PDB entry). **A** – whole prion protein structure. **B** – close-up view of the 136 position region. The valine$_{136}$ has been marked in pink and is indicated in arrows.

6.2.3.2 Comparison of PrP models of different species

In order to better understand whether the effective therapeutic for prion disease could work among other species, the similarities in prion protein sequences were investigated. Prion protein sequences are highly conserved between mammalian species. The protein sequences for ovine (P23907), bovine (P10279), human (P04156), mouse (P04925) and hamster PrP (P04273) from UniProt database were compared using ClustalW (Higgins, Thompson and Gibson, 1996; The UniProt Consortium, 2019). The degree of homology between species could be an indicator of using a potential therapeutic for TSEs across

species. For all species, alanine was present at 136 position (ovine position) **(Figure 6.2.7, A)**. Moreover, the sequences comparison showed that ovine PrP shared 70 % sequence alignment with bovine, 89 % with human, 83 % with mouse and 85 % with hamster PrP. The lower percent of similarity between ovine and bovine PrP was a result of an additional octapeptide repeat in bovine PrP. In addition, to visualise the PrP structures, PDB entries for ovine (2N53), bovine (1DWY), hamster (1B10), mouse (1XYX), and human (1QLX) were used (James *et al.*, 1997; Zahn *et al.*, 2000; Lopez Garcia *et al.*, 2002; Gossert *et al.*, 2005; Munoz-Montesino *et al.*, 2016). The deposited database entry for ovine PrP included the ARQ variant, the partial alignment between full ovine PrP (P23907) and Protein Data Bank entry for ovine PrP (2N53) was performed **(Figure 6.2.7, B)**. The pdb entry contained a shorter sequence, that started with a poly-his tag and did not contain the octapeptide repeats within the N-terminal protein end. The first amino acid that was common for pdb and Uniport entry was N_{103}. The similarity between full ovine PrP and 2N53 was 86 %, however this analysis included the whole N-terminus of full-length protein and poly-his tag of 2N53 followed by residues not common in ovine PrP in these models. Additionally, when ovine PrP fragment 103 (N) – 234 (S) fragment and 2N53 sequence were compared, the sequences similarities were at 99 % with differences being at 136 position (A/V) and 171 position (R/Q), which are natural polymorphisms observed previously (Belt *et al.*, 1995; Goldmann, 2008). Moreover, sequences for all other full-length PrP were aligned to pdb entries. The similarities were 99 %, 99 %, 100 % and 100 % for bovine, human, mouse and hamster sequences, respectively (data not shown). For bovine data, only one aa substitution was found at position 131 (A/S), whereas in human data two positions 21 (L/G) and 22 (C/S). For human sequence, the differences at 21 and 22 residues are within the signal peptide that is being cleaved during the protein processing. Therefore, the presence of different amino acids at these positions could be an experiment variation rather than commonly found differences in protein sequence. Furthermore, in other species, alanine is presented naturally at the 136 position (as numbered in ovine sequence), but the ovine rPrP with alanine at this position was a less effective inhibitor than VRQ. Therefore, only structures that have valine at 136 were analysed.

Figure 6.2.7. Prion protein sequences alignment. **A** – full-length PrP alignment for ovine (P23907), bovine (P10279), human (P04156), hamster (P04273) and mouse (P04925) performed in ClustalW. Alanine at equivalent to 136 position in ovine PrP is marked with a red box. In all other species analysed, alanine is present at this position. The similarities between ovine and other species are: 70 %, 89 %, 83 % and 85 % for bovine, human, mouse and hamster, respectively. **B** – representative sequence alignment for full length PrP (P23907) and pdb entry (2N53) sequence for ovine PrP. The similarity of these two sequences was 86 %. The differences included include the presence of poly-his tag in 2N53 sequence and two amino acids substitutions: A/V_{136} and R/Q_{171}. Position 136 is indicated in red box. Analysis performed using ClustalW.

The ovine PrP structure with valine at 136 position (2N53) was compared in PyMOL to other PrP of mammalian species **(Figure 6.2.8)**. The structures alignment was only partial and did not include the whole flexible N-terminus. The structural analysis showed

that all compared PrPs contained three α-helices in the 3-D model. It was noticed that the valine$_{136}$ in ovine PrP was directed inside the protein chain, whereas for other proteins with alanine, this amino acid residue was directed to the outside of the molecular structure. Additionally, there were no large differences within the structure's alignment between PrPs.

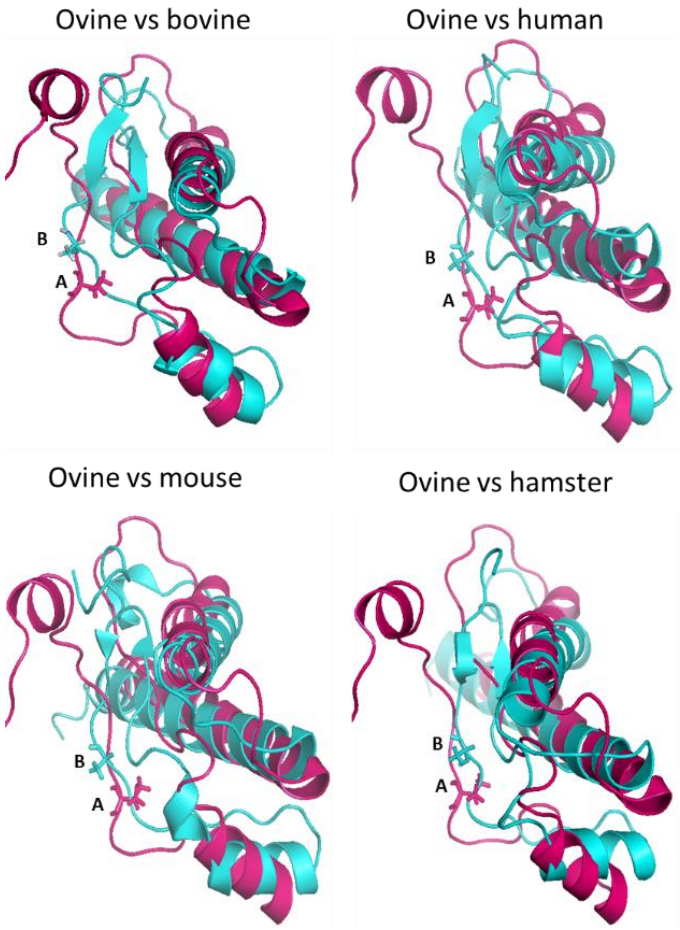

Figure 6.2.8. Ovine PrP (PDB entry 2N53, pink) superposition with bovine (1DWY), human (1QLX), mouse (1XYX) and hamster PrP (1B10) (all cyan). Valine at 136 position in ovine PrP is indicated on the images as A, whereas alanine in other models is indicated as B. All models were compared in PyMOL.

6.2.3.3 rPrP variants structural comparison

In order to generate the pdb files for PrP mutants at position 136, a web server - Dynamut – was used (Rodrigues, Pires and Ascher, 2018). Firstly, to investigate the differences between ARQ and VRQ, a structural model for ARQ was generated in Dynamut server (Rodrigues, Pires and Ascher, 2018). Using the pdb files obtained from

Dynamut distance lengths between carbons in both alanine and valine at 136 position to other amino acid were measured. Alanine is a short amino acid with a side chain methyl group attached to the central carbon. In comparison to alanine, the valine side chain contains an isopropyl group attached to central carbon (Hastings *et al.*, 2016). PyMOL analysis allowed comparison of the 3-D models of both VRQ and ARQ and measurement of the distances between the closest amino acid side chains **(Figure 6.2.9)**. It was identified that the closest side chains to both valine and alanine at 136 position were leucine at 141 position. Using Dynamut interatomic interactions file and PyMOL measurement tool, the distances were measured from C5 or C5' of leucine at 141 position to C3, C4 and C4'. The distances were as follows: ~3.6, 3.7 and 3.9 Ångstroms (Å), respectively. According to the software analysis there could be some interactions between these carbon atoms like hydrophobic bonds. In compare to this, only one possible interaction was mapped between C5 or C5' of leucine and C3 in alanine, however the measured distance value was similar (~3.5 Å).

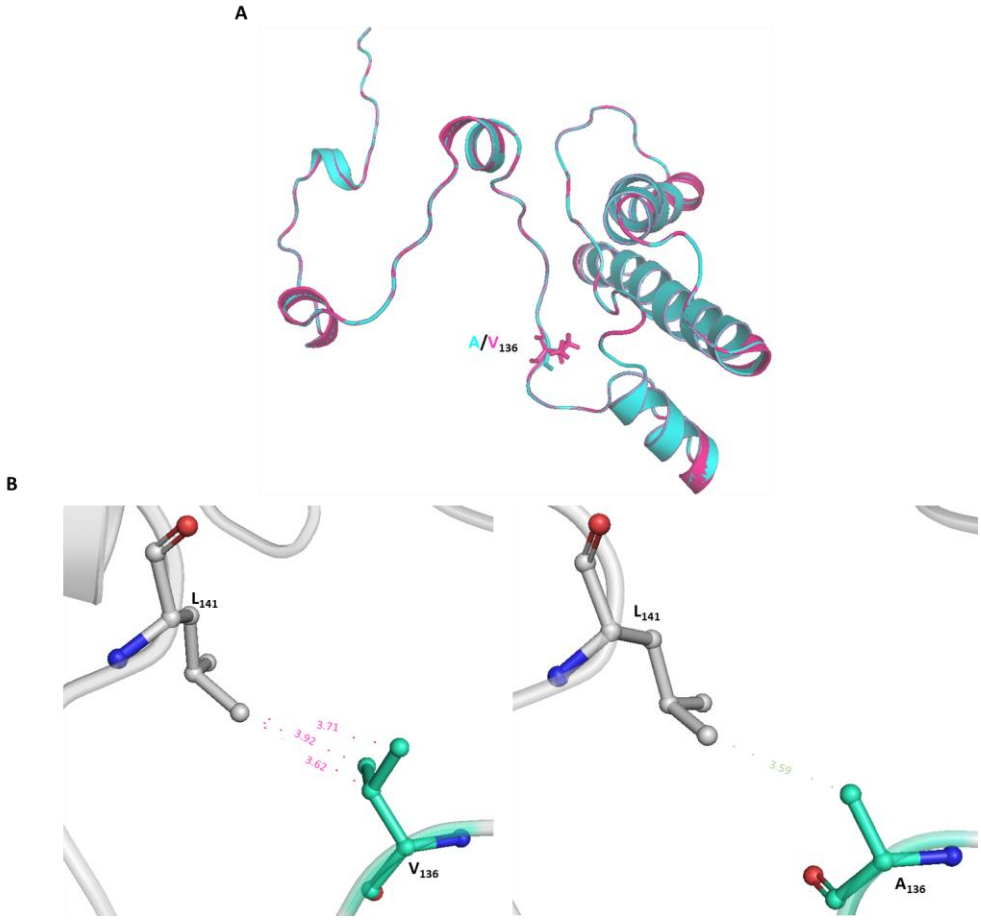

Figure 6.2.9. VRQ and ARQ structure comparison. **A** – Alignment of VRQ (valine at 136 position, pink) and ARQ (alanine at 136 position, cyan) 3-D models. **B** – Distances and possible interactions mapped between 136 position valine (V)/alanine (A) (green) and leucine (L) (grey) atoms at 141 position. The interatomic interactions files were generated using Dynamut and distances were measured using PyMOL tool 'measurement'. There are 3 possible interactions between valine carbons (C3, C4, C4') and C5 or C5' of leucine at 141 position (lengths: ~3.6, 3.7 and 3.9 Å), whereas only one interaction between alanine C3 and leucine was mapped (length ~3.5 Å). Oxygen atoms are indicated in red, nitrogen atoms are blue.

Next, the structure of VRQ was compared to structure with R at 136 position (RRQ). Arginine contains a three-carbon chain that ends with a guanidino group (Hastings *et al.*, 2016). The arginine carbon chain is longer than the previously analysed alanine or valine carbon chains. Again, whole 3-D models were compared between these two proteins and atoms interactions. Interatomic interactions were analysed using the Dynamut generated files **(Figure 6.2.10)** and then uploaded into PyMOL. The analysis revealed one potential linkage between arginine C4 and carbonyl group in S_{138}. In addition, four interactions between C5 or C5' of L_{141} and carbonyl group, C3, C4 and C5 of arginine were shown. These could involve hydrophobic, hydrogen bonds or other undefined connections. In addition, the distances between these atoms varied from ~3.4 to ~3.7 Å. More atomic interactions were determined with $arginine_{136}$ than $valine_{136}$.

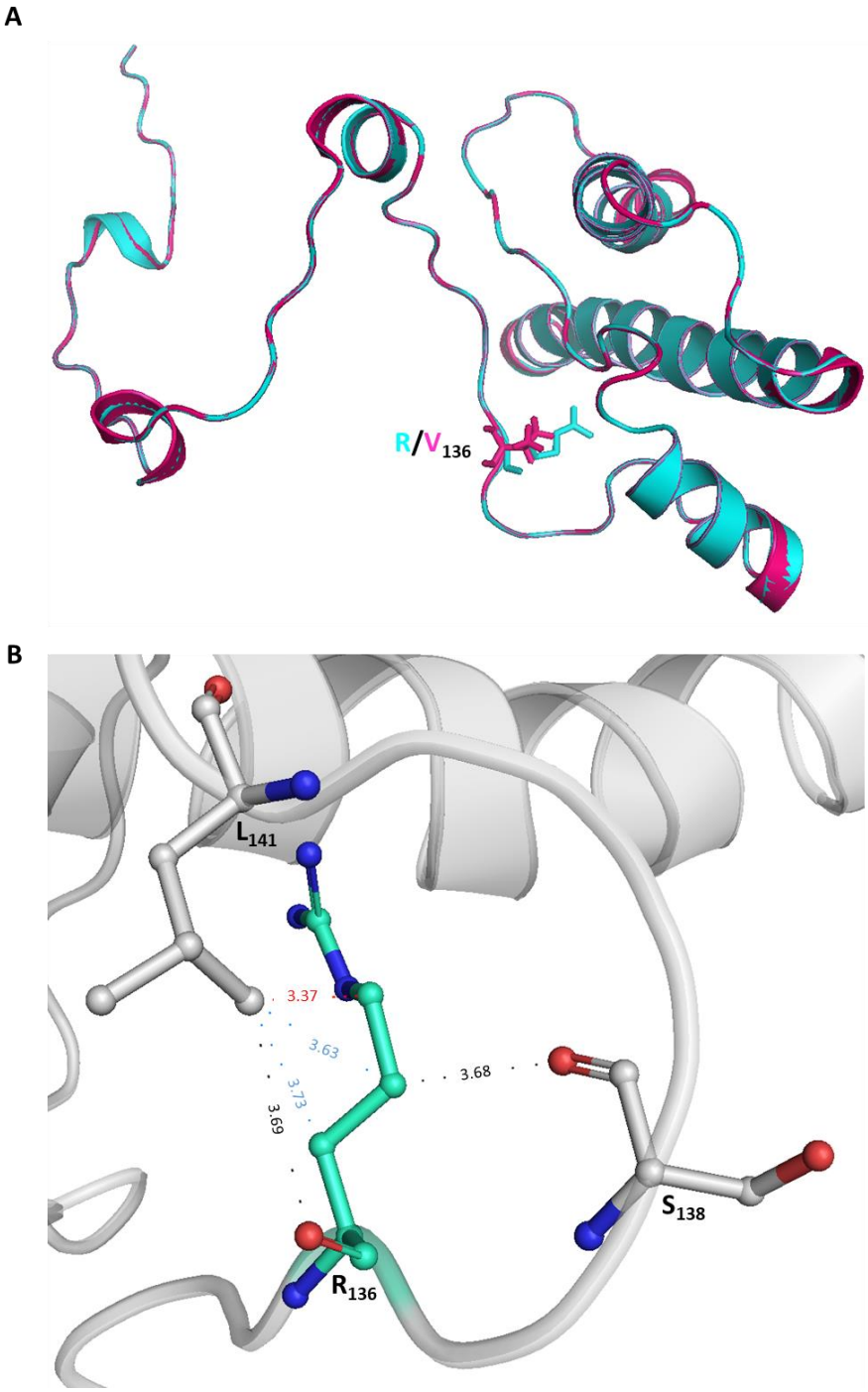

Figure 6.2.10. RRQ (cyan) and VRQ (pink) structures comparison (**A**) and mapped arginine (R) interactions with serine (S) at 138 position and leucine (L) at 141 position (**B**) in a protein amino acid chain. A first interaction (black) was mapped between carbonyl in arginine and C5 (or C5') of leucine at 141 position (~3.7 Å). A second interaction (black) was outlined between the C4 of arginine$_{136}$ and carbonyl group of serine at 138 position (~3.7 Å). Analysis also showed interactions (blue) between C3 and C4 of arginine$_{136}$ and C5 (or C5') of leucine at 141 position (3.7 Å and 3.6 Å, respectively). In addition, a linkage (red) was created between C5 of arginine$_{136}$ and C5

(or C5') of leucine$_{141}$ with distance measured 3.4 Å. Oxygen atoms are indicated in red, nitrogen atoms are blue.

Similarly to VRQ and RRQ, structures for KRQ and PRQ were also analysed **(Figure 6.2.11** and **Figure 6.2.12)**. Firstly, the whole PrP chains alignment was looked at. Since VRQ differs from KRQ and PRQ by only one amino acid, the protein 3-D models were aligned with only exemption of the analysed amino acid at 136 position. Then, the possible interactions between amino acids were analysed. It was found that lysine$_{136}$ C3, C4 and C5 potentially created hydrophobic bonds with leucine$_{141}$ C5 or C5'. The measured distances between atoms were ~3.4, 3.9 and 3.5 Å, respectively. In comparison, proline$_{136}$ atoms C4 and C5 also created interactions: two with C5 (or C5') of leucine$_{141}$ (~3.4 and 4.4 Å, respectively) and one between C4 of P$_{136}$ and glutamine$_{163}$ C4 with a distance of ~4 Å.

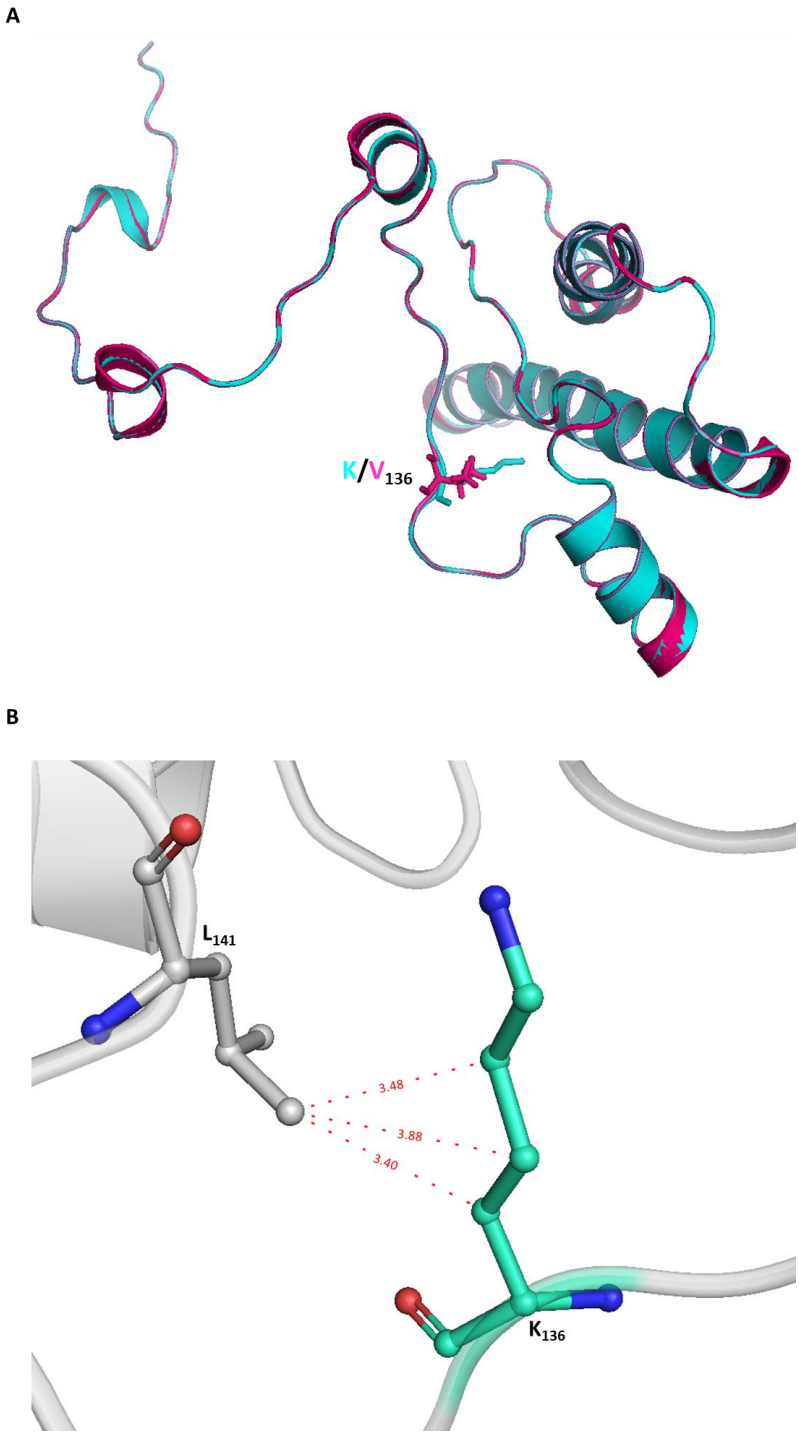

Figure 6.2.11. Structural differences between VRQ (pink) and KRQ (cyan). **A** – whole PrP structure alignment for VRQ/KRQ. **B** – atomic interactions with K_{136}. Structural analysis using Dynamut and PyMOL revealed three possible hydrophobic interactions for KRQ between C5 (or C5') of $leucine_{141}$ and C3, C4 and C5 carbon atoms in lysine with distance lengths ~3.4, 3.9 and 3.5 Å, respectively. Oxygen atoms are indicated in red, nitrogen atoms are blue.

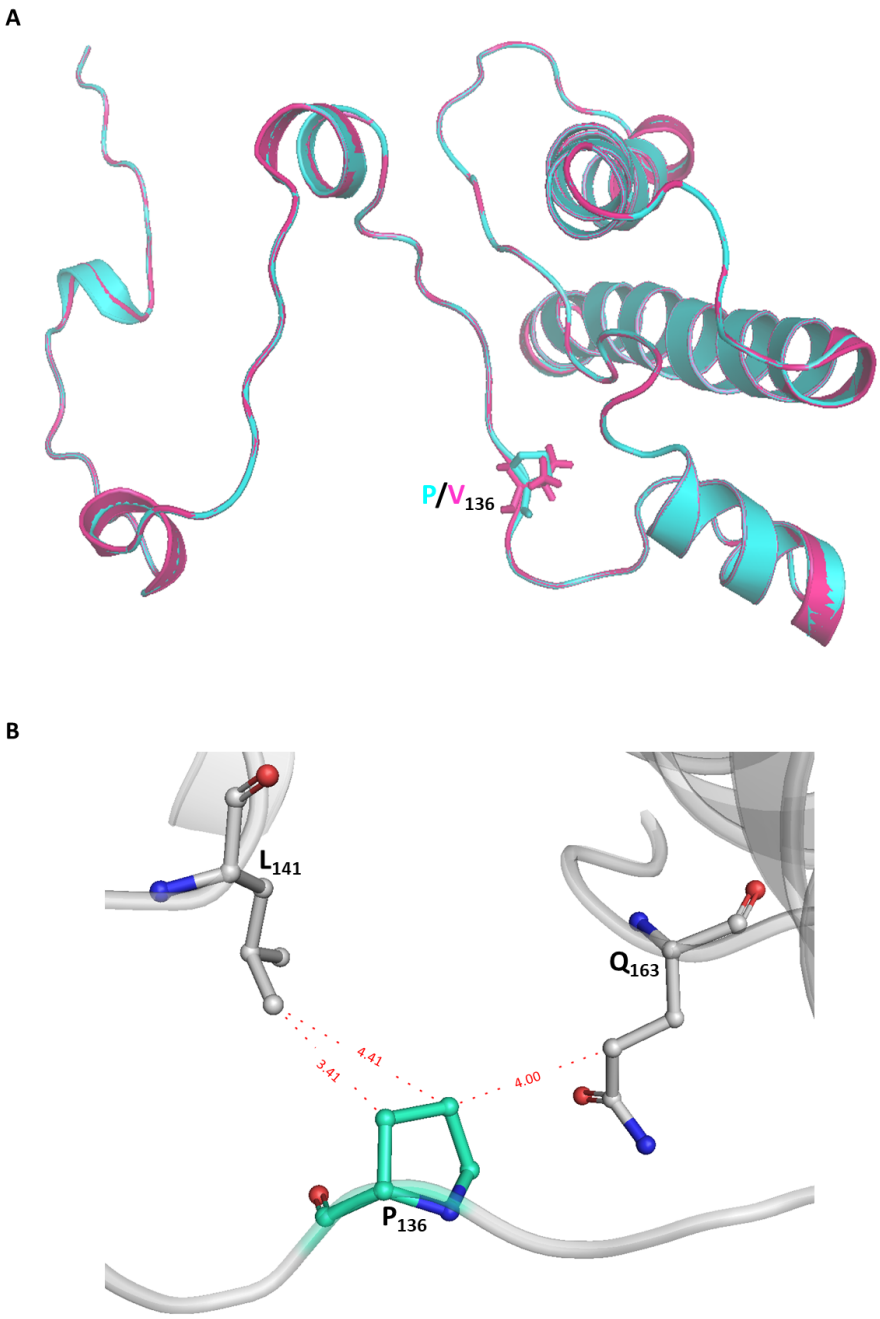

Figure 6.2.12. Structural differences between VRQ (pink) and PRQ (cyan). **A** – whole PrP structure alignment for VRQ/PRQ. **B** – atomic interactions with P_{136} (green). Structural analysis using Dynamut and PyMOL revealed two possible hydrophobic contacts for proline$_{136}$ C3, C4 with C5 (or C5') of leucine$_{141}$ (~3.4 and 4.4 Å) and one interaction of proline C4 with C4 of glutamine$_{163}$ (Q) (distance measured ~4 Å). Oxygen atoms are indicated in red, nitrogen atoms are blue.

6.2.3.4 Protein surface analysis for prion proteins with valine, arginine, lysine and proline at 136 position

The charge distribution on the molecules globular part surface was analysed, in particular the region around the position 136. The PYMOL generated images showed that the electrostatic potential around the analysed position differed between PrPs. VRQ, RRQ and KRQ images showed a positively charged (blue) region, whereas the proline within the PRQ had a charge lower than that for the other analysed proteins which was close to 0 kT/e (white) due to it missing a second basic residue. Furthermore, the surfaces coloured by electrostatic potential of the molecules are shown **(Figure 6.2.13, A)** with a schematic representation of the secondary PrP structure **(Figure 6.2.13, B)**. It was noticed that on the opposite site of position 136 in each analysed protein, a structural 'pocket' was present. This space was made by amino acids residues 209-216 (MERVVEQM) from the 3rd α-helix. It was clear that for RRQ and KRQ, the arginine and lysine long side chains went into that pocket, whereas the valine and proline side chains were not large enough to fill this space.

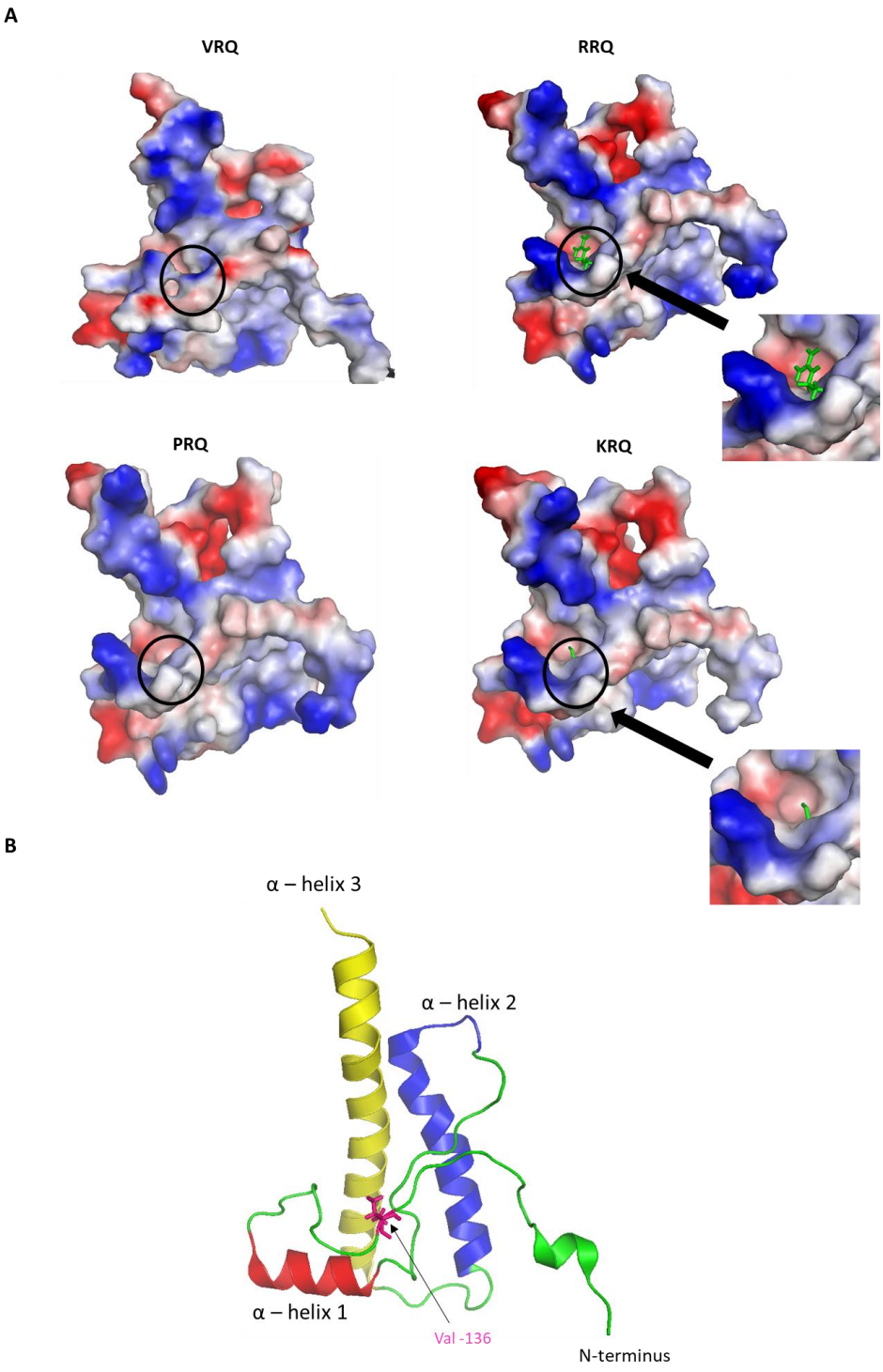

Figure 6.2.13. Electrostatic surface representation for the globular part of VRQ, RRQ, KRQ and PRQ. **A** – position 136 in all proteins was marked with a black circle. For RRQ and KRQ, position 136 was enlarged for better visualisation. The longer amino acids at 136 position were displayed in green (RRQ and KRQ), whereas shorter amino acid sticks are not visible on the protein surface. Red – negative charge, blue – positive charge, white – uncharged. **B** – Positioning of structural parts of PrP globular domains (VRQ as

an example). The displayed position was the same for all shown proteins. Position 136 is shown in pink, α-helix 1 in red, α-helix 2 in blue, α-helix 3 in yellow.

6.3 Discussion

The study has demonstrated that recombinant PrPs could act as inhibitors for *in vitro* prion protein amplification. Here, this was expanded to investigate the shortest possible fragment of the most potent rPrPs that could inhibit the *in vitro* amplification of prion protein misfolding. For this purpose, we tested rRRQ, rKRQ, rPRQ and rVRQ derived peptides with different lengths. All tested peptides consisted of the amino acid at 136 position in ovine PrP. Moreover, the 33 amino acids long peptides also contained the hydrophobic sequence AGAAAAGA, which had been reported to be essential for the inhibitory effects of hamster PrP derived peptides on PrP^{sen} conversion into PrP^{res} in cell-free conversion assay (Chabry, Caughey and Chesebro, 1998). In addition, peptides without the hydrophobic sequence (18 amino acids long) were designed and produced. Both, 33 (Ov112-144) and 18 amino acids long (Ov122-139) ovine PrP derived peptides were equivalent to hamster derived peptides previously presented in the literature (hamster 109-141 and 119-136, respectively) (Chabry, Caughey and Chesebro, 1998) where the ovine position 136 is equivalent to position 133 in the hamster PrP sequence. In addition, a 43 amino acids long peptide was also designed and its sequence included all three polymorphic positions within the ovine PrP, 136, 154 and 171, but not the hydrophobic sequence. This peptide was produced and designed only for rRRQ. In addition, one peptide with randomised amino acids sequence was designed and produced as a control. For peptides, powder resuspensions used the buffers recommended by the manufacturer. Some were resuspended in water, other buffers were checked to determine if they interfered with *in vitro* prion protein amplification. It appeared that the presence of 2.7 % acetonitrile in the samples significantly inhibited the *in vitro* misfolding of ovine scrapie prion protein (ARQ/VRQ, PG1361/05). The 2.7 % of acetonitrile is present when using 50 µM OvR112-144, therefore, this was the highest concentration of this peptide used. It was shown that 1 µM and 100 nM of OvR112-144 did not inhibit scrapie prion misfolding. Furthermore, 33 amino acids long peptides with other mutations at 136 position (for OvV, OvK and OvP) had no inhibitory effects at concentrations 1 µM and 100 nM. When analysing shorter peptides (Ov122-139) only OvR122-139 at 50 µM decreased the signal of PMCA amplified PrP^{Sc} on dotblots. However, higher concentration of this peptide did not affect the PMCA indicating the peptide did not consistently inhibit prion replication. In addition, the 50 nM of the rRRQ did not inhibit the PMCA reaction as previously described. This could suggest that were some problems with either PMCA process or with the recombinant rRRQ. For the other shorter peptides (Ov122-139) there were no inhibitory effects on ovine scrapie misfolding. Additionally, the longer peptide OvR130-173 was tested at concentrations of 50 µM – 1 nM and there was no peptide inhibition effects on the ovine PrP misfolding.

Chabry *et al.*, showed that the synthetic hamster peptides inhibited the conversion of PrP^{sen} in cell-free conversion assay. Moreover, the researchers tested a range of different peptides lengths and clearly stated that the peptides derived from the central part of hamster PrP had the highest inhibitory rate. In addition to that, they also showed that

the presence of the highly hydrophobic sequence AGAAAAGA was essential for inhibition of the PrP^{res} formation and the IC50 increased as the number of hydrophobic amino acid residues in the sequence decreased (Chabry, Caughey and Chesebro, 1998). To support this, the AGAAAAGA sequence has been described as highly amyloidogenic and crucial for the conversion of PrP^{C} into PrP^{res} (Gasset *et al.*, 1992; Hölscher, Delius and Bürkle, 1998). The inability of our peptides to inhibit the prion protein misfolding could be due to the methodology used for prion conversion. Chabry *et al*., used cell-free conversion assay, which differs from PMCA. In cell-free conversion assays, recombinant cellular PrP is incubated with PrP^{Sc} that has been purified and denatured by guanidine hydrochloride (Gdn-HCl), whereas in our PMCA model both PrP^{C} and PrP^{Sc} were derived from whole brain homogenates. In addition, in PMCA sonication and incubation steps were used, whereas in cell-free conversion assays recombinant PrP and PrP^{Sc} required only an incubation step (Kocisko *et al.*, 1994; Saborio, Permanne and Soto, 2001). Moreover, PrP^{Sc} formation using PMCA generated greater amounts of misfolded PrP and the formation was highly efficient in comparison to the cell-free conversion assay. Furthermore, the generated PrP^{Sc} in PMCA shares biochemical properties of PrP^{Sc} isolated from TSE infected brains (Saborio, Permanne and Soto, 2001). The inhibition of PMCA misfolding could possibly require the presence of whole recombinant prion protein and/or both its C- and N-terminus. To support this hypothesis, Yuan *et al.,* tested the conversion of human PrP^{Sc} during PMCA. Similar to current research, his group showed that the full-length human recombinant PrP was able to inhibit the *in vitro* misfolding of human iCJD brain derived PrP^{Sc}. Moreover, the inhibition depended on the rPrP dose used and the inhibition mechanism involved the recombinant prion protein C- and N-termini regions (Yuan *et al.*, 2013).

The differences in the protein sequences and structures between rPrPs from different species were investigated to assess the stability and flexibility of 136 region, which seems to have a significant impact on the inhibitory efficacy of rPrPs. The structure of rVRQ ovine PrP (residues 92-234) was analysed and shown the presence of 3 α-helices (α-helix 1: 146-156, α-helix 2: 174-194 and α-helix 3: 202-233) within the core PrP. The presence of $valine_{136}$, $arginine_{154}$ and $glutamine_{171}$ were confirmed in the ovine PrP sequence. Moreover, multiple NMR ensembles were analysed for region 136. It was shown that N-terminal part of protein was highly flexible and presented large variations between NMR ensembles. These variations existed until $tyrosine_{131}$, from which models created a more ordered structure, however the NMR coordinates for position 136 differed between entries. Therefore, it was hypothesised that region 136 is flexible. Additionally, sequences and structures of PrP from distinct species were examined. The potential similarities of PrP whole sequence/structure and/or 136 region between species could help to determine whether ovine PrP could act as a universal prion replication inhibitor. For this purpose, the full length mature ovine PrP with an ARR variant was compared to bovine, hamster, mouse and human PrP (Goldmann *et al.*, 1990). Slight differences in the sequence were noticed and also reported previously

(Groschup, Harmeyer and Pfaff, 1997; Baral *et al.*, 2015). First of all, the bovine PrP sequence was longer (264 amino acids) than the other species PrP because of additional octapeptide repeats within the N-terminus (Yoshimoto *et al.*, 1992). Additionally, the lengths of other tested PrPs were 254 aa (mouse and hamster) and 253 aa (human) (Oesch *et al.*, 1985; Kretzschmar *et al.*, 1986). Moreover, ovine prion protein has three highly polymorphic positions: 136, 154 and 171 (Belt *et al.*, 1995; Goldmann, 2008). Furthermore, the differences between PrP sequences were single amino acid substitutions alongside the sequence chain (Groschup, Harmeyer and Pfaff, 1997). Overall, the found differences between analysed PrP sequences resulted in the ovine PrP similarity to bovine in 70 %, human in 89 %, mouse in 83 % and hamster in 85 %. Previous data from the multiple sequences alignment for prion mammalian prion proteins confirmed the high protein sequence homology between species, however the exact percentage value could differ between bioinformatic tools (Groschup, Harmeyer and Pfaff, 1997). As indicated from the sequence analysis, the presence of alanine at the equivalent to ovine 136 position is a common feature between species. In the current research, structures for different species and ovine prion proteins were compared. The NMR files that were used during the structural analysis (from protein data bank files) contained the globular, C-terminus part of the protein. All analysed PrP structures contained three α-helices, where for ovine these included residues 146-156 (α-helix 1), 174-194 (α-helix 2) and 202-232 (α-helix 3). These results were similar to reported previously by Haire and co-workers (Haire *et al.*, 2004). Moreover, the NMR coordinates for other species α-helices were similar to ovine PrP, however the region 121-135 in ovine and equivalent residues in other species was the most disordered part of the C-terminus (Pastore and Zagari, 2007). Moreover, the 129-131 region structurally created β-sheet (Haire *et al.*, 2004; Pastore and Zagari, 2007). In contrast to analysis of PrP in other species, the β-sheet was not marked on the ovine PrP entry but this was due to the focus on the ovine α-helices structures (Munoz-Montesino *et al.*, 2016). The similarity between different species PrP could indicate that recombinant ovine PrP could be used as an universal therapeutic that can bind and mimic the PrP.

Tested in the current research ovine PrP mutants at 136 position showed different inhibition performance in PMCA. Therefore, the main aim of the structural analysis was to compare the rPrP versions. The analysis could give an insight on why some of the amino acid substitutions at 136 position showed the differences in inhibition of prion protein misfolding. In order to analyse the implemented changes at position 136 in ovine PrP and its effects on protein structure. rPrP structures were generated using Dynamut server and analysed in PyMOL. First of all, the two natural variants: VRQ and ARQ were compared. Alanine in comparison to valine is a shorter amino acid (Hastings *et al.*, 2016). The length of each amino acid at 136 position could result in differences in formation of atomic interactions between different amino acids within the protein chain. As observed, both alanine and valine side chains could form some interactions with side chains of $lysine_{141}$, however valine side chains could form three, whereas according to

software analysis, alanine could form only one connection. Furthermore, comparison of ovine natural variants: ARQ, VRQ and ARR was performed in previous research. The authors looked at the whole molecule and noticed that position 136 as well as the other polymorphic residues in ovine PrP, were on the protein surface and exposed to water and other solvents and of course were accessible to interact with other proteins or other PrP molecules. Moreover, it was described that in the VRQ, an additional hydrogen bond between N_{162} side chain and R_{139} stabilised the molecule more in comparison to ARQ (Eghiaian *et al.*, 2004). In addition, we also tested the number of possible interactions for the best inhibitory PrPs: RRQ, KRQ, PRQ. R and K have longer amino acids. As the analysis revealed, R chain atoms were shown to form different interactions with L_{141} and Ser_{138}. These could include hydrophobic and hydrogen bonds. For KRQ hydrophobic interactions were shown only for L_{141} atoms. In addition, to that, proline atoms were found to interact with L_{141} and Q_{163}. Among all the analysed structures R_{136} atoms created the most interatomic bonds. We could speculate that the greater number of connections between atoms could increase the protein stability. This would indicate that VRQ, RRQ, KRQ, PRQ had more stable structures around residue 136 compared to ARQ and this increased stability may present a more stable interaction region for binding to PrP^C and/or PrP^{Sc} during prion conversion and enhance inhibition. The distances of atoms forming connections were also estimated, however these only indicated the distance for formed bonds rather than analysis of differences between the distances between atoms. Furthermore, the amino acids variations could change the electrostatic potential of the PrP surfaces and this could influence their interaction with PrP^C and/or PrP^{Sc} during prion conversion (Baral *et al.*, 2015). In the current research, the changes of the surface electrostatic potential due to amino acid change were observed. In compare to VRQ (positive charge), PRQ neutralised the charge, whereas R and K, as charged amino acids, maintained the positive charge of proteins region. These slight variations in charge distribution on the PrP surface could modify the protein's features like binding properties or even already discussed interatomic interactions (Baral *et al.*, 2015). Furthermore, the presence of proline in the amino acids chain could lower the flexibility of the protein backbone and therefore affects the formation of protein secondary structures and increase protein stability (Choi and Mayo, 2006). In addition, the structural 'pocket' was observed on the opposite site of position 136 in ovine PrP. This space was created by amino acids contained within α-helix 2. Data also indicated that introduction of the longer amino acids at position 136 in ovine PrP did not implement further changes within the whole structure.

The change of the single amino acids in ovine PrP resulted in significant changes of the inhibition process of *in vitro* prion protein misfolding. Here, it was shown that even large fragments of the rPrPs failed to inhibit prion replication and only full-length protein was effective. Preliminary structural analysis revealed new insights on these prion protein variants. The amino acids changes could influence some local changes in terms of

domain stability and surface charge which could trigger the change in the whole protein properties including the inhibition efficacy (Baral *et al.*, 2015).

Chapter 7: Infections and treatment model of scrapie infected cells

7.1 Introduction

Cell cultures provide an extremely model for various physiological and disease associated processes. They are incredibly practical for screening for and testing candidate therapeutic compounds for various diseases, including TSEs (Kocisko and Caughey, 2006a). For prion diseases, cell culture experiments could also deliver details about the conversion mechanisms of PrP^{C} into PrP^{res} and PrP^{res} transmission between cells (Solassol, Crozet and Lehmann, 2003). In addition, metabolism of both resistant and cellular PrP have been analysed in *in vitro* cell culture experiments (Caughey *et al.*, 1999). For now, only a very limited number of cells lines have been described as permissive to prion from natural TSE isolates (Vilette *et al.*, 2001; Solassol, Crozet and Lehmann, 2003; Courageot *et al.*, 2008). Therefore it was hypothesised that the amplification of prions in cells could require additional, unknown factors (Courageot *et al.*, 2008). Previously, RK13 cell line (rabbit epithelial kidney cells) derived Rov9 cells were described as permissive to natural scrapie isolates due to a lack of endogenous PrP^{C} and the presence of doxycycline induced ovine PrP^{C} (VRQ equivalent) (Vilette *et al.*, 2001; Neale *et al.*, 2010). The Rov9 cells not only successfully replicated the resistant PrP from infectious inoculas but also stably infected over time and multiple passages (Vilette *et al.*, 2001). In addition, RK13 cells were also engineered into expressing bank vole and mouse PrP^{C} and propagated both voles and mouse prions (Courageot *et al.*, 2008).

In addition, research using cell lines has included screening for agents that inhibit PrP^{res} infection. Potential inhibitors of PrP conversion have been identified including PPS, Congo Red, quinacrine and mefloquine, and a range of monoclonal antibodies (Caughey and Race, 1992; Caughey and Raymond, 1993; Doh-ura, Iwaki and Caughey, 2000; Birkett *et al.*, 2001; Peretz *et al.*, 2001; Beringue *et al.*, 2004; Kocisko and Caughey, 2006b; Bian, Kang and Telling, 2014). Interestingly, the potential drugs were screened in experiments that either cured persistently infected cells or prevented initial cell infections (Beringue *et al.*, 2004). Furthermore, a library of 2000 potential drugs and natural products were screened in RML scrapie infected ScN2 cells in order to identify new therapeutic candidates for TSEs (Kocisko *et al.*, 2003). In addition, the effects of recombinant prion proteins and PrP derived peptides on PrP^{res} aggregation was investigated in cells persistently infected with TSE agent. Priola *et al*., studied how the co-expression of heterologous (hamster) PrP affect the PrP^{res} accumulation in scrapie infected MNB cells. They found that the presence of recombinant pion protein expressed by the murine cells significantly interfered with PrP^{C} conversion in those cells (Priola *et al.*, 1994). Later, other research showed promising results with using recombinant prion proteins and its fragments to cure cells infected with PrP^{res} (Chabry *et al.*, 1999; Yuan *et al.*, 2013).

Here, Rov9 cells expressing the VRQ ovine prion protein after induction with doxycycline were used as the model to screen various classical scrapie isolates for their ability to

infect the cells. For these tests, 5 scrapie isolates/strains were used: SSBP1 (VRQ/VRQ), PG1361/05 (ARQ/VRQ), PG1207/03 (VRQ/VRQ), PG1212/03 (VRQ/VRQ) and PG1517/01 (VRQ/VRQ). In addition, we tested infection efficiencies with both brain homogenates and purified PrP^{Sc}. Once, an infection model was established, the ability to prevent infections and cure persistently infected cells with rPrPs was determined.

7.2 Results

7.2.1 Presence of PrP^C in induced Rov9 cells

The level of PrP^C in Rov9 cells was determined with and without induction with 1 µg/ml doxycycline. For this purpose, the Rov9 cells were seeded on 12 well plate with the density 0.1 x 10^6 cells per well and grown for 48 h after which cells were induced with 1 µg/ml doxycycline for 48 h. The result showed that only the doxycycline induced cells displayed detectable ovine PrP^C after detection with SHA31 antibodies on western blots **(Figure 7.2.1, A)**.

In addition, the PK concentration used for digestion of PrP^C was optimised **(Figure 7.2.1, B)**. 40 µg of total protein content was digested with 0.01, 0.05 and 0.1 mg/ml of PK. Induced and digested samples were compared to non-induced, digested samples on the western blot. The result showed that 0.01 mg/ml of PK was sufficient to fully digest the ovine PrP^C.

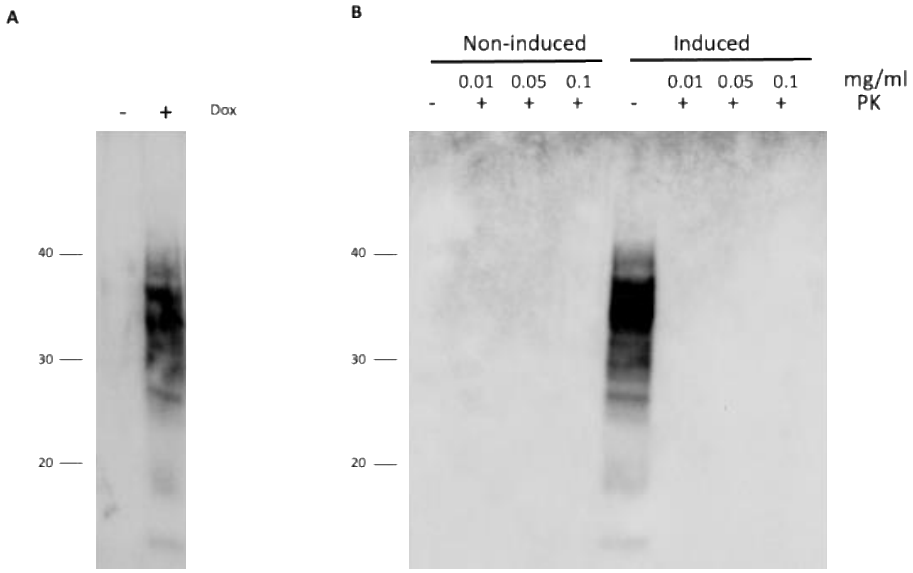

Figure 7.2.1. Rov9 cells produce ovine PrP^C after induction with 1 µg/ml doxycycline. **A** – Rov9 cells lysates with and without doxycycline treatment, 40 µg of total protein content was mixed with 4 x sample buffer and analysed on western blot. **B** – optimisation of proteinase K concentrations to digest the ovine PrP^C from Rov9 cells. Lysates containing 40 µg of protein from induced and non-induced cells were digested with 0.01, 0.05 and 0.1 mg/ml of PK and 20 µl of each sample was analysed on the western blot. Protein markers are indicated on the left side of the blot. Dox – doxycycline, PK – proteinase K;

7.2.2 Analysis of PrP^{Sc} in brain homogenates and PMCA products used as inocula

In order to assess the amount of PrP^{Sc} in the scrapie brain homogenates, 10 % brains of SSBP1 (VRQ/VRQ), PG1361/05 (ARQ/VRQ), PG1207/03 (VRQ/VRQ), PG1212/03 (VRQ/VRQ) and PG1517/01 (VRQ/VRQ) were digested with 100 µg/ml of PK and analysed on western blot **(Figure 7.2.2)**. The result showed that for all samples the characteristic 3 band pattern for classical ovine scrapie was produced. The analysis of SSBP1 scrapie showed the lowest level of PrP^{Sc} in the 10 % brain homogenate. In addition, 5 rounds of PMCA were performed for all the scrapie brain homogenates in VRQ/VRQ substrate (TSE negative brain homogenate 16). For PG1207/03, PG1212/03, PG1517/01 and PG1361/05 round 1 and 5 of serial PMCA was analysed. In all cases, the amplification of PrP^{Sc} was successful and showed high amount of PrP^{Sc} in round 1 and 5 PMCA products. For SSBP1, both round 1 and round 5 were analysed, however this scrapie brain showed no detectable on western blotting levels of PrP^{Sc} after round 1 (data not shown). Moreover, PMCA round 5 analysis showed that SSBP1 isolate amplified. These results demonstrated that all tested scrapie isolates amplified in VRQ/VRQ substrate and so should be able to replicate in the Rov9 cells.

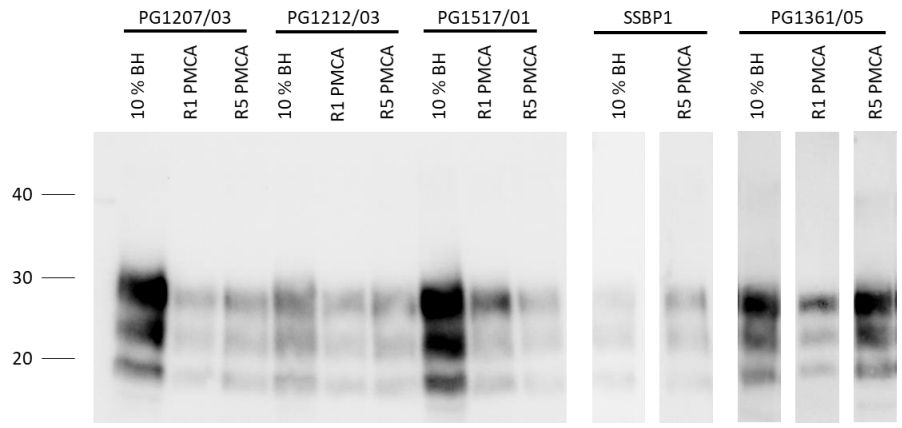

Figure 7.2.2. PrP^{Sc} levels in scrapie 10 % brain homogenates and PMCA products. This was determined for SSBP1 (VRQ/VRQ), PG1361/05 (ARQ/VRQ), PG1207/03 (VRQ/VRQ), PG1212/03 (VRQ/VRQ) and PG1517/01 (VRQ/VRQ). For round 1 of PMCA, 10 µl of each 10 % brain was amplified in 90 µl of TSE negative brain homogenate (B16) over 24 h. Round 2-5 were prepared by 1/3 dilution of previous round products in TSE negative brain homogenate (B16). Scrapie 10 % brain homogenates and PMCA products were digested with 100 µg/ml of proteinase K and 15 µl of each sample was analysed on the western blot. Protein marker is indicated on the left side of the blot.

7.2.3 Optimisation of Rov9 cell infection with brain homogenates

7.2.3.1 Infections with 1/500 diluted 10 % brain homogenates

The first attempt involved infection with 1/500 diluted 10 % brain homogenates (2 µl of 10 % brain per 1 ml of cell culture media) of PG1361/05 (ARQ/VRQ), SSBP1 (VRQ/VRQ) and PG1207/03 (VRQ/VRQ). This method was used because it previously showed successful Rov9 cells infection and allowed to reduce the impact of detergents contained within brain homogenates on the cells. In addition, to test the impact of PMCA and brain homogenate buffer on cells, equivalent volumes of PMCA and brain homogenate buffer were also added to the cells. Moreover, all samples were applied to non-induced and induced cells. The results showed that the presence of doxycycline for 48 h in cell media induced the ovine PrP^C in Rov9 cells, and this was fully digested with 5 µg/ml of PK **(Figure 7.2.3, A)**. In contrast, the Rov9 cells that were not induced with doxycycline showed no PrP^C band on western blot for all samples **(Figure 7.2.3, B)**. Furthermore, the addition of brain homogenate or PMCA buffer and scrapie brain homogenates (SSBP1, PG1361/05 and PG1207/03) did not infect the cells or cause cell loss.

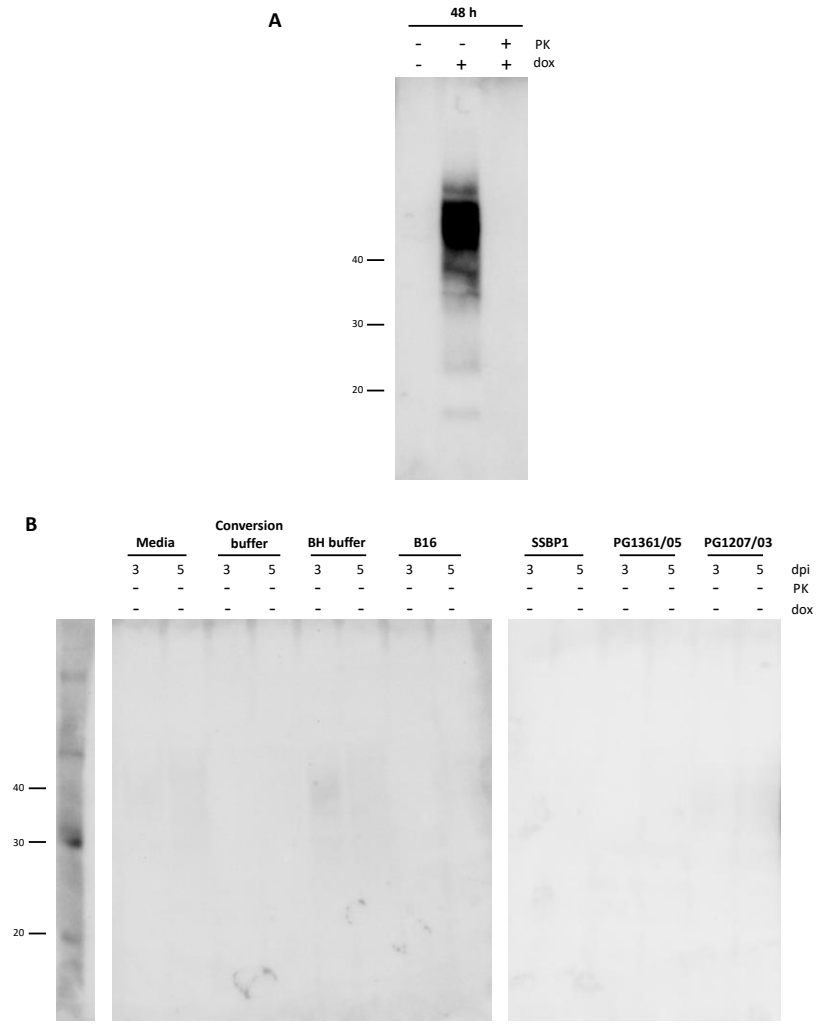

Figure 7.2.3. Infection of Rov9 cells with 1/500 diluted scrapie isolates. **A** - representative western blot shows presence of PrP^{C} in Rov9 cells induced with 1 µg/ml doxycycline for 48 h. The PrP^{C} is fully digested with 5 µg/ml of PK. **B** – western blots show that there is no PrP^{C} in non-induced cells. Cells were lysed at two different timepoints: 3 (72 h) and 5 (120 h) days post infection (dpi). In samples inoculated with media, PMCA (conversion) buffer, brain homogenate (BH) buffer, B16 (VRQ/VRQ) or scrapie samples SSBP1 (VRQ/VRQ), PG1361/05 (ARQ/VRQ) or PG1207/03 (VRQ/VRQ), PrP^{Sc} was not detected. 20 µl of each cell lysate was analysed. Dpi – days post infection, PK – proteinase K, dox – doxycycline;

Furthermore, the induced cells were inoculated with scrapie isolates (SSBP1 (VRQ/VRQ), PG1361/05 (ARQ/VRQ) and PG1207/03 (VRQ/VRQ)) and analysed 3-, 5-, 16- and 32-days post infection. Only representative result for SSBP1 infection is shown **(Figure 7.2.4)**. The outcome showed that the cells were not infected with any of the scrapie isolates at any point during the experiment. In addition, around 20 µg of total protein was loaded on the gel for 3 and 5 dpi, whereas for 16 and 32 dpi (3^{rd} and 5^{th} passage) 60-100 µg of total protein was loaded on the gel. Analysis of this high level of protein

for latter timepoints clearly demonstrated that the cells were not infected with any scrapie isolate. Moreover, the controls with brain homogenate and conversion buffer had no impact on PrP^C induction or protein content (not shown).

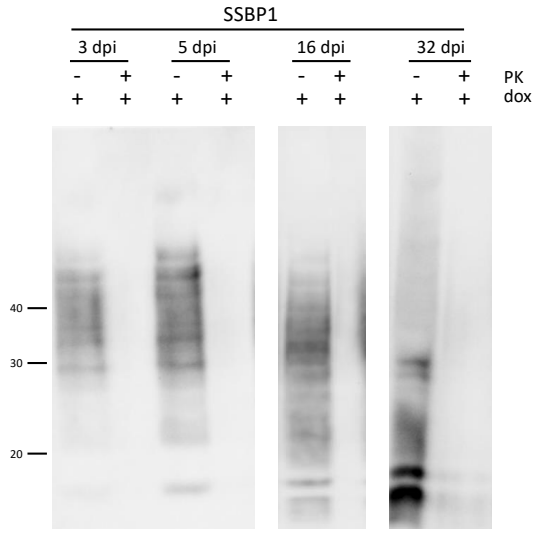

Figure 7.2.4. Infection of Rov9 cells with SSBP1. Representative western blot showing no PrP^{res} in cell lysates after inoculation with scrapie isolate SSBP1 (VRQ/VRQ) after 3-, 5-, 16- (3rd passage) and 32-days (5th passage) post infection. Rov9 cells were induced with 1 µg/ml of doxycycline and non-digested cell lysates were compared to samples digested with 5 µg/ml proteinase K. For 3 and 5 dpi samples, 20 µg of total protein, and for 16 and 32 dpi 60-100 µg of total protein was used for western blot analysis. Protein markers are indicated on the left side of the image. PK – proteinase K, dox – doxycycline, dpi – days post infection.

7.2.3.2 Infections with 1/40 diluted brain homogenates

Another infection trial, in which 1/40 diluted brain homogenates (25 µl of 10 % brain per 1 ml of media) were added on the cells was performed. After 3 dpi, it was noted that the majority of cells that were exposed to 1/40 dilution of brain homogenate and conversion buffer were dead. In addition, incubation with negative brain homogenate (B16, VRQ/VRQ) and scrapie isolate PG1361/05 (ARQ/VRQ) also resulted in noticeable cell loss in comparison to media control cells, therefore these were not analysed further. Furthermore, SSBP1 and PG1207/03 scrapie incubated samples survived the infection, however with some cell loss for SSBP1 isolate and were analysed on western blots **(Figure 7.2.5, A, B)**. In cells incubated with SSBP1 scrapie, no PrP^{Sc} was detected in samples from 5 until 17 dpi (passage 2). For ovine scrapie VRQ/VRQ (PG1207/03), a very faint scrapie triplet band was recorded on the western blot at timepoint 5 dpi. Therefore, these cells were passaged further until 5th passage (82 dpi), however at all passages up to this timepoint no PrP^{res} was detected (data not shown).

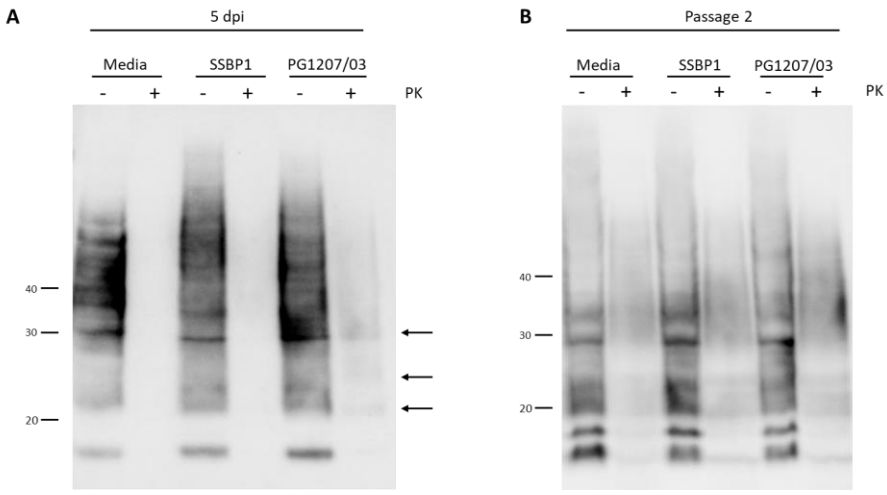

Figure 7.2.5. Representative western blots showing the effect of infections with ovine scrapie SSBP1 (VRQ/VRQ) and PG1207/03 (VRQ/VRQ) (1/40, 25 µl of 10 % brain in 1 ml of media) in comparison to media control (dox induced Rov9 cells). **A** – western blot shows the analysis of cell lysates collected 5 days post infection. Triple band pattern after infection with PG1207/07 is indicated with arrows on the right side of the blot. 30 µg of total protein content was analysed on western blot. **B** – western blot shows the analysis of cell lysates collected after passage 2 (17 days post infection). 100 µg of total protein content was digested with 5 µg/ml of PK and analysed on western blot. Rov9 cells were induced with 1 µg/ml of doxycycline and infected with 1/40 diluted scrapie SSB1 and PG1207/03 brain homogenates. Protein marker is indicated on the left side of each blot. PK – proteinase K; dpi – days post infection;

7.2.3.3 Optimisation of PrP^{res} detection in cell lysates

To further investigate the potential presence of cell infection in samples inoculated with 1/40 (25 µl of scrapie in 1 ml of media) of 10 % scrapie brains (PG1207/03 and SSBP1) two different approaches were tested to detect PrP^{Sc}: PMCA **(Figure 7.2.6, A, B)** and protein concentration by centrifugation **(Figure 7.2.6, C)**. Firstly, 5 rounds PMCA experiment was used. PMCA was performed on cell lysates for the cells inoculated with media, PG1207/03 and SSBP1 and samples taken at 120 h post infection (5 dpi) and passage 1 (10 dpi). Briefly, 10 µl of each cell lysate was mixed with 90 µl of 10 % negative brain homogenate (B16) and amplified for 5 rounds. PMCA products were digested with PK and analysed firstly on dotblot (15 µg/ml PK) and then positive samples and representatives of negative samples were analysed on western blot (50 and 100 µg/ml PK). For an amplification positive control, 10 % brain homogenate PG1361/05 (ARQ/VRQ) was used and for a negative control 10 % negative brain homogenate was used (B16) without seed. Each sample was amplified in triplicate. Dotblot analysis showed the presence of PrP^{res} in cell culture lysates after 120 h post infection and 1st passage for cells infected with PG1207/03. On the other hand, there was no PrP^{res} signal from SSBP1 infected samples in either 120 h post infection or 1st passage. Control

scrapie isolate (PG1361/05, ARQ/VRQ) amplified in the VRQ/VRQ brain (B16) in the presence of lysis buffer, and PrP^C only showed no signal. On western blot, PMCA products were digested with 50 (data not shown) and 100 µg/ml of PK. Data confirmed dotblot analysis that only PG1207/03 infection derived cell lysates (both 120 h post infection and 1st passage) amplified during PMCA.

A second approach to analyse cell lysates for PrP^{res} used digestion with 20 µg/ml PK and concentration of 500 µg of total protein content. In this approach, all samples available to date were analysed for cells inoculated with 1/40 (25 µl of 10 % brain in 1 ml of media) SSBP1 and PG1207/03 (both VRQ/VRQ). Results showed the presence of PrP^{res} in samples infected only with 10 % PG1207/03 brain homogenate (**Figure 7.2.6, C**). Interestingly, the highest signal came from samples collected 72 h (3 dpi) and 120 h post infection (5 dpi), after which signal dropped significantly down to undetectable levels in passage 3 (24 dpi) samples. This could indicate that the detected of PrP^{res} with both PMCA and concentration protocols came from the scrapie inoculum rather than infected cells.

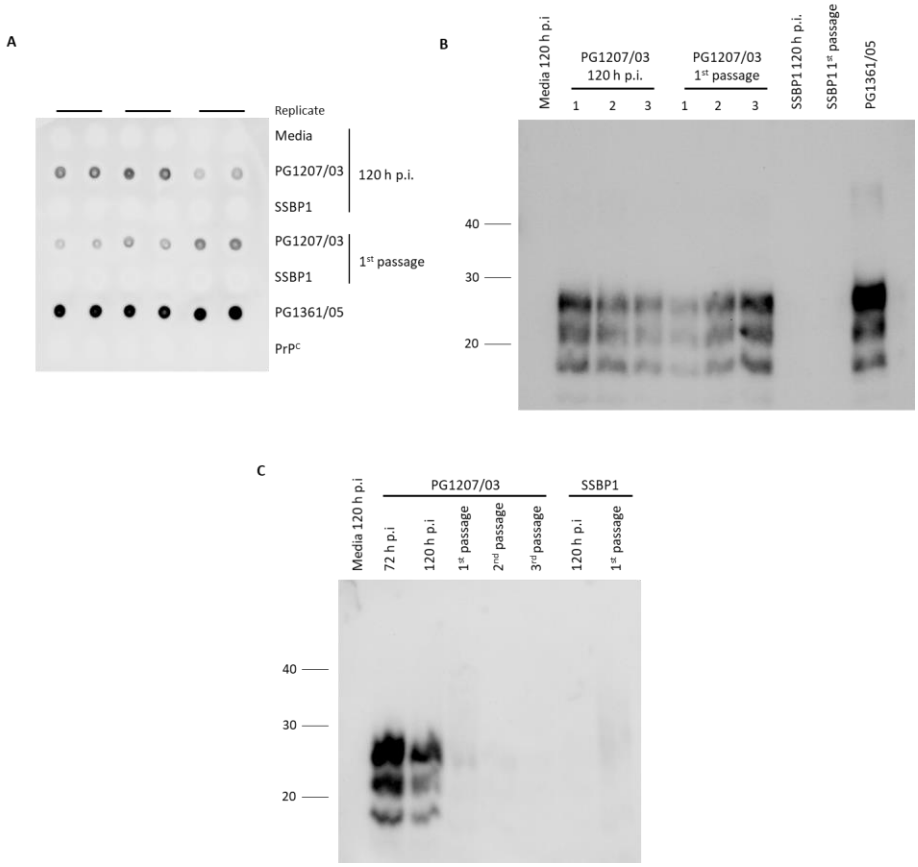

Figure 7.2.6. Infection of Rov9 cells analysed by amplification or concentration of PrP^{Sc} in cell lysates. Analysis of the presence of PrP^{res} using two approaches: PMCA (**A, B**) and concentration by centrifugation (**C**) for samples infected with 1/40 of 10 % brain homogenates for PG1207/03 (VRQ/VRQ), SSBP1 (VRQ/VRQ) and cells in OPTI MEM media with 1 µg/ml doxycycline as a control. PMCA experiment was designed for samples from 120 h (5 days) post infection and 1st passage (10 days post infection). PMCA was performed over 5 rounds and products were digested with 15 µg/ml (**A**) and 100 µg/ml (**B**) PK. 2.5 µl of each PK digested sample replicates was added on the dotblot (**A**) or 20 µl was added on the western blot (**B**). 10 % scrapie brain PG1361/05 (ARQ/VRQ) was used as an amplification control and PrP^{C} as a digestion control. On western blot (**B**) all samples with positive signal for PrP^{res} in dotblots were analysed alongside representatives of samples where there was no PrP^{res} detection on the dotblot. Samples replicates in **A** are indicated above the dotblot. **C** – second approach for detection of PrP^{res} in cell lysates used the concentration of 500 µg of total protein content. 500 µg of total protein was digested with PK (20 µg/ml) and concentrated by centrifugation and analysed on western blot. Samples from 72 h post infection (3 days post infection), 120 h (5 days post infection), 1st passage (10 dpi), 2nd passage (17 dpi), 3rd passage (24 dpi) were analysed. 1, 2, 3 – sample replicates, h p.i. – hours post infection, dpi – days post infection.

It was also investigated, if higher levels of protein needed to be concentrated in order to detect PrP^{res} from cell lysates. For this purpose, 1000 µg of total protein at passage 4 (61 dpi) and 5 (82 dpi) of cells infected with scrapie isolate PG1207/03 (VRQ/VRQ) samples was used. Western blot analysis showed no PrP^{res} in cell lysates (data not shown).

Overall, the protocol using concentration of 500 µg of total protein content was used for further experiments.

7.2.3.4 Optimisation of brain homogenate dilutions and treatment before inoculation on cells

Firstly, the maximum amount of brain that could be used for cell infection but not affect cells survival, was determined. For this purpose, 10 % brain homogenates SSBP1, PG1207/03, PG1212/03 and PG1517/01 (all VRQ/VRQ) were used and kept on the cells for 3 days (72 h). During microscopic examination of the cells (data not shown), it was found that the addition of 25 µl per 1 ml of media (1/40 brain/media ratio) of 10 % brains PG1207/03, PG1212/03 and PG1517/01 did not affect the cell survival. Therefore, this amount of brain was used for further infections for PG1207/03, PG1212/03 and PG1517/01. However, addition of 25 µl (per 1 ml of media) of 10 % SSBP1 reduced the cells survival, whereas the 12.5 µl per 1 ml of media (1/80 brain/media ratio) did not cause any cell loss (data not shown). Therefore, for cell infections with 10 % SSBP1, 12.5 µl of 10 % brain was used in 1 ml of OPTI MEM media (1/80). Moreover, the 1/40 dilutions of both brain homogenate and conversion buffer in cell culture media resulted in noticeably cell loss (data not shown).

Secondly, it was investigated whether brain homogenate pre-treatments like heating for 20 minutes at 80 °C followed by 2 minutes sonication increased the infection rates (Vilette *et al.*, 2001). For this purpose, 10 % SSBP1, PG1207/03, PG1212/03 and PG1517/01 brain homogenates were heated and sonicated and the brains were added on the cells with dilutions 1/40 (25 µl per 1 ml of media) for PG1207/03, PG1212/03 and PG1517/01 and 1/80 (12.5 µl of brain per 1 ml of media) for 10 % SSBP1. As a comparison, cells were also infected with the same dilution of unprocessed brains. The treated cells were observed under microscope after 3 days and passaged after 5 days post infection and no cell loss was observed.

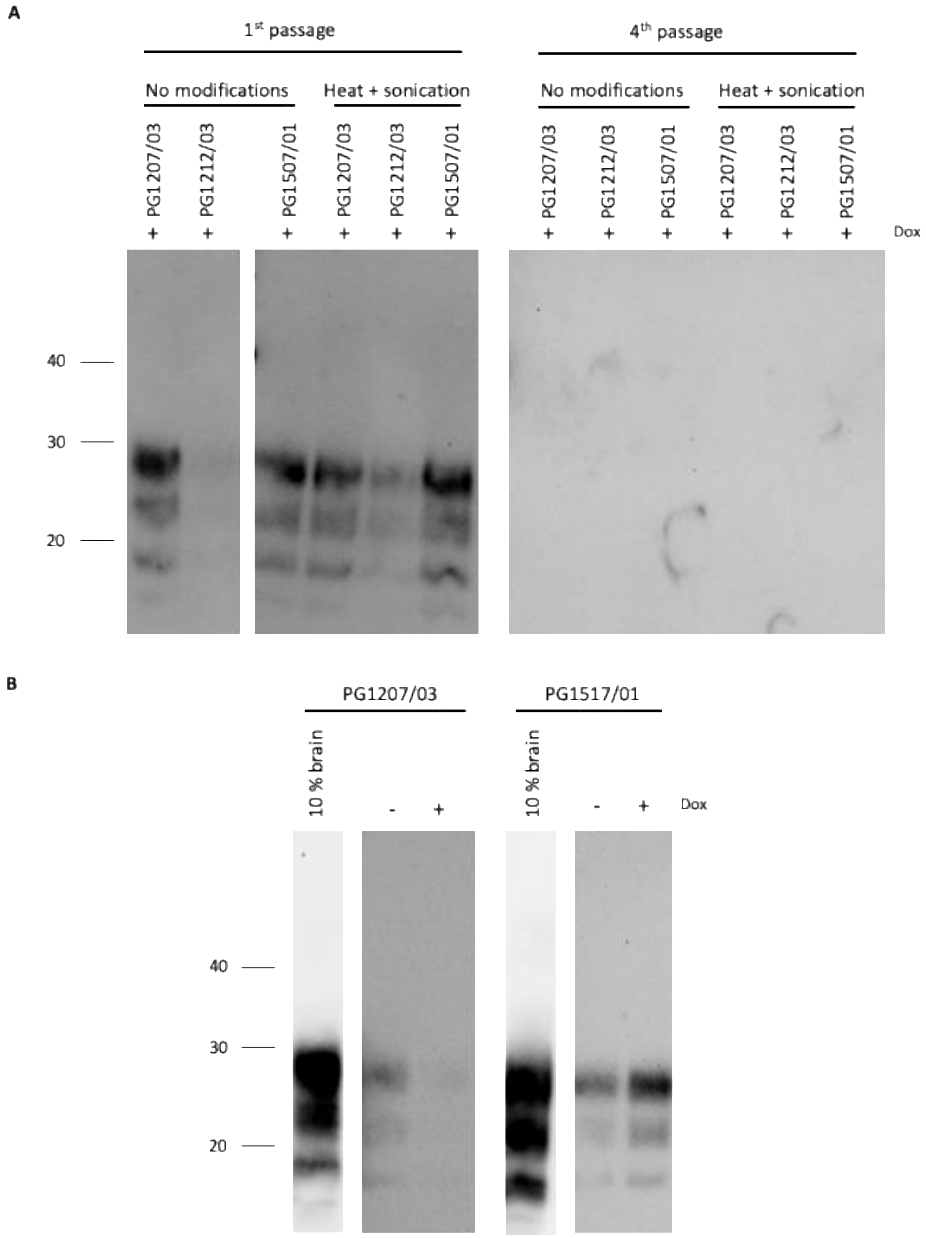

Figure 7.2.7. Rov9 cells infection with heated and sonicated and unmodified 10 % scrapie brain homogenate. Scrapie PG1207/03, PG1212/03 and PG1517/01 (all VRQ/VRQ) were used and cells were inoculated with 25 µl of 10 % brain per 1 ml of media (1/40). **A** – passage 1 (11 dpi) and passage 4 (38 dpi) cell lysate analysis. All Rov9 cells were induced with 1 µg/ml doxycycline for 48 h and infected with brain samples heated for 20 minutes at 80 °C and sonicated for 2 minutes or unmodified scrapie brain homogenates. 500 µg of total protein content was digested with 20 µg/ml PK and analysed on the western blot for each sample. **B** – passage 1 (11 dpi) for non-induced (-) and induced (+) Rov9 cells. Cells were infected with brain homogenate heated for 20 minutes at 80 °C and sonicated for 2 minutes for PG1207/03 and PG1517/01 scrapie. For each sample, 500 µg of protein content was digested with 20 µg/ml PK and analysed on the western blot. Alongside, 20 µl of 10 % scrapie brains

digested with 100 µg/ml PK were run for signal comparison. Protein markers are indicated on the left side of each blot. Dox – doxycycline;

For cells infected with brain homogenates PG1207/03 and PG1517/01 there were no differences in PrP^{res} detection was observed in cells infection after passage 1 (11 dpi) when comparing using the heated and sonicated brain or unmodified brain **(Figure 7.2.7, A)**. However, higher levels of PrP^{res} were detected in cells infected with heated and sonicated PG1212/03 rather than unmodified brain in passage 1 samples (11 dpi) **(Figure 7.2.7, A)**. The cells infection for all three scrapie isolates was not stable and after analysis of passage 2 (17 dpi), 3 (31 dpi) (data not shown) and 4 (38 dpi) no PrP^{res} was detected on the western blot in any of the tested samples **(Figure 7.2.7, A)**. In addition, because of its poor performance in cell infection assays, isolate PG1212/03 was not used in further experiments.

The loss of PrP^{res} signal over multiple cell passages suggested that the PrP^{res} could came from the original inoculum rather than from the infected cells or could be only transiently replicating in the cells. In order to investigate that issue, non-induced and induced cells were infected with heated and sonicated PG1207/03 and PG1517/01 scrapie brain homogenates. The cell lysates were analysed after passage 1 (11 dpi) and showed the presence of PrP^{res} in cells not induced with doxycycline for both scrapie isolates **(Figure 7.2.7, B)** indicating the PrP^{Sc} is from the original inoculum and this is diluted out and no longer detected by passage 2.

For infections with 1/80 dilution of SSPP1 (12.5 µl of 10 % brain per 1 ml of media), heated and sonicated or unmodified brains were used. For heated and sonicated infections, brain homogenates were added on non-induced and induced cells. Here, after 1^{st} passage (12 dpi) PrP^{res} was detected only in samples induced with doxycycline **(Figure 7.2.8, A)**. This could suggest that the resistant PrP signal came from replication within the infected cells rather than the scrapie inoculum. Moreover, PrP^{res} was not detected during passage 2 (19 dpi) and 3 (26 dpi), however it was detected on western blot in later passages (passage 4 (34 dpi), 5 (41 dpi) and 6 (47 dpi)). Similarly, only induced cells were infected with unmodified brain SSBP1 at a 1/80 scrapie:media ratio in comparison to non-induced cells. The western blots showed the presence of PrP^{res} at passage 1 (17 dpi), 2 (24 dpi), 4 (46 dpi), 5 (53 dpi) and 6 (59 dpi). There was no PrP^{res} in sample after passage 3 (38 dpi) probably due to PrP^{res} pellet loss during the concentration procedure **(Figure 7.2.8, B)**. Overall, the persistent infection of Rov9 cells with scrapie brain homogenate SSBP1 was demonstrated. However, inoculation with PG1207/03 and PG1517/01 scrapie did not result in prion replication within the cells. The SSBP1 infection method was used in further experiments.

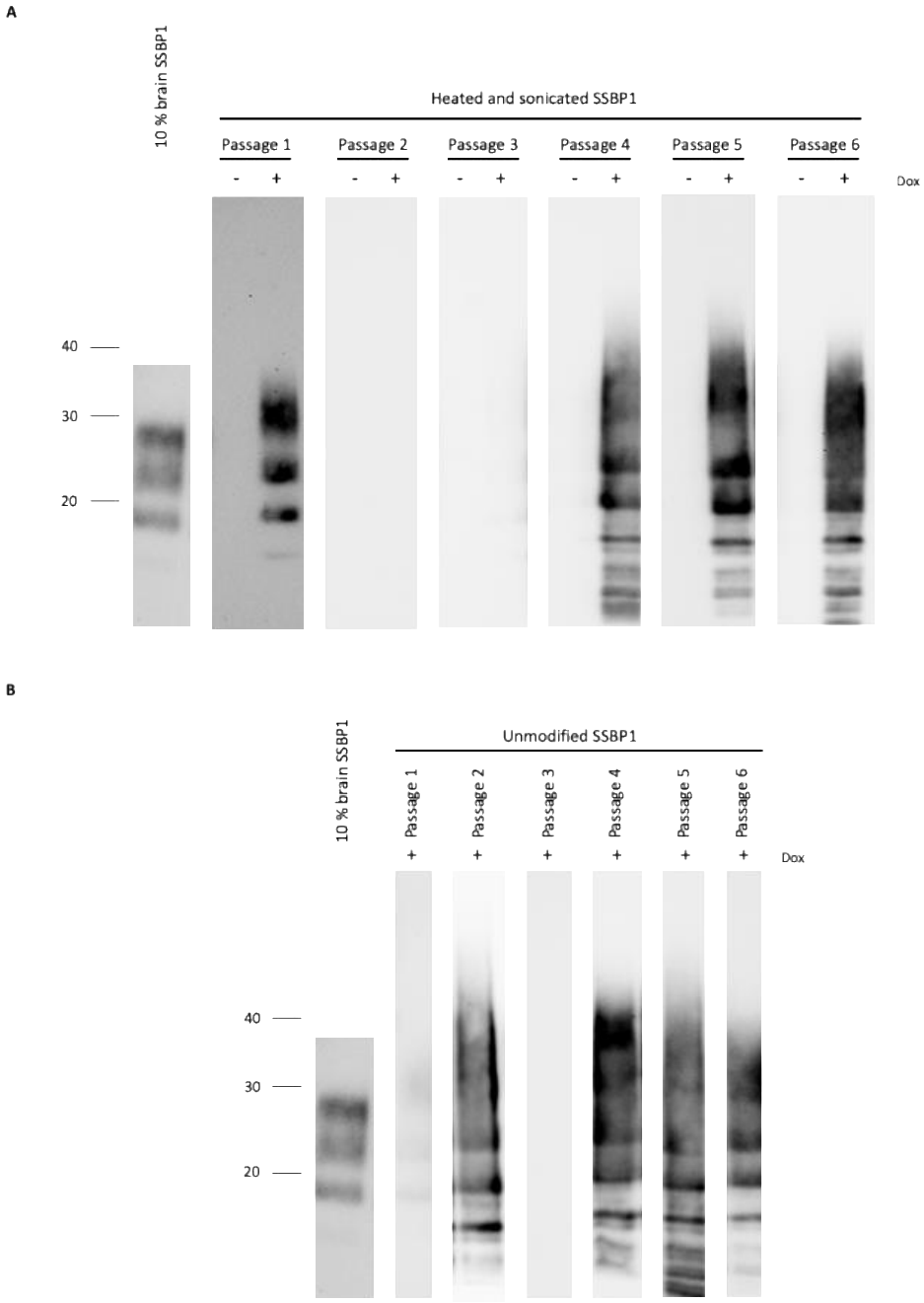

Figure 7.2.8. Rov9 cell infections with heated and sonicated and unprocessed 10 % SSBP1 scrapie brain homogenate (VRQ/VRQ). Cells were infected with 12.5 µl of 10 % brain homogenate per 1 ml of media (1/80 dilution). **A** – passage 1 – 6 (12 – 47 dpi) of induced and non-induced cells inoculated with heated and sonicated SSBP1 brain. **B** – passage 1 – 6 (17 – 59 dpi) of induced cells infected with unprocessed SSBP1 brain. 500 µg of total protein from samples were digested with 20 µg/ml PK and analysed on western blots. Protein markers are indicated on the left side of each blot. 10 % SSBP1 brain was digested with 100 µg/ml PK and 20 µl of the digestion product was analysed on the western as a control. Dox – doxycycline;

7.2.3.5 Rov9 cell morphology and phenotypes

When infected with SSBP1 10 % brain homogenate, Rov9 cells were observed under a light microscope. The morphology of these cells was compared to independent Rov9 cells permanently infected with SSBP1 (Dr Fiona Houston, Roslin Institute) and also uninduced but cultured in the presence of SSBP1 Rov9 cells **(Figure 7.2.9)**. Accumulation of large or small vacuoles was observed in the SSBP1 infected Rov9 cells produced in this study. No accumulation of vacuoles was observed in uninfected, induced cells that were grew in OPTI MEM complete media. Also, less accumulation of vacuoles was observed in cell obtained from the Roslin Institute.

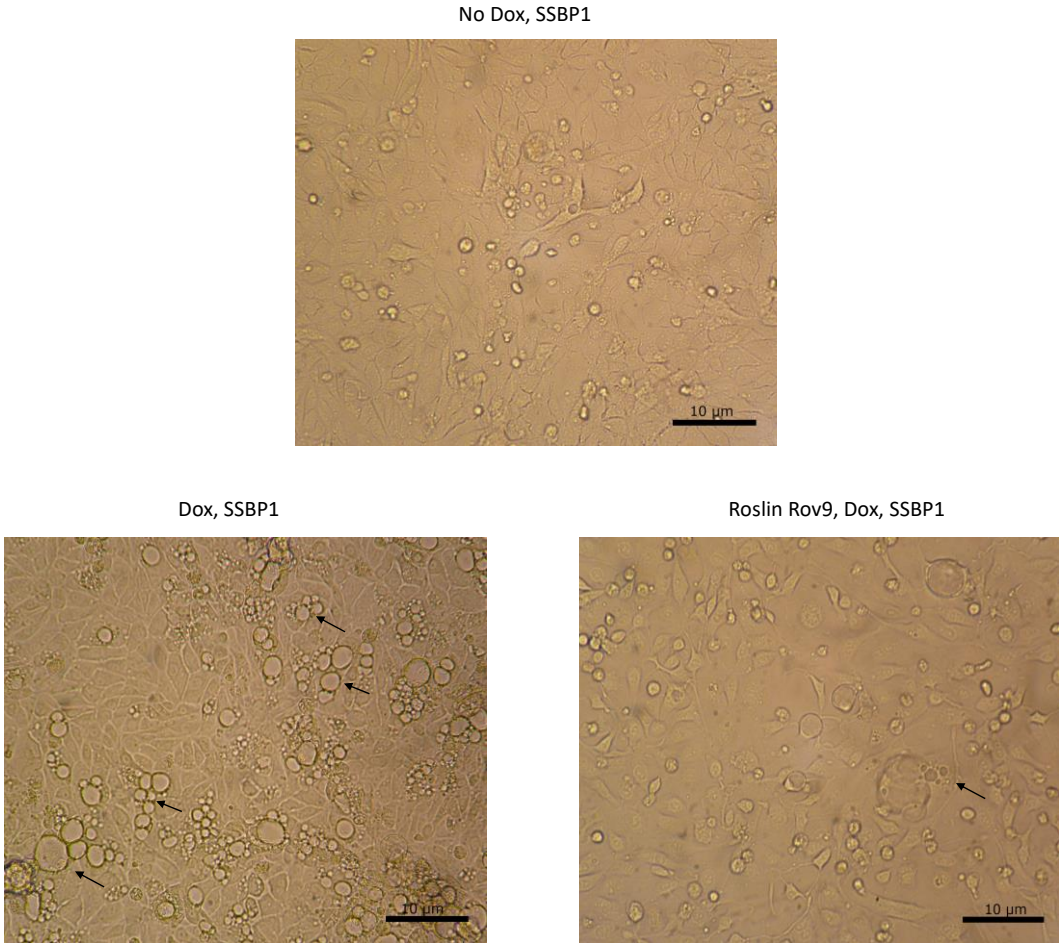

Figure 7.2.9. Representative Rov9 light microscopy images showing vacuole accumulation in Rov9 cells infected with SSBP1 (VRQ/VRQ). Infected cells were either produced in the present study or were obtained from the Roslin Institute. Representative vacuole accumulation was marked on images with black arrows. Scale bars were indicated on each image. Dox – doxycycline;

7.2.3.6 Protease resistance of PrP^{Sc} in Rov9 cells infected with SSBP1

The protease resistance of PrP^{res} produced in SSBP1 infected Rov9 cells was tested. Lysates from passage 9 for infected cells produced in the present study and those obtained from the Roslin Institute were digested with a range of PK concentrations **(Figure 7.2.10)**. The PrP^{res} was resistant to at least 100 µg/ml of PK (passage 9 – 65 dpi). The absence of PrP^{res} bands in the sample digested with 20 µg/ml of PK was very likely a result of losing the PrP^{res} pellet during the experiment procedure. In addition, the band pattern for infected cells were similar for both sources of infected cells. The bands for di- , mono- and un-glycosylated bands of PrP^{res} had similar sizes and both samples had additional lower molecular weight bands.

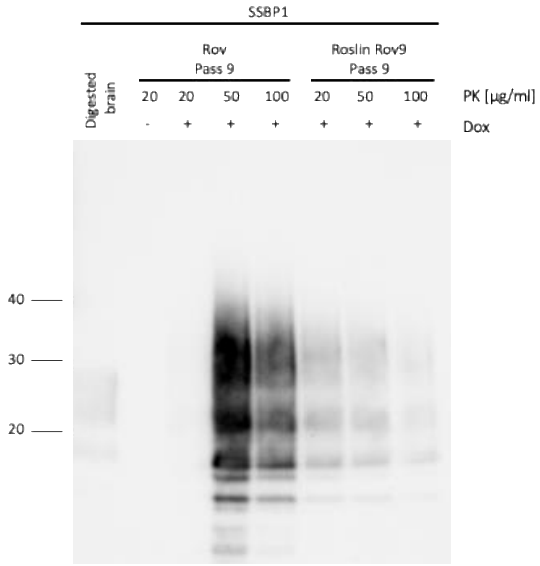

Figure 7.2.10. Proteinase K resistance of PrP^{res} isolated from Rov9 cells infected with scrapie isolate SSBP1 (VRQ/VRQ) (passage 9 – 65 dpi). 500 µg of total protein amount for non-induced and induced cells was digested with 20, 50 or 100 µg/ml of PK and analysed on the western blot. 20 µl of 10 % SSBP1 brain homogenate was digested with 100 µg/ml and analysed on the western blot. Two sources of infected cells were used, one produced in the present study and one from The Roslin Institute. Protein marker is indicated on the left side of the blot. PK – proteinase K, dox – doxycycline, pass – passage;

7.2.4 Inoculation of Rov9 cells with SiO_2 precipitated PrP^{Sc}

7.2.4.1 SiO_2 binding fractions analysis

Following initial failed attempts to infect Rov9 cells with brain homogenate, the PrP^{Sc} inoculum was concentrated and purified on SiO_2 before application to cells (Rees *et al.*, 2009). 25 µl of 10 % brain homogenate for each isolate was used for SiO_2 capture. In order to estimate the amount of PrP^{Sc} bound to SiO_2 slurry, fractions after binding ('bind'), washing and elution ('final') were collected and analysed **(Figure 7.2.11)**. Fractions 'bind', 'wash' and 'final' for SSBP1 (VRQ/VRQ) and B16 (VRQ/VRQ) were analysed with and without PK digestion, whereas 'final' fractions for PG1361/05 (ARQ/VRQ) and PG1207/03 (VRQ/VRQ) were only analysed as PK digested products. For all scrapie isolates and despite the low signal for SSBP1, PrP^{Sc} was present in the 'final' fractions. Moreover, B16 derived PrP^{C} was also found to bind to SiO_2 slurry and was present in the 'final' fraction and was full digested with PK (50 µg/ml).

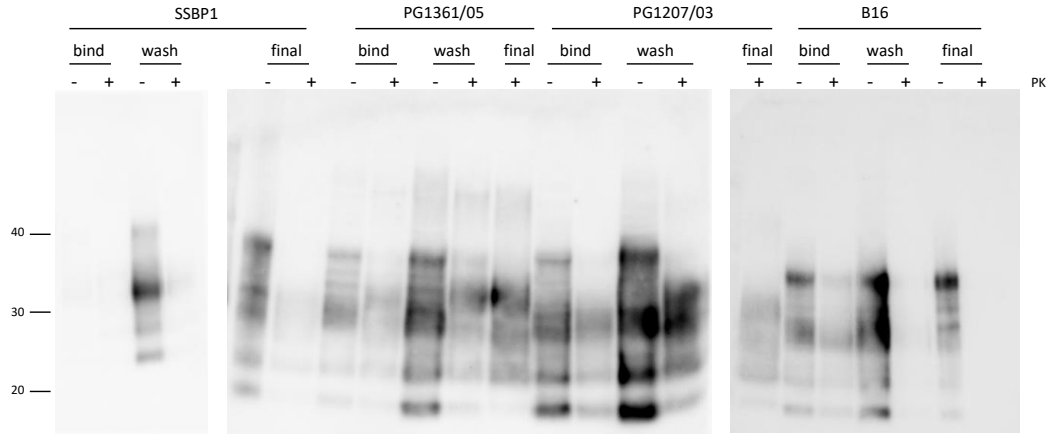

Figure 7.2.11. Levels of PrP^{Sc} in different SiO_2 precipitation fractions. Scrapie SSBP1 (VRQ/VRQ), PG1361/05 (ARQ/VRQ), PG1207/03 (VRQ/VRQ) and TSE negative brain homogenate B16 (VRQ/VRQ) were mixed with SiO_2 and incubated at RT. After centrifugation the 'bind' fraction was collected and analysed. SiO_2 slurry was washed ('wash' fraction) and also analysed. 'Final' fraction was collected in 1 % SDS, precipitated in MeOH and resuspended in PBS. Fractions were digested with 50 µg/ml of PK and 20 µl of each product was analysed on western blot. Protein markers are indicated on the left side of the blots.

7.2.4.2 Inoculation of Rov9 cells with SiO_2 precipitated PrP^{Sc} and PrP^{C}

10 or 20 µl of SiO_2 and MeOH precipitated PrP^{Sc} or PrP^{C} was added to Rov9 cells per well and kept for 3 days. Firstly, no cell loses or toxic effects on cells were observed during and after incubation with PrP^{C} or PrP^{Sc}. The Rov9 cells looked healthy and viable. After first passage (10 dpi) no PrP^{res} was observed in samples from cells treated with either 10 or 20 µl of SiO_2 purified PrP^{Sc} **(Figure 7.2.12)**.

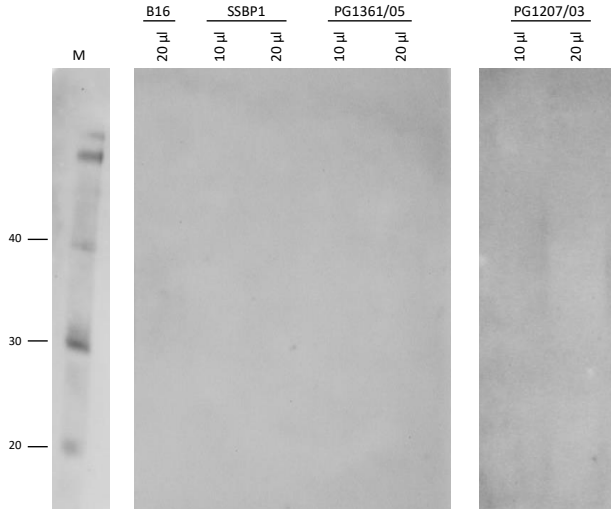

Figure 7.2.12. Representative western blots show absence of PrP^{Sc} in passage 1 (10 dpi) in Rov9 cell lysates. 20 µl of PrP^{C} (B16) and 10 or 20 µl of SiO_2 purified and MeOH precipitated PrP^{Sc} from scrapie SSBP1 (VRQ/VRQ), PG1361/05 (ARQ/VRQ) and PG1207/03 (VRQ/VRQ) was added in media complete with 1 µg/ml of doxycycline on the cells and incubated. 500 µg of total protein was digested with 20 µg/ml PK and analysed on western blots. Protein marker is indicated on the left side on the blot.

7.2.5 Inoculation of Rov9 cells with NaPTA precipitated PrP^{Sc}

Following initial failed attempts to infect Rov9 cells with brain homogenate, the PrP^{Sc} inoculum was concentrated NaPTA before application to cells (Safar *et al.*, 1998). NaPTA precipitated PrP^{Sc} from 10 % brain homogenates SSBP1 (VRQ/VRQ), PG1361/05 (ARQ/VRQ) and PG1207/03 (VRQ/VRQ) was added on Rov9 induced with 1 µg/ml doxycycline. PrP^{res} was observed in Rov9 infected with SSBP1 derived PrP^{Sc} in passage 1 samples (17 dpi). Furthermore, the Rov9 cells were persistently infected with SSBP1 as the presence of PrP^{res} in cell lysates was detected throughout passages (passage 1: 17 dpi, passage 6: 59 dpi) **(Figure 7.2.13)**. The lack of PrP^{res} in passage 3 (38 dpi) was probably due to PrP^{res} pellet loss during the experiment. In contrast, the other scrapie isolates did not infect the cells (data not shown). In addition, the Rov9 cells that were inoculated with PG1361/05 derived PrP^{Sc} died during the first 3 days post infection.

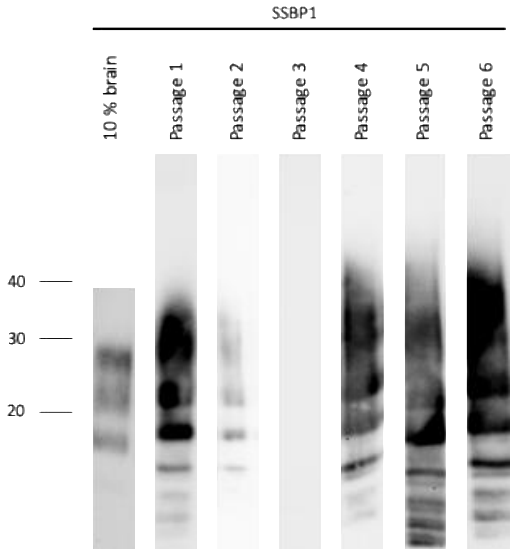

Figure 7.2.13. Rov9 infections with NaPTA precipitated PrP^{Sc} from 10 % SSBP1 brain homogenate (VRQ/VRQ). 30 µl of NaPTA precipitated SSBP1 PrP^{Sc} was added on induced cells. 500 µg of total protein count from each cell lysate was digested with 20 µg/ml of PK and analysed on western blot. 10 % SSBP1 brain homogenate was digested with 100 µg/ml of PK and 20 µl was analysed on western blot. Protein markers are indicated on the left side of each blot. Passage 1 – 17 dpi, passage 2 – 24 dpi, passage 3 – 38 dpi, passage 4 – 46 dpi, passage 5 – 53 dpi, passage 6 – 59 dpi.

7.2.6 Preventing infections with SSBP1 derived PrP^{Sc} with rPrP

Having established an infection protocol for infecting Rov9 cells with heat treated and sonicated SSBP1, this was used to determine whether rPrPs could inhibit or prevent infection. rPrPs were preincubated in media with the 10 % heated and sonicated SSBP1 brain (VRQ/VRQ). The samples for non-induced cells inoculated with SSBP1 had no PrP^{res} detected in any of the passages and experimental repeats. This result showed that the PrP^{res} bands on western blots for doxycycline induced samples came from replication in infected cells rather than brain inoculum. In addition, passage 1 (11 dpi) was also analysed for induced cells where only rPrPs at 250 nM were added. The outcome showed no PrP^{res} in cell lysates after 1st passage (data not shown). Furthermore, the PrP^{res} was detected in induced cells inoculated with SSBP1 from passage 1 onwards. The scrapie 10 % brain was included on each blot for signal reference. The addition of 50 nM of rRRQ had no effect on prevention of the SSBP1 Rov9 cells infection over two passages, therefore rPrPs were only analysed at 250 nM **(Figure 7.2.14, A)**. For no rPrP, 250 nM rRRQ and 250 nM rARR, three independent experiment repeats were performed, whereas rKRQ, rPRQ and rVRQ were analysed in two experiment repeats. Calculated in ImageJ signal value was standardized against average signal for scrapie brains controls. The results were standarised against 10 % SSBP1 brain controls because the signal from it was more consistent between experiments than no rPrP (inhibition) signal. Following this adjustment, one-way ANOVA ($F=14.16$, $p<0.05$) followed by Dunnett's multiple comparisons test was carried out and revealed significant differences in PrP^{res} levels between rRRQ ($p=0.0067$), rARR ($p=0.0064$) and no rPrP in passage 1 samples **(Figure 7.2.14, B)**. Both rRRQ and rARR significantly inhibited the infection with scrapie SSPB1. Moreover, the data for rKRQ, rPRQ and rVRQ **(Figure 7.2.14, C)** was not analysed statistically due to low number of replicates. Preliminary results for rKRQ and rPRQ showed that these rPrPs could also inhibited the scrapie infection of Rov9 cells. In contrast, rVRQ showed high variations between experiments therefore its role in the experiment needs to be further investigated. Additionally, when western blot passage 2 (18 dpi) data was analysed (data not shown) low infection level was maintained for rRRQ and rPRQ, whereas it was variable between repeats for rKRQ, rVRQ and rARR.

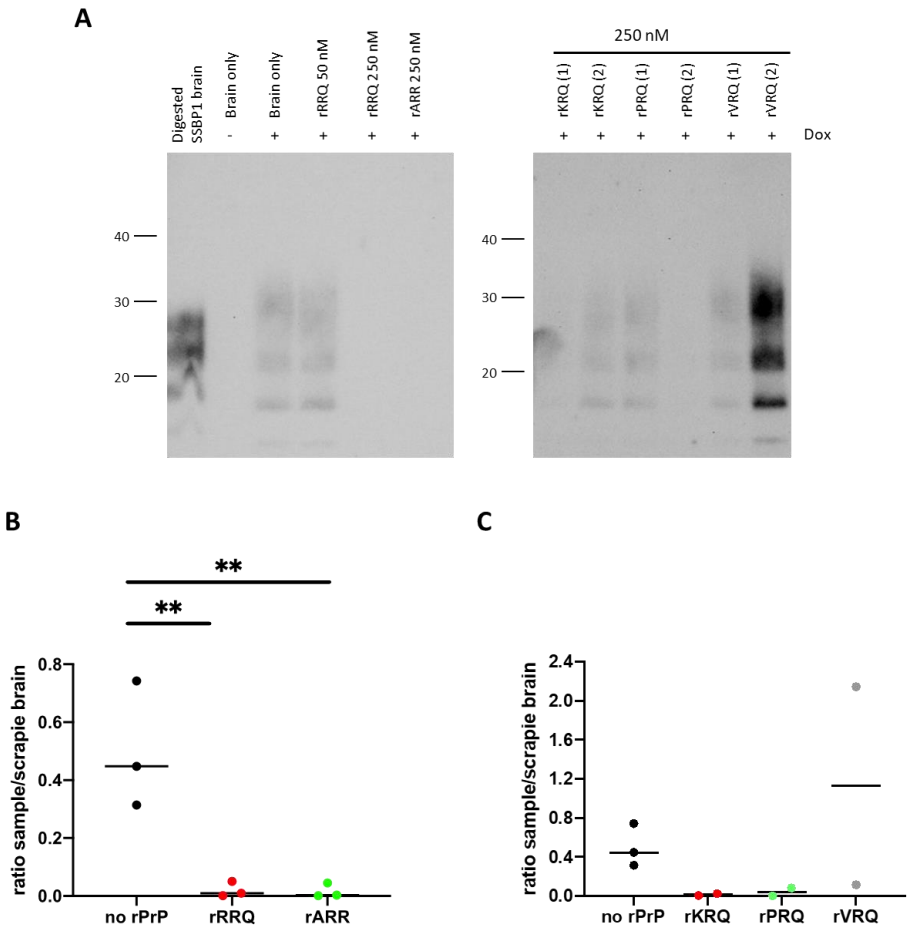

Figure 7.2.14. Passage 1 analysis for preventing infections of Rov9 cells with rPrPs. **A** - representative western blot shows passage 1 (11 dpi) for Rov9 cells infected with SSBP1 in the presence of rRRQ (50 nM or 250 nM), rKRQ, rPRQ, rVRQ, rARR (250 nM). 10 % SSBP1 brain homogenate was heated for 20 minutes at 80 °C and sonicated for 2 minutes then mixed with rPrP in OPTI MEM media complete with or without 1 µg/ml doxycycline and incubated for 1 h at 37 °C. The inoculum was then added to Rov9 cells. 500 µg of total protein from passage 1 cell lysates was digested with 20 µg/ml PK and analysed on western blot. PK digested 10 % SSBP1 brain homogenate was put on blot for signal reference. SSBP1 brain was digested with 100 µg/ml PK and 20 µl was analysed on western blot. Protein markers are indicated on the left side of each blot. **B** – graph shows the calculated ratio for each sample signal/the average signal for scrapie brain controls for rRRQ and rARR. Displayed data came from three independent experiments. One-way ANOVA ($F=14.16$, $p<0.05$) with Dunnett's multiple comparisons test showed significant differences between 250 nM rRRQ and rARR and the no rPrP control (p values: rRRQ=0.0067, rARR=0.0064). * - $p\geq 0$ .05, ** - $p\geq 0.01$, *** - $p\geq 0.001$, **** - $p\geq 0.0001$. **C** – graph shows the calculated ratio for each sample signal/the average signal for scrapie brain controls for rKRQ, rPRQ and rVRQ in compare to no rPrP samples. Displayed data came from two independent experiments. Dox – doxycycline, 1, 2 – sample replicates.

For two experimental repeats samples were analysed up to passage 4 (31 dpi) **(Figure 7.2.15)**. In these experiments only rRRQ at 50 and 250 nM and rARR at 250 nM were studied. These were compared to non-induced and induced cells infected with SSBP1 scrapie isolate. In non-induced cells, no PrP^{res} was detected, whereas in dox induced cells, cells were infected with scrapie SSBP1 and the PrP^{res} was present in cell lysates. In addition, in passage 3 (24 dpi) rRRQ at 50 nM had no inhibition effect on preventing cells infection, whereas in passage 4 samples showed some effect, however this could be sample variation rather than inhibition effect of rRRQ at 50 nM. Moreover, the experiments also showed that in passage 3 and 4 both 250 nM of rRRQ and rARR still had an impact on reducing the efficiency of the infection with SSBP1.

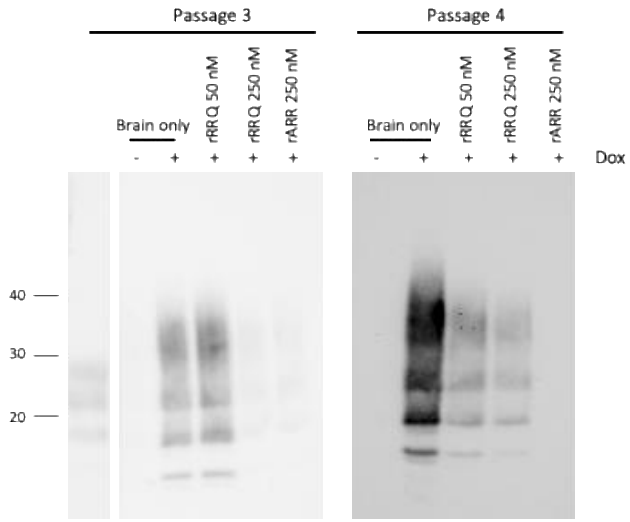

Figure 7.2.15. Preventing infections of Rov9 cells by treatment with rPrP. rRRQ (at 50 and 250 nM) and rARR (250 nM) were assessed. Representative western blots show passages 3 (24 dpi) and 4 (31 dpi) for Rov9 cells infected with SSBP1 preincubated with rPrP. 10 % SSBP1 brain homogenate was heated for 20 minutes at 80 °C and sonicated for 2 minutes. Processed brain was mixed with rPrP in OPTI MEM media complete with or without 1 µg/ml doxycycline and incubated for 1 h at 37 °C. 500 µg of total protein from passage 3 and passage 4 cell lysates was digested with 20 µg/ml PK and analysed on western blot. PK digested 10 % SSBP1 brain homogenate was put on blot for reference. SSBP1 brain was digested with 100 µg/ml PK and 20 µl was analysed on western blot. Protein markers are indicated on the left side of each blot. Dox – doxycycline.

Overall, the infection of Rov9 cells with scrapie isolate SSBP1 (VRQ/VRQ) could be inhibited or efficiency reduced using rPrPs at 250 nM when 10 % scrapie brain was preincubated with rPrPs before addition on the cells. The preliminary data suggest that between all tested rPrPs – rRRQ showed the most promising results.

7.2.7 Curing SSBP1 infected Rov9 cells with rPrPs

Induced Rov9 cells were infected with heated and sonicated SSBP1 brain homogenate (VRQ/VRQ) and exhibited stable infection over multiple passages. These persistently infected cells were used in four independent curing experiments. The scrapie 10 % brain was included on each blot in duplicates for signal reference **(Figure 7.2.16, A)**. PrP^{res} levels were estimated by densitometry and the blots were analysed. The ratio of signal for each sample versus the average signal for scrapie brain blotting controls was calculated. For this data, Kruskal-Wallis test with multiple comparison Dunn's test analysis was carried out ($H=6.810$, $p<0.05$) and showed no significant differences between samples (p value: rRRQ=0.86, rKRQ>0.99, rPRQ=0.20, rVRQ>0.99, rARR>0.99) and the no rPrP control **(Figure 7.2.16, B)**.

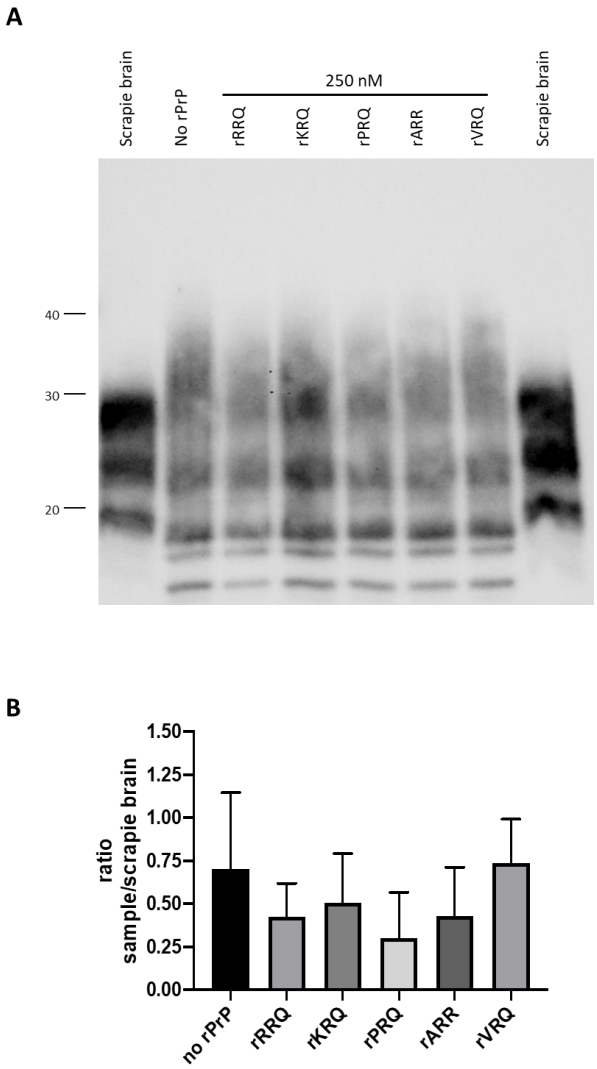

Figure 7.2.16. The effect of 250 nM rRRQ, rKRQ, rPRQ, rARR and rVRQ on PrP^{res} levels in persistently infected Rov9 cells. **A** - the blot shows representative result from four experiments. Persistently infected Rov9 cells were incubated with 250 nM of each rPrP for 4 days. 500 µg of total protein from each cell lysate was digested with 20 µg/ml of PK and analysed on western blot. 10 % classical scrapie brain homogenates were digested with 100 µg/ml of PK and 20 µl of the product was analysed on the blot as a signal reference. Protein marker is indicated on the left side of the blot. **B** – graph shows the calculated ratio for each sample signal/the average signal for scrapie brain controls. Displayed data came from four independent experiments. Kruskal-Wallis test ($H=6.810$, $p<0.05$) with multiple comparisons Dunn's test showed no significant differences between any of the rPrP and the no rPrP control (p values: rRRQ=0.85, rKRQ>0.99, rPRQ=0.20, rVRQ>0.9999, rARR>0.99).

7.3 Discussion

Rov9 cells are derived from rabbit epithelial kidney cells. The level of endogenous PrP^C in these cells is very low and they have been used for ovine PrP^C plasmid transfection (Vilette *et al.*, 2001). As a result, expression of ovine PrP^C (VRQ equivalent) could be induced by the presence of 1 µg/ml of doxycycline. These cells were used in this study to provide a model for infection with ovine scrapie prions.

First, it was investigated whether cells were producing ovine PrP^C. Expression of PrP^C in the Rov9 cells at the time of exposure to infectious inocula was necessary for successful infection with the TSE agent (Paquet, Daude, *et al.*, 2007). Data showed that induction with doxycycline resulted in ovine PrP^C production and in addition, the PrP^C was fully digested with PK at 10 µg/ml. In comparison, the non-induced cells had no ovine PrP^C in the cell lysates (Vilette *et al.*, 2001). In addition, during the cell infection preparation procedure, the media was swapped from EMEM to OPTI MEM and cells induced in OPTI MEM. It was previously found that the Rov9 cells maintained infection better in OPTI MEM and the PrP^{res} signal after infections with TSE agent was 4 x higher (Kocisko *et al.*, 2005).

Some cell lines susceptible to prion infection required isolates that have been previously passaged in rodents (Clarke and Haig, 1970; Taraboulos *et al.*, 1990; Schatzl *et al.*, 1997). This was in part due to a species barrier as the cells used for infections usually came from rodents (*etc*. mice) (Vilette *et al.*, 2001). Because of the expression of ovine PrP^C, Rov9 cells were described as being susceptible to natural ovine TSEs, that were not experimentally adapted to rodents (Vilette *et al.*, 2001; Neale *et al.*, 2010). Here, 5 scrapie isolates: PG1207/03 (VRQ/VRQ), PG1212/03 (VRQ/VRQ), PG1517/01 (VRQ/VRQ), PG1361/05 (ARQ/VRQ) and SSBP1 (VRQ/VRQ) were used in infection trials. Firstly, the levels of PrP^{Sc} were determined in 10 % brain homogenates and after amplification in VRQ/VRQ substrate. In all samples, 10 % brain homogenate contained readily detectable PrP^{Sc} on the western blot, however the SSBP1 displayed the lowest PrP^{Sc} content in comparison to other brain samples. The difference between levels of PrP^{Sc} in brain homogenates was not expected to have an impact on the Rov9 cells infection as it was previously reported that the amount of PrP^{Sc} in the scrapie brains did not correlate with the *de novo* PrP^{res} formation (Neale *et al.*, 2010). Therefore, here, we analysed the 10 % brains to determine the PrP^{res} band patterns rather than PrP^{Sc} level estimation. In addition, all tested isolates amplified over 5 rounds of PMCA in VRQ/VRQ substrate. For four isolates (PG1207/03, PG1212/03, PG1517/01 and PG1361/05) the amplification product was detectable on western blot after only 1 PMCA round. In contrast, for SSBP1 scrapie isolate, there was no product detected after rounds 1-4 of PMCA, but this was present after round 5. Successful PMCA amplification indicated these scrapie isolates will amplify in VRQ/VRQ substrate and so should be able to replicate in the Rov9 cells.

Preliminary infection experiments involved testing 3 of the scrapie isolates (PG1361/05, SSBP1 and PG1207/03). For these, 2 µl of 10 % brain was added per 1 ml of cell culture media (1/500 dilution). It was shown previously that the addition of as little as 0.1 µl (1/10,000 dilution) of 10 % brain homogenate of mouse passaged 22L isolate was enough to infect the RK13 cells expressing mouse PrP. In addition, PrP^{res} was also present for infections using 1000- and 100-fold dilutions of inocula (1 µl and 10 µl of 10 % brain per 1 ml of media, respectively) after three weeks post infection (Arellano-Anaya *et al.*, 2017). Therefore, as a first attempt in the current study, 500-fold dilution of 10 % brain homogenates were used. SSBP1 was used as it was a VRQ/VRQ brain and was previously reported as being able to persistently infect Rov9 cells (Neale *et al.*, 2010). In addition, another VRQ/VRQ scrapie – PG1207/03 – was also chosen along with the heterozygotic VRQ isolate (ARQ/VRQ PG1361/05). This latter classical scrapie isolate was tested as it was the primary isolate used in the PMCA model for examining the efficacy of rPrPs in blocking prion replication. Moreover, it was also previously shown that the Rov9 cells could be infected with field cases of scrapie from VRQ/VRQ or VRQ heterozygous isolates (Neale *et al.*, 2010). In this experiment, each sample was analysed 3 dpi, 5 dpi and then in weekly intervals. Moreover, the impact on possible buffers on cells survival and PrP^{C} expression was also tested. The brain homogenates had been previously prepared in two different buffers: brain homogenate buffer and conversion buffer. Both of these contain detergents such as triton X-100 or NP-40 and additionally, conversion buffer contained EDTA, whereas brain homogenate buffer sodium deoxycholate. Analysis demonstrated that the addition of either of the buffers to the equivalent level present in 1/500 diluted brain inocula had no impact on cell survival and PrP^{C} expression. As a further control, TSE negative brain homogenate (VRQ/VRQ) was included in cell infections, this did not cause cell death and the brain derived PrP^{C} was not detected in non-induced cells. For all 3 scrapie isolates, PrP^{res} was not detected at any timepoint (up to 32 dpi – 5^{th} passage) meaning there was no cell infections with a 1/500 diluted of 10 % brain homogenates PG1361/05, SSBP1 and PG1207/03. At this stage, two possible reasons for the lack of infection were considered. Firstly, the cells could be infected but because of the small dose of the infectious inocula, a small number of cells could present the PrP^{res} but this was below the limit of detection on western blot when analysing up to 100 µg of total protein. This scenario would also indicate that transmission between cells was not efficient (Arellano-Anaya *et al.*, 2011). Secondly, the amount of PrP^{Sc} that is present in the scrapie inoculum was not enough to infect the Rov9 cells, whereas this is in contrast to the mouse PrP^{C} expressing RK13 cells (Arellano-Anaya *et al.*, 2017).

Next, cell infections using a much higher amount of inocula was carried out. Cells were challenged with a 1/40 dilution (25 µl of 10 % brain in 1 ml of media) of isolates (and buffers as controls) in media complete. Using 12.5 times more of each inoculum resulted in loss of noticeably number of cells for classical scrapie PG1361/05 inocula and buffers controls, suggesting that the amount of detergents in the buffers was high and caused

cellular death. Rov9 cells that were infected with PG1207/03 and SSBP1 survived the infection as observed at 3 dpi timepoint with some cell loss for SSBP1 infections. After 5 dpi, there was a very faint characteristically triple band pattern for scrapie in cell lysates infected with PG1207/03 but not with SSBP1. However, this potential infection signal was lost during subsequent passages. No PrP^{res} bands were detected in SSBP1 treated cells in passage 2. At this point, it was also assessed whether the detection of PrP^{res} in cell lysates could be made more sensitive. The analysis of PMCA samples found that cell lysates from infections with PG1207/03 (5 dpi and 1st passage) contained PrP^{res}. In contrast, no resistant prion signal was detected with SSBP1. In conclusion, this step confirmed that there was PrP^{res} present in the cell lysates from PG1207/03 infected Rov9 cells. In addition, PrP^{res} in cell lysates were concentrated by centrifugation and 500 µg of total protein analysed for each sample. Using this approach, it was confirmed that PrP^{res} was present in samples at 5 dpi and after 1st passage for PG1207/03. In addition, PrP^{res} was also present at 3 dpi timepoint and 2nd passage (24 dpi) of that isolate. The level of PrP^{res} decreased between passages suggesting that the infection was not stable or that the observed PrP^{res} was from the scrapie inoculum rather than due to *de novo* production in infected Rov9 cells. As the centration of samples before analysis seemed to increase sensitivity and was much more rapid than PMCA, this was adopted as the standard analysis method.

Next, processing of brain homogenates before addition on cells was attempted to try and improve infection efficacy. The protocol was taken from Vilette *et al.* and involved heating the brain homogenates at 80 °C for 20 minutes and sonicating for 2 minutes (Vilette *et al.*, 2001). These steps could potentially create more infectious resistant prion oligomers to act as seeds for *de novo* prion replication, however this step was not usually included in TSE cell culture methods (Vilette *et al.*, 2001; Falanga *et al.*, 2006; Courageot *et al.*, 2008; Salamat *et al.*, 2011; Arellano-Anaya *et al.*, 2017). This new modification resulted in PrP^{res} detection for all tested scrapie isolates (PG1207/03, PG1212/03 and PG1517/01) after passage 1. Furthermore, isolates PG1207/03 and PG1517/01 also produce PrP^{res} signals without this pre-treatment. Moreover, it appeared that cells infected with any of these scrapie isolates was not persistent and the PrP^{res} signal was undetectable by passage 4. It was investigated whether the detected PrP^{res} came from replication in cells or from the scrapie inoculum. For this purpose, non-induced and induced with doxycycline Rov9 cells were infected with 1/40 processed 10 % brain homogenates PG1207/03 and PG1517/01. It was found that for both isolates non-induced and induced Rov9 cells had resistant PrP bands. This experiment showed that the PrP^{res} detected in cells inoculated for PG1517/01 and PG1207/03 infected samples came from scrapie infectious inocula rather than infected cells. This also explained the PrP^{res} signal loss over multiple passages, a result of diluting the inocula.

The approach of processing the brain homogenate before cells infection was also tested for SSPB1 brain. Here, it was observed that the addition of 1/40 (brain:media ratio) on

the cells resulted in some cell loss. This was not consistent between experiments potentially due to factors like usage of different brain aliquots or suboptimal cells growth. A 1/80 dilution of 10 % (12.5 µl of 10 % brain in 1 ml of media) SSBP1 was found to not reduce the cells survival when a visual investigation was performed after 3 dpi. In addition, unprocessed and processed SSBP1 homogenate were used to inoculate non-induced and induced cells. Here, samples at 3 and 5 dpi samples were not analysed as they could produce false positives from the scrapie inoculum signal. After 1st passage (11 dpi) the PrP^{res} was detected only in cells expressing the ovine PrP and not in the non-induced cells. This result showed that the original inoculum of SSBP1 was not detected in neither induced nor non-induced cells. In compare the PG1207/03 and PG1517/01, the 10 % SSBP1 had less PrP^{Sc} in the original inoculum. Additionally, the amount of SSBP1 brain added on the cells during infections was reduced from 1/40 (for PG1207 and PG1517/01) to 1/80. Furthermore, PrP^{res} was detected in passage 1 of both experiments, and there was more PrP^{res} in cells infected with processed brain compared to those challenges with unmodified SSBP1. This suggested that the heating and sonicating procedure created more infectious seed for Rov9 cell infection. The infection with both processed and non-processed SSBP1 was also stable over 6 passages. A technical challenge in the assay was that after the concentration of PrP^{res} by centrifugation, the resistant PrP pellet was very small and not always visible. This resulted in some pellets being lost and no PrP^{res} detected for such samples.

Because the presence of detergents in brain homogenates reduced the amount of brain to media ratio needed for successful infections, it was also investigated whether the use of purified PrP^{Sc} from brain homogenates improved cell infection. Two PrP^{Sc} purification methods were used. First, mineral particles were used to precipitate bind PrP^{Sc} (Johnson *et al.*, 2006; Rees *et al.*, 2009; Jacobson, Kuech and Pedersen, 2013; Horie *et al.*, 2014). SiO_2 was used to purify the PrP^{Sc} from SSBP1 (VRQ/VRQ), PG1361/05 (ARQ/VRQ) and PG1207/03 (VRQ/VRQ) (Rees *et al.*, 2009). In order to assess the presence of PrP^{Sc} during the purification and in final preparation, each fraction was examined on western blot. High levels of PrP^{Sc} were detected in both PG1207/03 and PG1361/05 isolates in the final fraction. In compare to this, lower level of PrP^{Sc} was detected in final preparation of SSBP1. The cells treated with SiO_2 – purified PrP^{Sc} were not infected with any of the tested scrapie isolates when passage 1 was analysed. The second method used NaPTA precipitation of the PrP^{Sc} (Safar *et al.*, 1998). Infection with NaPTA precipitated ARQ/VRQ PG1361/05 scrapie isolate resulted in cell death during 3 dpi. We cannot exclude here the possibility that the purification was not complete, and the detergents present in brain homogenate were not completely removed. Furthermore, it was also noticed previously that the 1/40 dilution of 10 % brain homogenate (25 µl of 10 % brain in 1 ml of media) for PG1361/05 also killed the cells. These two results could be an impact of presence of detergents or presence of PrP^{Sc} that was highly infectious and, as a result, caused cell death. On the other hand, cells infected with PrP^{Sc} derived from SSBP1 scrapie isolate showed PrP^{res} in first passage

samples. The amount of brain used in NaPTA precipitation was higher than in infection with 10 % SSBP1 brain homogenates, however, the potential losses of PrP^{Sc} during the purification procedure cannot be excluded. Consequently, the signal for PrP^{res} was higher than for cells infected with 1/80 of SSBP1 brain homogenate. Moreover, this infection was stable over 6 passages.

When applying the model of Rov9 cell infections, a few factors require consideration. Firstly, the *PRNP* genotype of the isolates. Neale and co-workers assessed the permissiveness of Rov9 cells to a panel of sheep scrapie from a range of genotypes. In these experiments only scrapie isolates from VRQ/VRQ homozygotes and VRQ heterozygotes were able to infect the Rov9 cells. In addition to that, not all VRQ homo- or heterozygous scrapie sheep brains infected cells (Neale *et al.*, 2010). These outcomes suggested that the homology between PrP genotypes between cells and inoculum might be required and Rov9 cell infection could depend on PrP^{C} sequence (Sabuncu *et al.*, 2003; Neale *et al.*, 2010). Secondly, the dilution of brain homogenate should be optimal so that it contains sufficient infectious material but at the same time is not toxic for cells. In previously reported research, the brains used for cell infections were homogenised in sterile PBS or sterile glucose solution (Vilette *et al.*, 2001; Falanga *et al.*, 2006; Neale *et al.*, 2010; Stanton *et al.*, 2012). Here, the disadvantage of our prion isolates was that the isolates contained detergents and the solutions used for their preparation were not classed as sterile. Therefore, we had to investigate different brain:media dilutions and observe its effect on cells. Finally, for successful Rov9 cells infections with SSBP1 scrapie isolate we used a dilution of 1/80 of a 10% brain homogenate in media. This dilution of 10 % SSBP1 brain homogenate was also been used previously to persistently infect Rov9 cells (Falanga *et al.*, 2006). In contrast, a study using sterile 5 % glucose solution to prepare 10 % (w/v) brain from PG127 scrapie isolate, applied 1/4 dilution of natural sheep and mouse-passaged 10 % brain homogenates on cells (Vilette *et al.*, 2001). Other research used PG127 scrapie isolate and found that inoculation with 1/10 dilution of 10 % of brain homogenate was enough to infect the Rov9 cells (Salamat *et al.*, 2011). Additionally, successful infections with 1/40 dilution of PG127 sheep isolate and 1/1000 dilution of 10 % scrapie field isolates were described (Paquet, Daude, *et al.*, 2007; Neale *et al.*, 2010). Because our brain homogenates could be non-sterile and contain large PrP^{Sc} aggregates we processed the brain using the heating and sonication steps before adding into cell culture media (Vilette *et al.*, 2001). Surprisingly, the processing was not performed in all published research even though the infection of Rov9 cells was successful (Falanga *et al.*, 2006; Salamat *et al.*, 2011). The other important factor was the incubation time for cells and infectious inocula to allow the PrP^{Sc} cell uptake. A report suggested that RML derived PrP^{Sc} was endocytosed in 1 minute from the exposure time in novel and a neuroblastoma cell line (Goold *et al.*, 2011). For Rov9 cells, published methods used exposure times from 5 to 48 h (Vilette *et al.*, 2001; Falanga *et al.*, 2006; Paquet, Daude, *et al.*, 2007). In addition, quantitative analysis showed that in 6 h after infection only 5-10 % of total

PrP^{Sc} from the inoculum could be taken up by Rov9 cells, whereas when the time was increased to 24 h the total uptake was increased to 82 % (Paquet, Daude, *et al.*, 2007). To maximise cellular uptake of the infecting prions, the current study allowed inocula to be in contact with cells for 72 h.

Overall, SSBP1 isolate could be used to stably infect Rov9 cells by direct application of a 1/80 dilution of the 10 % brain homogenate in the cell media. This could be enhanced in terms of the PrP^{res} signal at passage 1 by either pre-treating the inocula by heating and sonication or by NaPTA precipitating the inocula. Considering ease of use and efficacy, the use of heat treated/sonicated SSBP1 inocula was the optimum method used in this study. Additionally, to maximise the cellular uptake of prions, the scrapie inoculum was kept on cells for 72 h.

Once the infection with SSBP1 brain homogenate was established, the PrP^{res} band pattern was compared for SSBP1 brain, the infected cells and also an independent source of Rov9 cells infected with SSBP1 (a gift from Dr Fiona Houston, Roslin Institute). Both infections were analysed at passage 9. The difference in band pattern for PrP^{res} from infected Rov9 cells compared to SSBP1 brain homogenate was consistent for independent sources of infected cells and demonstrated that Rov9 cells were infected and produced *de novo* PrP^{res} with distinct glycosylation/cleavage profile compared to the infecting PrP^{Sc} from brain homogenate (Vilette *et al.*, 2001).

It was noted that the morphology of infected cells was distinct from uninfected cells. In infected Rov9 cells the accumulation of vacuoles was observed. These structures were present in all SSBP1 infected cells irrespective of the pre-treatment or precipitation of the inoculum. The vacuoles presence was also observed in the infected Rov9 cells supplied by The Roslin Institute, however with much lower occurrence. These structures have not been reported in the literature for Rov9 cell infections. On the other hand, this type of vacuole aggregation was found in association with florid plaques in vCJD cases (Ironside and Bell, 1997; Takashima *et al.*, 1997; Grigoriev *et al.*, 1999; Armstrong *et al.*, 2002). In addition, these structures were also observed in iCJD (dura mater or growth hormone cases) (Takashima *et al.*, 1997; Shimizu *et al.*, 1999; Cali *et al.*, 2015). Moreover, all the described changes were reported in brain tissue and not epithelial cells (Grigoriev *et al.*, 1999; Asante *et al.*, 2006; Cali *et al.*, 2015).

The main aim of this chapter was to investigate whether the rPrPs have an inhibition impact on *de novo* PrP^{res} formation in Rov9 cells. For this purpose, two experiments were designed to determine if rPrPs can prevent infections and whether they can cure stably infected cells. In the preventing infection experiment, the three potentially best inhibitors for *in vitro* PrP^{Sc} amplification were used: rRRQ, rKRQ, rPRQ. In addition, also natural variants – rVRQ and rARR were tested. rARR was shown to be the least potent inhibitor in previous PMCA experiments, therefore we investigated its effect on PrP^{res} accumulation in Rov9 cells as a comparison to the variants that were far more potent

inhibitors of PrP^{Sc} replication in PMCA (Workman, Maddison and Gough, 2017). In all three replicate experiments, the Rov9 cells were persistently infected with SSBP1 and the PrP^{res} signal did not come from the inoculum. Furthermore, 50 nM of rRRQ was tested but it appeared to have little impact on preventing the infections with SSBP1 over multiple passages. Moreover, statistical analysis between no rPrP and 250 nM of rRRQ and rARR showed that all these mutants reduced the PrP^{res} amount in cell cultures when passage 1 was analysed (11 dpi). Because of the lower number of repeats for rKRQ, rPRQ and rVRQ we could not perform the statistical analysis on these rPrP. However preliminary data for rKRQ and rPRQ suggest that these could act as potential inhibitors for Rov9 cells infection with SSBP1 scrapie. For rVRQ, the results were variable, therefore we could potentially argue that the presence of natural variant rVRQ did not prevent the infection of Rov9 cells as effectively. Further passages for 250 nM of rRRQ and rARR showed that these two rPrP reduced the PrP^{res} level in infected Rov9 cells. The infection was not prevented in 100 %, and it cannot be predicted how many cells were infected, or the way that the cells would proliferate and transmitted the PrP^{res} between them. Infection of Rov9 cells has been previously shown to be inhibited by sulfated glycans. It was found that the glycans had no inhibition effect on the PrP^{Sc} uptake by the Rov9 cells when pre-incubated with sulfated glycans for 24 h prior to infection. In contrast, the presence of sulphated glycans at the time of infection with PrP^{Sc} and cultured in the presence of glycans for a week inhibited the Rov9 cells infection (Paquet, Daude, *et al.*, 2007).

A second experiment tested the impact of 250 nM of each rPrP on persistently infected Rov9 cells. The cells were incubated with rPrPs over 4 days and then the changes in PrP^{res} profile and signal were analysed, over four independent experiments. The data showed high variations for all samples and changes were not significant, however the trend was that the rRRQ and rPRQ were the most likely to reduce the PrP^{res} levels. These experiments could be furter developed and new experimental approaches could be tested. For example, peristently infected Rov9 cells could be incubated with rPrPs for longer periods of time and with higher rPrPs concentrations. Moreover, additional control that has been described in the literature and have been proved to have PrP^{res} reducing capabilities in persistently infected cells could be added as an inhibiton control.

Persistently infected Rov9 cells have been used to screen a range of therapeutic compounds that were found to inhibit PrP^{res} production in N2a cells. It was found that some compounds such as the tannic acid and PPS inhibited the PrP^{res} accumulation in infected Rov9 cells, whereas for example curcumin had no effect on PrP^{res} in Rov9 cells (Kocisko *et al.*, 2005). The data indicates that different cell models of prion replication can produce very different results when assessing potential therapeutic agents. In addition, Beringue and co-workers tested the impact on different monoclonal antibodies of PrP^{res} accumulation in Rov9 cells. The antibodies were produced in mice immunised with truncated human rPrP (sequence 91-231) (Beringue *et al.*, 2003). The

accumulation of PrP^{res} was inhibited in scrapie infected Rov9 cells that where treated with antibodies that recognised residues 96-109 according to mouse PrP sequence numbering (Beringue *et al.*, 2004). In comparison to the current study, Beringue *et al.* treated the cells with the antibodies for a much longer time-frame than (3 weeks), and this could be potentially beneficial for investigating inhibition mechanisms in cells actively propagating scrapie infection (Beringue *et al.*, 2004). On the other hand, to the date no recombinant prion proteins have been tested in scrapie infected Rov9 cells, however rPrPs have been tested in other prion infected cells. Recombinant human PrP was found to inhibit the murine PrP^{Sc} accumulation in ScN2a cells in a concentration dependent manner over 4 days of incubation. The significant decrease in PrP^{res} signal from infected N2a cells was observed when 100 nM of human rPrP was added to the cells; the EC50 value reported for the same rPrP in PMCA was 60 nM (Yuan *et al.*, 2013). Moreover, other scrapie infected cells – MNB – were tested with two hamster PrP derived peptides and their impact on PrP^{res} accumulation over 3-4 days. The peptide containing hamster positions 119-136 in the sequence effectively reduced the PrP conversion, with an IC50 values between 68 – 75 μM in a cell-free conversion assays (for different isolates) and 11 μM in cell culture (Chabry *et al.*, 1999). In our experiments, 250 nM of each rPrP were tested in persistently infected cells. The experiment showed that 250 nM of rRRQ had no effect on PrP^{res} accumulation in cell culture. In addition, other mutants (rKRQ, rPRQ) or natural variants (rVRQ and rARR) that were tested had no significant effect on the resistant prion propagation in the infected cells.

The results reported in the cell culture research differ from results obtained from PMCA. In PMCA lower concentration of inhibitors were required to noticeably inhibit the amplification of scrapie prion protein whereas in cell culture experiments much higher amounts of rPrP were used but still with different outcome. As an example, the average IC50 value from PMCA experiment for rRRQ was 11 nM, whereas in cell culture experiments 250 nM was used and prevented the infection with scrapie. That amount of inhibitor was 22x more than IC50 value reported from PMCA. In contrast, 50 nM of rRRQ had no effect in preventing infections with SSBP1. In addition, rARR that was previously reported to have higher IC50 value (505 nM) than rVRQ (122 nM), was found to prevent the cellular infections with prions at the same level and similarly to other tested at the same concentration rPrPs but did not reduce the PrP^{res} levels in persistently infected cells (Workman, Maddison and Gough, 2017). There are multiple factors that could be causing these differences in rPrPs performance. Firstly, these changes could be triggered by using a different TSE isolate. PMCA was performed for natural classical scrapie PG1361/05 (ARQ/VRQ), whereas in cell culture experiments experimental SSBP1 (VRQ/VRQ) isolate was used. Secondly, the SSBP1 isolate was not tested in the inhibition PMCA, in which other isolates (that also needed multiple rounds to amplify) were inhibited using higher amounts of rPrPs (50 nM). Thirdly, PMCA is a method specifically designed for amplification of misfolded prion protein. Experiments using cell cultures are more complex and many possible processes are associated in prion uptake

and propagation. Moreover, different mechanisms could be involved in the primary prion uptake by the cells and cell to cell spreading. To enhance the contact of rPrPs with scrapie PrP^{Sc} and allow potential rPrP-PrP^{Sc} binding, in preventing infections experiment, the rPrPs were pre-incubated with SSBP1 in cell culture media. The current results described high impact of some of rPrPs in preventing infections but not curing infections experiments. The previously published data suggest that transmission of PrP^{res} between cells could occur through the contact to neighbouring cells via endocytosis or direct penetration of cell membrane by PrP^{Sc} monomers from cell culture media (Fevrier *et al.*, 2004; Guo and Lee, 2014; Aguzzi and Lakkaraju, 2016). Additionally, the transport could also occur to more distant cells via TNTs (Gousset *et al.*, 2009; Victoria *et al.*, 2016). Whereas the present in media PrP^{Sc} would be accessible to potential binders (like rPrPs), PrP^{res} located in endosomes and TNTs could not be easily available for inhibitors. Furthermore, none of these PrP^{res} spreading mechanisms might be exclusive (Paquet, Langevin, *et al.*, 2007). Therefore, we could not exclude the possibility that the rPrPs reduce the accessible fraction of PrP^{res} in persistently infected cells but the difference could not be measured using used in the current research tools leading to the detected high level of PrP^{res}.

The reported cell culture experiments investigated if the rPrPs that were previously found to be potent inhibitors of prion replication in *in vitro* prion amplification, reduce the infection of cells and/or can cure infection in persistently infected cells. The rPrPs tested (except for rVRQ) were effective at reducing infection efficiency or preventing cell infection with prions but could not (under the conditions tested) reduce prion replication in already infected cells. This may indicate that the rPrPs used in this research bound to PrP^{Sc} inoculum and that this interaction prevented the PrP^{Sc} from either being taken up by the cells and/or from binding PrP^{C} or cofactors required for prion replication. However, the rPrPs could not interact with cell surface or intracellular PrP^{Sc}. Whether the rPrPs would have been more effective at reducing infection in infected cells over a longer duration or following passage remains to be established. Overall, the data demonstrates that the ovine rPrPs can effectively inhibit prion replication in PMCA and also prevent prion from infecting cells.

Chapter 8: General Discussion

8.1 Introduction

This study focused on the development of candidate therapeutics for transmissible spongiform encephalopathies. The work included production and use of recombinant XRQ mutants as inhibitors for *in vitro* prion misfolding for different TSE isolates. The most effective rPrPs were then analysed structurally. Moreover, the recombinant PrPs were also used in a cell culture model of scrapie infection to determine their efficacy in preventing and curing infection.

8.2 Analysis of the ability of rPrP mutants at position 136 to inhibit prion replication

The current study focused on producing and testing rPrPs with substitutions at position 136 in an *in vitro* prion replication assay and their effect was compared to natural variant rVRQ. Previously, rVRQ was reported to inhibit prion amplification *in vitro* for different species regardless of the prion disease isolate or genotype (Workman, Maddison and Gough, 2017). Moreover, this PrP genotype was a more efficient inhibitor than the other rPrPs tested, for example rARQ was reported to have an IC50 of 228 nM, rARR 505 nM and rVRQ 122 nM. This result clearly suggested that the position 136 in ovine PrP could have a significant impact on misfolding of the prion protein during PMCA (Workman, 2017; Workman, Maddison and Gough, 2017). In addition, previous research showed the ability of human, mouse, bank vole, bovine and hamster rPrP to inhibit the amplification of human prion protein in PMCA (Yuan *et al.*, 2013; Skinner *et al.*, 2015). At the beginning of the current study, the rVRQ inhibition of a classical ovine scrapie was verified and the result was consistent with previous outcomes with similar IC50 values reported in the two independent studies (Workman, 2017; Workman, Maddison and Gough, 2017). Moreover, this study was the first to demonstrate the use of mutated rPrPs inhibitors, genetically modified at position 136 of ovine rPrPs with non-natural mutations. It was shown here that the change in amino acid at 136 position had an impact on the inhibition effectiveness in the PMCA. All 20 amino acids variants at position 136 were tested and arginine, lysine and proline were found to create the most potent rPrPs inhibitors were more effective than previously reported rVRQ with rRRQ being 22x more effective than rVRQ (Workman, Maddison and Gough, 2017). This novel result showed the importance of position 136 in ovine PrP in inhibition. Previously, the 136 position was found as crucial when determining the disease susceptibility or resistance in sheep (Goldmann, 2008). This, together with previous research could suggest that modified ovine rPrPs, could potentially be used as a therapeutic for prion diseases (Yuan *et al.*, 2013; Skinner *et al.*, 2015; Seelig, Goodman and Skinner, 2016). More research in this filed could focus on further characterisation of rPrP mutants for other species, for instance position 129 in human rPrP is polymorphic. It was found that V/V_{129} and M/M_{129} are more susceptible for sCJD and vCJD than heterozygotes M/V (Mead, 2006; Mastrianni, 2010; Brown *et al.*, 2012; Acevedo-Morantes and Wille, 2014). Research

focusing on investigating recombinant human PrP in the inhibition of *in vitro* prion protein misfolding could be designed with focus on position 129 and also other amino acids substitutions could be implemented in human PrP at position 129. Moreover, the mechanisms of rPrP action could be investigated to determine whether the rPrPs added into PMCA act as a PrP^{C} binder to block access to substrate or a PrP^{Sc} binder to block the sites for PrP conversion. Yuan and co-workers using magnetic beads binding assays demonstrated that recombinant human PrP bound to the PrP^{Sc} but not the PrP^{C}. They described that human rPrP had higher than PrP^{C} affinity to the same binding site within the PrP^{Sc}. This suggests that rPrPs and PrP^{C} are likely to be the active competitors for PrP^{Sc} binding (Yuan *et al.*, 2013). Additionally, RT-QuIC has been described as another method of misfolding the PrP protein (Atarashi, Sano, *et al.*, 2011). This assay presents a model for the misfolding of a wide range of TSEs using bank vole rPrP substrate and so could be developed to further screen the best inhibitors (Orrú, Groveman, *et al.*, 2015). Moreover, using the RT-QuIC could help improve the inhibitors screening not only for ovine rPrP but also human in order to develop and could potentially give more accurate results. This method could also improve the quality and quantity of the data and help to produce IC50 values for rPrPs.

In the current research the shortest possible peptide with inhibition abilities containing the 136 position was sought. The ovine PrP derived peptides were applied to PMCA and their inhibitory properties determined. The PrP derived peptides were smaller in size than the full-length protein which could be beneficial in production and drug delivery, as the small molecules could pass the brain blood barrier more efficiently (Soto *et al.*, 2000). The result presented here showed that none of the peptides exhibited the inhibition observed for ovine full-length proteins. This was consistent with previous research investigating the impact on human PrP on PMCA misfolding. Authors found that the full-length recombinant human PrP was the most efficient inhibitor of PMCA, with the C- or N-terminally truncated peptides being less effective (Yuan *et al.*, 2013). On the other hand, using a cell-free conversion assay, Chabry *et al*., presented data that indicated the potential for PrP derived peptides with the same inhibition properties as the full length PrP (Chabry, Caughey and Chesebro, 1998; Chabry *et al.*, 1999). This could indicate that the power of inhibition of PrP derived peptides depends on the model of prion misfolding being used and would differ between assays and types of isolates. Furthermore, the possibility that the PrP derived peptides formed aggregates and therefore lost their inhibitory properties cannot be excluded. This problem was observed with Aβ derived peptides, that self-assembled into fibrils and did not inhibit the misfolding of amyloid β (Yan *et al.*, 2013). To further investigate the use of PrP derived peptides, it should be investigated whether the peptides were in a monomeric or aggregated state. Moreover, these peptides could be applied in different methods of protein misfolding such as RT-QuIC and the results could be compared to those obtained with PMCA. In addition, peptides could also be used alongside rPrP in preventing infections of cells or curing perisistently infected cells. This experiment could act as an

addition to PMCA and RT-QuIC and would help to investigate peptides effect of blocking the cells infection with prion protein. Using the peptides in further experiment could help in providing new data and ideas about the inhibition mechanisms.

One of the tested recombinant PrPs was rPRQ (P_{136}). Interestingly, the presence of proline in the protein sequences was observed in unstructured regions of the protein. Moreover, the thermodynamic studies showed that prolines were not compatible with β-sheets and also could prevent or even disturbs forming β sheet rich structures (Smith, Regan and Withka, 1994; Li *et al.*, 1996; Williams *et al.*, 2004). Additionally, introduction of prolines into the peptide or protein chains helped with the whole molecule solubility and reduced the potential of amyloid formation (Wood *et al.*, 1995; Williams *et al.*, 2004). Because of these features, β-sheet breaker peptides with extra proline residues were described in AD models (Soto *et al.*, 1996, 1998; Shuaib *et al.*, 2019). These consisted of partial Aβ sequence with additional proline inserted into the peptide chain (Soto *et al.*, 1998). A similar approach was also tested in PrP studies, where β-sheet blocker peptides with additional prolines inserted in the peptide sequence were designed. Purified PrP^{Sc} from both mice infected with scrapie 139A isolate and human sCJD and vCJD were incubated with specific peptides. The result showed that the incubation with proline rich peptide (β-sheet blocker) reduced the amount of PK resistant protein however, the effect was species specific. Moreover, the proline-rich peptide reduced the misfolding of prion more effectively than the non-modified PrP sequence derived peptides (Soto *et al.*, 2000). In the current research, proline was introduced into the polypeptide chain in an unstructured region, however this was a substitution rather than insertion of an additional amino acid. Further research could look into expanding the PrP-derived peptides into creating β-sheet breaker peptides by introducing more proline residues into the polypeptide chain.

The study also presented preliminary insights into the structural analysis of ovine PrP variants. The outcome showed that each of the ovine rPrP mutants analysed exhibited similar structure to natural ovine VRQ. The PrP molecule consisted of a flexible N-terminus and globular C-terminus, with three α-helices (Haire *et al.*, 2004). Results confirmed the hypothesis that the newly produced prion proteins differed only in amino acid at position 136 and the protein substitution did not have an impact on the secondary structure of distant regions or the whole molecule. In addition to that, when investigating the differences between of presence of valine, alanine, arginine, lysine and proline at 136 position, it was noticed that two amino acids that were present in PrP mutants – arginine and lysine – had longer side chains. This feature allowed for more interactions with other amino acids within the structure and could potentially stabilise the whole PrP molecule. These interactions did not influence more distant sites in the whole PrP molecule possibly due to the presence of a structural pocket created by the region in α-helix 2. These preliminary insights into the structural analysis of rPrP inhibitors could be developed into more detailed analysis. The further research could

involve the investigation of whether the rPrP bind to PrP^{C} or PrP^{Sc}, which could then be followed by some molecular dynamic's simulations. Previously, similar analysis was performed for the complexes of prion protein with phenothiazine compounds (promazine and chlorpromazine). The authors revealed the crystal structure of prion-promazine complexes and found that the these compounds prevented the misfolding of PrP^{C} by using the protein stabilisation mechanisms (Baral *et al.*, 2014).

The structural analysis of the most effective rPrP inhibitors could indicate that not only one but perhaps more mechanisms were involved in the rPrP inhibition in PMCA. These could be further analysed both *in vitro* and *in silico*.

8.3 Recombinant prion proteins as inhibitors across prion diseases

What would be the best rPrPs for prion amplification inhibition research? Based on the ovine system as a model of the prion diseases therapeutic development, we could hypothesize that an effective inhibitor would not only be characterised by the lowest IC50 value but it would need to show its effectiveness among many tested TSE isolates and distinct TSE diseases. The main focus for developing successful therapeutic would be on human prion diseases – *e.g.,* sCJD, vCJD, FFI, GGS. Investigating an ovine system of prion disease could give insights on some processes and features that could be reflected to those seen in human TSEs. In the current research, we reported three inhibitors that exhibited both: very low IC50 value in comparison to other natural and mutant variants of rPrP and the ability to inhibit different prion disease isolate from field and experimental cases. These included ovine classical scrapie isolates, bovine BSE and experimental ovine BSE. This together with previously reported research that rVRQ was found to inhibit the misfolding of multiple TSE isolates, could suggest that these proteins could act as inhibitors across different TSE isolates and in different species. This finding is consistent with previously reported data for ovine rVRQ that also worked across different TSE isolates (Workman, Maddison and Gough, 2017). In contrast, a contrary hypothesis was reported by Yuan *et al*., who indicated that the inhibition of PMCA with recombinant PrP was species specific (Yuan *et al.*, 2013). Findings reported here could be enhanced by analysing the most effective rPrP in more prion diseases from more genotypes across many different TSE isolates. More importantly, the testing of rPrP should be implemented in human TSE models (PMCA, RT-QuIC and cell culture) in order to help creating a new inhibitor for human prion protein misfolding.

In addition, the recombinant ovine PrPs were also tested as inhibitors for other protein misfolding diseases. In the current research, the inhibition of α-synuclein misfolding during PMCA was investigated. The rationale was that the rPrP could act as a β-sheet breaker, which were described for amyloid beta inhibition research (Soto *et al.*, 1996, 1998; Shuaib *et al.*, 2019). The current research showed no effects of recombinant PrPs on the misfolding of α-synuclein during PMCA. However, this analysis could be expanded into testing also natural rPrPs, like VRQ, with α-synuclein PMCA. Additionally, misfolded

α-synuclein could also be produced using the RT-QuiC assay (Fairfoul *et al.*, 2016). The use of recombinant PrP could be implemented in that assay in order to analyse the possible inhibition mechanisms. Additionally, rPrPs could also be tested, as potent inhibitors for amyloid β and tau misfolding using established *in vitro* misfolding assays (Nieznanska *et al.*, 2018).

8.4 A cell culture model for investigation of rPrP inhibition of scrapie propagation

In the current research, the inhibition of prion protein misfolding *in vitro* with rPrPs was further validated using a cell culture model of scrapie infection. Cell cultures are incredibly practical in testing therapeutic compounds for various diseases including TSEs (Kocisko and Caughey, 2006b). Here, the optimisations steps for the infection of ovine VRQ Rov9 cells were described. The research produced Rov9 cells persistently infected with scrapie SSBP1. These protocols were previously described, but they were implemented and modified in the current research (Vilette *et al.*, 2001; Falanga *et al.*, 2006; Neale *et al.*, 2010). The introduced modified cell infection resulted in a cell phenotype, the widespread occurrence of vacuoles, that has not been reported before for TSE infections in Rov9 cells. Ovine rPrPs were tested for preventing or curing infection with SSBP1. rRRQ, rKRQ, rPRQ and rARR were found to prevent infection with SSBP1, whereas natural rVRQ gave inconsistent results when passage 1 was analysed. Furthermore, low infection level was also maintained for latter passages for rRRQ and rARR, but the reproducibility for others – rKRQ, rPRQ, rVRQ – was poor. This data demonstrated that ovine rPrP could have a significant impact on preventing the infections with scrapie isolates. On the other hand, the rPrPs were tested for the possibility of clearing the PrP^{res} in the persistently infected cells. The data showed a trend for some clearance of PrP^{Sc} in the cells for mutant rPrPs and natural rARR but not the natural rVRQ. This research could be further pursued by increasing the time of incubation of persistently infected cells with rPrP. In addition, higher concentrations of rPrPs could be used in the cell treatment. Additionally, previously reported agents that decreased the PrP^{res} in infected cells like PPS, quinacrine or antibodies could be tested alongside the ovine rPrP to determine their relative efficacies (Beringue *et al.*, 2003; Kocisko *et al.*, 2005). Moreover, other infected with scrapie infected cell lines *e.g.* ScN2a or MNB could be used in testing ovine rPrPs as inhibitors of PrP^{res} formation (Chabry *et al.*, 1999; Yuan *et al.*, 2013). Once successful in cell culture models, ovine rPrPs could be validated in *in vivo* TSE mouse models (Seelig, Goodman and Skinner, 2016).

The cell culture results showed that the time of delivery of the successful therapeutic agent could significantly increase its effectiveness (Panegyres and Armari, 2013). The data presented in this thesis showed that when cells were treated with the therapeutic agent (rPrPs) at the time of infection with prions, the infection was less effective in comparison to rPrP treatment of persistently infected cells. Indicating that early

diagnosis could improve the effectiveness of any treatment of prion diseases (Collinge, 2005).

Reseach using prion protein and prion diseases isolates has many limitations. Because of the prions infectious nature (and proved BSE transmissibility to humans), all experiments have to be performed in higher biosafety security laboratory and in fully controlled environment. Extra caution needs to be taken when working with prion diseases brain homogenates and PMCA products. Because of these conditions, the number and sort of experiments was determined by the instruments localised within the laboratory. However, the type of experiments presented in this work allowed to fully investigate the subject and produce a great amount of work and information about the topic. Range of methodology, starting from protein purification, PMCA and towards cell culture experiments allowed to show and analyse the subject in many details and provide proper scientific data.

Overall, the current study demonstrates that mutant rPrPs are effective inhibitors of TSE propagation in an *in vitro* protein misfolding model. The mutants were considerably more effective than the natural PrP variants tested. Furthermore, mutant rPrP was also effective at preventing infection of cells. Further optimisation for the rPrPs at other amino acid residues known to be important in TSE propagation in ovine disease, such as 154 and 171 could be further mutated and tested. Finally, the study is based on a model TSE, scrapie in sheep, therapeutic intervention is required for human TSE diseases. The ovine rPrP mutants could be tested against models of human TSEs to determine their direct therapeutic potential and an analogous strategy for mutating and testing human rPrPs could be followed.

Appendix

Representative dotblots show inhibition of ovine scrapie PG1361/05 (ARQ/VRQ) with rKRQ, OvK and randomised peptide (OvRND112-144) **(A)**, rPRQ and OvP **(B)**, rVRQ and OvV peptides **(C and D)**. In all cases, there was no peptide inhibition of scrapie ARQ/VRQ PG1361/0550 nM rRRQ, 1 µM and 100 nM of peptides were compared to PG1361/05 amplified in relevant buffers. PrP^C controls amplified in PBS, 0.05 % acetronitrile and 0.04 % HCOOH, 0.3 % acetonitrile were included as a PK digestion control. Amplification products were PK digested and 2.5 µl of each sample were added on the dotblot in duplicate. PrP^C – negative brain homogenate.

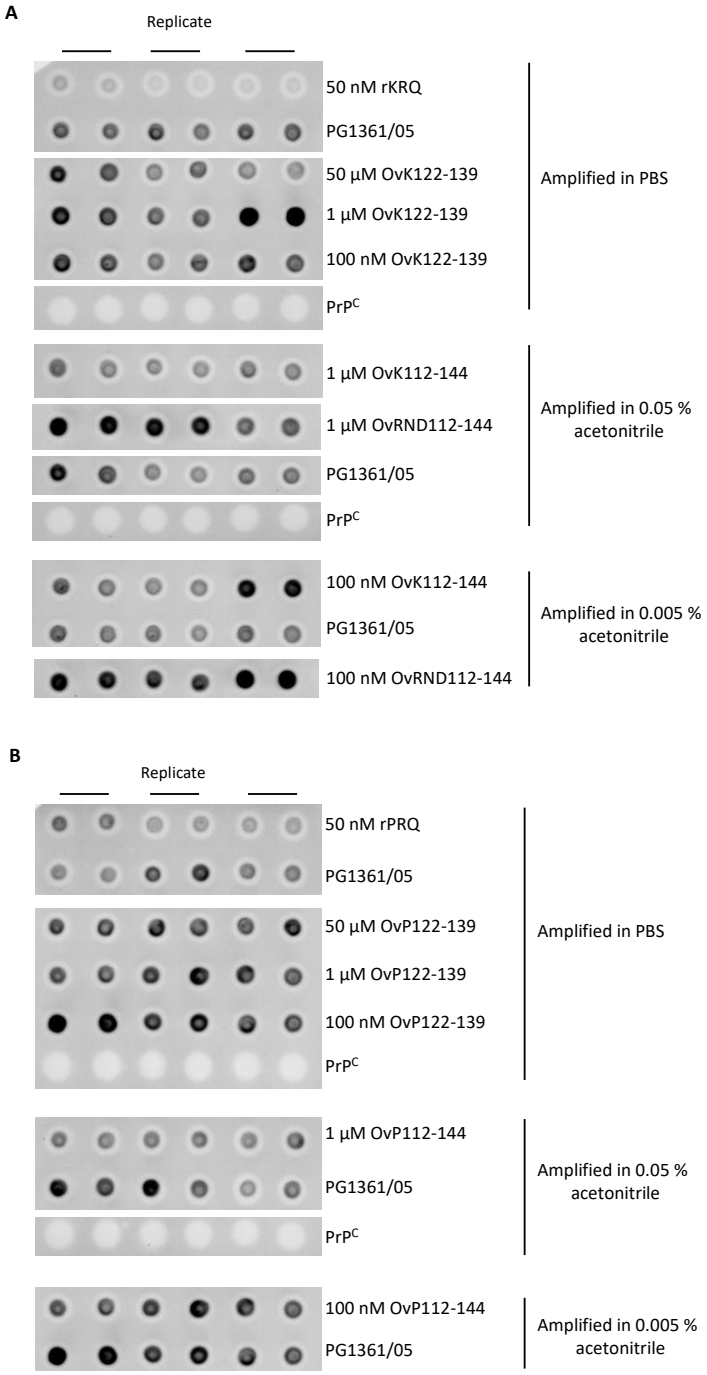

C

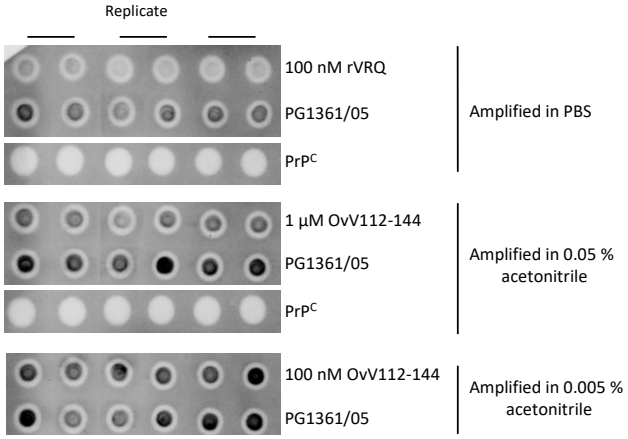
Replicate
100 nM rVRQ
PG1361/05
PrP^C
Amplified in PBS
1 µM OvV112-144
PG1361/05
PrP^C
Amplified in 0.05 % acetonitrile
100 nM OvV112-144
PG1361/05
Amplified in 0.005 % acetonitrile

D

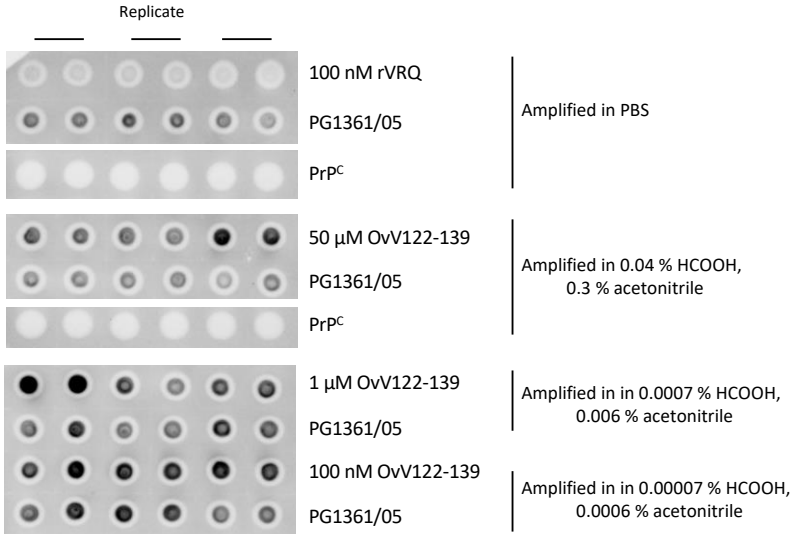
Replicate
100 nM rVRQ
PG1361/05
PrP^C
Amplified in PBS
50 µM OvV122-139
PG1361/05
PrP^C
Amplified in 0.04 % HCOOH, 0.3 % acetonitrile
1 µM OvV122-139
PG1361/05
Amplified in in 0.0007 % HCOOH, 0.006 % acetonitrile
100 nM OvV122-139
PG1361/05
Amplified in in 0.00007 % HCOOH, 0.0006 % acetonitrile

PIPS Reflective Statement

Note to examiners:

This statement is included as an appendix to the thesis in order that the thesis accurately captures the PhD training experienced by the candidate as a BBSRC Doctoral Training Partnership student.

The Professional Internship for PhD Students is a compulsory 3-month placement which must be undertaken by DTP students. It is usually centred on a specific project and must not be related to the PhD project. This reflective statement is designed to capture the skills development which has taken place during the student's placement and the impact on their career plans it has had.

PIPS Reflective Statement

I have spent 3 months of my Professional Internship for PhD Students (PIPS) working as a Research Associate in Arden Biotechnology Ltd in Lincoln. The company's main research focus is to develop a novel biocontrol for *Clostridium perfringens* – anaerobic, Gram-positive bacteria that causes necrotic enteritis in poultry.

During this placement, I was a part of the molecular lab team and involved in different projects. My main project was focused on the analysis of the *Clostridium perfringens* bacteriophages protein profiles. The aim of this project was to design an experiment using the SDS-PAGE electrophoresis in order to see differences in an environmental bacteriophage profiles. The methodology was familiar to me, however I had to use many online resources like scientific publications and articles available in the company to fully understand the topic. It allowed me to learn basic information about the bacteria and the disease – necrotic enteritis. By the end of the placement, I successfully managed to design and optimize the SDS-PAGE electrophoresis conditions for environmental bacteriophage proteins. Furthermore, I analysed and compared 25 different bacteriophages profiles. All the data I have obtained, were described, handled and explained to my Line Manager and the Director of Research. By doing this I have improved my communication and presenting scientific data skills. In addition, completing this project was very beneficial for the company, as my presence, knowledge and work allowed them to learn all the necessary skills required for protein analysis.

Moreover, I also took part in bacteriophage DNA analysis project. During this project, I learned new methods like Pulse Field Gel Electrophoresis, which allowed us to determine our environmental bacteriophage genomes size. Furthermore, I was involved in a sequencing project, in which we used one of the newest sequencing technology developed by Oxford Nanopore Technologies – MinION. My part in this project involved

PIPS Reflective Statement

DNA extraction and the DNA preparation for the sequencing. Then, I had the great opportunity to observe the sequencing process but unfortunately not the DNA sequences analysis process. self-confidence in exploring and trying out new, previously unknown methods has increased.

These two events taught me not to be afraid of any challenges, especially in terms of applying new technology in research. In addition, my self-confidence in exploring and trying out new, previously unknown methods has increased.

The placement helped me to refresh existing and obtain some new microbiology skills. For the first time during my career, I learned how to grow anaerobic bacteria but also, I had an opportunity to gain experience in phage enumeration and propagation techniques.

In addition, my placement gave me the opportunity to observe infection models using the Wax moth larvae – *Galleria mellonella* and *Clostridium perfringens*. That expanded my knowledge in using different organisms as infection/disease models.

During my placement, I was also asked to prepare a written report for the company funder, explaining the progress and all the used methods. That allowed me to practise scientific reports writing and will be beneficial in both my PhD work and future career.

The placement in Arden Biotechnology gave me some important ideas about my future career planning. It allowed me to meet new people and learn how they started a company from scratch and gave a better understanding of the possible funding sources. Furthermore, my work and the performance helped to develop the company product which will be beneficial in the future. Moreover, the work from the placement in Arden Biotechnology has a potential to be published. However, the biggest take away from this placement is that I realised that I am passionate about science and I am happy to plan my future career in the research environment.

References

Abdulrahman, B. A. *et al.* (2017) 'The celecoxib derivatives AR-12 and AR-14 induce autophagy and clear prion-infected cells from prions', *Scientific Reports*, 7(1), pp. 1–12. doi: 10.1038/s41598-017-17770-8.

Abramov, E. *et al.* (2009) 'Amyloid-B as a positive endogenous regulator of release probability at hippocampal synapses', *Nature Neuroscience*, 12(12), pp. 1567–1576. doi: 10.1038/nn.2433.

Acevedo-Morantes, C. Y. and Wille, H. (2014) 'The structure of human prions: From biology to structural models — considerations and pitfalls', *Viruses*, 6(10), pp. 3875–3892. doi: 10.3390/v6103875.

Acutis, P. L. *et al.* (2006) 'Identification of prion protein gene polymorphisms in goats from Italian scrapie outbreaks', *Journal of General Virology*, 87(4), pp. 1029–1033. doi: 10.1099/vir.0.81440-0.

Adjou, K. T. *et al.* (2007) 'Alpha-synuclein Accumulates in the Brain of Scrapie-affected Sheep and Goats', *Journal of Comparative Pathology*, 137(1), pp. 78–81. doi: 10.1016/j.jcpa.2007.03.007.

Agrimi, U. *et al.* (2008) 'Prion protein amino acid determinants of differential susceptibility and molecular feature of prion strains in mice and voles', *PLoS Pathogens*, 4(7), pp. 2–10. doi: 10.1371/journal.ppat.1000113.

Aguzzi, A. and Frontzek, K. (2020) 'New paradigms of clinical trial design for genetic prion diseases', *The Lancet Neurology*. Elsevier Ltd, 19(4), pp. 284–285. doi: 10.1016/S1474-4422(20)30029-6.

Aguzzi, A. and Lakkaraju, A. K. K. (2016) 'Cell Biology of Prions and Prionoids: A Status Report', *Trends in Cell Biology*. Elsevier Ltd, 26(1), pp. 40–51. doi: 10.1016/j.tcb.2015.08.007.

Ahmed, K. A. and Xiang, J. (2011) 'Mechanisms of cellular communication through intercellular protein transfer', *Journal of Cellular and Molecular Medicine*, 15(7), pp. 1458–1473. doi: 10.1111/j.1582-4934.2010.01008.x.

Akimov, S. *et al.* (2008) 'Persistent Propagation of Variant Creutzfeldt-Jakob Disease Agent in Murine Spleen Stromal Cell Culture with Features of Mesenchymal Stem Cells', *Journal of Virology*, 82(21), pp. 10959–10962. doi: 10.1128/jvi.01085-08.

Alais, S. *et al.* (2008) 'Mouse neuroblastoma cells release prion infectivity associated with exosomal vesicles', *Biology of the Cell*, 100(10), pp. 603–618. doi: 10.1042/bc20080025.

Alvarez, L. *et al.* (2011) 'Genetic variability in the prion protein gene in five indigenous Turkish sheep breeds', *Small Ruminant Research*. Elsevier B.V., 99(2–3), pp. 93–98. doi: 10.1016/j.smallrumres.2011.03.043.

Andréoletti, O. *et al.* (2002) 'PrPSc accumulation in placentas of ewes exposed to natural scrapie: Influence of foetal PrP genotype and effect on ewe-to-lamb transmission', *Journal of General Virology*, 83(10), pp. 2607–2616. doi: 10.1099/0022-1317-83-10-2607.

Andréoletti, O. *et al.* (2011) 'Atypical/Nor98 scrapie infectivity in sheep peripheral tissues', *PLoS Pathogens*, 7(2), pp. 1–14. doi: 10.1371/journal.ppat.1001285.

Angers, R. C. *et al.* (2009) 'Chronic Wasting Disease Prions in Elk Antler Velvet', *Emerging Infectious Diseases*, 15(5), pp. 696–703. doi: 10.3201/eid1505.081458.

Animal and Plant Health Agency (2019a) *Overview of Great Britain Statistics*. Available at: https://assets.publishing.service.gov.uk/government/uploads/system/uploads/attachment_data/file/817375/pub-tse-stats-gboverview.pdf (Accessed: 25 July 2019).

Animal and Plant Health Agency (2019b) *TSE surveillance statistics : sheep Summary of the number of confirmed cases of scrapie in sheep each year in Great Britain*. Available at: https://assets.publishing.service.gov.uk/government/uploads/system/uploads/attachment_data/file/817365/pub-tse-stats-sheep.pdf (Accessed: 25 July 2019).

Archer, F. *et al.* (2004) 'Cultured Peripheral Neuroglial Cells Are Highly Permissive to Sheep Prion Infection', *Journal of Virology*, 78(1), pp. 482–490. doi: 10.1128/JVI.78.1.482.

Arellano-Anaya, Z. E. *et al.* (2011) 'A simple, versatile and sensitive cell-based assay for prions from various species', *PLoS ONE*, 6(5). doi: 10.1371/journal.pone.0020563.

Arellano-Anaya, Z. E. *et al.* (2015) 'Prion strains are differentially released through the exosomal pathway', *Cellular and Molecular Life Sciences*, 72(6), pp. 1185–1196. doi: 10.1007/s00018-014-1735-8.

Arellano-Anaya, Z. E. *et al.* (2017) *Prions. Methods and Protocols*. Edited by V. A. Lawson and J. M. Walker. Hatfield: Humana Press.

Arima, K. *et al.* (1999) 'Cellular co-localization of phosphorylated tau- and NACP/α-synuclein-epitopes in Lewy bodies in sporadic Parkinson's disease and in dementia with Lewy bodies', *Brain Research*, 843(1–2), pp. 53–61. doi: 10.1016/S0006-8993(99)01848-X.

Arima, K. *et al.* (2005) 'Biological and Biochemical Characteristics of Prion Strains Conserved in Persistently Infected Cell Cultures', *Journal of Virology*, 79(11), pp. 7104–

7112. doi: 10.1128/jvi.79.11.7104-7112.2005.

Arjona, A. *et al.* (2004) 'Two Creutzfeldt-Jakob disease agents reproduce prion protein-independent identities in cell cultures', *Proceedings of the National Academy of Sciences of the United States of America*, 101(23), pp. 8768–8773. doi: 10.1073/pnas.0400158101.

Armstrong, R. A. *et al.* (2002) 'Florid prion protein (PrP) plaques in patients with varian Creutzfeldt-Jakob Disease (vCJD) are spatially related to blood vessels', *Neuroscience Research Communications*, 32(1), pp. 29–36.

Arsac, J. N. *et al.* (2007) 'Similar biochemical signatures and prion protein genotypes in atypical scrapie and Nor98 cases, France and Norway', *Emerging Infectious Diseases*, 13(1), pp. 58–65. doi: 10.3201/eid1301.060393.

Asante, E. A. *et al.* (2006) 'Dissociation of pathological and molecular phenotype of variant Creutzfeldt-Jakob disease in transgenic human prion protein 129 heterozygous mice', *Proceedings of the National Academy of Sciences of the United States of America*, 103(28), pp. 10759–10764. doi: 10.1073/pnas.0604292103.

Atarashi, R. *et al.* (2008) 'Simplified ultrasensitive prion detection by recombinant PrP conversion with shaking GFP fails to inhibit actin-myosin interactions in vitro', *Nature Methods*, 5(3), pp. 211–212.

Atarashi, R., Sano, K., *et al.* (2011) 'Real-time quaking-induced conversion: A highly sensitive assay for prion detection', *Prion*, 5(3), pp. 150–153. doi: 10.4161/pri.5.3.16893.

Atarashi, R., Satoh, K., *et al.* (2011) 'Ultrasensitive human prion detection in cerebrospinal fluid by real-time quaking-induced conversion', *Nature Medicine*. Nature Publishing Group, 17(2), pp. 175–178. doi: 10.1038/nm.2294.

Baig, M. H. *et al.* (2018) 'Peptide based therapeutics and their use for the treatment of neurodegenerative and other diseases', *Biomedicine and Pharmacotherapy*. Elsevier, 103(February), pp. 574–581. doi: 10.1016/j.biopha.2018.04.025.

Ballatore, C., Lee, V. M. Y. and Trojanowski, J. Q. (2007) 'Tau-mediated neurodegeneration in Alzheimer's disease and related disorders', *Nature Reviews Neuroscience*, 8(9), pp. 663–672. doi: 10.1038/nrn2194.

Baral, P. K. *et al.* (2014) 'Structural basis of prion inhibition by phenothiazine compounds', *Structure*. Elsevier Ltd, 22(2), pp. 291–303. doi: 10.1016/j.str.2013.11.009.

Baral, P. K. *et al.* (2015) 'X-ray structural and molecular dynamical studies of the globular domains of cow, deer, elk and Syrian hamster prion proteins', *Journal of Structural Biology*. Elsevier Inc., 192(1), pp. 37–47. doi: 10.1016/j.jsb.2015.08.014.

Di Bari, M. A. *et al.* (2008) 'The bank vole (Myodes glareolus) as a sensitive bioassay for sheep scrapie', *Journal of General Virology*, 89(12), pp. 2975–2985. doi: 10.1099/vir.0.2008/005520-0.

Di Bari, M. A. *et al.* (2013) 'Chronic Wasting Disease in Bank Voles: Characterisation of the Shortest Incubation Time Model for Prion Diseases', *PLoS Pathogens*, 9(3). doi: 10.1371/journal.ppat.1003219.

Baron, G. S. *et al.* (2006) 'Mouse-Adapted Scrapie Infection of SN56 Cells: Greater Efficiency with Microsome-Associated versus Purified PrP-res', *Journal of Virology*, 80(5), pp. 2106–2117. doi: 10.1128/jvi.80.5.2106-2117.2006.

Barret, A. *et al.* (2003) 'Evaluation of Quinacrine Treatment for Prion Diseases', *Journal of Virology*, 77(15), pp. 8462–8469. doi: 10.1128/jvi.77.15.8462-8469.2003.

Barria, M. A. *et al.* (2018) 'Rapid amplification of prions from variant Creutzfeldt–Jakob disease cerebrospinal fluid', *Journal of Pathology: Clinical Research*, 4(2), pp. 86–92. doi: 10.1002/cjp2.90.

Barrow, C. J. *et al.* (1992) 'Solution conformations and aggregational properties of synthetic amyloid b-peptides of Alzheimer's disease', *Journal of Molecular Biology*, 225, pp. 1075–1093.

Bartz, J. C., Kincaid, A. E. and Bessen, R. A. (2002) 'Retrograde Transport of Transmissible Mink Encephalopathy within Descending Motor Tracts', *Journal of Virology*, 76(11), pp. 5759–5768. doi: 10.1128/jvi.76.11.5759-5768.2002.

Baskakov, I. V. *et al.* (2019) 'The prion 2018 round tables (I): the structure of PrPSc', *Prion*, 13(1), pp. 46–52. doi: 10.1080/19336896.2019.1569450.

Bayer, T. A. *et al.* (1999) 'It all sticks together - The APP-related family of proteins and Alzheimer's disease', *Molecular Psychiatry*, 4(6), pp. 524–528. doi: 10.1038/sj.mp.4000552.

Beekes, M. and McBride, P. A. (2000) 'Early accumulation of pathological PrP in the enteric nervous system and gut-associated lymphoid tissue of hamsters orally infected with scrapie', *Neuroscience Letters*, 278(3), pp. 181–184. doi: 10.1016/S0304-3940(99)00934-9.

Belay, E. D. (1999) 'Transmissible Spongiform Encephalopathies in Humans', *Annual Review of Microbiology*, 53, pp. 283–314.

Bell, M. R. *et al.* (2013) 'To fuse or not to fuse: What is your purpose?', *Protein Science*, 22(11), pp. 1466–1477. doi: 10.1002/pro.2356.

Belt, P. B. G. M. *et al.* (1995) 'Identification of five allelic variants of the sheep PrP gene and their association with natural scrapie', *Journal of General Virology*, 76(3), pp. 509–517. doi: 10.1099/0022-1317-76-3-509.

Benestad, S. L. *et al.* (2003) 'Cases of scrapie with unusual features in Norway and designation of a new type, Nor98', *Veterinary Record*, 153(7), pp. 202–208. doi: 10.1136/vr.153.7.202.

Benestad, S. L. *et al.* (2008) 'Atypical/Nor98 scrapie: Properties of the agent, genetics, and epidemiology', *Veterinary Research*, 39(4), pp. 1–14. doi: 10.1051/vetres:2007056.

Benestad, S. L. *et al.* (2012) 'Healthy goats naturally devoid of prion protein', *Veterinary Research*, 43(1), pp. 2–5. doi: 10.1186/1297-9716-43-87.

Beringue, V. *et al.* (2003) 'Regional heterogeneity of cellular prion protein isoforms in the mouse brain', *Brain*, 126(9), pp. 2065–2073. doi: 10.1093/brain/awg205.

Beringue, V. *et al.* (2004) 'PrPSc binding antibodies are potent inhibitors of prion replication in cell lines', *Journal of Biological Chemistry*, 279(38), pp. 39671–39676. doi: 10.1074/jbc.M402270200.

Bernoulli, C., Siegfried, J. and Baumgartner, G. (1977) 'Dangers of accidental person to person transmission of Creutzfeldt Jakob disease by surgery', *Lancet*, 1(8009), pp. 478–479. doi: 10.1016/S0140-6736(77)91944-4.

Bertsch, U. *et al.* (2005) 'Systematic Identification of Antiprion Drugs by High-Throughput Screening Based on Scanning for Intensely Fluorescent Targets', *Journal of Virology*, 79(12), pp. 7785–7791. doi: 10.1128/JVI.79.12.7785.

Besnier, L. S. *et al.* (2015) 'The cellular prion protein PrPc is a partner of the Wnt pathway in intestinal epithelial cells', *Molecular Biology of the Cell*, 26(18), pp. 3313–3328. doi: 10.1091/mbc.E14-11-1534.

Bett, C. *et al.* (2012) 'Biochemical properties of highly neuroinvasive prion strains', *PLoS Pathogens*, 8(2), pp. 32–34. doi: 10.1371/journal.ppat.1002522.

Biacabe, A. G. *et al.* (2004) 'Distinct molecular phenotypes in bovine prion diseases', *EMBO Reports*, 5(1), pp. 110–115. doi: 10.1038/sj.embor.7400054.

Biacabe, A. G. *et al.* (2007) 'H-type Bovine Spongiform Encephalopathy', *Prion*, 1(1), pp. 61–68.

Bian, J. *et al.* (2010) 'Cell-Based Quantification of Chronic Wasting Disease Prions', *Journal of Virology*, 84(16), pp. 8322–8326. doi: 10.1128/jvi.00633-10.

Bian, J., Kang, H. E. and Telling, G. C. (2014) 'Quinacrine promotes replication and conformational mutation of chronic wasting disease prions', *Proceedings of the National Academy of Sciences of the United States of America*, 111(16), pp. 6028–6033. doi: 10.1073/pnas.1322377111.

Billinis, C. *et al.* (2004) 'Prion protein gene polymorphisms in healthy and scrapie-

affected sheep in Greece', *Journal of General Virology*, 85(2), pp. 547–554. doi: 10.1099/vir.0.19520-0.

Birkett, C. R. *et al.* (2001) 'Scrapie strains maintain biological phenotypes on propagation in a cell line in culture', *The EMBO Journal*, 20(13), pp. 3351–3358.

Bons, N. *et al.* (1999) 'Natural and experimental oral infection of nonhuman primates by bovine spongiform encephalopathy agents', *Proceedings of the National Academy of Sciences of the United States of America*, 96(7), pp. 4046–4051. doi: 10.1073/pnas.96.7.4046.

Bourkas, M. E. C. *et al.* (2019) 'Engineering a murine cell line for the stable propagation of hamster prions', *Journal of Biological Chemistry*, 294(13), pp. 4911–4923. doi: 10.1074/jbc.RA118.007135.

Bove-Fenderson, E. *et al.* (2017) 'Cellular prion protein targets amyloid-β fibril ends via its C-terminal domain to prevent elongation', *Journal of Biological Chemistry*, 292(41), pp. 16858–16871. doi: 10.1074/jbc.M117.789990.

Bradford, B. M., Crocker, P. R. and Mabbott, N. A. (2014) 'Peripheral prion disease pathogenesis is unaltered in the absence of sialoadhesin (Siglec-1/CD169)', *Immunology*, 143(1), pp. 120–129. doi: 10.1111/imm.12294.

Brandner, S. *et al.* (1996) 'Normal host prion protein (PrPc) is required for scrapie spread within the central nervous system', *Proceedings of the National Academy of Sciences of the United States of America*, 93(23), pp. 13148–13151. doi: 10.1073/pnas.93.23.13148.

Brown, P. (1997) 'B lymphocytes and neuroinvasion', *Nature*, 390, pp. 662–663. doi: 10.1080/08940889508602829.

Brown, P. *et al.* (2012) 'Iatrogenic creutzfeldt-Jakob disease, final assessment', *Emerging Infectious Diseases*, 18(6), pp. 901–907. doi: 10.3201/eid1806.120116.

Brown, P. and Gajdusek, D. C. (1991) 'Survival of scrapie virus after 3 years' interment', *The Lancet*, 337(8736), pp. 269–270. doi: 10.1016/0140-6736(91)90873-N.

Bruce, M. E. *et al.* (1997) 'Transmissions to mice indicate that "new variant" CJD is caused by the BSE agent', *Nature*, 389, pp. 498–501.

Bruce, M. E. *et al.* (2002) 'Strain characterization of natural sheep scrapie and comparison with BSE', *Journal of General Virology*, 83(3), pp. 695–704. doi: 10.1099/0022-1317-83-3-695.

Buée, L. *et al.* (2000) 'Tau protein isoforms, phosphorylation and role in neurodegenerative disorders11These authors contributed equally to this work.', *Brain Research Reviews*, 33(1), pp. 95–130. doi: 10.1016/S0165-0173(00)00019-9.

Buschmann, A. *et al.* (2004) 'Atypical scrapie cases in Germany and France are identified by discrepant reaction patterns in BSE rapid tests', *Journal of Virological Methods*, 117(1), pp. 27–36. doi: 10.1016/j.jviromet.2003.11.017.

Cali, I. *et al.* (2015) 'Distinct pathological phenotypes of Creutzfeldt-Jakob disease in recipients of prion-contaminated growth hormone', *Acta neuropathologica communications*. Acta Neuropathologica Communications, 3, p. 37. doi: 10.1186/s40478-015-0214-2.

Cartoni, C. *et al.* (2005) 'Identification of the pathological prion protein allotypes in scrapie-infected heterozygous bank voles (Clethrionomys glareolus) by high-performance liquid chromatography-mass spectrometry', *Journal of Chromatography A*, 1081(1 SPEC. ISS.), pp. 122–126. doi: 10.1016/j.chroma.2005.04.035.

Casalone, C. *et al.* (2004) 'Identification of a second bovine amyloidotic spongiform encephalopathy: Molecular similarities with sporadic Creutzfeldt-Jakob disease', *Proceedings of the National Academy of Sciences*, 101(9), pp. 3065–3070. doi: 10.1073/pnas.0305777101.

Castilla, J. *et al.* (2005) 'In vitro generation of infectious scrapie prions', *Cell*, 121(2), pp. 195–206. doi: 10.1016/j.cell.2005.02.011.

Castro-Seoane, R. *et al.* (2012) 'Plasmacytoid dendritic cells sequester high prion titres at early stages of prion infection', *PLoS Pathogens*, 8(2). doi: 10.1371/journal.ppat.1002538.

Caughey, B. *et al.* (1999) 'Methods for studying prion protein (PrP) metabolism and the formation of protease-resistant PrP in cell culture and cell-free systems: An update', *Applied Biochemistry and Biotechnology - Part B Molecular Biotechnology*, 13(1), pp. 45–55. doi: 10.1385/mb:13:1:45.

Caughey, B. *et al.* (2009) 'Getting a grip on prions: oligomers, amyloids and pathological membrane interactions', *Annual Review of Biochemistry*, 78, pp. 177–204. doi: 10.1146/annurev.biochem.78.082907.145410.Getting.

Caughey, B. and Race, R. E. (1992) 'Potent Inhibition of Scrapie-Associated PrP Accumulation by Congo Red', *Journal of Neurochemistry*, 59(2), pp. 768–771. doi: 10.1111/j.1471-4159.1992.tb09437.x.

Caughey, B. and Raymond, G. J. (1993) 'Sulfated polyanion inhibition of scrapie-associated PrP accumulation in cultured cells', *Journal of virology*, 67(2), pp. 643–650.

Centers for Disease Contol (1985) 'Fatal degenerative neurologic disease in patients who received pituitary-derived human growth hormone', *MMWR. Morbidity and Mortalilty Weekly Report*, 34(24), pp. 365–6.

Centers for Disease Control and Prevention (2019). doi:

10.1097/JOM.0000000000001045.

Cervenakova, L. *et al.* (2011) 'Fukuoka-1 strain of transmissible spongiform encephalopathy agent infects murine bone marrow-derived cells with features of mesenchymal stem cells', *Transfusion*, 51(8), pp. 1755–1768. doi: 10.1111/j.1537-2995.2010.03041.x.

Chabry, J. *et al.* (1999) 'Species-Independent Inhibition of Abnormal Prion Protein (PrP) Formation by a Peptide Containing a Conserved PrP Sequence', *Journal of Virology*, 73(8), pp. 6245–6250. doi: 10.1080/10584589808202090.

Chabry, J., Caughey, B. and Chesebro, B. (1998) 'Specific Inhibition of in Vitro Formation of Protease-resistant Prion Protein by Synthetic Peptides', *The Journal of Biological Chemistry*, 273(21), pp. 13203–13207.

Chen, S., Yadav, S. P. and Surewicz, W. K. (2010) 'Interaction between human prion protein and amyloid-β (Aβ) oligomers: Role of N-terminal residues', *Journal of Biological Chemistry*, 285(34), pp. 26377–26383. doi: 10.1074/jbc.M110.145516.

Cheng, Y. C. *et al.* (2016) 'Early and non-invasive detection of chronic wasting disease prions in elk feces by real-time quaking induced conversion', *PLoS ONE*, 11(11), pp. 1–18. doi: 10.1371/journal.pone.0166187.

Chesebro, B. (2003) 'Introduction to the transmissible spongiform encephalopathies or prion diseases.', *Br Med Bull*, 66, pp. 1–20. doi: 10.1093/bmb/dg66.001.

Choi, E. J. and Mayo, S. L. (2006) 'Generation and analysis of proline mutants in protein G', *Protein Engineering, Design and Selection*, 19(6), pp. 285–289. doi: 10.1093/protein/gzl007.

Clarke, M. . and Haig, D. . (1970) 'Evidence for the multiplication of scrapie agent in cell culture', *Nature*, 225, pp. 100–101.

Cobb, N. J. and Surewicz, W. K. (2009) 'Prion Diseases and their biochemical mechanisms', *Biochemistry*, 48(12), pp. 2574–2585. doi: 10.1038/jid.2014.371.

Colby, D. W. and Prusiner, S. B. (2011) 'Prions', *Cold Spring Harbor Perspectives in Biology*, 3, p. a006833. doi: 10.1016/B978-012373944-5.00200-5.

Coleman, B. M. *et al.* (2012) 'Prion-infected cells regulate the release of exosomes with distinct ultrastructural features', *FASEB Journal*, 26(10), pp. 4160–4173. doi: 10.1096/fj.11-202077.

Collinge, J. *et al.* (1996) 'Molecular analysis of prion strain variation and the etiology of nvCJD', *Nature*, 383, pp. 685–690.

Collinge, J. (2005) 'Molecular neurology of prion disease', *Journal of Neurology, Neurosurgery and Psychiatry*, 76(7), pp. 906–919. doi: 10.1136/jnnp.2004.048660.

Collinge, J. *et al.* (2007) 'A General Model of Prion Strains and Their Pathogenicity', *Science*, 318(November), pp. 930–936. doi: 10.1126/science.1138718.

Collinge, J. *et al.* (2009) 'Safety and efficacy of quinacrine in human prion disease (PRION-1 study): a patient-preference trial', *The Lancet Neurology*. Elsevier Ltd, 8(4), pp. 334–344. doi: 10.1016/S1474-4422(09)70049-3.

Conde-Vancells, J. and Falcon-Perez, J. M. (2012) 'Isolation of urinary exosomes from animal models to unravel noninvasive disease biomarkers', *Methods in Molecular Biology*, 909(4), pp. 321–340. doi: 10.1007/978-1-61779-959-4_21.

Corbett, G. T. *et al.* (2020) 'PrP is a central player in toxicity mediated by soluble aggregates of neurodegeneration-causing proteins', *Acta Neuropathologica*. Springer Berlin Heidelberg, 139(3), pp. 503–526. doi: 10.1007/s00401-019-02114-9.

Corsaro, A. *et al.* (2002) 'Expression in E. coli and purification of recombinant fragments of wild type and mutant human prion protein', *Neurochemistry International*, 41(1), pp. 55–63. doi: 10.1016/S0197-0186(01)00137-1.

Courageot, M. P. *et al.* (2008) 'A cell line infectible by prion strains from different species', *Journal of General Virology*, 89(1), pp. 341–347. doi: 10.1099/vir.0.83344-0.

Cronier, S. *et al.* (2007) 'Prion Strain- and Species-Dependent Effects of Antiprion Molecules in Primary Neuronal Cultures', *Journal of Virology*, 81(24), pp. 13794–13800. doi: 10.1128/jvi.01502-07.

Cronier, S., Laude, H. and Peyrin, J. M. (2004) 'Prions can infect primary cultured neurons and astrocytes and promote neuronal cell death', *Proceedings of the National Academy of Sciences of the United States of America*, 101(33), pp. 12271–12276. doi: 10.1073/pnas.0402725101.

Cunningham, A. A. *et al.* (2004) 'Distribution of bovine spongiform encephalopathy in greater kudu (Tragelaphus strepsiceiros)', *Emerging Infectious Diseases*, 10(6), pp. 1044–1049. doi: 10.3201/eid1006.030615.

Davies, G. A. *et al.* (2006) 'Prion diseases and gastrointestinal tract', *Canadian Journal of Gastroenterology*, 20(1), pp. 18–24. doi: 10.1155/2006/184528.

DEFRA (2001) 'National Scrapie Plan for Great Britain', 1(July), pp. 1–28.

Denkers, N. D. *et al.* (2013) 'Aerosol Transmission of Chronic Wasting Disease in White-Tailed Deer', *Journal of Virology*, 87(3), pp. 1890–1892. doi: 10.1128/JVI.02852-12.

Denkers, N. D., Telling, G. C. and Hoover, E. A. (2011) 'Minor Oral Lesions Facilitate Transmission of Chronic Wasting Disease', *Journal of Virology*, 85(3), pp. 1396–1399. doi: 10.1128/JVI.01655-10.

Doh-ura, K., Iwaki, T. and Caughey, B. (2000) 'Lysosomotropic Agents and Cysteine

Protease Inhibitors Inhibit Scrapie-Associated Prion Protein Accumulation', *Journal of Virology*, 74(10), pp. 4894–4897.

Donne, D. *et al.* (1997) 'Structure of the recombinant full-length hamster prion protein PrP(29-231): the N terminus is highly flexible.', *Proceedings of the National Academy of Sciences of the United States of America*, 94(25), pp. 13452–7. doi: 10.1073/pnas.94.25.13452.

Dyer, C. (2018) 'British man with CJD gets experimental treatment in world first', *BMJ (Clinical research ed.)*, 363(October), p. k4608. doi: 10.1136/bmj.k4608.

Eghiaian, F. *et al.* (2004) 'Insight into the PrPc → PrPSc conversion from the structures of antibody-bound ovine prion scrapie-susceptibility variants', *Proceedings of the National Academy of Sciences of the United States of America*, 101(28), pp. 10254–10259. doi: 10.1073/pnas.0400014101.

Enari, M., Flechsig, E. and Weissmann, C. (2001) 'Scrapie prion protein accumulation by scrapie-infected neuroblastoma cells abrogated by exposure to a prion protein antibody.', *Proceedings of the National Academy of Sciences of the United States of America*, 98(16), pp. 9295–9299. doi: 10.1073/pnas.151242598.

Ersdal, C. *et al.* (2003) 'Accumulation of pathogenic prion protein (PrPSc) in nervous and lymphoid tissues of sheep with subclinical scrapie', *Veterinary Pathology*, 40(2), pp. 164–174. doi: 10.1354/vp.40-2-164.

Fairfoul, G. *et al.* (2016) 'Alpha-synuclein RT-QuIC in the CSF of patients with alpha-synucleinopathies', *Annals of Clinical and Translational Neurology*, 3(10), pp. 812–818. doi: 10.1002/acn3.338.

Falanga, P. B. *et al.* (2006) 'Selection of ovine PrP high-producer subclones from a transfected epithelial cell line', *Biochemical and Biophysical Research Communications*, 340(1), pp. 309–317. doi: 10.1016/j.bbrc.2005.11.153.

Fediaevsky, A. *et al.* (2009) 'A case-control study on the origin of atypical scrapie in sheep, France', *Emerging Infectious Diseases*, 15(5), pp. 710–718. doi: 10.3201/eid1505.081119.

Féraudet, C. *et al.* (2005) 'Screening of 145 anti-PrP monoclonal antibodies for their capacity to inhibit PrPSc replication in infected cells', *Journal of Biological Chemistry*, 280(12), pp. 11247–11258. doi: 10.1074/jbc.M407006200.

Ferreira, D. G. *et al.* (2017) 'α-synuclein interacts with PrP C to induce cognitive impairment through mGluR5 and NMDAR2B', *Nature Neuroscience*, 20(11), pp. 1569–1579. doi: 10.1038/nn.4648.

Fevrier, B. *et al.* (2004) 'Cells release prions in association with exosomes', *Proceedings of the National Academy of Sciences of the United States of America*, 101(26), pp.

9683–9688. doi: 10.1073/pnas.0308413101.

Fluharty, B. R. *et al.* (2013) 'An N-terminal fragment of the prion protein binds to amyloid-β oligomers and inhibits their neurotoxicity in vivo', *Journal of Biological Chemistry*, 288(11), pp. 7857–7866. doi: 10.1074/jbc.M112.423954.

Follet, J. *et al.* (2002) 'PrP Expression and Replication by Schwann Cells: Implications in Prion Spreading', *Journal of Virology*, 76(5), pp. 2434–2439. doi: 10.1128/jvi.76.5.2434-2439.2002.

Forloni, G. *et al.* (2013) 'Therapy in prion diseases.', *Current Topics in Medicinal Chemistry*, 13(19), pp. 2465–76. doi: CTMC-EPUB-56317 [pii].

Forloni, G. *et al.* (2015) 'Preventive study in subjects at risk of fatal familial insomnia: Innovative approach to rare diseases', *Prion*, 9(2), pp. 75–79. doi: 10.1080/19336896.2015.1027857.

Forno, L. S. (1995) 'Neuropathology of Parkinson's Disease', *Journal of Neuropathology and Experimental Neurology*, 55(3), pp. 259–272. Available at: http://www.ghbook.ir/index.php?name=های رسانه و فرهنگ نوین&option=com_dbook&task=readonline&book_id=13650&page=73&chkhashk=ED9C9491B4&Itemid=218&lang=fa&tmpl=component.

Foster, J. D. and Dickinson, A. G. (1988) 'The unusual properties of CH1641, a sheep-passaged isolate of scrapie.', *Veterinary Record*, 123(1), pp. 5–8.

Frootan, F. *et al.* (2012) 'Prion protein coding gene (prnp) variability in sheep from turkey and Iran', *Biochemical Genetics*, 50(3–4), pp. 277–284. doi: 10.1007/s10528-011-9470-4.

Funke, S. A. and Willbold, D. (2012) 'Peptides for Therapy and Diagnosis of Alzheimer's Disease', *Current Pharmaceutical Design*, 18(6), pp. 755–767. doi: 10.2174/138161212799277752.

Gale, P. and Roberts, H. (2018) 'Update on Chronic Wasting Disease in Europe', (April), pp. 1–4.

Gambetti, P. *et al.* (2008) 'A Novel Human Disease with Abnormal Prion Protein Sensitive to Protease', *Annals of Neurology*, 63(6), pp. 697–708. doi: 10.1002/ana.21420.A.

Gasset, M. *et al.* (1992) 'Predicted a-helical regions of the prion protein when synthesized as peptides form amyloid (scrapie/13-sheet/proteln secondary structure/amylold flbrils)', *Biochemistry*, 89(November), pp. 10940–10944. Available at: https://www.pnas.org/content/pnas/89/22/10940.full.pdf.

Genovesi, S. *et al.* (2007) 'Direct detection of soil-bound prions', *PLoS ONE*, 2(10), pp. 1–6. doi: 10.1371/journal.pone.0001069.

Georgakis, N. *et al.* (2020) 'Determination of Half-Maximal Inhibitory Concentration of an Enzyme Inhibitor', in *Targeting Enzymes for Pharmaceutical Development*, pp. 41–46.

Georgsson, G., Sigurdarson, S. and Brown, P. (2006) 'Infectious agent of sheep scrapie may persist in the environment for at least 16 years', *Journal of General Virology*, 87(12), pp. 3737–3740. doi: 10.1099/vir.0.82011-0.

Gerdes, H. H. and Carvalho, R. N. (2008) 'Intercellular transfer mediated by tunneling nanotubes', *Current Opinion in Cell Biology*, 20(4), pp. 470–475. doi: 10.1016/j.ceb.2008.03.005.

Geschwind, M. D. *et al.* (2013) 'Quinacrine treatment trial for sporadic creutzfeldt-Jakob disease', *Neurology*, 81(23), pp. 2015–2023. doi: 10.1212/WNL.0b013e3182a9f3b4.

Giaccone, G. and Moda, F. (2020) 'PMCA Applications for Prion Detection in Peripheral Tissues of Patients with Variant Creutzfeldt-Jakob Disease', *Biomolecules*, 10(3). doi: 10.3390/biom10030405.

Giasson, B. I. *et al.* (2003) 'Initiation and synergistic fibrillization of tau and alpha-synuclein', *Science*, 300(5619), pp. 636–640. doi: 10.1126/science.1082324.

Gibbs, C. *et al.* (1985) 'Clinical and pathological features and laboratory confirmation of Creutzfeldt-Jakob disease in a recipient of pituitary-derived human growth hormone.', *N Engl J Med*, 313, pp. 734–738.

Gilch, S. *et al.* (2003) 'Polyclonal anti-PrP auto-antibodies induced with dimeric PrP interfere efficiently with PrPSc propagation in prion-infected cells', *Journal of Biological Chemistry*, 278(20), pp. 18524–18531. doi: 10.1074/jbc.M210723200.

Glatzel, M. *et al.* (2001) 'Sympathetic innervation of lymphoreticular organs is rate limiting for prion neuroinvasion', *Neuron*, 31(1), pp. 25–34. doi: 10.1016/S0896-6273(01)00331-2.

Glatzel, M. and Aguzzi, A. (2000) 'Peripheral pathogenesis of prion diseases', *Microbes and Infection*, 2(6), pp. 613–619. doi: 10.1016/S1286-4579(00)00364-6.

Glenner, G. G. and Wong, C. W. (1984) 'Alzheimer's disease: Initial report of the purification and characterization of a novel cerebrovascular amyloid protein', *Biochemical and Biophysical Research Communications*, 120(3), pp. 885–890. doi: 10.1016/S0006-291X(84)80190-4.

Goldfarb, L. G. *et al.* (1991) 'Transmissible familial Creutzfeldt-Jakob disease associated with five, seven, and eight extra octapeptide coding repeats in the PRNP gene', *Proceedings of the National Academy of Sciences of the United States of America*, 88(23), pp. 10926–10930. doi: 10.1073/pnas.88.23.10926.

Goldmann, W. *et al.* (1990) 'Two alleles of a neural protein gene linked to scrapie in

sheep.', *Proceedings of the National Academy of Sciences of the United States of America*, 87(7), pp. 2476–80. doi: 10.1073/pnas.87.7.2476.

Goldmann, W. *et al.* (1994) 'PrP genotype and agent effects in scrapie: Change in allelic interaction with different isolates of agent in sheep, a natural host of scrapie', *Journal of General Virology*, 75(5), pp. 989–995. doi: 10.1099/0022-1317-75-5-989.

Goldmann, W. *et al.* (2005) 'Frequencies of PrP gene haplotypes in British sheep flocks and the implications for breeding programmes', *Journal of Applied Microbiology*, 98(6), pp. 1294–1302. doi: 10.1111/j.1365-2672.2005.02568.x.

Goldmann, W. (2008) 'PrP genetics in ruminant transmissible spongiform encephalopathies', *Veterinary Research*, 39(4). doi: 10.1051/vetres:2008010.

Goldmann, W. *et al.* (2011) 'Caprine prion gene polymorphisms are associated with decreased incidence of classical scrapie in goat herds in the United Kingdom', *Veterinary Research*, 42(1), pp. 1–8. doi: 10.1186/1297-9716-42-110.

González, L. *et al.* (2005) 'Phenotype of disease-associated PrP accumulation in the brain of bovine spongiform encephalopathy experimentally infected sheep', *Journal of General Virology*, 86(3), pp. 827–838. doi: 10.1099/vir.0.80299-0.

González, L., Martin, S. and Jeffrey, M. (2003) 'Distinct profiles od PrPd immunoreactivity in the brain of scrapie- and BSE-infected sheep: Implications for differential cell targetting and PrP processing', *Journal of General Virology*, 84(5), pp. 1339–1350. doi: 10.1099/vir.0.18800-0.

Goold, R. *et al.* (2011) 'Rapid cell-surface prion protein conversion revealed using a novel cell system', *Nature Communications*, 2(1). doi: 10.1038/ncomms1282.

Gossert, A. D. *et al.* (2005) 'Prion protein NMR structures of elk and of mouse/elk hybrids', *Proceedings of the National Academy of Sciences of the United States of America*, 102(3), pp. 646–650. doi: 10.1073/pnas.0409008102.

Gough, K., Baker, C., *et al.* (2015) 'Circulation of prions within dust on a scrapie affected farm', *Veterinary Research*. ???, 46(1), pp. 10–13. doi: 10.1186/s13567-015-0176-1.

Gough, K., Rees, H., *et al.* (2015) 'Methods for Differentiating Prion Types in Food-Producing Animals', *Biology*, 4(4), pp. 785–813. doi: 10.3390/biology4040785.

Gough, K. C. *et al.* (2012) 'The Oral Secretion of Infectious Scrapie Prions Occurs in Preclinical Sheep with a Range of PRNP Genotypes', *Journal of Virology*, 86(1), pp. 566–571. doi: 10.1128/JVI.05579-11.

Gough, K. C., Bishop, K. and Maddison, B. C. (2014) 'Highly sensitive detection of small ruminant bovine spongiform encephalopathy within transmissible spongiform encephalopathy mixes by serial protein misfolding cyclic amplification', *Journal of Clinical Microbiology*, 52(11), pp. 3863–3868. doi: 10.1128/JCM.01693-14.

Gough, K. C. and Maddison, B. C. (2010) 'Prion transmission: Prion excretion and occurrence in the environment', *Prion*, 4(4), pp. 275–282. doi: 10.4161/pri.4.4.13678.

Gousset, K. *et al.* (2009) 'Prions hijack tunnelling nanotubes for intercellular spread', *Nature Cell Biology*, 11(3), pp. 328–336. doi: 10.1038/ncb1841.

Govaerts, C. *et al.* (2004) 'Evidence for assembly of prions with left-handed β-helices into trimers', *Proceedings of the National Academy of Sciences of the United States of America*, 101(22), pp. 8342–8347. doi: 10.1073/pnas.0402254101.

Grassmann, A. *et al.* (2013) *Cellular aspects of prion replication in vitro*, *Viruses*. doi: 10.3390/v5010374.

Grigoriev, V. *et al.* (1999) 'Submicroscopic immunodetection of PrP in the brain of a patient with a new-variant of Creutzfeldt-Jakob disease', *Neuroscience Letters*, 264(1–3), pp. 57–60. doi: 10.1016/S0304-3940(99)00146-9.

Groschup, M. H., Harmeyer, S. and Pfaff, E. (1997) 'Antigenic features of prion proteins of sheep and of other mammalian species', *Journal of Immunological Methods*, 207(1), pp. 89–101. doi: 10.1016/S0022-1759(97)00121-X.

Groveman, B. R. *et al.* (2017) 'Role of the central lysine cluster and scrapie templating in the transmissibility of synthetic prion protein aggregates', *PLoS Pathogens*, 13(9), pp. 1–24. doi: 10.1371/journal.ppat.1006623.

Groveman, B. R. *et al.* (2019) 'Sporadic Creutzfeldt-Jakob disease prion infection of human cerebral organoids', *Acta neuropathologica communications*. Acta Neuropathologica Communications, 7(1), p. 12. doi: 10.1186/s40478-019-0742-2.

Grundke-iqbals, I. *et al.* (1986) 'Microtubule-associated Protein Tau', *The Journal of Biological Chemistry*, 261(13), pp. 6084–6089.

Gu, Y. *et al.* (2003) 'Identification of cryptic nuclear localization signals in the prion protein', *Neurobiology of Disease*, 12(2), pp. 133–149. doi: 10.1016/S0969-9961(02)00014-1.

Gu, Y., Oyama, F. and Ihara, Y. (2002) 'τ Is Widely Expressed in Rat Tissues', *Journal of Neurochemistry*, 67(3), pp. 1235–1244. doi: 10.1046/j.1471-4159.1996.67031235.x.

Guan, F. *et al.* (2011) 'Polymorphisms of the prion protein gene and their effects on litter size and risk evaluation for scrapie in Chinese Hu sheep', *Virus Genes*, 43(1), pp. 147–152. doi: 10.1007/s11262-011-0609-5.

Guo, J. L. and Lee, V. M. Y. (2014) 'Cell-to-cell transmission of pathogenic proteins in neurodegenerative diseases', *Nature Medicine*. Nature Publishing Group, 20(2), pp. 130–138. doi: 10.1038/nm.3457.

Hachiya, N. S. *et al.* (2005) 'Mitochondrial localization of cellular prion protein (PrPC) invokes neuronal apoptosis in aged transgenic mice overexpressing PrPC', *Neuroscience Letters*, 374(2), pp. 98–103. doi: 10.1016/j.neulet.2004.10.044.

Hadlow, W. J. (1959) 'Scrapie and Kuru', *Lancet*, 274(7097), pp. 289–290.

Hadlow, W. J. *et al.* (1980) 'Brain tissue from persons dying of creutzfeldt-jakob disease causes scrapie-like encephalopathy in goats', *Annals of Neurology*, 8(6), pp. 628–631. doi: 10.1002/ana.410080615.

Hadlow, W. J., Race, R. E. and Kennedy, R. C. (1987) 'Temporal distribution of transmissible mink encephalopathy virus in mink inoculated subcutaneously', *Journal of Virology*, 61(10), pp. 3235–3240.

Haïk, S. *et al.* (2000) 'Dementia with Lewy bodies in a neuropathologic series of suspected Creutzfeldt-Jakob disease', *Neurology*, 55(9), pp. 1401–1404. doi: 10.1212/WNL.55.9.1401.

Haïk, S. *et al.* (2002) 'Alpha-synuclein-immunoreactive deposits in human and animal prion diseases', *Acta Neuropathologica*, 103(5), pp. 516–520. doi: 10.1007/s00401-001-0499-z.

Haïk, S. *et al.* (2003) 'The sympathetic nervous system is involved in variant Creutzfeldt-Jakob disease', *Nature Medicine*, 9(9), pp. 1121–1123. doi: 10.1038/nm922.

Haïk, S. *et al.* (2014) 'Doxycycline in Creutzfeldt-Jakob disease: A phase 2, randomised, double-blind, placebo-controlled trial', *The Lancet Neurology*, 13(2), pp. 150–158. doi: 10.1016/S1474-4422(13)70307-7.

Haire, L. F. *et al.* (2004) 'The Crystal Structure of the Globular Domain of Sheep Prion Protein', *Journal of Molecular Biology*, 336(5), pp. 1175–1183. doi: 10.1016/j.jmb.2003.12.059.

Haley, N. J. *et al.* (2009) 'Detection of CWD prions in urine and saliva of deer by transgenic mouse bioassay', *PLoS ONE*, 4(3). doi: 10.1371/journal.pone.0004848.

Haley, N. J. *et al.* (2013) 'Prion-seeding activity in cerebrospinal fluid of deer with chronic wasting disease', *PLoS ONE*, 8(11), pp. 1–12. doi: 10.1371/journal.pone.0081488.

Haley, N. J. *et al.* (2014) 'Detection of chronic wasting disease in the lymph nodes of free-ranging cervids by real-time quaking-induced conversion', *Journal of Clinical Microbiology*, 52(9), pp. 3237–3243. doi: 10.1128/JCM.01258-14.

Haley, N. J. *et al.* (2016) 'Antemortem detection of chronic wasting disease prions in nasal brush collections and rectal biopsies from white-tailed deer by real time quaking-induced conversion.', *J Clin Microbiol*, 54(4). doi: 10.1128/JCM.02699-15.

Haley, N. J. and Richt, J. A. (2017) 'Evolution of diagnostic tests for chronic wasting disease, a naturally occurring prion disease of cervids', *Pathogens*, 6(3). doi: 10.3390/pathogens6030035.

Han, J. *et al.* (2006) 'Study on interaction between microtubule associated protein tau and prion protein', *Science in China, Series C: Life Sciences*, 49(5), pp. 473–479. doi: 10.1007/s11427-006-2019-9.

Hannaoui, S. *et al.* (2014) 'Cycline efficacy on the propagation of human prions in primary cultured neurons is strain-specific', *Journal of Infectious Diseases*, 209(7), pp. 1144–1148. doi: 10.1093/infdis/jit623.

Harris, D. A. (1999) 'Cellular biology of prion diseases', *Clinical Microbiology Reviews*, 12(3), pp. 429–444. doi: 10.1128/cmr.12.3.429.

Hastings, J. *et al.* (2016) 'ChEBI in 2016: Improved services and an expanding collection of metabolites', *Nucleic Acids Research*, 44(D1), pp. D1214–D1219. doi: 10.1093/nar/gkv1031.

Henderson, D. M. *et al.* (2013) 'Rapid antemortem detection of CWD prions in deer saliva.', *PloS one*, 8(9), pp. 1–12. doi: 10.1371/journal.pone.0074377.

Herbst, A. *et al.* (2013) 'Infectious Prions Accumulate to High Levels in Non Proliferative C2C12 Myotubes', *PLoS Pathogens*, 9(11). doi: 10.1371/journal.ppat.1003755.

Herva, M. E. *et al.* (2014) 'Anti-amyloid Compounds Inhibit alpha-Synuclein Aggregation Induced by Protein Misfolding Cyclic Amplification (PMCA)', *Journal of Biological Chemistry*, 289(17), pp. 11897–11905. doi: 10.1074/jbc.M113.542340.

Higgins, D. G., Thompson, J. D. and Gibson, T. J. (1996) 'Using CLUSTAL for multiple sequence alignments', *Methods in Enzymology*, 266(1988), pp. 383–400. doi: 10.1016/s0076-6879(96)66024-8.

Hill, A. F. *et al.* (1998) 'Molecular screening of sheep for bovine spongiform encephalopathy', *Neuroscience Letters*, 255(3), pp. 159–162. doi: 10.1016/S0304-3940(98)00736-8.

Ho, A. and Sudhof, T. C. (2004) 'Binding of F-spondin to amyloid- precursor protein: A candidate amyloid- precursor protein ligand that modulates amyloid- precursor protein cleavage', *Proceedings of the National Academy of Sciences*, 101(8), pp. 2548–2553. doi: 10.1073/pnas.0308655100.

Hölscher, C., Delius, H. and Bürkle, A. (1998) 'Overexpression of Nonconvertible PrPcΔ114–121 in Scrapie-Infected Mouse Neuroblastoma Cells Leads to trans-Dominant Inhibition of Wild-Type PrPSc Accumulation', *Journal of Virology*, 72(2), pp. 1153–1159. doi: 10.1128/jvi.72.2.1153-1159.1998.

Hoover, C. E. *et al.* (2017) 'Pathways of Prion Spread during Early Chronic Wasting

Disease in Deer', *Journal of Virology*, 91(10), pp. e00077-17. doi: 10.1128/JVI.00077-17.

Hope, J. *et al.* (1986) 'The major polypeptide of scrapie-associated fibrils (SAF) has the same size, charge distribution and N-terminal protein sequence as predicted for the normal brain protein (PrP).', *The EMBO journal*, 5(10), pp. 2591–7. Available at: http://www.pubmedcentral.nih.gov/articlerender.fcgi?artid=1167157&tool=pmcentrez&rendertype=abstract.

Horie, M. *et al.* (2014) 'Evaluation of cellular effects of silicon dioxide nanoparticles', *Toxicology Mechanisms and Methods*, 24(3), pp. 196–203. doi: 10.3109/15376516.2013.879505.

Horiuchi, M. *et al.* (2000) 'Interactions between heterologous forms of prion protein: Binding, inhibition of conversion, and species barriers', *Proceedings of the National Academy of Sciences*, 97(11), pp. 5836–5841. doi: 10.1073/pnas.110523897.

Hsiao, K. *et al.* (1989) 'Linkage of a prion protein missense variant to Gerstmann-Straussler syndrome', *Nature*, 338(March), pp. 342–345.

Hsiao, K. *et al.* (1992) 'Mutant prion proteins in Gerstmann-Sträussler-Scheinker disease with neurofibrillary tangles', *Nature Genetics*, 1, pp. 68–71. doi: 10.1038/ng0492-68.

Hu, N. W. *et al.* (2018) 'Extracellular Forms of Aβ and Tau from iPSC Models of Alzheimer's Disease Disrupt Synaptic Plasticity', *Cell Reports*. ElsevierCompany., 23(7), pp. 1932–1938. doi: 10.1016/j.celrep.2018.04.040.

Hunter, N. (2003) 'Scrapie and experimental BSE in sheep', *British Medical Bulletin*, 66(April), pp. 171–183. doi: 10.1093/bmb/66.1.171.

Ironside, J. W. and Bell, J. E. (1997) 'Florid plaques and new variant Creutzfeldt-Jakob disease [3]', *Lancet*, 350(9089), p. 1475. doi: 10.1016/S0140-6736(05)64239-0.

Ishizawa, T. *et al.* (2003) 'Colocalization of tau and α-synuclein epitopes in Lewy bodies', *Journal of Neuropathology and Experimental Neurology*, 62(4), pp. 389–397. doi: 10.1093/jnen/62.4.389.

Iwamaru, Y. *et al.* (2017) 'Chronic wasting disease prion infection of differentiated neurospheres', *Prion*, 11(4), pp. 277–283. doi: 10.1080/19336896.2017.1336273.

Jackson, G. S. *et al.* (1999) 'Multiple folding pathways for heterologously expressed human prion protein', *Biochimica et Biophysica Acta - Protein Structure and Molecular Enzymology*, 1431(1), pp. 1–13. doi: 10.1016/S0167-4838(99)00038-2.

Jacobs, J. G. *et al.* (2007) 'Molecular discrimination of atypical bovine spongiform encephalopathy strains from a geographical region spanning a wide area in Europe', *Journal of Clinical Microbiology*, 45(6), pp. 1821–1829. doi: 10.1128/JCM.00160-07.

Jacobs, J. G. *et al.* (2011) 'Differentiation of ruminant transmissible spongiform encephalopathy isolate types, including bovine spongiform encephalopathy and CH1641 scrapie', *Journal of General Virology*, 92(1), pp. 222–232. doi: 10.1099/vir.0.026153-0.

Jacobson, K. H., Kuech, T. R. and Pedersen, J. A. (2013) 'Attachment of Pathogenic Prion Protein to Model Oxide Surfaces Kurt', *Environmental Science and Technology*, 47(13), pp. 6925–6934. doi: 10.1038/jid.2014.371.

James, T. L. *et al.* (1997) 'Solution structure of a 142-residue recombinant prion protein corresponding to the infectious fragment of the scrapie isoform', *Proceedings of the National Academy of Sciences of the United States of America*, 94(19), pp. 10086–10091. doi: 10.1073/pnas.94.19.10086.

Jarret, J. T., Berger, E. P. and Lansbury, P. T. ~Jr. (1993) 'The carboxy terminus of β amyloid protein is critical for the seeding of amyloid formation: Implications for the pathogenesis of Alzheimer's disease', *Biochem.*, 32, pp. 4693–4697.

Jarrett, J. T. and Lansburry, P. T. (1993) 'Seeding "one dimensional cristallization" of amyloid: a pathogenic mechanism in Alzheimer's disease and scrapie?', *Cell*, 73, pp. 1055–1058. doi: 10.1016/0092-8674(93)90635-4.

Jeffrey, M. *et al.* (2001) 'Differential diagnosis of infections with the bovine spongiform encephalopathy (BSE) and scrapie agents in sheep', *Journal of Comparative Pathology*, 125(4), pp. 271–284. doi: 10.1053/jcpa.2001.0499.

Jeffrey, M., Martin, S., *et al.* (2006) 'Immunohistochemical Features of PrPd Accumulation in Natural and Experimental Goat Transmissible Spongiform Encephalopathies', *Journal of Comparative Pathology*, 134(2–3), pp. 171–181. doi: 10.1016/j.jcpa.2005.10.003.

Jeffrey, M., González, L., *et al.* (2006) 'Ovine infection with the agents of scrapie (CH1641 isolate) and bovine spongiform encephalopathy: Immunochemical similarities can be resolved by immunohistochemistry', *Journal of Comparative Pathology*, 134(1), pp. 17–29. doi: 10.1016/j.jcpa.2005.06.005.

John, T. R., Schätzl, H. M. and Gilch, S. (2013) 'Early detection of chronic wasting disease prions in urine of pre-symptomatic deer by real-time quaking-induced conversion assay', *Prion*, 7(3), pp. 253–258. doi: 10.4161/pri.24430.

Johnson, C. *et al.* (2003) 'Prion Protein Gene Heterogeneity in Free-Ranging White-Tailed Deer Within the Chronic Wasting Disease Affected Region of Wisconsin', *Journal of Wildlife Diseases*, 39(3), pp. 576–581. doi: 10.7589/0090-3558-39.3.576.

Johnson, C. J. *et al.* (2006) 'Prions adhere to soil minerals and remain infectious', *PLoS Pathogens*, 2(4), pp. 296–302. doi: 10.1111/j.1745-5871.2006.00403.x.

Jung, B. C. *et al.* (2017) 'Amplification of distinct α-synuclein fibril conformers through protein misfolding cyclic amplification', *Experimental and Molecular Medicine*, 49(4), pp. 1–8. doi: 10.1038/emm.2017.1.

Kang, H. E. *et al.* (2017) 'Prion Diagnosis: Application of Real-Time Quaking-Induced Conversion', *BioMed Research International*, 2017. doi: 10.1155/2017/5413936.

Kanu, N. *et al.* (2002) 'Transfer of scrapie prion infectivity by cell contact in culture', *Current Biology*, 12(7), pp. 523–530. doi: 10.1016/S0960-9822(02)00722-4.

Katorcha, E. *et al.* (2017) 'Cross-seeding of prions by aggregated alpha-synuclein leads to transmissible spongiform encephalopathy', *PLoS Pathog*, 13(8), p. e1006563. doi: 10.1371/journal.ppat.1006563.

Kayed, R. *et al.* (2003) 'Common structure of soluble amyloid oligomers implies common mechanism of pathogenesis', *Science*, 300(5618), pp. 486–489. doi: 10.1126/science.1079469.

Van Keulen, L. J. M., Vromans, M. E. W. and Van Zijderveld, F. G. (2002) 'Early and late pathogenesis of natural scrapie infection in sheep', *Apmis*, 110(1), pp. 23–32. doi: 10.1034/j.1600-0463.2002.100104.x.

Kim, J.-I. *et al.* (2009) 'The role of glycophospatidylinositol anchor in the amplification of the scrapie isoform of prion protein in vitro', *FEBS*, 583(22), pp. 3671–3675. doi: 10.1111/j.1743-6109.2008.01122.x.Endothelial.

Kimberlin, R. H., Hall, S. M. and Walker, C. A. (1983) 'Pathogenesis of mouse scrapie. Evidence for direct neural spread of infection to the CNS after injection of sciatic nerve', *Journal of the Neurological Science*, 61, pp. 315–325.

Kimple, M. E., Brill, A. L. and Pasker, R. L. (2013) 'Overview of affinity tags for protein purification', *Current Protocols in Protein Science*, (73), p. Unit-9.9. doi: 10.1002/0471140864.ps0909s73.

Kitamoto, T., Lizuka, R. and Tateishi, J. (1993) 'An amber mutation of prion protein in Gerstmann-Sträussler Syndrome with mutant PrP plaques', *Biochemical and Biophysical Research Communications*, pp. 525–531. doi: 10.1006/bbrc.1993.1447.

Kobayashi, A. *et al.* (2015) 'The influence of PRNP polymorphisms on human prion disease susceptibility: an update', *Acta Neuropathologica*. Springer Berlin Heidelberg, 130(2), pp. 159–170. doi: 10.1007/s00401-015-1447-7.

Koch, T. K. *et al.* (1985) 'Creutzfeldt–Jakob Disease in a Young Adult with Idiopathic Hypopituitarism — Possible Relation to the Administration of Cadaveric Human Growth Hormone', *New England Journal of Medicine*, 313, pp. 731–733.

Kocisko, D. A. *et al.* (1994) 'Cell-free formation of protease-resistant prion protein', *Letters to Nature*, 370, pp. 471–474.

Kocisko, D. A. *et al.* (2003) 'New inhibitors of scrapie-associated prion protein formation in a library of 2000 drugs and natural products.', *Journal of virology*, 77(19), pp. 10288–94. doi: 10.1128/JVI.77.19.10288.

Kocisko, D. A. *et al.* (2005) 'Comparison of protease-resistant prion protein inhibitors in cell cultures infected with two strains of mouse and sheep scrapie', *Neuroscience Letters*, 388(2), pp. 106–111. doi: 10.1016/j.neulet.2005.06.053.

Kocisko, D. and Caughey, B. (2006a) 'Mefloquine, an Antimalaria Drug with Antiprion Activity In Vitro, Lacks Activity In Vivo', *Journal of Virology*, 80(2), pp. 1044–1046. doi: 10.1128/JVI.80.2.1044.

Kocisko, D. and Caughey, B. (2006b) 'Searching for Anti-Prion Compounds: Cell-Based High-Throughput In Vitro Assays and Animal Testing Strategies', *Methods in Enzymology*, 412(06), pp. 223–234. doi: 10.1016/S0076-6879(06)12014-5.

Kondo, J. *et al.* (1988) 'The carboxyl third of tau is tightly bound to paired helical filaments', *Neuron*, 1(9), pp. 827–834. doi: 10.1016/0896-6273(88)90130-4.

Konold, T. *et al.* (2008) 'Evidence of scrapie transmission via milk', *BMC Veterinary Research*, 4, pp. 1–10. doi: 10.1186/1746-6148-4-14.

Konold, T. *et al.* (2015) 'Objects in Contact with Classical Scrapie Sheep Act as a Reservoir for Scrapie Transmission', *Frontiers in Veterinary Science*, 2(September), pp. 1–7. doi: 10.3389/fvets.2015.00032.

Koutsoumanis, K. *et al.* (2019) 'Update on chronic wasting disease (CWD) III', *EFSA Journal*, 17(11). doi: 10.2903/j.efsa.2019.5863.

Kovacs, G. G. *et al.* (2011) 'Genetic Creutzfeldt-Jakob disease associated with the E200K mutation: Characterization of a complex proteinopathy', *Acta Neuropathologica*, 121(1), pp. 39–57. doi: 10.1007/s00401-010-0713-y.

Kramm, C. *et al.* (2019) 'In Vitro detection of Chronic Wasting Disease (CWD) prions in semen and reproductive tissues of white tailed deer bucks (Odocoileus virginianus)', *PloS one*, 14(12), p. e0226560. doi: 10.1371/journal.pone.0226560.

Krejciova, Z. *et al.* (2017) 'Human stem cell-derived astrocytes replicate human prions in a PRNP genotype-dependent manner', *Journal of Experimental Medicine*, 214(12), pp. 3481–3495. doi: 10.1084/jem.20161547.

Kretzschmar, H. A. *et al.* (1986) 'Molecular Cloning of a Human Prion Protein cDNA', *Dna*, 5(4), pp. 315–324. doi: 10.1089/dna.1986.5.315.

Krüger, D. *et al.* (2009) 'Faecal shedding, alimentary clearance and intestinal spread of prions in hamsters fed with scrapie', *Veterinary Research*, 40(1). doi: 10.1051/vetres:2008042.

Ladogana, A. *et al.* (1995) 'Proteinase-resistant protein in human neuroblastoma cells infected with brain material from Creutzfeldt-Jakob patient', *The Lancet*, 345, pp. 594–595.

Lancaster, M. A. and Knoblich, J. A. (2014) 'Generation of Cerebral Organoids from Human Pluripotent Stem Cells', *Nature Protocols*, 9(10), pp. 2329–2340. doi: 10.1038/nprot.2014.158.Generation.

Langeveld, J. P. M. *et al.* (2006) 'Rapid and discriminatory diagnosis of scrapie and BSE in retro-pharyngeal lymph nodes of sheep', *BMC Veterinary Research*, 2, pp. 1–14. doi: 10.1186/1746-6148-2-19.

Laplanche, J. L. *et al.* (1999) 'Prominent psychiatric features and early onset in an inherited prion disease with a new insertional mutation in the prion protein gene', *Brain*, 122(12), pp. 2375–2386. doi: 10.1093/brain/122.12.2375.

Lau, J. L. and Dunn, M. K. (2018) 'Therapeutic peptides: Historical perspectives, current development trends, and future directions', *Bioorganic and Medicinal Chemistry*. The Authors, 26(10), pp. 2700–2707. doi: 10.1016/j.bmc.2017.06.052.

Laurén, J. *et al.* (2009) 'Cellular prion protein mediates impairment of synaptic plasticity by amyloid-β Oligomers', *Nature*, 457(7233), pp. 1128–1132. doi: 10.1038/nature07761.Cellular.

Lawson, V. A. *et al.* (2008) 'Mouse-adapted sporadic human Creutzfeldt-Jakob disease prions propagate in cell culture', *International Journal of Biochemistry and Cell Biology*, 40(12), pp. 2793–2801. doi: 10.1016/j.biocel.2008.05.024.

Lear, S. and Cobb, S. L. (2016) 'Pep-Calc.com: A set of web utilities for the calculation of peptide and peptoid properties and automatic mass spectral peak assignment', *Journal of Computer-Aided Molecular Design*. Springer International Publishing, 30(3), pp. 271–277. doi: 10.1007/s10822-016-9902-7.

Lee, J. *et al.* (2008) 'Adaptor protein sorting nexin 17 regulates amyloid precursor protein trafficking and processing in the early endosomes', *Journal of Biological Chemistry*, 283(17), pp. 11501–11508. doi: 10.1074/jbc.M800642200.

Lee, V. M.-Y., Goedert, M. and Trojanowski, J. Q. (2001) 'Neurodegenerative Tauopathies', *Annual Review of Neuroscience*, 24(1), pp. 1121–1159. doi: 10.1146/annurev.neuro.24.1.1121.

Levavasseur, E. *et al.* (2017) 'Detection and partial discrimination of atypical and classical bovine spongiform encephalopathies in cattle and primates using real-time quaking-induced conversion assay', *PLoS ONE*, 12(2), pp. 1–15. doi: 10.1371/journal.pone.0172428.

Li, S. *et al.* (1996) 'a-Helical , but not B-sheet , propensity of proline is determined by

peptide environment', *Proc. Natl. Acad. Sci. USA*, 93(June), pp. 6676–6681.

Liu, P.-P. *et al.* (2019) 'History and progress of hypotheses and clinical trials for Alzheimer's disease', *Signal Transduction and Targeted Therapy*. Springer US, 4(1). doi: 10.1038/s41392-019-0071-8.

Liu, T. *et al.* (2002) 'Intercellular transfer of the cellular prion protein', *Journal of Biological Chemistry*, 277(49), pp. 47671–47678. doi: 10.1074/jbc.M207458200.

Llewelyn, C. A. *et al.* (2004) 'Possible transmission of variant Creutzfeldt-Jakob disease by blood transfusion', *Lancet*, 363(9407), pp. 417–421. doi: 10.1016/S0140-6736(04)15486-X.

Lopez Garcia, F. *et al.* (2002) 'NMR structure of the bovine prion protein', *Proceedings of the National Academy of Sciences*, 97(15), pp. 8334–8339. doi: 10.1073/pnas.97.15.8334.

Luhken, G. *et al.* (2007) 'Epidemiological and genetical differences between classical and atypical scrapie cases', *Veterinary Research*, 38, pp. 65–80.

Maddison, B., Baker, C., *et al.* (2010) 'Environmental Sources of Scrapie Prions', *Journal of Virology*, 84(21), pp. 11560–11562. doi: 10.1128/JVI.01133-10.

Maddison, B., Rees, H., *et al.* (2010) 'Prions Are Secreted into the Oral Cavity in Sheep with Preclinical Scrapie', *The Journal of Infectious Diseases*, 201(11), pp. 1672–1676. doi: 10.1086/652457.

Maddison, B. *et al.* (2015) 'Incubation of ovine scrapie with environmental matrix results in biological and biochemical changes of PrPScover time', *Veterinary Research*, 46(1), pp. 1–6. doi: 10.1186/s13567-015-0179-y.

Maddison, B. C. *et al.* (2009) 'Prions Are Secreted in Milk from Clinically Normal Scrapie-Exposed Sheep', *Journal of Virology*, 83(16), pp. 8293–8296. doi: 10.1128/JVI.00051-09.

Maddison, B. C., Whitelam, G. C. and Gough, K. C. (2007) 'Cellular prion protein in ovine milk', *Biochemical and Biophysical Research Communications*, 353(1), pp. 195–199. doi: 10.1016/j.bbrc.2006.12.006.

Mahal, S. P. *et al.* (2007) 'Prion strain discrimination in cell culture: The cell panel assay', *Proceedings of the National Academy of Sciences of the United States of America*, 104(52), pp. 20908–20913. doi: 10.1073/pnas.0710054104.

Maiti, N. R. and Surewicz, W. K. (2001) 'The Role of Disulfide Bridge in the Folding and Stability of the Recombinant Human Prion Protein', *Journal of Biological Chemistry*, 276(4), pp. 2427–2431. doi: 10.1074/jbc.M007862200.

Makarava, N. and Baskakov, I. V. (2013) 'The Evolution of Transmissible Prions: The

Role of Deformed Templating', *PLoS Pathogens*, 9(12), pp. 1–3. doi: 10.1371/journal.ppat.1003759.

Mandal, P. K. *et al.* (2006) 'Interaction between Aβ peptide and α synuclein: Molecular mechanisms in overlapping pathology of Alzheimer's and Parkinson's in dementia with Lewy body disease', *Neurochemical Research*, 31(9), pp. 1153–1162. doi: 10.1007/s11064-006-9140-9.

Manson, J. *et al.* (1992) 'The prion protein gene: a role in mouse embryogenesis?', *Development (Cambridge, England)*, 115, pp. 117–122.

Manuelidis, L. *et al.* (2007) 'Cells infected with scrapie and Creutzfeld-Jakob disease agents produce intracellular 25-nm virus-like particles', *Proceedings of the National Academy of Sciences of the United States of America*, 104(6), pp. 1965–1970. doi: 10.1073/pnas.0610999104.

Masliah, E. *et al.* (2001) 'β-Amyloid peptides enhance α-synuclein accumulation and neuronal deficits in a transgenic mouse model linking Alzheimer's disease and Parkinson's disease', *Proceedings of the National Academy of Sciences of the United States of America*, 98(21), pp. 12245–12250. doi: 10.1073/pnas.211412398.

Masliah, E. *et al.* (2012) 'Prion infection promotes extensive accumulation of α-synuclein in aged human α-synuclein transgenic mice', *Prion*, 6(2), pp. 184–190. doi: 10.4161/pri.19806.

Massignan, T. *et al.* (2016) 'A cationic tetrapyrrole inhibits toxic activities of the cellular prion protein', *Scientific Reports*. Nature Publishing Group, 6(February), pp. 1–14. doi: 10.1038/srep23180.

Mastrianni, J. A. (2010) 'The genetics of prion diseases', *Genetics in Medicine*, 12(4), pp. 187–195. doi: 10.1097/GIM.0b013e3181cd7374.

Masujin, K. *et al.* (2016) 'Detection of Atypical H-Type Bovine Spongiform Encephalopathy and Discrimination of Bovine Prion Strains by Real-Time Quaking-Induced Conversion', *Journal of Clinical Microbiology*, 54(3), pp. 676–686. doi: 10.1128/JCM.02731-15.

Mathiason, C. K. *et al.* (2006) 'Infectious prions in the saliva and blood of deer with chronic wasting disease', *Science*, 314(October), pp. 133–136.

Mattei, V. *et al.* (2009) 'Paracrine diffusion of PrPc and propagation of prion infectivity by plasma membrane-derived microvesicles', *PLoS ONE*, 4(4). doi: 10.1371/journal.pone.0005057.

McCulloch, L. *et al.* (2011) 'Follicular dendritic cell-specific prion protein (PrP c) expression alone is sufficient to sustain prion infection in the spleen', *PLoS Pathogens*, 7(12). doi: 10.1371/journal.ppat.1002402.

McGuire, L. I. *et al.* (2016) 'Cerebrospinal fluid real-time quaking-induced conversion is a robust and reliable test for sporadic creutzfeldt–jakob disease: An international study', *Annals of Neurology*, 80(1), pp. 160–165. doi: 10.1002/ana.24679.

Mead, S. (2006) 'Prion disease genetics', *European Journal of Human Genetics*, 14(3), pp. 273–281. doi: 10.1038/sj.ejhg.5201544.

Mead, S., Lloyd, S. and Collinge, J. (2019) 'Genetic Factors in Mammalian Prion Diseases', *Annual Review of Genetics*, 53(1), pp. 117–147. doi: 10.1146/annurev-genet-120213-092352.

Medori, R. *et al.* (1992) 'Fatal Familial Insomnia, a prion disease with a mutation at codon 178 of the prion protein fene', *N Engl J Med*, 326(7), pp. 444–479. doi: 10.1016/j.physbeh.2017.03.040.

Medori, R. and Tritschler, H. J. (1993) 'Prion protein gene analysis in three kindreds with fatal familial insomnia (FFI): Codon 178 mutation and codon 129 polymorphism', *American Journal of Human Genetics*, 53(4), pp. 822–827.

Mehlhorn, I. *et al.* (1996) 'High-level expression and characterization of a purified 142-residue polypeptide of the prion protein', 35(17), pp. 5528–5537.

van der Merwe, J. *et al.* (2015) 'The standard scrapie cell assay: Development, utility and prospects', *Viruses*, 7(1), pp. 180–198. doi: 10.3390/v7010180.

Meydan, H. *et al.* (2012) 'Prion protein gene polymorphism and genetic risk evaluation for scrapie in all Turkish native sheep breeds', *Virus Genes*, 45(1), pp. 169–175. doi: 10.1007/s11262-012-0744-7.

Meyer, V. *et al.* (2014) 'Amplification of Tau Fibrils from Minute Quantities of Seeds', *Biochemistry*, 53(36), pp. 5804–5809. doi: 10.1021/bi501050g.

Milhavet, O. *et al.* (2006) 'Neural Stem Cell Model for Prion Propagation', *Stem Cells*, 24(10), pp. 2284–2291. doi: 10.1634/stemcells.2006-0088.

Miller, M. W. *et al.* (2004) 'Environmental sources of prion transmission in mule deer', *Emerging Infectious Diseases*, 10(6), pp. 1003–1006. doi: 10.3201/eid1006.040010.

Miller, M. W. and Williams, E. S. (2003) 'Horizontal prion transmission in mule deer', *Nature*, 425(6953), pp. 35–36. doi: 10.1038/425035a.

Mironov, A. *et al.* (2003) 'Cytosolic prion protein in neurons.', *The Journal of neuroscience : the official journal of the Society for Neuroscience*, 23(18), pp. 7183–7193. doi: 23/18/7183 [pii].

Miyazawa, K., Emmerling, K. and Manuelidis, L. (2011) 'Replication and spread of CJD, kuru and scrapie agents in vivo and in cell culture', *Virulence*, 2(3), pp. 188–199. doi: 10.4161/viru.2.3.15880.

Moda, F., Bolognesi, M. L. and Legname, G. (2019) 'Novel screening approaches for human prion diseases drug discovery', *Expert Opinion on Drug Discovery*. Taylor & Francis, 14(10), pp. 983–993. doi: 10.1080/17460441.2019.1637851.

Mok, T. *et al.* (2017) 'Variant Creutzfeldt – Jakob Disease in a Patient with Heterozygosity at PRNP Codon 129', *The New England Journal of Medicine*, 376(3).

Moore, R. A., Taubner, L. M. and Priola, S. A. (2009) 'Prion protein misfolding and disease', *Current Opinion in Structural Biology*, 19(1), pp. 14–22. doi: 10.1016/j.sbi.2008.12.007.

Morales, R. *et al.* (2010) 'Molecular Cross Talk between Misfolded Proteins in Animal Models of Alzheimer's and Prion Diseases', *Journal of Neuroscience*, 30(13), pp. 4528–4535. doi: 10.1523/JNEUROSCI.5924-09.2010.

Morales, R., Green, K. and Soto, C. (2009) 'Cross currents in protein misfolding disorders: interactions and therapy', *CNS and Neurological Disorders - Drug Targets*, 8(5), pp. 363–371. doi: 10.1016/j.asieco.2008.09.006.EAST.

Morales, R., Moreno-Gonzalez, I. and Soto, C. (2013) 'Cross-Seeding of Misfolded Proteins: Implications for Etiology and Pathogenesis of Protein Misfolding Diseases', *PLoS Pathogens*, 9(9), pp. 1–4. doi: 10.1371/journal.ppat.1003537.

Morel, E. *et al.* (2004) 'The Cellular Prion Protein PrP ^{c} Is Expressed in Human Enterocytes in Cell-Cell Junctional Domains', *Journal of Biological Chemistry*, 279(2), pp. 1499–1505. doi: 10.1074/jbc.M308578200.

Morel, E. *et al.* (2008) 'The cellular prion protein PrPc is involved in the proliferation of epithelial cells and in the distribution of junction-associated proteins', *PLoS ONE*, 3(8). doi: 10.1371/journal.pone.0003000.

Moreno-Gonzalez, I. and Soto, C. (2011) 'Misfolded protein aggregates: Mechanisms, structures and potential for disease transmission', *Seminars in Cell and Developmental Biology*. Elsevier Ltd, 22(5), pp. 482–487. doi: 10.1016/j.semcdb.2011.04.002.

Mougenot, A. L. J. *et al.* (2011) 'Transmission of prion strains in a transgenic mouse model overexpressing human A53T mutated α-synuclein', *Journal of Neuropathology and Experimental Neurology*, 70(5), pp. 377–385. doi: 10.1097/NEN.0b013e318217d95f.

Moum, Truls *et al.* (2005) 'Polymorphisms at codons 141 and 154 in the ovine prion protein gene are associated with scrapie Nor98 cases', *Journal of General Virology*, 86(1), pp. 231–235. doi: 10.1099/vir.0.80437-0.

Munoz-Montesino, C. *et al.* (2016) 'Generating Bona Fide Mammalian Prions with Internal Deletions', *Journal of Virology*, 90(15), pp. 6963–6975. doi: 10.1128/jvi.00555-16.

Muntané, G. *et al.* (2008) 'Phosphorylation of tau and α-synuclein in synaptic-enriched fractions of the frontal cortex in Alzheimer's disease, and in Parkinson's disease and related α-synucleinopathies', *Neuroscience*, 152(4), pp. 913–923. doi: 10.1016/j.neuroscience.2008.01.030.

Murayama, Y. *et al.* (2007) 'Urinary excretion and blood level of prions in scrapie-infected hamsters', *Journal of General Virology*, 88(10), pp. 2890–2898. doi: 10.1099/vir.0.82786-0.

Murdoch, B. M. and Murdoch, G. K. (2015) 'Genetics of prion disease in cattle', *Bioinformatics and Biology Insights*, 9, pp. 1–10. doi: 10.4137/BBi.s29678.

Nalls, A. V. *et al.* (2013) 'Mother to Offspring Transmission of Chronic Wasting Disease in Reeves' Muntjac Deer', *PLoS ONE*, 8(8). doi: 10.1371/journal.pone.0071844.

Narayanan, V. and Scarlata, S. (2001) 'Membrane binding and self-association of α-synucleins', *Biochemistry*, 40(33), pp. 9927–9934. doi: 10.1021/bi002952n.

Naslavsky, N. *et al.* (1997) 'Characterization of detergent-insoluble complexes containing the cellular prion protein and its scrapie isoform', *Journal of Biological Chemistry*, 272(10), pp. 6324–6331. doi: 10.1074/jbc.272.10.6324.

Natale, G. *et al.* (2011) 'Transmission of prions within the gut and toward the central nervous system', *Prion*, 5(3), pp. 142–149. doi: 10.4161/pri.5.3.16328.

NCJDRSU (2019) *Creutzfeldt-Jakob Disease in the UK*, *National CJD Research & Surveillance Unit*. Available at: http://www.cjd.ed.ac.uk/documents/figs.pdf (Accessed: 25 July 2019).

Neale, M. H. *et al.* (2010) 'Infection of Cell Lines with Experimental and Natural Ovine Scrapie Agents', *Journal of Virology*, 84(5), pp. 2444–2452. doi: 10.1128/jvi.01855-09.

Negro, A. *et al.* (1997) 'The complete mature bovine prion protein highly expressed in Escherichia coli: Biochemical and structural studies', *FEBS Letters*. Federation of European Biochemical Societies, 412(2), pp. 359–364. doi: 10.1016/S0014-5793(97)00798-9.

Nentwig, A. *et al.* (2007) 'Diversity in neuroanatomical distribution of abnormal prion protein in atypical scrapie', *PLoS Pathogens*, 3(6), pp. 0743–0751. doi: 10.1371/journal.ppat.0030082.

Newman, P. K. *et al.* (2014) 'Postmortem findings in a case of variant Creutzfeldt-Jakob disease treated with intraventricular pentosan polysulfate', *Journal of Neurology, Neurosurgery and Psychiatry*, 85(8), pp. 919–922. doi: 10.1136/jnnp-2013-305590.

Nieznanska, H. *et al.* (2018) 'Identification of prion protein-derived peptides of potential use in Alzheimer's disease therapy', *Biochimica et Biophysica Acta - Molecular Basis of Disease*. Elsevier, 1864(6), pp. 2143–2153. doi: 10.1016/j.bbadis.2018.03.023.

Nieznanski, K. *et al.* (2012) 'Soluble prion protein inhibits amyloid-β (Aβ) fibrillization and toxicity', *Journal of Biological Chemistry*, 287(40), pp. 33104–33108. doi: 10.1074/jbc.C112.400614.

Nieznanski, K. *et al.* (2014) 'Interaction between prion protein and Aβ amyloid fibrils revisited', *ACS Chemical Neuroscience*, 5(5), pp. 340–345. doi: 10.1021/cn500019c.

Nishida, N. *et al.* (2000) 'Successful Transmission of Three Mouse-Adapted Scrapie Strains to Murine Neuroblastoma Cell Lines Overexpressing Wild-Type Mouse Prion Protein', *Journal of Virology*, 74(1), pp. 320–325. doi: 10.1128/jvi.74.1.320-325.2000.

Nonno, R. *et al.* (2006) 'Efficient transmission and characterization of Creutzfeldt-Jakob disease strains in bank voles', *PLoS Pathogens*, 2(2), pp. 0112–0120. doi: 10.1371/journal.ppat.0020012.

Nonno, R. *et al.* (2019) 'Variable protease-sensitive prionopathy transmission to bank voles', *Emerging Infectious Diseases*, 25(1), pp. 73–81. doi: 10.3201/eid2501.180807.

O'Brien, R. J. and Wong, P. C. (2011) 'Amyloid Precursor Protein processing and Alzheimer's Disease', *Annual Review of Microbiology*, 34, pp. 185–204. doi: 10.1146/annurev-neuro-061010-113613.Amyloid.

O'Rourke, K. I. *et al.* (1999) 'PrP genotypes of captive and free-ranging Rocky Mountain elk (Cervus elaphus nelsoni) with chronic wasting disease', *Journal of General Virology*, 80(10), pp. 2765–2769. doi: 10.1099/0022-1317-80-10-2765.

Oelschlegel, A. M. *et al.* (2015) 'A bovine cell line that can be infected by natural sheep scrapie prions', *PLoS ONE*, 10(1), pp. 1–15. doi: 10.1371/journal.pone.0117154.

Oesch, B. *et al.* (1985) 'A cellular gene encodes scrapie PrP27-30 protein', *Cell*, 40(4), pp. 735–746. Available at: http://files/54/Oesch et al. - 1985 - A cellular gene encodes scrapie PrP 27-30 protein.pdf%5Cnhttp://www.ncbi.nlm.nih.gov/pubmed/2859120.

Ondrejcak, T. *et al.* (2018) 'Cellular prion protein mediates the disruption of hippocampal synaptic plasticity by soluble tau in vivo', *Journal of Neuroscience*, 38(50), pp. 10595–10606. doi: 10.1523/JNEUROSCI.1700-18.2018.

Orrú, C. D. *et al.* (2009) 'Human variant Creutzfeldt-Jakob disease and sheep scrapie PrPresdetection using seeded conversion of recombinant prion protein', *Protein Engineering, Design and Selection*, 22(8), pp. 515–521. doi: 10.1093/protein/gzp031.

Orrú, C. D. *et al.* (2014) 'A Test for Creutzfeldt–Jakob Disease Using Nasal Brushings', *New England Journal of Medicine*, 371(6), pp. 519–529. doi: 10.1056/NEJMoa1315200.

Orrú, C. D., Groveman, B. R., *et al.* (2015) 'Bank Vole Prion Protein As an Apparently Universal Substrate for RT-QuIC-Based Detection and Discrimination of Prion Strains', *PLoS Pathogens*, 11(6), pp. 1–20. doi: 10.1371/journal.ppat.1004983.

Orrú, C. D., Favole, A., *et al.* (2015) 'Detection and discrimination of classical and atypical L-Type bovine spongiform encephalopathy by real-time quaking-induced conversion', *Journal of Clinical Microbiology*, 53(4), pp. 1115–1120. doi: 10.1128/JCM.02906-14.

Owen, J. P. *et al.* (2007) 'Use of thermolysin in the diagnosis of prion diseases', *Molecular Biotechnology*, 35(2), pp. 161–170. doi: 10.1007/BF02686111.

Paik, S. R. *et al.* (1998) 'Self-oligomerization of NACP , the precursor protein of the non-amyloid β/A4 protein (Aβ) component of Alzheimer's disease amyloid , observed in the presence of a C-terminal Aβ fragment (residues 25-35)', *FEBS Letters*, 421, pp. 73–76.

Pan, K. *et al.* (1993) 'Conversion of alpha-helices into beta-sheets features in the formation of the scrapie prion proteins', *Biochemistry*, 90(December), pp. 10962–10966. doi: VL - 90.

Pan, K. -M, Stahl, N. and Prusiner, S. B. (1992) 'Purification and properties of the cellular prion protein from Syrian hamster brain', *Protein Science*, 1(10), pp. 1343–1352. doi: 10.1002/pro.5560011014.

Panegyres, P. K. and Armari, E. (2013) 'Therapies for human prion diseases.', *American journal of neurodegenerative disease*, 2(3), pp. 176–86. Available at: http://www.ncbi.nlm.nih.gov/pmc/articles/PMC3783831/%5Cnhttp://www.ncbi.nlm.nih.gov/pubmed/24093082%5Cnhttp://www.pubmedcentral.nih.gov/articlerender.fcgi?artid=PMC3783831.

Papasavva-Stylianou, P. *et al.* (2011) 'PrP gene polymorphisms in Cyprus goats and their association with resistance or susceptibility to natural scrapie', *Veterinary Journal*. Elsevier Ltd, 187(2), pp. 245–250. doi: 10.1016/j.tvjl.2009.10.015.

Paquet, S., Langevin, C., *et al.* (2007) 'Efficient dissemination of prions through preferential transmission to nearby cells', *Journal of General Virology*, 88(2), pp. 706–713. doi: 10.1099/vir.0.82336-0.

Paquet, S., Daude, N., *et al.* (2007) 'PrPc Does Not Mediate Internalization of PrPSc but Is Required at an Early Stage for De Novo Prion Infection of Rov Cells', *Journal of Virology*, 81(19), pp. 10786–10791. doi: 10.1128/jvi.01137-07.

Pastore, A. and Zagari, A. (2007) 'A structural overview of the vertebrate prion proteins.', *Prion*, 1(3), pp. 185–197. doi: 10.4161/pri.1.3.5281.

Peoc'h, K. *et al.* (2000) 'Identification of three novel mutations (E196K, V203I, E211Q) in the prion protein gene (PRNP) in inherited prion diseases with Creutzfeldt-Jakob disease phenotype.', *Human mutation*, 15(5), p. 482. doi: 10.1002/(SICI)1098-1004(200005)15:5<482::AID-HUMU16>3.0.CO;2-1.

Peretz, D. *et al.* (2001) 'Antibodies inhibit prion propagation and clear cell cultures of

prion infectivity', *Nature*, 412(6848), pp. 739–743. doi: 10.1038/35089090.

Peretz, D. (2001) 'Strain-specified relative conformational stability of the scrapie prion protein', *Protein Science*, 10(4), pp. 854–863. doi: 10.1110/ps.39201.

Pergami, P., Jaffe, H. and Safar, J. (1996) 'Semipreparative chromatographic method to purify the normal cellular isoform of the prion protein in nondenatured form', *Analytical Biochemistry*, 236(1), pp. 63–73. doi: 10.1006/abio.1996.0132.

Perucchini, M. *et al.* (2008) 'PrP genotypes of free-ranging wapiti (Cervus elaphus nelsoni) with chronic wasting disease', *Journal of General Virology*, 89(5), pp. 1324–1328. doi: 10.1099/vir.0.83424-0.

Pir, G. J. *et al.* (2019) 'Suppressing Tau Aggregation and Toxicity by an Anti-Aggregant Tau Fragment', *Molecular Neurobiology*. Molecular Neurobiology, 56, pp. 3751–3767.

Priola, S. A. *et al.* (1994) 'Heterologous PrP molecules interfere with accumulation of protease-resistant PrP in scrapie-infected murine neuroblastoma cells.', *Journal of virology*, 68(8), pp. 4873–8. Available at: http://www.pubmedcentral.nih.gov/articlerender.fcgi?artid=236427&tool=pmcentrez&rendertype=abstract.

Pritzkow, S. *et al.* (2015) 'Grass Plants Bind, Retain, Uptake, and Transport Infectious Prions', *Cell Reports*. The Authors, 11(8), pp. 1168–1175. doi: 10.1016/j.celrep.2015.04.036.

Pritzkow, S. *et al.* (2018) 'Efficient prion disease transmission through common environmental materials', *Journal of Biological Chemistry*, 293(9), pp. 3363–3373. doi: 10.1074/jbc.M117.810747.

Prusiner, S. B. (1982) 'Novel proteinaceous infectious particles cause scrapie', *Science*, 216(4542), pp. 136–144. doi: 10.1126/science.6801762.

Prusiner, S. B. (1998) 'Prions', *Proceedings of the National Academy of Sciences of the United States of America*, 95(November), pp. 13363–13383.

Prusiner, S. B. (2004) 'Prion biology and diseases.', *Cold Spring Harbor Laboratory Press, Cold Spring Harbor, N.Y.* doi: 10.1101/087969547.38.1.

Puoti, G. *et al.* (2012) 'Sporadic human prion diseases: Molecular insights and diagnosis', *The Lancet Neurology*. Elsevier Ltd, 11(7), pp. 618–628. doi: 10.1016/S1474-4422(12)70063-7.

Race, R. E., Fadness, L. H. and Chesebro, B. (1987) 'Characterization of scrapie infection in mouse neuroblastoma cells', *Journal of General Virology*, 68(5), pp. 1391–1399. doi: 10.1099/0022-1317-68-5-1391.

Race, R., Jenny, A. and Sutton, D. (1998) 'Scrapie Infectivity and Proteinase K-Resistant

Prion Protein in Sheep Placenta, Brain, Spleen, and Lymph Node: Implications for Transmission and Antemortem Diagnosis', *The Journal of Infectious Diseases*, 178(4), pp. 949–953. doi: 10.1086/515669.

Race, R., Oldstone, M. and Chesebro, B. (2000) 'Entry versus Blockade of Brain Infection following Oral or Intraperitoneal Scrapie Administration: Role of Prion Protein Expression in Peripheral Nerves and Spleen', *Journal of Virology*, 74(2), pp. 828–833. doi: 10.1128/jvi.74.2.828-833.2000.

Raymond, G. J. *et al.* (2006) 'Inhibition of Protease-Resistant Prion Protein Formation in a Transformed Deer Cell Line Infected with Chronic Wasting Disease', *Journal of Virology*, 80(2), pp. 596–604. doi: 10.1128/jvi.80.2.596-604.2006.

Redaelli, V. *et al.* (2017) 'Detection of prion seeding activity in the olfactory mucosa of patients with Fatal Familial Insomnia', *Scientific Reports*. Nature Publishing Group, 7(January), pp. 1–8. doi: 10.1038/srep46269.

Rees, H. C. *et al.* (2009) 'Concentration of disease-associated prion protein with silicon dioxide', *Molecular Biotechnology*, 41(3), pp. 254–262. doi: 10.1007/s12033-008-9129-5.

Requena, J. R. and Wille, H. (2014) 'The structure of the infectious prion protein', *Prion*, 8(1). doi: 10.4161/pri.28368.

Resenberger, U. K. *et al.* (2011) 'The cellular prion protein mediates neurotoxic signalling of B-sheet-rich conformers independent of prion replication', *EMBO Journal*, 30(10), pp. 2057–2070. doi: 10.1038/emboj.2011.86.

Rezaei, H. *et al.* (2000) 'High yield purification and physico-chemical properties of full-length recombinant allelic variants of sheep prion protein linked to scrapie susceptibility', *European Journal of Biochemistry*, 267(10), pp. 2833–2839. doi: 10.1046/j.1432-1033.2000.01347.x.

Riek, R. *et al.* (1997) 'NMR characterization of the full-length recombinant murine prion protein, mPrP(23-231)', *FEBS Letters*, 413(2), pp. 282–288. doi: 10.1016/S0014-5793(97)00920-4.

Riesner, D. (2003) 'Biochemistry and structure of PrP C and PrP Sc', *British Medical Bulletin*, 66(ii), pp. 21–33. doi: 10.1093/bmb/dg66.021.

Robertson, C. *et al.* (2006) 'Cellular prion protein is released on exosomes from activated platelets', *Blood*, 107(10), pp. 3907–3911. doi: 10.1182/blood-2005-02-0802.

Robinson, S. J. *et al.* (2012) 'The role of genetics in chronic wasting disease of North American cervids', *Prion*, 6(2), pp. 153–162. doi: 10.4161/pri.19640.

Rochet, J.-C. (2007) 'Novel therapeutic strategies for the treatment of protein-

misfolding diseases', *Expert Reviews in Molecular Medicine*, 9(17), pp. 1–34. doi: 10.1017/S1462399407000385.

Rodrigues, C. H. M., Pires, D. E. V. and Ascher, D. B. (2018) 'DynaMut: Predicting the impact of mutations on protein conformation, flexibility and stability', *Nucleic Acids Research*. Oxford University Press, 46(W1), pp. W350–W355. doi: 10.1093/nar/gky300.

Rosano, G. L. and Ceccarelli, E. A. (2014) 'Recombinant protein expression in Escherichia coli: Advances and challenges', *Frontiers in Microbiology*, 5(APR), pp. 1–17. doi: 10.3389/fmicb.2014.00172.

Roy, S. *et al.* (2005) 'Axonal transport defects: A common theme in neurodegenerative diseases', *Acta Neuropathologica*, 109(1), pp. 5–13. doi: 10.1007/s00401-004-0952-x.

Rubenstein, R. *et al.* (1991) 'Alterations in neurotransmitter-related enzyme activity in scrapie-infected PC12 cells', *Journal of General Virology*, 72(6), pp. 1279–1285. doi: 10.1099/0022-1317-72-6-1279.

Rubenstein, R., Carp, R. I. and Callahan, S. M. (1984) 'In vitro replication of scrapie agent in a neuronal model: Infection of PC12 cells', *Journal of General Virology*, 65(12), pp. 2191–2198. doi: 10.1099/0022-1317-65-12-2191.

Rustom, A. *et al.* (2004) 'Nanotubular Highways for Intercellular Organelle Transport', *Science*, 303(5660), pp. 1007–1010. doi: 10.1126/science.1093133.

Saá, P., Castilla, J. and Soto, C. (2006) 'Presymptomatic detection of prions in blood', *Science*, 313(5783), pp. 92–94. doi: 10.1126/science.1129051.

Saborio, G. P., Permanne, B. and Soto, C. (2001) 'Sensitive detection of pathological prion protein by cyclic amplication of protein misfolding', *Nature*, 411(June), pp. 1–4. doi: 10.1038/35081095.

Sabuncu, E. *et al.* (2003) 'PrP Polymorphisms Tightly Control Sheep Prion Replication in Cultured Cells', *Journal of Virology*, 77(4), pp. 2696–2700. doi: 10.1128/jvi.77.4.2696-2700.2003.

Safar, J. *et al.* (1998) 'Eight prion strains have PrP(Sc) molecules with different conformations', *Nature Medicine*, 4(10), pp. 1157–1165. doi: 10.1038/2654.

Salamat, M. K. *et al.* (2011) 'Prion Propagation in Cells Expressing PrP Glycosylation Mutants', *Journal of Virology*, 85(7), pp. 3077–3085. doi: 10.1128/jvi.02257-10.

Sander, P. *et al.* (2004) 'Analysis of sequence variability of the bovine prion protein gene (PRNP) in German cattle breeds', *Neurogenetics*, 5(1), pp. 19–25. doi: 10.1007/s10048-003-0171-y.

Sano, K. *et al.* (2013) 'Early Detection of Abnormal Prion Protein in Genetic Human Prion Diseases Now Possible Using Real-Time QUIC Assay', *PLoS ONE*, 8(1), pp. 8–11. doi:

10.1371/journal.pone.0054915.

Sano, K. *et al.* (2017) 'Prion-Like Seeding of Misfolded α-Synuclein in the Brains of Dementia with Lewy Body Patients in RT-QUIC', *Molecular Neurobiology*. Molecular Neurobiology, 55(5), pp. 3916–3930. doi: 10.1007/s12035-017-0624-1.

Saunders, G. C. *et al.* (2006) 'PrP genotypes of atypical scrapie cases in Great Britain', *Journal of General Virology*, 87(11), pp. 3141–3149. doi: 10.1099/vir.0.81779-0.

Schatzl, H. M. *et al.* (1997) 'A Hypothalamic Neuronal Cell Line Persistently Infected with Scrapie Prions Exhibits Apoptosis', *Journal of virology*, 71(11), pp. 8821–8831.

Schläpfer, J. *et al.* (1999) 'A new allelic variant in the bovine prion protein gene (PRNP) coding region', *Animal Genetics*, 30(5), pp. 382–383. doi: 10.1046/j.1365-2052.1999.00526.x.

Schneider, C. A., Rasband, W. S. and Eliceiri, K. W. (2012) 'NIH Image to ImageJ: 25 years of image analysis', *Nature Methods*. Nature Publishing Group, 9(7), pp. 671–675. doi: 10.1038/nmeth.2089.

Schrodinger, L. (2010) 'The PyMOL Molecular Graphics System'.

Seelig, D. M., Goodman, P. A. and Skinner, P. J. (2016) 'Potential approaches for heterologous prion protein treatment of prion diseases', *Prion*, 10(1), pp. 18–24. doi: 10.1080/19336896.2015.1123372.

Sharon, R. *et al.* (2001) 'A-Synuclein Occurs in Lipid-Rich High Molecular Weight Complexes, Binds Fatty Acids, and Shows Homology To the Fatty Acid-Binding Proteins', *Proceedings of the National Academy of Sciences of the United States of America*, 98(16), pp. 9110–9115. doi: 10.1073/pnas.171300598.

Shibuya, S. *et al.* (1998) 'Protective prion protein polymorphisms against sporadic Creutzfeldt-Jakob disease', *The Lancet*, 351, p. 419.

Shikiya, R. A. and Bartz, J. C. (2011) 'In Vitro Generation of High-Titer Prions', *Journal of Virology*, 85(24), pp. 13439–13442. doi: 10.1128/jvi.06134-11.

Shimizu, S. *et al.* (1999) 'Creutzfeldt-Jakob disease with florid plaques after cadaveric dura mater grafting', *Arch Neurol*, 56, pp. 357–362. doi: 10.1046/j.1440-1789.2003.00489.x.

Shin, W. *et al.* (2008) 'Cloning and expression of a prion protein (PrP) gene from Korean bovine (Bos taurus coreanae) and production of rabbit anti-bovine PrP antibody', *Biotechnology Letters*, 30(10), pp. 1705–1711. doi: 10.1007/s10529-008-9768-4.

Shuaib, S. *et al.* (2019) 'Computational design and evaluation of β - sheet breaker peptides for destabilizing Alzheimer ' s amyloid - β 42 protofibrils', *Journal of Cellular Biochemistry*, 120, pp. 17935–17950. doi: 10.1002/jcb.29061.

Sigurdson, C. J. *et al.* (1999) 'Oral transmission and early lymphoid tropism of chronic wasting disease PrP(res) in mule deer fawns (Odocoileus hemionus)', *Journal of General Virology*, 80(10), pp. 2757–2764. doi: 10.1099/0022-1317-80-10-2757.

Silva, C. J. *et al.* (2018) 'Determining the Relative Susceptibility of Four Prion Protein Genotypes to Atypical Scrapie', *Analytical Chemistry*, 90(2), pp. 1255–1262. doi: 10.1021/acs.analchem.7b03985.

Sisakhtnezhad, S. and Khosravi, L. (2015) 'Emerging physiological and pathological implications of tunneling nanotubes formation between cells', *European Journal of Cell Biology*. Elsevier GmbH., 94(10), pp. 429–443. doi: 10.1016/j.ejcb.2015.06.010.

Sisó, S. *et al.* (2007) 'Neuropathological and molecular comparison between clinical and asymptomatic bovine spongiform encephalopathy cases', *Acta Neuropathologica*, 114(5), pp. 501–508. doi: 10.1007/s00401-007-0283-9.

Skinner, P. J. *et al.* (2015) 'Treatment of prion disease with heterologous prion proteins', *PLoS ONE*, 10(7), pp. 1–17. doi: 10.1371/journal.pone.0131993.

Smith, C. K., Regan, L. and Withka, J. M. (1994) 'A Thermodynamic Scale for the β-Sheet Forming Tendencies of the Amino Acids', *Biochemistry*, 33(18), pp. 5510–5517. doi: 10.1021/bi00184a020.

Sohn, H. J. *et al.* (2002) 'A case of chronic wasting disease in an elk imported to Korea from Canada', *Journal of Veterinary Medical Science*, 64(9), pp. 855–858. doi: 10.1292/jvms.64.855.

Solassol, J., Crozet, C. and Lehmann, S. (2003) 'Prion propagation in cell culture', *British Medical Bulletin*, 66, pp. 87–97. doi: 10.1385/1-59259-874-9:227.

Somerville, R. A. *et al.* (2019) 'BSE infectivity survives burial for five years with only limited spread', *Archives of Virology*. Springer Vienna, 164(4), pp. 1135–1145. doi: 10.1007/s00705-019-04154-8.

Sorice, M. *et al.* (2012) 'Trafficking of PrPCto mitochondrial raft-like microdomains during cell apoptosis', *Prion*, 6(4), pp. 354–358. doi: 10.4161/pri.20479.

Soto, C. *et al.* (1996) 'Inhibition of Alzheimer ' s Amyloidosis by Peptides That Prevent b -Sheet Conformation', *Biochemical and Biophysical Research Communications*, 680, pp. 672–680.

Soto, C. *et al.* (1998) 'B-sheet breaker peptides inhibit fibrillogenesis in a rat brain model of amyloidosis: Implications for Alzheimer's therapy', *Nature Medicine*, 4(July), pp. 822–826.

Soto, C. *et al.* (2000) 'Reversion of prion protein conformational changes by synthetic b -sheet breaker peptides', *The Lancet*, 355, pp. 192–197.

Soto, C. (2001) 'Protein misfolding and disease: protein refolding and therapy', *FEBS Letters*, 498, pp. 204–207. doi: 10.1385/1592593941.

Soto, C. (2003) 'Unfolding the role of protein misfolding in neurodegenerative diseases', *Nature Reviews Neuroscience*, 4(1), pp. 49–60. doi: 10.1038/nrn1007.

Soto, C. and Estrada, L. (2005) 'Amyloid Inhibitors and p-Sheet Breakers', in *Alzheimer's Disease*, pp. 351–364.

Soto, C., Estrada, L. and Castilla, J. (2006) 'Amyloids, prions and the inherent infectious nature of misfolded protein aggregates', *Trends in Biochemical Sciences*, 31(3), pp. 150–155. doi: 10.1016/j.tibs.2006.01.002.

Spagnolli, G. *et al.* (2019) 'Full atomistic model of prion structure and conversion', *PLoS Pathogens*, 15(7), pp. 1–18. doi: 10.1371/journal.ppat.1007864.

Spillantini, G. M. *et al.* (1997) 'Alpha-Synuclein in Lewy bodies', *Nature*, pp. 839–840. doi: 10.1038/42166.

Spillantini, M. G. *et al.* (1998) 'alpha-Synuclein in filamentous inclusions of Lewy bodies from Parkinson' s disease and dementia with Lewy bodies', *Proceedings of the National Academy of Sciences*, 95(11), pp. 6469–6473. doi: 10.1073/pnas.95.11.6469.

Spiropoulos, J. *et al.* (2011) 'Isolation of prion with BSE properties from farmed goat', *Emerging Infectious Diseases*, 17(12), pp. 2253–2261. doi: 10.3201/eid1712.110333.

Stack, M. J., Chaplin, M. J. and Clark, J. (2002) 'Differentiation of prion protein glycoforms from naturally occurring sheep scrapie, sheep-passaged scrapie strains (CH1641 and SSBP1), bovine spongiform encephalopathy (BSE) cases and Romney and Cheviot breed sheep experimentally inoculated with BSE using', *Acta Neuropathologica*, 104(3), pp. 279–286. doi: 10.1007/s00401-002-0556-2.

Stanton, J. B. *et al.* (2012) 'Discovery of a Novel, Monocationic, Small-Molecule Inhibitor of Scrapie Prion Accumulation in Cultured Sheep Microglia and Rov Cells', *PLoS ONE*, 7(11). doi: 10.1371/journal.pone.0051173.

Stöckel, J. *et al.* (1998) 'Prion protein selectively binds copper(II) ions', *Biochemistry*, 37(20), pp. 7185–7193. doi: 10.1021/bi972827k.

Stockman, S. (1913) 'Scrapie: An Obscure Disease of Sheep', *Journal of Comparative Pathology and Therapeutics*. Elsevier, 26(October), pp. 317–327. doi: 10.1016/S0368-1742(13)80060-4.

Suh, T. Y. *et al.* (2017) 'Biological and biochemical characterization of M2B cells: Classical BSE prion is conserved in transgenic mice overexpressing bovine prion protein gene', *Prion*, 11(6), pp. 405–414. doi: 10.1080/19336896.2017.1331809.

Taema, M. M. *et al.* (2012) 'Differentiating ovine BSE from CH1641 scrapie by serial

protein misfolding cyclic amplification', *Molecular Biotechnology*, 51(3), pp. 233–239. doi: 10.1007/s12033-011-9460-0.

Takashima, S. *et al.* (1997) 'Creutzfeldt-Jakob disease with florid plaques after cadaveric dural graft in a Japanese woman [7]', *Lancet*, 350(9081), pp. 865–866. doi: 10.1016/S0140-6736(05)62035-1.

Taraboulos, A. *et al.* (1990) 'Acquisition of protease resistance by prion proteins in scrapie-infected cells does not require asparagine-linked glycosylation.', *Proceedings of the National Academy of Sciences of the United States of America*, 87(21), pp. 8262–8266. doi: 10.1073/pnas.87.21.8262.

Tark, D. *et al.* (2015) 'Generation of a persistently infected MDBK cell line with natural bovine spongiform encephalopathy (BSE)', *PLoS ONE*, 10(2), pp. 1–11. doi: 10.1371/journal.pone.0115939.

Teng, S. *et al.* (2010) 'Structural assessment of the effects of Amino Acid Substitutions on protein stability and protein-protein interaction', *International Journal of Computational Biology and Drug Design*, 3(4), pp. 334–349. doi: 10.1504/IJCBDD.2010.038396.

Teruya, K. and Doh-Ura, K. (2017) 'Insights from therapeutic studies for PrP prion disease', *Cold Spring Harbor Perspectives in Medicine*, 7(3). doi: 10.1101/cshperspect.a024430.

Thackray, A., Muhammad, F., *et al.* (2012) 'Prion-induced toxicity in PrP transgenic Drosophila', *Experimental and Molecular Pathology*. Elsevier Inc., 92(2), pp. 194–201. doi: 10.1016/j.yexmp.2012.01.005.

Thackray, A., Hopkins, L., *et al.* (2012) 'Propagation of ovine prions from "poor" transmitter scrapie isolates in ovine PrP transgenic mice', *Experimental and Molecular Pathology*. Elsevier Inc., 92(1), pp. 167–174. doi: 10.1016/j.yexmp.2011.11.004.

Thackray, A. M. *et al.* (2008) 'Molecular and Transmission Characteristics of Primary-Passaged Ovine Scrapie Isolates in Conventional and Ovine PrP Transgenic Mice', *Journal of Virology*, 82(22), pp. 11197–11207. doi: 10.1128/jvi.01454-08.

Thackray, A. M. *et al.* (2017) 'Genetic human prion disease modelled in PrP transgenic Drosophila', *Biochemical Journal*, 474(19), pp. 3253–3267. doi: 10.1042/BCJ20170462.

Thadani, V. *et al.* (1988) 'Creutzfeldt-Jakob disease probably acquired from a cadaveric dura mater graft. Case report', *Journal of Neurosurgery*, 69(5), pp. 766–769. doi: 10.3171/jns.1988.69.5.0766.

Thapa, S. *et al.* (2018) 'Overexpression of quality control proteins reduces prion conversion in prion-infected cells', *Journal of Biological Chemistry*, 293(41), pp. 16069–16082. doi: 10.1074/jbc.RA118.002754.

The UniProt Consortium (2019) 'UniProt: A worldwide hub of protein knowledge', *Nucleic Acids Research*. Oxford University Press, 47(D1), pp. D506–D515. doi: 10.1093/nar/gky1049.

Thompson, A. G. B. *et al.* (2013) 'The medical research council prion disease rating scale: A new outcome measure for prion disease therapeutic trials developed and validated using systematic observational studies', *Brain*, 136(4), pp. 1116–1127. doi: 10.1093/brain/awt048.

Thomzig, A. *et al.* (2007) 'Accumulation of pathological prion protein PrPSc in the skin of animals with experimental and natural scrapie', *PLoS Pathogens*, 3(5), pp. 0659–0667. doi: 10.1371/journal.ppat.0030066.

Thuring, C. M. A. *et al.* (2004) 'Discrimination between Scrapie and Bovine Spongiform Encephalopathy in Sheep by Molecular Size, Immunoreactivity, and Glycoprofile of Prion Protein', *Journal of Clinical Microbiology*, 42(3), pp. 972–980. doi: 10.1128/JCM.42.3.972-980.2004.

Tjernberg, L. O. *et al.* (1996) 'Arrest of β-amyloid fibril formation by a pentapeptide ligand', *Journal of Biological Chemistry*, 271(15), pp. 8545–8548. doi: 10.1074/jbc.271.15.8545.

Trevitt, C. R. and Collinge, J. (2006) 'A systematic review of prion therapeutics in experimental models', *Brain*, 129(9), pp. 2241–2265. doi: 10.1093/brain/awl150.

Tsigelny, I. F. *et al.* (2008) 'Mechanisms of hybrid oligomer formation in the pathogenesis of combined Alzheimer's and Parkinson's diseases', *PLoS ONE*, 3(9). doi: 10.1371/journal.pone.0003135.

Tsuboi, Y., Doh-Ura, K. and Yamada, T. (2009) 'Continuous intraventricular infusion of pentosan polysulfate: Clinical trial against prion diseases: Symposium: Prion diseases - Updated', *Neuropathology*, 29(5), pp. 632–636. doi: 10.1111/j.1440-1789.2009.01058.x.

Tuo, W. *et al.* (2001) 'PrP-C and PrP-Sc at the Fetal-Maternal Interface', *Journal of Biological Chemistry*, 276(21), pp. 18229–18234. doi: 10.1074/jbc.M008887200.

Tuo, W. *et al.* (2002) 'Pregnancy status and fetal prion genetics determine PrPSc in placentomes of scrapie-infected sheep', *Proceedings of the National Academy of Sciences of the United States of America*, 99(9), pp. 6310–6315. doi: 10.1073/pnas.072071199.

Turk, E. *et al.* (1988) 'Purification and properties of the cellular and scrapie hamster prion proteins', *European Journal of Biochemistry*, 176(1), pp. 21–30. doi: 10.1111/j.1432-1033.1988.tb14246.x.

Ueda, K. *et al.* (1993) 'Molecular cloning of cDNA encoding an unrecognized component

of amyloid in Alzheimer disease.', *Proceedings of the National Academy of Sciences of the United States of America*, 90(23), pp. 11282–11286. doi: 10.1073/pnas.90.23.11282.

Um, J. W. *et al.* (2012) 'Alzheimer amyloid- β oligomer bound to postsynaptic prion protein activates Fyn to impair neurons', *Nature Neuroscience*. Nature Publishing Group, 15(9), pp. 1227–1235. doi: 10.1038/nn.3178.

Um, J. W. and Strittmatter, S. M. (2013) 'Amyloid-β induced signaling by cellular prion protein and Fyn kinase', *Prion*, 7(1), pp. 37–41.

Vaccari, G. *et al.* (2007) 'Prion Protein Alleles Showing a Protective Effect on the Susceptibility of Sheep to Scrapie and Bovine Spongiform Encephalopathy', *Journal of Virology*, 81(13), pp. 7306–7309. doi: 10.1128/jvi.02880-06.

Vascellari, M. *et al.* (2007) 'PrPSc in salivary glands of scrapie-affected sheep', *J Virol*, 81(9), pp. 4872–4876. doi: 10.1128/JVI.02148-06.

Vázquez-Fernández, E. *et al.* (2016) 'The Structural Architecture of an Infectious Mammalian Prion Using Electron Cryomicroscopy', *PLoS Pathogens*, 12(9), pp. 1–21. doi: 10.1371/journal.ppat.1005835.

Vella, L. J. *et al.* (2007) 'Packaging of prions into exosomes is associated with a novel pathway of PrP processing', *Journal of Pathology*, 211, pp. 582–590. doi: 10.1002/path.

Vella, L. J. *et al.* (2008) 'The role of exosomes in the processing of proteins associated with neurodegenerative diseases', *European Biophysics Journal*, 37(3), pp. 323–332. doi: 10.1007/s00249-007-0246-z.

Victoria, G. S. *et al.* (2016) 'Astrocyte-to-neuron intercellular prion transfer is mediated by cell-cell contact', *Scientific Reports*. Nature Publishing Group, 6(August 2015), pp. 25–28. doi: 10.1038/srep20762.

Vidal, E. *et al.* (2008) 'Lack of PrPsc immunostaining in intracranial ectopic lymphoid follicles in a sheep with concomitant non-suppurative encephalitis and Nor98-like atypical scrapie: A case report', *Veterinary Journal*, 177(2), pp. 283–288. doi: 10.1016/j.tvjl.2007.04.014.

Viegas, P. *et al.* (2006) 'Junctional expression of the prion protein PrPC by brain endothelial cells: a role in trans-endothelial migration of human monocytes', *Journal of Cell Science*, 119(22), pp. 4634–4643. doi: 10.1242/jcs.03222.

Vilette, D. *et al.* (2001) 'Ex vivo propagation of infectious sheep scrapie agent in heterologous epithelial cells expressing ovine prion protein', *Proceedings of the National Academy of Sciences*, 98(7), pp. 4055–4059. doi: 10.1073/pnas.061337998.

Vilette, D. (2008) 'Cell models of prion infection', *Veterinary Research*, 39(10). doi: 10.1051/vetres.

Vilette, D. *et al.* (2018) 'Cellular mechanisms responsible for cell-to-cell spreading of prions', *Cellular and Molecular Life Sciences*. Springer International Publishing, 75(14), pp. 2557–2574. doi: 10.1007/s00018-018-2823-y.

Vital, A. *et al.* (2007) 'A sporadic case of Creutzfeldt-Jakob disease with beta-amyloid deposits and alpha-synuclein inclusions', *Neuropathology*, 27(3), pp. 273–277. doi: 10.1111/j.1440-1789.2007.00755.x.

Vital, A. *et al.* (2009) 'The nigrostriatal pathway in Creutzfeldt-Jakob disease', *Journal of Neuropathology and Experimental Neurology*, 68(7), pp. 809–815. doi: 10.1097/NEN.0b013e3181abdae8.

La Vitola, P. *et al.* (2019) 'Cellular prion protein neither binds to alpha-synuclein oligomers nor mediates their detrimental effects', *Brain*, 142(2), pp. 249–254. doi: 10.1093/brain/awy318.

Völkel, D., Blankenfeldt, W. and Schomburg, D. (1998) 'Large-scale production, purification and refolding of the full-length cellular prion protein from Syrian golden hamster in Escherichia coli using the glutathione S-tranferase-fusion system', *European Journal of Biochemistry*, 251(1–2), pp. 462–471. doi: 10.1046/j.1432-1327.1998.2510462.x.

Vorberg, I. *et al.* (2003) 'Multiple Amino Acid Residues within the Rabbit Prion Protein Inhibit Formation of Its Abnormal Isoform', *Journal of Virology*, 77(3), pp. 2003–2009. doi: 10.1128/jvi.77.3.2003-2009.2003.

Vorberg, I. *et al.* (2004) 'Susceptibility of Common Fibroblast Cell Lines to Transmissible Spongiform Encephalopathy Agents', *The Journal of Infectious Diseases*, 189(3), pp. 431–439. doi: 10.1086/381166.

Walia, R. *et al.* (2019) 'Gene-edited murine cell lines for propagation of chronic wasting disease prions', *Scientific reports*, 9(1), p. 11151. doi: 10.1038/s41598-019-47629-z.

Wang, X. F. *et al.* (2008) 'Human tau protein forms complex with PrP and some GSS- and fCJD-related PrP mutants possess stronger binding activities with tau in vitro', *Molecular and Cellular Biochemistry*, 310(1–2), pp. 49–55. doi: 10.1007/s11010-007-9664-6.

Watts, J. C. *et al.* (2014) 'Evidence That Bank Vole PrP Is a Universal Acceptor for Prions', *PLoS Pathogens*, 10(4). doi: 10.1371/journal.ppat.1003990.

Waxman, E. A. and Giasson, B. I. (2011) 'Induction of Intracellular Tau Aggregation Is Promoted by -Synuclein Seeds and Provides Novel Insights into the Hyperphosphorylation of Tau', *Journal of Neuroscience*, 31(21), pp. 7604–7618. doi: 10.1523/JNEUROSCI.0297-11.2011.

Weidemann, A. *et al.* (1989) 'Identification, biogenesis, and localization of precursors of

Alzheimer's disease A4 amyloid protein', *Cell*, 57(1), pp. 115–126. doi: 10.1016/0092-8674(89)90177-3.

Weingarten, M. D. *et al.* (1975) 'A protein factor essential for microtubule assemby', *Proceedings of the National Academy of Sciences of the United States of America*, 72(5), pp. 1858–1862.

Weiss, S. *et al.* (1995) 'Overexpression of active Syrian golden hamster prion protein PrPc as a glutathione S-transferase fusion in heterologous systems.', *Journal of virology*, 69(8), pp. 4776–4783. doi: 10.1128/jvi.69.8.4776-4783.1995.

Wells, G. A. *et al.* (1987) 'A novel progressive spongiform encephalopathy in cattle.', *The Veterinary record*. doi: 10.1136/vr.121.18.419.

White, A. R. *et al.* (2003) 'Monoclonal antibodies inhibit prion replication and delay the development of prion disease', *Nature*, 422(6927), pp. 80–83. doi: 10.1038/nature01457.

White, M. D. and Mallucci, G. R. (2009) 'Therapy for prion diseases: Insights from the use of RNA interference', *Prion*, 3(3), pp. 121–128. doi: 10.4161/pri.3.3.9289.

Wickner, R. B. *et al.* (2018) 'Yeast Prions Compared to Functional Prions and Amyloids', *Journal of Molecular Biology*. Elsevier Ltd, 430(20), pp. 3707–3719. doi: 10.1016/j.jmb.2018.04.022.

Will, R. G. *et al.* (1996) 'A new variant of Creutzfeldt-Jakob disease in the UK', *The Lancet*, 347(9006), pp. 921–925. doi: 10.5555/uri:pii:S0140673696914129.

Will, R. G. (2003) 'Acquired prion disease: Iatrogenic CJD, variant CJD, kuru', *British Medical Bulletin*, 66, pp. 255–265. doi: 10.1093/bmb/66.1.255.

Will, R. G. and Matthews, W. B. (1982) 'Evidence for case-to-case transmission of Creutzfeldt-Jakob disease', (45), pp. 235–238.

Wille, H. *et al.* (2002) 'Structural studies of the scrapie prion protein by electron crystallography', *Proceedings of the National Academy of Sciences of the United States of America*, 99(6), pp. 3563–3568. doi: 10.1073/pnas.052703499.

Wille, H. and Requena, J. (2018) 'The Structure of PrPSc Prions', *Pathogens*, 7(1), p. 20. doi: 10.3390/pathogens7010020.

Williams, A. D. *et al.* (2004) 'Mapping Aβ amyloid fibril secondary structure using scanning proline mutagenesis', *Journal of Molecular Biology*, 335(3), pp. 833–842. doi: 10.1016/j.jmb.2003.11.008.

Williams, E. S. (2005) 'Chronic wasting disease', *Veterinary Pathology*, 42(5), pp. 530–549. doi: 10.1354/vp.42-5-530.

Williams, E. S. and Young, S. (1980) 'Chronic wasting disease of captive mule deer: a

spongiform encephalopathy', *Journal of Wildlife Diseases*, 16(1).

Williamson, R. A. *et al.* (1998) 'Mapping the Prion Protein Using Recombinant Antibodies', *Journal of Virology*, 72(11), pp. 9413–9418. doi: 10.1128/jvi.72.11.9413-9418.1998.

Wirak, D. O. *et al.* (1991) 'Regulatory region of human amyloid precursor protein (APP) gene promotes neuron-specific gene expression in the CNS of transgenic mice', *Embo J*, 10(2), pp. 289–296. Available at: http://www.ncbi.nlm.nih.gov/pubmed/1899371.

Wood, S. J. *et al.* (1995) 'Prolines and Amyloidogenicity in Fragments of the Alzheimer's Peptide B/A4', *Biochemistry*, 34, pp. 724–730. doi: 10.1021/bi00003a003.

Workman, R. (2017) *The Development of Candidate Therapeutic and Diagnostic Ligands for Prion Diseases By*.

Workman, R. G., Maddison, B. C. and Gough, K. C. (2017) 'Ovine recombinant PrP as an inhibitor of ruminant prion propagation in vitro', *Prion*, 11(4), pp. 265–276. doi: 10.1080/19336896.2017.1342919.

World Organisation for Animal Health (2019) 'Bovine Spongiform Encephalopathy', in *Terrestrial Animal Health Code*, pp. 1–16. doi: 10.21775/9781910190951.08.

Wulf, M.-A., Senatore, A. and Aguzzi, A. (2017) 'The biological function of the cellular prion protein: an update', *BMC Biology*. BMC Biology, 15(1), p. 34. doi: 10.1186/s12915-017-0375-5.

Yan, L. M. *et al.* (2013) 'Selectively N-methylated soluble IAPP mimics as potent IAPP receptor agonists and nanomolar inhibitors of cytotoxic self-assembly of both IAPP and Aβ40', *Angewandte Chemie - International Edition*, 52(39), pp. 10378–10383. doi: 10.1002/anie.201302840.

Yin, S. M., Zheng, Y. and Tien, P. (2003) 'On-column purification and refolding of recombinant bovine prion protein: Using its octarepeat sequences as a natural affinity tag', *Protein Expression and Purification*, 32(1), pp. 104–109. doi: 10.1016/S1046-5928(03)00195-5.

Yoshimoto, J. *et al.* (1992) 'Comparative sequence analysis and expression of bovine PrP gene in mouse L-929 cells', *Virus Genes*, 6(4), pp. 343–356. doi: 10.1007/BF01703083.

Younan, N. D. *et al.* (2018) 'Prion protein stabilizes amyloid- (A) oligomers and enhances A neurotoxicity in a Drosophila model of Alzheimer's disease', *Journal of Biological Chemistry*, 293(34), pp. 13090–13099. doi: 10.1074/jbc.RA118.003319.

Yuan, J. *et al.* (2013) 'Recombinant Human Prion Protein Inhibits Prion Propagation in vitro', *Scientific Reports*, 3(1), p. 2911. doi: 10.1038/srep02911.

Zahn, R. *et al.* (2000) 'NMR solution structure of the human prion protein', *Proceedings of the National Academy of Sciences*, 97(1), pp. 145–150. doi: 10.1073/pnas.97.1.145.

Zou, W. *et al.* (2010) 'Variably Protease-Sensitive Prionopathy: A New Sporadic Disease', *Ann Neurol*, 68(2), pp. 162–172. doi: 10.1002/ana.22094.Variably.

Zou, W. Q. *et al.* (2013) 'Prions in variably protease-sensitive prionopathy: An update', *Pathogens*, 2(3), pp. 457–471. doi: 10.3390/pathogens2030457.